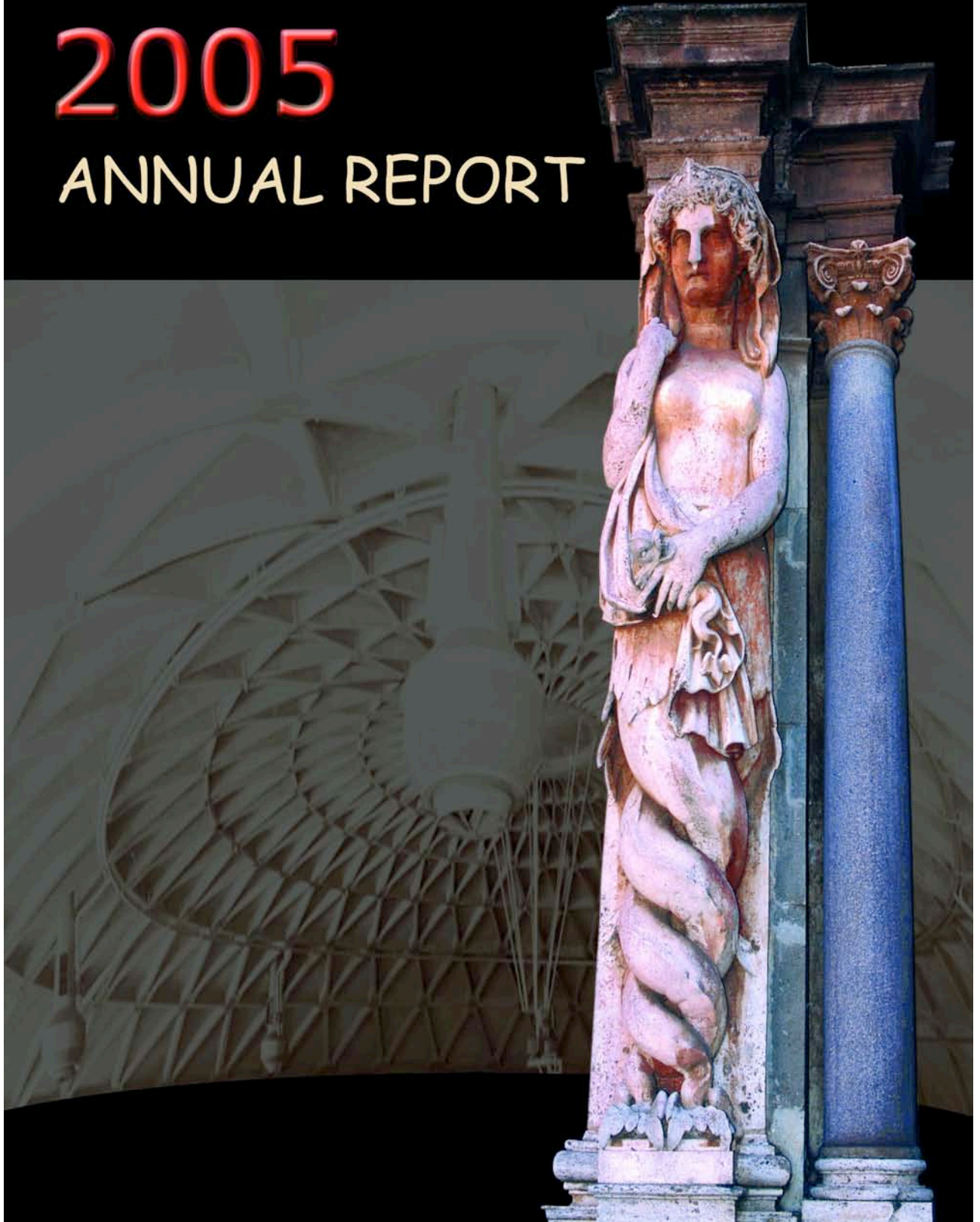


istituto nazionale di fisica nucleare  
laboratori nazionali di Frascati

2005

ANNUAL REPORT





Cover:

Background: *Inside view of the Adone dome (ing. C. Cestelli-Guidi & ing. A. Giuffrè) now hosting the DAΦNE Accelerator of the INFN-LNF. (Photo Claudio Federici)*

Foreground: *Cariatide by Ippolito Buzzi (1562-1634) decorating the "Teatro delle Acque" (Water theater) of Villa Aldobrandini in Frascati. (Photo Claudio Federici)*

Cover artwork: *Claudio Federici*



istituto nazionale di fisica nucleare  
laboratori nazionali di Frascati

2005

# ANNUAL REPORT

**LNF-06/10 (IR)**  
March, 2006

*Editor*  
Enrico Nardi

*Technical Editor*  
Luigina Invidia

*Published by*  
*SIS-Pubblicazioni*  
*P.O.Box 13 – I-00044 Frascati (Italia)*

Available at [www.lnf.infn.it/rapatt](http://www.lnf.infn.it/rapatt)

Mario Calvetti  
*LNF Director*

Maria Curatolo  
*Head, Research Division*

Miro Andrea Preger  
*Scientific Head, Accelerator Division*

Claudio Sanelli  
*Technical Head, Accelerator Division*

*LNF Scientific Coordinators*

Riccardo De Sangro  
*Particle Physics*

Marco Ricci  
*Astroparticle Physics*

Valeria Muccifora  
*Nuclear Physics*

Calogero Natoli  
*Theory and Phenomenology*

Roberto Cimino  
*Techn. and Interdisciplinary Research*

## FOREWORD

### **Laboratori Nazionali di Frascati – Frascati National Laboratories (LNF): Present and Future**

#### **Introduction**

The Frascati National Laboratories (LNF), situated on a hill just south of Rome, is the largest laboratory of the Italian Institute of Nuclear Physics (INFN). The laboratory is organized into three sub-structures: the Accelerator Division, the Research Division and the Administration, for a total of about 380 staff members.

The Accelerator Division runs the DAΦNE accelerator complex, an  $e^+ e^-$  storage ring, used to produce  $\phi$  mesons at a high rate. Three experiments, KLOE, FINUDA and SIDDHARTA, study the  $\phi$  decays, the charged and neutral kaon decays, the kaonic nuclei, produced when a negative kaon is absorbed in a nucleus, and the properties of any other of the particles produced in the  $\phi$  decay chain.

A linear accelerator (the Linac) accelerates electrons and positrons to fill the storage rings. The very clean electron and positron beams, with variable energy in the interval between 50 MeV and 850 MeV, variable intensity from 1 to  $10^{10}$  electrons per bunch, at a rate of 50 Hz, can be deflected into an experimental area, the Beam Test Facility (BTF), where a photon-tagged beam, of variable energy, is also available.

The BTF facility is continuously used by internal and external users. Last year, for example, the photon calorimeter of the AGILE satellite was calibrated using the energy tagged photon beam, and the properties of several detectors, used by the LHC experiments, were also measured.

Experiments with cryogenic detectors, channelling of positron with undulated crystals for x ray production, and other experiments, are planned for the coming years.

The Accelerator Division participates in the construction of the CNAO (Centro Nazionale di Adroterapia Oncologica), a 1.2 GeV proton synchrotron used for cancer therapy in Pavia.

A free electron laser, named SPARC, is being assembled at the LNF, in collaboration with ENEA (the Italian National Agency for New Technologies, Energy and the Environment). The scientific goal of the SPARC project consists in producing 10 ps electron bunches, with emittance smaller than 2 mm mrad, able to induce the self amplified green synchrotron laser light in the magnetic undulator placed downstream the electron gun.

A very intense LASER, able to produce 200 TW of 0.8 micron wave length for 10 fs (the Frascati Laser for Acceleration and Multidisciplinary Experiments, FLAME) is being assembled nearby the SPARC linac. The possibility to accelerate a bunch of electrons in the plasma waves produced by the light in a gaseous target will be explored.

The proton synchrotron in Pavia (CNAO), the SPARC free electron laser and the FLAME laser will be operational by the end of the year 2008.

Physicists and engineers of the Accelerator Division also participate in the research and development in the field of accelerator technology. The construction of CTF3, the CLIC Test Facility at CERN, the TTFII, the Tesla Test Facility at DESY, the work for the future Linear Collider and the study for a possible future Super B-factory as well, are part of our research program.

The DAΦNE accelerator, which is continuously being improved, produces synchrotron radiation light used by many experimental groups.

The very intense infrared light from a synchrotron source is available at DAΦNE. At the moment we have three lines running, the Infra Red line, the X ray line and the UV line, a second x-ray line is under construction. More than a hundred users, in the context of the European research funding TARI program, used this facility last year.

The Research Division is composed of physicists and engineers working in many experiments at the LNF, at CERN (ATLAS, LHCb, DIRAC), at FNAL (CDFII), at SLAC (BABAR), at JLAB (AICE), at DESY (HERMES), in Grenoble (GRAAL), at the Gran Sasso National Laboratories – LNGS (OPERA, ICARUS), at Cascina (VIRGO), in space borne experiments within the WIZARD program, and also, locally, in the search for gravitational waves with a cryogenic bar (NAUTILUS).

### **Short range future at LNF**

The scientific program of DAΦNE has been decided for the coming three years 2006, 2007, 2008.

In the spring of 2006 KLOE will be removed from the DAΦNE ring and placed in the assembly hall, while the FINUDA detector will be placed on the machine. We expect to collect  $1 \text{ fb}^{-1}$  with FINUDA before the installation of the SIDDHARTA detector by the end of 2007.

SIDDHARTA will take data in 2007 while a new run in 2008 - 2009 for FINUDA is possible.

DAΦNE is a beautiful opportunity to study machine physics at its cutting edge. Several possible modifications of the accelerator can be implemented to increase the luminosity. New technologies will be applied, like fast kickers, to increase the injection efficiencies, kickers that could be used for the ILC dumping rings, crab cavities, wigglers with shaped poles, to follow the particle trajectory in the alternating magnetic fields, and so on.

An adequate fraction of the beam time will be dedicated to machine studies, because it is important to understand the machine limits, the new technologies and the new ideas.

The LNF are also very active in the field of scientific communication. In fact, every year we have more than a thousand visitors, mainly students and teachers. Every autumn we organize a week long meeting, with lectures, discussions, visits to the labs, attended

by more than 250 secondary school teachers of physics and philosophy. In the year 2005 our Scientific Information Services has organized 23 conferences.

### **Long range future – The LNF roadmap**

The main research programs of the LNF, the CNAO, the SPARC, the FLAME projects, will either have ended or be in smooth running conditions by the end of 2008, similarly for the LNF groups that collaborate with the LHC experiments. We consider it very important to have a strong physics research program, to be pursued at Frascati beyond the year 2010.

A major upgrade of the present accelerator is under evaluation, aiming at a machine able to deliver more than  $50 \text{ fb}^{-1}$  at the  $\Phi$  resonance, in 4 or 5 years of data taking, starting in 2011, and to operate with a centre of mass energy in the interval 1GeV - 2.5 GeV. Recently we have stimulated an intense effort to study the physics case of this new accelerator named DANAE. Five Letters of Intent on different research topics have recently been received and will be evaluated in the framework of this possible new future initiative.

The letters of intent and the proposal for the new accelerator can be found at the following address <http://www.lnf.infn.it/lnfadmin/direzione/roadmap.html>.

New collaborators for the experiments and the construction of a top class accelerator would be welcome at LNF.

Prof. Mario Calvetti  
Director of LNF



## **ACKNOWLEDGMENTS**

I would like to thank Luigina Invidia for her very efficient and pleasant collaboration in the production of this report, and Claudio Federici for the beautiful realization of the cover page. I also acknowledge Stefano Bianco, Annette Donkerlo, Maria Rita Ferrazza and Matthew Moulson for their help and suggestions. I am grateful to all the authors that contributed to this report by making an effort to submit their contribution within schedule.

A special acknowledgment should also go to the many colleagues whose activity, not being strictly related to scientific work, is not represented in this report: without their collaboration any kind of research at the LNF would hardly be possible.

Enrico Nardi  
Editor

# Laboratori Nazionali di Frascati

## 2005 ANNUAL REPORT

### CONTENTS

<i>Foreword</i> .....	VII
<i>Acknowledgments</i> .....	XI
COMMUNICATION and OUTREACH .....	1
CRESCERE .....	6
FISICA in AUTOBUS .....	9
SCIENZA per TUTTI .....	11
<i>1 – Particle Physics</i>	
ATLAS .....	15
BABAR .....	27
BTEV .....	36
CDF .....	37
KLOE .....	46
LHC-b .....	63
<i>2 – Astroparticle Physics</i>	
BENE .....	72
ICARUS .....	73
LARES .....	74
NEMO .....	77
OPERA .....	78
PVLAS .....	88
RAP .....	90
ROG .....	93
WIZARD .....	100

### ***3 – Nuclear Physics***

AIACE .....	103
FINUDA .....	109
GRAAL .....	114
HERMES .....	119
$\bar{P}$ ANDA .....	131
SIDDHARTA .....	134
VIP .....	140

### ***4 – Theory and Phenomenology***

FA-51 .....	144
LF-21 .....	145
LF-61 .....	151
MI-11 .....	156
MI-12 .....	158
PI-11 .....	166
PI-31 .....	167

### ***5 – Technological and Interdisciplinary Research***

ARCHIMEDE .....	168
CAPIRE .....	170
E-CLOUD .....	173
FLUKA2 .....	177
FREETHAI .....	178
FREETHALDEUTER .....	186
MARIMBO .....	190
MINCE .....	193
POLYX .....	197
PRESS-MAG-0 .....	199
SAFTA2 .....	202
SALAF .....	204
SI-RAD .....	208
SUE .....	211

## ***6 – Accelerator Physics***

CSAX .....	214
DAΦNE .....	216
DAΦNE-BTF .....	229
DAΦNE-L Lab .....	239
GILDA .....	247
NTA CANDIA .....	249
NTA CLIC .....	251
NTA TTF .....	253
RADIATION SAFETY .....	255
SPARC .....	258
<i>LNF Publications</i> .....	267
<i>Glossary</i> .....	276

## COMMUNICATION AND OUTREACH

R. Centioni, V. Ferretti (art. 15), S. Miozzi (art. 2222), L. Sabatini, S. Vannucci (Resp.)  
Office of Education and Public Relations  
Scientific Information Service

The “Laboratori Nazionali di Frascati dell’INFN” (LNF) provides basic education in Physics for the general public, students and teachers. The LNF Educational and Public Relation programmes are made possible by the enthusiastic involvement of the laboratory graduate students, postdocs, researchers, engineers and technicians. This report describes 2005 activity including special events organized for World Year of Physics (WYP 2005).

### 1 LNF guided tours, “Scientific Week”, “Open Day” and ScienzaOrienta

<http://www.lnf.infn.it/edu/>

A well established laboratory tradition: 4500 people/year for general public, students and teachers.  
Scientific coordinators: L. Benussi, P. Gianotti, G. Mazzitelli, C. Petrascu, B. Sciascia.  
82 volunteers have received 127 groups. A typical visit consists of:

- history of the laboratory;
- presentation of INFN-LNF activities on site and abroad;
- visit to the “en plain air museum”;
- visit to experimental areas.

#### **LNF Scientific Week, Open day and ScienzaOrienta: about 1000 visitors.**

Most of LNF employees are in action to present their research center, answer questions and care for their guests. Since 1990 this is organized as:

- guided tours;
- conferences and public lectures;
- scientific videos;
- exhibitions of students’ projects;
- Open Day.

### 2 Outreach: Scientific Itineraries

The aim is to offer a more complete view of the scientific institutions operating in the area and improve the communication with the general public. In collaboration with:

- CNR Tor Vergata;
- ENEA Frascati;



Figure 1: *Wyp 2005 Event: Viaggi e Miraggi Theatre Company in "I Fisici", F. Duerrenmatt, LNF June 16-17, 2005. Organized during LNF Summer Stages (INFN-LNF photo).*

- ESA-ESRIN Frascati;
- INAF Astronomical Observatory of Rome, Monte Porzio Catone;
- COPIT, Rome;
- Frascati Municipality;
- International non-government organizations;
- University of Rome Tor Vergata.

### **3 High school students' programme**

<http://www.lnf.infn.it/edu/stagelnf/>

LNF Stages, Scientific Coordinator: D. Babusci.

Goal: enable students to acquire the knowledge and understanding of INFN research activities.

- Winter stages, 2-4 weeks: 37 students with 19 tutors;
- Masterclasses 2005, 1 week: 35 students with 15 tutors;
- Summer stages, 3 weeks: 82 students with 23 tutors;
- Lectures at school by LNF researchers, 2-3 days: 864 students with 16 tutors.

## Special Program for Primary School: QUASAR

<http://www.lnf.infn.it/edu/quasar/>

Care of F. Murtas and B. Sciascia.

Age: 8 - 14.

First meeting with the children at their school to introduce the world of research and some concepts of modern physics. Then, visit to the Frascati National Laboratories by small groups. Total of children and teachers in visit: 70.

## 4 High school teachers' programme

### "Incontri di Fisica"

<http://www.lnf.infn.it/edu/incontri/>

Organizing Committee: S. Bertolucci, D. Babusci (chair), S. Bianco, M. Calvetti, L.E. Casano, R. Centioni, S. Miozzi, L. Sabatini, S. Vannucci.

- Lectures and Experiments for high-school science teachers and scientific journalists.
- Goal: stimulate teachers' professional training and provide an occasion for interactive and hands-on contact with the latest developments in physics.

Fifth edition (October 4-6, 2005): 190 participants and 64 LNF Tutors (researchers, engineers and technicians).

## 5 Online resources for teachers and students: Lezioni di Fisica, Live lectures by scientists

<http://www.lnf.infn.it/media/lezionifisica.html/>

Care of M. Calvetti, O. Ciaffoni, G. Di Giovanni.

R. Barbieri: "Matter Waves, Principle of Uncertainty".

M. Mangano: "The forces".

G. Altarelli: Principle of Relativity, Space-Time.

## 6 General public programme

### Seminars

<http://www.lnf.infn.it/edu/seminaridivulgativi/>

Upon request, LNF researchers give seminars to high school students and the general public on:

- INFN Activities and Elementary Particles;
- Modern Physics and Cosmology;
- Synchrotron Light;
- Gravitational waves.



Figure 2: *Wyp 2005 Event: Concert, LNF June 8, 2005. Jack Liebeck (violin) and Charles Owen (piano). (photo by Roberto Baldini).*

## 7 Events

<http://www.lnf.infn.it/edu/wyp2005/>

### 1. Wyp 2005 Events

- Wyp Concert by Jack Liebeck and Charles Owen, LNF, 8 June 2005;
- I Fisici, F. Duerrenmatt, LNF 16-17, June 2005;
- La fisica e la motocicletta, LNF 4-6 October, 2005

### 2. Events

- VI Incontro con la Scienza, Conference given by Prof. Antonino Zichichi, Frascati November 3, 2005;
- Christmas Concert, Classico Concerto Bandistico Augusto Panizza Citt di Frascati, LNF 16 December, 2005.

## Conferences

International conferences, workshops and schools hosted and organized by the LNF:

1. Euridice Collaboration Meeting, LNF 8-12 February, 2005;
2. Riunione sulle prospettive della Fisica Astroparticellare nello spazio nell'INFN, LNF 16 February, 2005;
3. Mini-Workshop on Wiggler Optimization for Emittance Control, LNF 21-22 February, 2005;
4. Les Rencontres de Physique de la Valle d'Aoste, La Thuile, 27 February / 5 March, 2005
5. Modern Trends in Supersymmetric Mechanics, LNF 7-12 March, 2005;
6. Interaction.org Meeting, LNF 10-11 March, 2005;
7. Giornate di Studio SPARX e Applicazioni, LNF 9-10 May, 2005;
8. LNF Spring School "Bruno Touschek", LNF 15-19 May, 2005;
9. Spring Institute 2005, LNF 16 May / 18 July, 2005;
10. K-Rare Decays, LNF 26-27 May, 2005;
11. First Workshop on Quark Hadron Duality and the Transition to Perturbative QCD, LNF 6-8 June, 2005;
12. Fisica delle collisioni di ioni pesanti di altissima energia e Plasma di Quark-Gluoni, LNF 8-9, June 2005;
13. Piano Triennale INFN, 9-10 June, 2005;
14. 7th International Workshop on Neutrino Factories and Superbeams, LNF 21-26, June, 2005;
15. XII Mice Collaboration Meeting. LNF 26-29, June, 2005;
16. International Conference on X-Ray Optics and Microanalysis, 25-30 September, 2005;
17. Incontri di Fisica 2005, LNF 4-6 October, 2005;
18. The Physics and Applications of High Brightness Electron Beams, Erice 9-14 October, 2005;
19. VIII Scuola Nazionale di luce di Sincrotrone, LNF 10-21 October, 2005;
20. International Workshop on Nucleon Form Factors, 12-14 October, 2005;
21. Comunicare Fisica, LNF 24-27 October, 2005;
22. ICFA mini-workshop on "The Frontier of Short Bunches in Storage Rings", LNF 7-8 November, 2005;
23. Super B-Factory Meeting, LNF 11-12 November, 2005;
24. Jacow Team Meeting, LNF 14-18 November, 2005;
25. Nanoscience & Nanotechnology, Villa Mondragone, Monte Porzio Catone 14-16 November, 2005;
26. TESLA Technology Collaboration Meeting, LNF 5-7 December, 2005;
27. GDE Meeting, LNF 7-9 December, 2005.

## CRESCERE (Cosmic Rays Experiment in an European School Environment: a Remote Experiment)

Luigi Benussi, Stefano Bianco, Halina Bilokon, Orlando Ciaffoni, Franco Luigi Fabbri  
Maria Antonietta Frani, Paola Gianotti, Giuseppina Modestino, Giovanni Nicoletti  
Luciano Passamonti, Piero Patteri, Catalina Petrascu, Diana Sirghi  
Flavia Toti-Lombardozi, Luciano Trasatti

### 1 Introduction

The CRESCERE project (Cosmic Rays in a Europe School Environment: a Remote Experiment) aim to spuring young students to be engaged in a research activity, giving them the opportunity of using a modern scientific apparatus to carry on a web-controlled experiment, with the help of an on-line tutor. The project was born within the framework of activities of [www.scienzapertutti.net](http://www.scienzapertutti.net) exploiting a previous experience in cosmic ray measurement for didactic purpose.

The funding from the EC in the FP6 “Science and society” allowed its extention to Portugal and Romania, with the involvement respectively of FCUL (Faculdade de Ciências da Universidade de Lisboa) and LIP (Laboratório de Instrumentação and Física Experimental de Partículas, and IFIN-HH (Nat. Inst. for Physics and Nuclear Engeneering “Horia Holubei”). The schools participating to CRESCERE can choose among three experimental setups, housed at LNF or at LIP in Portugal, to measure cosmic ray muon speed, flux or lifetime, according to the experimental configuration. All raw data are available for analysis to everyone.



Figure 1: *The geographic distribution of the Italian schools involved in CRESCERE.*



Figure 2: A picture of a student presentation at the Lisbona meeting.

## 2 Scientific education in CRESCERE

The goal of the project is to stimulate the natural curiosity of young peoples toward the science, giving them a first hand feeling of the research activity in modern physics. Widespread use of web to communicate with the tutors and to operate the experiment is suited to get involvement of the students, since they are already acquainted with it for entertainment.

The tutorial activity supports the teachers and the students both before and after the on-line sessions. It starts after the enrollment in CRESCERE scheduling a visit of physicist to give a short introduction to modern physics and the role of cosmic ray in the science of XX century. An overview of the experiment and data analysis is given too. Moreover, these seminars present the INFN educational activities and the EC action to promote scientific careers; often this is the first personal contact of students with a researcher.

A booklet and a CD have been produced to summarize the activity and will be distributed to each student which participated in CRESCERE.

A closing meeting was held in Lisbona on 7th December 2005, to mark the next conclusion of the first stage of CRESCERE. It was attended by more than 100 students, coming from Italy, Portugal and Romania; it was planned so that some groups of students could present their work in the format of a typical scientific communication, emphasizing the importance of public dissemination of knowledge gained in research activity.

The on-line sessions were extended in the first months of 2006, to satisfy as much as possible the requests submitted by the schools. The geographic distribution of the schools involved in CRESCERE is shown in fig. 2.

### 3 The experimental setups and the on-line sessions

Three detectors, composed of scintillation counters and associated electronics (HV supply, discriminators, logic gates, TDC and crate controller) have been assembled; they are optimized for measurements of: a) Cosmic ray muon speed at LNF, b) Muon lifetime at FCUL, c) Cosmic ray flux at LIP. The participating schools have just to provide a fast internet connection, to allow video streaming, and a moderately recent hardware. The plugins required to get control of the experiment are available for download from the CRESCERE web site.

A few weeks before the data taking session the schools are requested to connect and test their configuration, although they have no real control in this stage (green code access). They can attend the presentation and send questions. Often the students exploits this opportunity to look at data sets taken in previous sessions to get acquainted with data analysis. The “green code” access was largely granted to teachers and single students wishing to give a look to CRESCERE on a personal basis even if their school cannot participate this year.

The on-line tutor gives a remind of the issue already presented in the visit, with greater details and live demonstration of the electronics. A few webcams can be switched to show different part of the detector setup, acquisition electronics and experimental room.

The time when a school has assigned the control (“red code” access) is mostly dedicate to chatting with the tutor to get a better insight of the detector behaviour and to discuss the best strategy of data acquisition. A screenshot of a remote session is shown in fig. 3.



Figure 3: A screenshot of a remote session.

### References

1. F.L. Fabbri, Presentation at Innovation in communication of Science - Forli, December 2005.
2. F. L. Fabbri *et al.* 'CRESCERE : un progetto europeo per la comunicazione' , XCI Congresso Nazionale SIF Catania, September 2005.
3. H. Bilokon, “Il progetto CRESCERE” , communication at Comunicare Fisica 2005 , LNF.
4. F.L. Fabbri, Researchers in Europe 2005 Initiative-Closing event-Dublin, 2 December 2005.
5. CRESCERE workshops at Madeira and Lisbona.

## PHYSICS ON THE BUS

H. Bilokon, F. L. Fabbri, C. Federici, G. Modestino, P. Patteri, A. Salemmè

### 1 “Physics on the bus”: a communication experiment

The project “Physics on the bus” has been conceived in the framework of the celebration for “2005 World Year of Physics”, aiming to give a close contact with some frontier issues of physics research to common peoples, namely commuter users of public transportation in a dozen of medium or large Italian cities. A simplified language, inspired by graphics and style of commercial advertising, has been used to get attention and to stimulate participation to web-based games. A number of aspects, uncommon to the physicists usual activity, had to be managed in order to carry on the project.

The posters of “Physics on the bus” are exposed on the buses or at bus stops, in the space usually occupied by commercial advertisings. The expositions started on July 2005, and will last until June 2006. A dozen of different posters will have been available for exposition by the end of the project.

Each poster presents a issue of modern physics, e.g. symmetry, order/disorder, black holes, antimatter, or more general hints on physics presence in everyday life, using an intriguing language and surprising graphic objects. It must catch attention and give some basic information at the first glimpse, as it is unlikely that a commuter, often in an uncomfortable position, can have time to read a complex text. On the other hand, we had to avoid an aggressive presentation, in a truly advertising style, for a number of reasons; firstly, we want to communicate a friendly image of physics and to make the reader conscious that the physics is in his world, even when it is not evident; moreover, since we were not acquainted at all to such a language, we would have to commit the work to a professional advertising agency, surely too much expensive for our budget and likely not willing to be constrained by our ideas; finally, even such limited displacement from the style of the usual educational communication, asked for a hard effort of simplification.

### 2 The accomplishment of the project

In the original project 12 themes had to be ready from the start, so that the posters could rotate among the cities each months; this implied that the web pages of [www.giocaonalbert.it](http://www.giocaonalbert.it) had been



Figure 1: The poster presenting the Nobel Prize winner Italian physicists.

ready too. Actually, both the delayed funding and the unforeseen complexity of the printing preparation make it impossible to follow this scheme. We adopted a more flexible sequence of poster release, starting from more general theme (Italian Nobel Prize winner, physical constants, antimatter, gravitation and so on) toward the physical applications, present and future, in the everyday life. This approach make easier to add or remove cities at any stage of the project, according to availability of expository spaces or local manpower. A number of higher schools were involved in the project, both supporting the local committee, and more often realizing limited exposition in schools and other public places in town were spaces on the public transportation were not available. The students have also the opportunity of proposing alternative graphical interpretations of the physical issues addressed by our posters; their works are presented in the web sites [www.giocaconalbert.it](http://www.giocaconalbert.it) or [scienzapertutti.lnf.infn.it](http://scienzapertutti.lnf.infn.it), and will participate to one of the annual challenges organized by Scienzapertutti. A summary of the cities involved and their contribution is reported in table 1.

Table 1: *The main data on poster exhibitions.*

City	no. poster	Start	Status
Bari	500		active
Bologna	200	9/1/05	active
Ferrara	40	7/25/05	active
Genova	?		scheduled
Lecce	60	9/1/05	active
Maglie	150	9/1/05	active
Milano	500	12/1/05	active
Pavia	100	9/1/05	active
Perugia	150	9/1/05	active
Pisa	350	9/1/05	active
Roma	100	10/1/05	ended
Trieste	40	9/1/05	ended

### 3 The web site [www.giocaconalbert.com](http://www.giocaconalbert.com)

A prize contest is linked to “Physics on the bus” in order to stimulate the participation of young students, after the first contact obtained by the poster exhibition. Each poster presents a few questions, in a really teasing and surprising formulation and the readers receive the hint to go to <http://www.giocaconalbert.com> for an insight. The contest is based on elementary questions, offering a multiple choice for the answer; a number of link are proposed, addressing to [scienzapertutti.lnf.infn.it](http://scienzapertutti.lnf.infn.it) and other educational sites, where a free help can be found with some good willing; alternatively, a simplification of the choices can be obtained at expense of the available score. The goal is that the challenger get a confirmation or an improvement of his knowledge on some fundamental items of physics. Up to now 700 peoples enrolled in the contest are actively participating. The web site and its forum of discussion is a reference point for people looking for events related to WYP2005; a proper study of the questions, discussions and interest of its visitor will provide an insight on how the physics appears to common people and young student.

### References

1. F. L. Fabbri, Congresso SIF Catania, September 2005.
2. P.Patteri *et al.*, “Fisica in autobus”, contributed paper (in italian) at the conference “Comunicare Fisica 2005”, to be published in the proceedings.

## ScienzaPerTutti: A SCIENCE DISSEMINATION PROJECT

L. Benussi (Art. 23), H. Bilokon, F.L. Fabbri (Resp.),  
G. Isidori, G. Modestino, G. Nicoletti, P. Patteri , C. Petrascu

### 1 Summary

After 3 years of activity the web site ScienzaPerTutti (<http://scienzapertutti.lnf.infn.it>) -also known as SxT- is a consolidated reality of the scientific communication web community. ScienzaPerTutti is a physics communication project addressed to the Italian general public with particular attention to young people, teachers and students. The project, wants to constitute moments of direct dialog between the researchers and the non generic public, through the technological transfer, of the products of scientific research. At the same time the project addresses itself to the galaxy of the youth world, offering, within the rigor of the contents, a humanized and user-friendly vision of science themes.

The organizational structure of ScienzaPerTutti is made up of:

- a promoting committee with the function of directing and guiding;
- a scientific editorial board which has the responsibility of the preparation of all the published tests, of the monthly updating of the columns, of the addressing the questions sent by the web surfers to a group of experts and of completing their answers with glossary, addenda, references and graphs;
- a group of more then 100 experts in different field of science which answer to the public;
- external collaborators (university and high school professors or students) which help the scientific board.

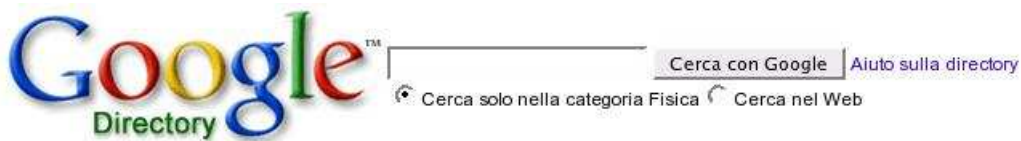
In addition o this, it also counts on the collaboration of several project leaders and researchers invited by the scientific editorial board, who write articles about scientific arguments for non specialized readers.

### 2 Activities

The success of ScienzaPerTutti is confirmed by the continuous and constant increase of the number of web surfers visiting our pages; since October 2002 the number of contacts are more then 3.7 millions (3,772,566), while Google ([www.google.com](http://www.google.com)) assign to SxT the 4th place for the page-rank relative to the physics educational web site

(<http://www.google.com/Top/World/Italiano/Scienza/Fisica/>)

The success of ScienzaPerTutti is also -and probably mainly- due to the philosophy of the project itself : SxT is a bi-directional communication web site in which our web surfers can strongly interact with the us to improve and propose the contents of the site; 30 articles have been realized by our “visitors” (schools, students and generic public) The great dynamism of the site, with monthly updates and new contents, the interactivity of the editors and the experts with the web-surfers, the projects developed with the schools make ScienzaPerTutti a very active and lively community constituted of researchers, teachers, students, generic public.



## Fisica

World > Italiano > Scienza > Fisica

### Categorie

Centri di Ricerca (10)  
 Dipartimenti e Facoltà Universitarie (34)  
 Meccanica Quantistica (4)  
 Musei (5)  
 Relatività (4)

Categoria Relativa:

World > Italiano > Scienza > Astronomia (385)

### Pagine Web

- CERN Document Server - <http://cdsweb.cern.ch/>  
 Propone, tramite ricerca semplice e avanzata, notizie bibliografiche e documenti a testo pieno di interess
- L'Avventura delle Particelle - [http://www.infn.it/multimedia/particle/paitaliano/adventure\\_home.html](http://www.infn.it/multimedia/particle/paitaliano/adventure_home.html)  
 Guida alla fisica delle particelle. Viene trattato il Modello Standard, con una presentazione delle particell  
 Guida storica e glossario sulla fisica delle particelle.
- SIF - Società Italiana di Fisica - <http://www.sif.it/>  
 Società fondata nel 1897 attorno alla rivista mensile "Il Nuovo Cimento". Presenta versioni elettroniche d  
 Scienza per Tutti - <http://scienzaper tutti.infn.it/>
- Percorsi divulgativi e tracciati di storia della fisica moderna. "Isola dei perché", glossario, concorsi e giochi
- Gabinetto di fisica - [http://spazioinwind.libero.it/gabinetto\\_di\\_fisica/frontits.htm](http://spazioinwind.libero.it/gabinetto_di_fisica/frontits.htm)  
 Museo virtuale di strumenti di laboratorio di fisica del XIX secolo e del primo novecento, dalle collezioni d
- Fisica delle Particelle Elementari - <http://xoomer.virgilio.it/lpassal/>  
 Un tutorial sulle particelle elementari come i leptoni e i quark. Completo di glossario, bibliografia e link.
- Fisica On Web - <http://www.fisicaonweb.it/>  
 Portale di Fisica diviso in tre sezioni, con possibilità' di interazione in tempo reale tra i visitatori, di redazic  
 sezione sulla storia della fisica e dei grandi scienziati.

Figure 1: Google web pages ([www.google.com](http://www.google.com)) of the scientific Italian web sites rank.

The questions addressed to SxT in the section “Chiedi all’esperto” by web surfers are more than 300 and the experts answering to the different questions are more than 150; experts came from several Italian Universities and research institutes (a great part from INFN) demonstrating again the success of the project and its prerogative of being an attraction pole in the scientific educational environment.

ScienzaPerTutti is the promoter of collateral activities as the annual contest “SpazioAperto” dedicated to Italian schools and which this year evolved in an international contest open also to foreign schools in which Italian is studied or by Italian institute abroad; this opening offered us the opportunity to enlarge our community to a non Italian audience for whom we added a multi-languages (French, Rumanian, Portugal and Russian) section in which we translated some articles present in the Italian site. Other SxT collateral activities are the CRESCERE project, the achievement of a modern experiment remotely operable via web and offered to schools, and the realization of specific projects for the Celebration of the Year of Physics as 12 Autobus, e GiocaConAlbert.

Fig.2(a) reports the LNF web log statistics and shows the distribution of the client domains accessing SxT in October 2005; in February 2006 fig2(b), due to the multi-languages sections of SxT, the number of contacts from non Italian domains are increased in percentage with respect to the Italian domains (from 20% to 60%).

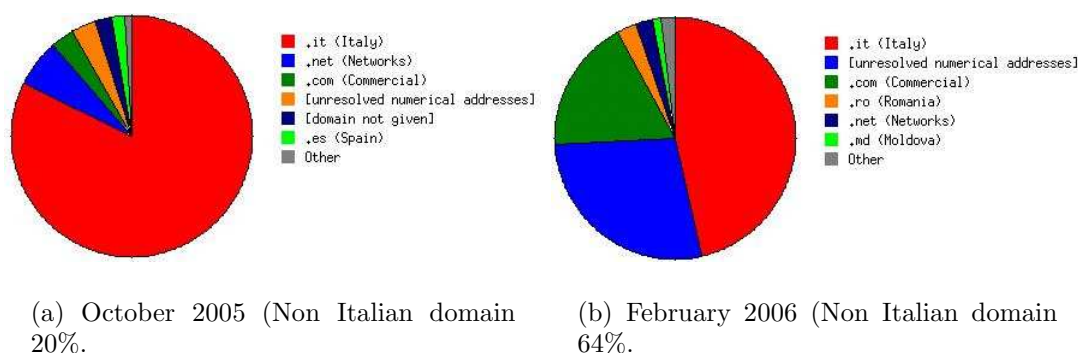


Figure 2: *Google web pages (www.google.com) of the scientific Italian web sites rank.*

## 2.1 The organizational structure of ScienzaPerTutti

### (b) Scientific editorial board

L. Benussi, H. Bilokon, E. Durante, F. L. Fabbri, G. Modestino, G. Nicoletti, P. Patteri, C. Petrascu, F. Toti Lombardozi.

### (c) Consultant experts

P. Agnoli, M. Alamanou, G. Amelino, R. Baiocchi, R. Baldini Celio, S. Barbanera, G. Barbiellini, E. Basile, M. Basile, G. Batignani, P.P. Battaglini, R. Battiston, P. Belli, G. Bellini, S. Bellucci, M. Biagini, H. Bilokon, C. Bini, C. Bloise, S. Boffi, F. Bossi, C. Bosio, C. Bruzzese, F. Buccella, E. Burattini, S. Calcaterra, C. Cannella, G. Capon, M. Caponero, M. Casolino, P. Catone, F. Celani, R. Cesario, O. Ciaffoni, I. Ciufolini, G. Corradi, L. Covi, G. D'Agostini, S. D'Argenio, O. da Pos, M. P. De Pascale, R. de Sangro, P. de Simone, L. Di Cesare, P. di Nezza, U. Dosselli, E. Durante, A. Ereditato, A. Esposito, F. L. Fabbri, V. Fafone, M. Falcetta, A. Farina, F. Felli, M. L. Ferrer, P. Ferretti, L. Foà, P. Franzini, S. Frullani, B. Gallavotti, M. Gasperini, M. Gobbino, M. Grandolfo, I. Guarneri, S. Guiducci, G. Iaselli, I. Iori, L. Iorio, G. Isidori, C. La Padula, P. Lariccia, A. Lorenzo, C. Luci, V. Lucherini, M. Lusignoli, C. Majorana, A. Marcelli, C. Matteuzzi, M. Mangano, G. Mannocchi, G. Mantovani, A. Marcelli, S. Marcello, S. Marini, A. Massarini, I. Modena, G. Modestino, A. Moneti, G. Mussardo, G. P. Murtas, E. Nardi, C. Natoli, G. Nicoletti, L. Orrù, G. Padovan, M. Pallotta, E. Pallante, G. Pancheri, A. Paolozzi, E. Paris, G. Parisi, L. Passamonti, P. Patteri, G. Penso, R. Peron, I. Peruzzi, C. Petrascu, M. Piccolo, D. Pierluigi, F. Pirri, G. Pizzella, F. Pompili, M. Primavera, L. Quintieri, S. Ratti, A. Reale, T. Regge, M. Ricci, R. Ricci, E. Righi, F. Romano, F. Rosati, G. Rossi, L. Ruggero, A. Russo, P. Santangelo, G. Saviano, F. Scaramuzzi, C. Schaerf, L. Schirone, F. Sebastiani, M. Serone, V. Sgrigna, A. Spallone, R. Sparvoli, P. Spillantini, P. Strolin, G. Susinno, G. Testera, S. Tomassini, L. Trasatti, G. Trenta, L. Trentadue, M. Vacca, A. Vacchi, G. Vilasi, F. Vissani, A. Venturelli, L. Zampieri.

### (e) Multilingual versions

Portuguese: H. Bilokon, I. Bediaga (Rio de Janeiro), A. Maio (Lisbon).

Romanian: C. Petrascu, D. Sirghi.

French: F.L.Fabbri, L. Benussi, C. Hadjidakis.

Russian: O. Shekhovtsova, O. Ryukina.

### **3 List of conference talks**

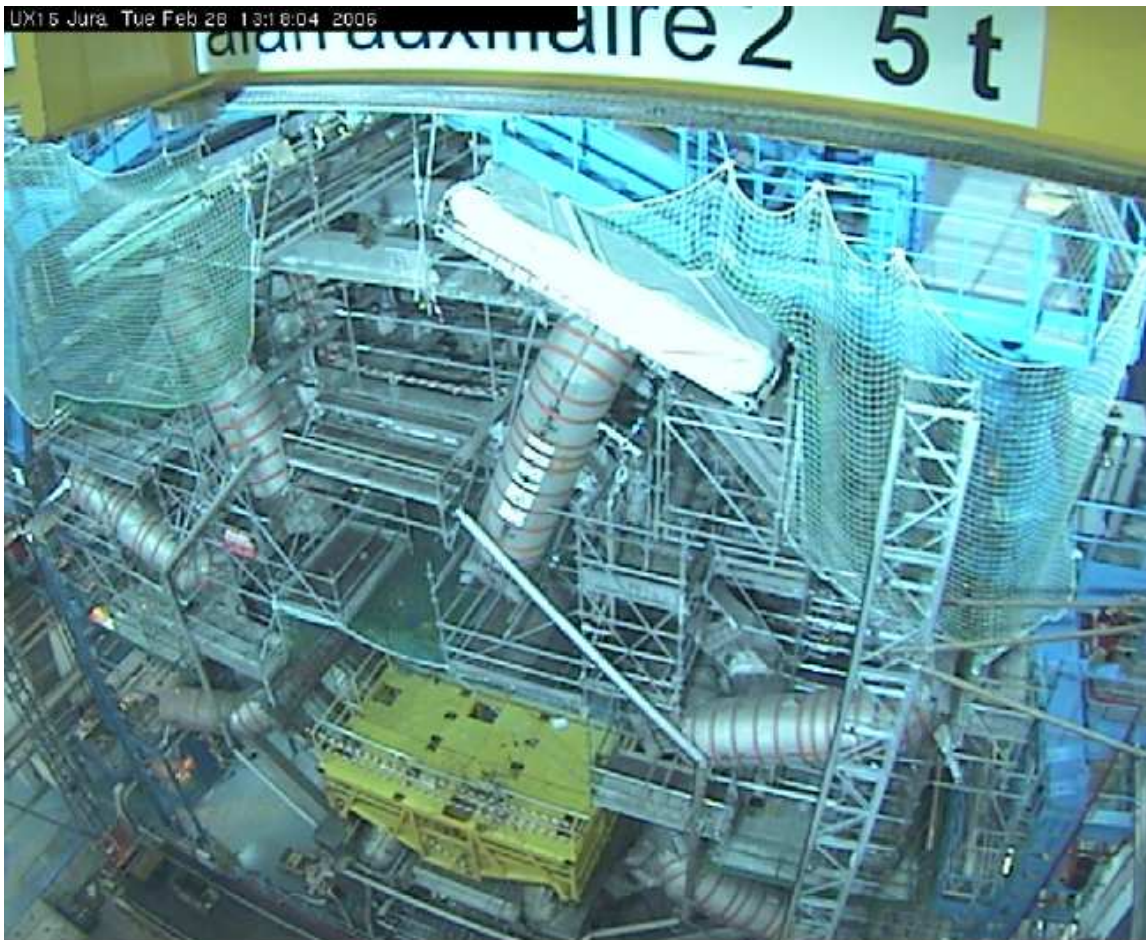
L. Benussi, “ScienzaPerTutti: la scienza nella rete, la rete della scienza” , Conferenza “Comunicare Fisica 2005”, Laboratori Nazionali di Frascati.

Modestino G. “ScienzaPerTutti: l’interattività della comunicazione scientifica”, Catania, XCI Congresso Nazionale SIF 2005.

## ATLAS

M. Antonelli, S. Argentati, M. Barone, M. Beretta, H. Bilokon, E. Capitolo (Tecn.), F. Cerutti, V. Chiarella, M. Curatolo, B. Dulach, B. Esposito(Resp.), M.L. Ferrer, S. Giovannella, K. Kordas, P. Laurelli, G. Maccarrone, A. Martini, W. Mei, S. Miscetti, G. Nicoletti, G. Pileggi (Tecn.), B. Ponzio(Tecn.), V. Russo(Tecn.), A. Sansoni, T. Vassilieva (Tecn.), S. Ventura (Dott.)

In collaboration with:  
Servizio Progettazione Apparati Sperimentali:  
C. Capoccia, S. Cerioni



## 1 Introduction

The Atlas experiment, one of the two general purpose experiments aimed at covering the full physics potential at the LHC, is based on an apparatus of unprecedented size, performances and complexity, to perform excellent inner tracking, electromagnetic and hadron calorimetry, and muon measurement. It has been designed and built by a world-wide collaboration of more than 150 Institutions.

Giant steps in the detector hardware construction, assembly, integration, installation and commissioning have been achieved during 2005. The time of the very first run is approaching and the Atlas collaboration is working very hard to be ready for this appointment with a very performing detector.

The LNF group has taken the responsibility of the construction of part of the precision tracking chambers, named Monitored Drift Tube (MDT) chambers, of the Atlas muon spectrometer. The group has participated in the design of the muon precision chambers with many original contributions to the project, developing an assembly method capable of insuring an extremely high and constant mechanical precision for all the produced chambers. The assembly method has been taken as baseline for all the production sites. Many other facilities have been designed and realized for the tube and chamber production. A very relevant one is the fully automated tube wiring machine, a multi-function machine particularly advanced from the point of view of the technical achievement. The Frascati automated wiring machine has been replicated in many other wiring sites. The chamber production in Frascati is finished since 2004 and all the chambers have been transported to Cern for the completion of the installation of the services, the successive integration with the trigger detectors RPC, the final tests and, finally, the installation into the Atlas spectrometer.

## 2 Chamber Commissioning in the BB5 area at Cern

The completion of the installation of the services (i.e. the gas system, the active FE electronics, the DCS components for the read-out of the alignment and temperature sensors and the full cabling) on all the MDT-BML chambers built at LNF was achieved before the end of 2005. Moreover, all the chambers underwent the foreseen tests to verify the integrity and the functionality of all the components and the correctness of the cabling connections. In fig. 1 the chamber cabling is shown.

The integration with the trigger detectors RPC into muon stations was pursued in the first half of the year. It was then interrupted because it was found that some RPC chambers needed modifications. It will be resumed in the year 2006. The number of BML stations integrated in 2005 is 47. In fig. 2 few integrated stations stored in the BB5 area are shown.

After the integration into stations, the “sag adjustment” ( i.e. the adjustment of the sagitta of the tubes in order to have the best achievable tube-wire concentricity) has to be performed. To establish the right procedure for the sag adjustment, a preliminary study was performed, positioning a BML station at the same inclination angles with respect to the horizontal plane (see fig. 3) as in the Atlas apparatus. The adjustment, which is realized by means of the appropriate mechanism mounted in each chamber spacer, has been performed on 22 stations.

A cosmic ray test of the complete stations is performed before leaving the BB5 area. The number of BML stations that have undergone in 2005 this cosmic ray test and are therefore declared ready for installation in Atlas is 18.



Figure 1: *Cabled MDT chamber.*

### 3 Chamber Installation in the Atlas detector

The installation of the muon stations in the Atlas spectrometer was started in summer 2005. Concerning the BML stations, 6 stations of the sector between the feet of the Atlas detector (sector 13) were successfully installed in July and correctly positioned in the Atlas spectrometer by means of auxiliary tooling designed and realized in Frascati. In the general schedule of Atlas, the installation of all the other BML stations has been delayed to 2006. The installation of the BML stations in sector 13 is shown in fig. 4, fig. 5 and fig. 6.

#### 3.1 Surface tests before installation (SX1)

After transportation from the Cosmic Test facility in BB5, the MDT chambers undergo a new set of tests before being down-loaded in the pit and installed in the muon spectrometer. Each single chamber is connected to the low voltages, and then readout from the CSM board via an optical fiber by a stand-alone PC to check the whole functionality of the FEE mounted on the chamber. Tests of the HV system, of the gas-tightness and of the optical alignment system are also performed. The mechanical integrity of the chamber is then surveyed by eye inspection. Two different kinds of data taking are carried out for the MDT's, a **noise run** and a **pulse run**:

- The noise run consists of acquiring events with a random trigger generated by an oscillator



Figure 2: *MDT stations stored in the BB5 area.*

at few kHz which tests the chamber occupancy as a function of the applied threshold on the discriminators. In this way, the detector noise can be determined and any problematic regions, or bad working discriminators, are spotted.

- Also the pulse run relies on the external oscillator but the trigger signal is split in two. The first replica of the trigger is used to generate the L1A, the second one is instead shaped and amplified to generate a narrow ( $< 25$  ns) signal of adjustable pulse height from 2 to 5 V which is sent to the HV input on the chamber. In this way, the electronics is fired by propagating the generate pulse along the chamber wires. The correct time-delay to acquire the generated signal on the TDC's, has been set by reading out the timing while controlling the input with an adjustable delay generator. This method has been developed in order to test the chambers without any need to flush the gas and to check, not only the amplifier and the TDC's in the FEE, but also the connection of the wire which could be damaged during transportation.

The pulse and noise runs allow a quick ( $< 10'$ ) check of the functionality of all system. Parallel testing of the RPC is also done. Gas leak tests, measurements of the pull-down current and, lately, a RPC pulse test are performed to check the functionality of the whole system and the cabling of the L1 trigger.



Figure 3: *Sag adjustment performed on a MDT station.*

#### 4 Cosmics data taking in Sector 13

An intense work of commissioning, to test not only the functionality of the MDT chambers but the whole system, (trigger, detector control system, data acquisition and online/offline monitoring) has started in autumn 2005. We quickly describe here the main achievements.

Sector 13 is the Barrel sector of the muon spectrometer in between the detector feet which has, therefore, the *easiest access* situation. Although most of the system services are not there yet, temporary services have been installed to perform both the noise study and to start reading the muon chambers from the USA15 station where the muon readout boards, the MROD's, are located. In sector 13, the final configuration of grounding and the dependence of noise from the applied threshold have been studied. The situation is very clean. Only few wires have single rates exceeding the kHz and, as expected, the average noise decreases of a factor two when increasing of 2 mV the applied threshold.

From the detector point of view, 3 BML and 3 BOL chambers have been set up in final position and then connected to a temporary gas many-fold to flush them with new gas. A simple scintillator trigger, formed by two  $3.0 \times 0.3$  m long scintillators readout at both ends by PM,  $S_j^{A,B}$ , has been prepared. The two scintillators have been positioned one above the other 30 cm along their longitudinal direction. The scintillators have then been put on the ground below the outer sector so to cover almost three chambers along  $\eta$ . The trigger required a 4-fold coincidence  $(S_1^A \times S_1^B) \times (S_2^A \times S_2^B)$  and counted  $\sim 1$  Hz in the pit, which has to be compared with a trigger



Figure 4: *The sliding of a BML station in the Atlas apparatus.*

counting of 30 Hz at the surface. The initialization of the chamber FEE was done by temporary hardware located in the pit (CAEN easy crates and PC's). Only the readout optical fibers were connected to the final patch-panels and brought to USA15 in a close-to-final configuration. The trigger was instead constituted by the 4-fold coincidence described above which was formed with NIM logic and then brought by a long cable to the USA15 room.

Data taking periods were restricted in time due to the difficulty to operate the chambers with HV and to turn ON the PM's during the continuous installation of the chambers. However,  $\sim 10$  runs of 1 hour each have been taken in two months, to monitor the functionality of the chambers. In fig. 7 the "home-made" event-display, run almost in real time to control the data-taking, shows very clean tracks through the BML's. In Fig. 8, a very clean time distribution is shown. The  $T_0$  and  $T_{max}$  of the spectrum have been extracted by fitting it with the standard curve used for the calibration procedure. First testing of the online monitoring and of the Offline calibration procedures have been started thanks to the acquired data. A rate of  $\sim 100$  Hz in the whole sector 13 can be estimated by triggering with the RPC system. This means that the  $T_0$  of each multilayer could be calibrated with the precision of  $\sim 1$  ns with 12 hours of data taking. If cross-calibration between the timing of the wires can be done by electronic pulsing of the FEE, a precise calibration of the apparatus can be performed with cosmics in-situ before the start of real  $p - p$  collisions.

To show the quality of the data collected, an event display of the cosmic sample done with the official Atlas-Offline display, Atlantis, is shown in fig. 9.



Figure 5: A BML station inside the ATLAS sector 13.

## 5 DAQ Commissioning

The activity in the Trigger and Data Acquisition (TDAQ) system of the ATLAS experiment has been concentrated during the year 2005 in two different aspects:

- Development in the event building part; TDAQ tests using a large cluster of PCs at CERN and commissioning using pre-series PCs interconnected via the almost final network configuration;
- Run TDAQ in the LNF cosmic ray stand.

ATLAS has a three-level trigger system. Until the 2nd level trigger the event selection is based on *regions of interest* (ROI) in the detector. The full event is built just before it is sent to the 3rd level trigger (*Event Filter* in ATLAS terminology). The event builder is implemented by the SFI (Sub Farm Input) process and this is the TDAQ part that, since November 2005, became full responsibility of the Frascati group.

The software infrastructure for the monitoring services of the TDAQ system was changed in the first part of 2005 in order to avoid bottlenecks and enhance the performance. Accordingly, the ability of the event building nodes to provide events to monitor processes has been re-implemented. Using test-beds at CERN and Linux PCs at Frascati, the cost in event-building performance, when the event builder nodes were also delivering events to monitoring tasks, was measured. For realistic monitoring fractions (less than about 1-10% of the events) the cost in event building rate was found to be less than 3%. However, this cost could reach 60% if 100% of the built events were also sent



Figure 6: A view of a BML station between the Atlas feet (sector 13).

to the monitoring tasks. This work triggered improvements on the side of the monitoring software which were used in a subsequent software release.

The Frascati group played a leading role in the 2005 Large Scale Tests (LST05) to assess the functionality of the TDAQ system and reveal the limitations of the existing software implementation. Given the availability of 700 PC's in LST05 (provided by CERN), the configurations with an event building system sized up to the full ATLAS scale<sup>1</sup> have been tested. A complete TDAQ slice (read-out, level-2 trigger, event-building and event-filter PCs) with and without algorithms on the trigger system was also tested. The emphasis of the tests was on the functionality of the control aspects of the TDAQ system. For example, the time needed for the whole system to complete a run-control transition, like *configuration*, *initialization*, *start run*, *etc.* has been measured. These tests revealed bugs and limitations of the current software which are not readily visible while testing the system in small tests. The problems have been fixed since then. The LST05 experience was surely positive, also because it represented a good training ground for the following items and enhanced the Frascati expertise in the whole TDAQ software chain.

In order to get ready for data-taking in 2007 with ATLAS, the TDAQ group has installed a prototype of the TDAQ system at the final location. This *pre-series* prototype is about 10% of the full ATLAS system with the final network topology and realistic PC's for the various TDAQ components. The LNF group has worked in the installation of the PC's and in the commissioning of

---

<sup>1</sup>This corresponds to 250 PC's: 100 event building nodes and 150 PC's playing the role of the detector-readout system.

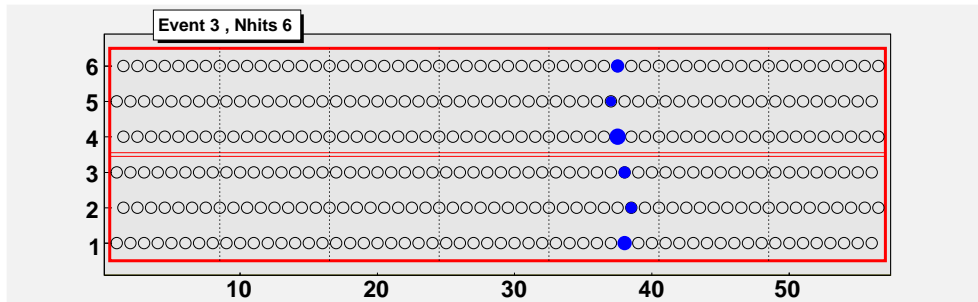


Figure 7: Example of the “home-made” event display to check the functionality of the acquired MDT chambers in real time.

the event-building part of the system. Moreover, the group has also participated in the exploitation of the system by measuring the event building performance in the case of output toward event monitors and/or Event Filter nodes.

A full event in ATLAS will be about 1.5 MB, recorded at a rate of 100 to 200 Hz. There are cases where there is no need to have the information from the whole ATLAS in the event; e.g. an event concerning the calibration of the muon detectors. In collaboration with other TDAQ experts, the LNF group is working to implement the ability of the system to build partial events, i.e. using only the data readout of specific sub-detectors. In this way, a higher rate for calibration events can be sustained. In parallel, there is the need to tag an event as good for physics, calibration, debugging etc, and stream it to the appropriate output according to a corresponding *stream tag*. The trigger part of the TDAQ system that will define the *stream tag* and the Data Collection part<sup>2</sup> has to act accordingly: build an event partially or fully, decide to which stream(s) to write it etc. So, the work on the partial event building is part of an effort to add flexible *streaming* functionality to the Data Collection system.

In addition to the work described above, a cosmic ray stand running the later TDAQ software is maintained at LNF to be ready to continue the MDT test when the installation at CERN will be completed and to test new hardware developed on-site for the MDT read-out.

## 6 Frascati Atlas Tier2

The TIER-2 of the ATLAS experiment at LNF started running on April 2004, in a very fruitful collaboration between the LNF Computing Service and the ATLAS-LNF group. The initial configuration based on 1 Storage element providing 1.2 TB of disk space, 1 Computing element and 3 Working nodes, has been running during 2005 with high efficiency. Apart from the interruption of the Computing Center activity due to a air conditioning problem, the TIER2 suffered only one major interruption in May 2005 due to the operating system upgrade, from Linux RedHat to Scientific Linux. The installation was running 97% of the time. The system has been accessed using

<sup>2</sup>The Data Collection part is responsible for the event building and the data movement between the various TDAQ components.

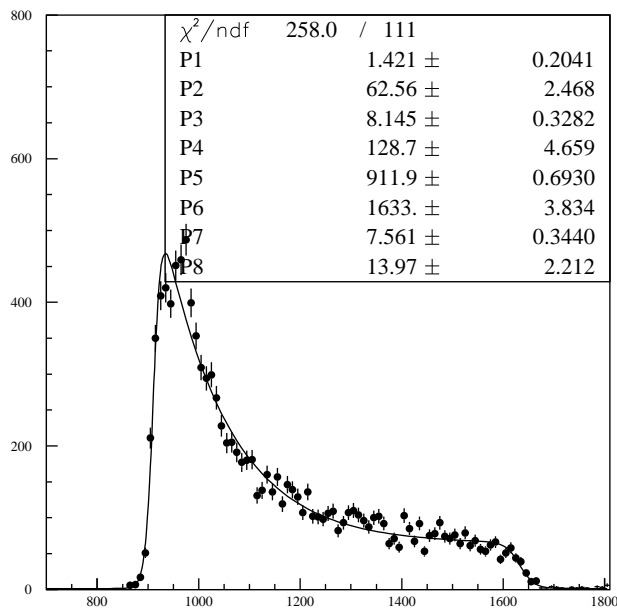


Figure 8: *Example of the Time distribution for the BML chambers in the pit for one multilayer after one hour of cosmic data taking with the Scintillator trigger.*

GRID tools by users from Atlas, dteam and gridit virtual organizations. Fig. 10 presents the use of the CPU during the first three months of 2005 when the ATLAS DataChallenge2 production was running. Fig. 11 shows the production of jobs for the Rome ATLAS physics workshop held in 2005.

Hardware upgrades were financed by INFN to increase the CPU power and the disk storage. This hardware was ordered in November 2005 and will be running in 2006.

## 7 Software and Analysis

The Frascati group is interested both in the Standard Model Physics and in the Search for New Physics, the preferred signature being the presence of high pT muons in the final states.

Because of the interest in the muon signature, the group has contributed to the construction of the muon detector and to the test beam and commissioning work and intends to contribute actively to the verification of the calibration and the reconstruction of the muons.

The physics topics which are being at present the object of the studies made can be summarized as follows:

1.  $H \rightarrow 4\mu$  (in collaboration with Cosenza);
2.  $h_0/A \rightarrow 2\mu$  (in collaboration with Roma1);
3.  $\tau \rightarrow 3\mu$ .

In addition to that, the study of  $W \rightarrow \mu\nu, Z \rightarrow \mu\mu$  and  $J/\psi \rightarrow \mu\mu$  has been started with the double purpose of:

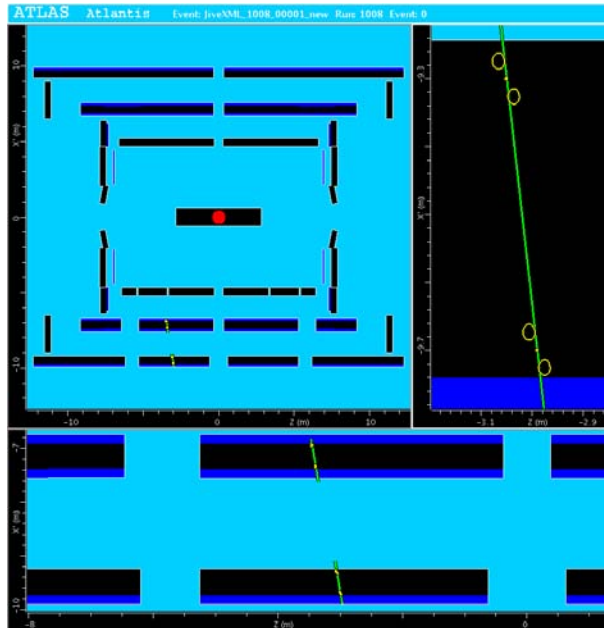


Figure 9: *Example of one cosmic track passing through a BML and BOL chamber as view by the Atlantis display.*

1. investigating the above physics processes since the initial phase of LHC;
2. using the above processes for the calibration of the detector in general and the  $\mu$  detector in particular (momentum reconstruction scale, resolution, efficiency).

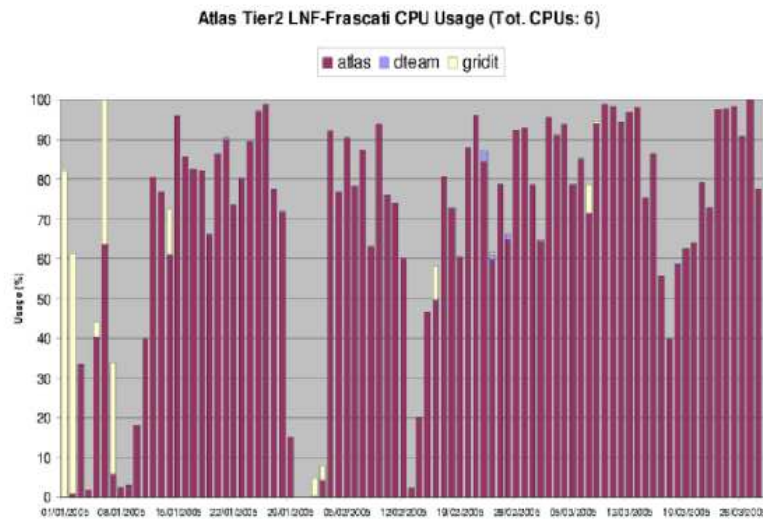


Figure 10: *The Atlas LNF TIER2 CPU usage (Ntot CPU : 6)*



## BaBar

F. Anulli, R. Baldini Ferroli, A. Calcaterra, L. Daniello(Tecn.), R. de Sangro  
G. Finocchiaro, P. Patteri, I. Peruzzi(Resp.), M. Piccolo, A. Zallo

### 1 Introduction

BaBar (in fig. 1) is the experiment running at the SLAC asymmetric  $B$ -factory PEP-II; the physics program is centered on, but not limited to, the study of the  $CP$  violation effects in the decay of neutral  $B$  mesons. The  $B$  system is the best suited to study  $CP$  violation because the expected effects are large, and appear in many final states and, most importantly, can be directly related to the Standard Model parameters. The large data sample now being collected has already allowed significant advances in a large number of topics in  $B$ , charm and tau lepton physics; all three angles of the Unitarity Triangle have been measured, direct  $CP$  violation has been established in  $B$  decays, several new  $B$  decay modes have been measured, and new charmed states have been discovered.

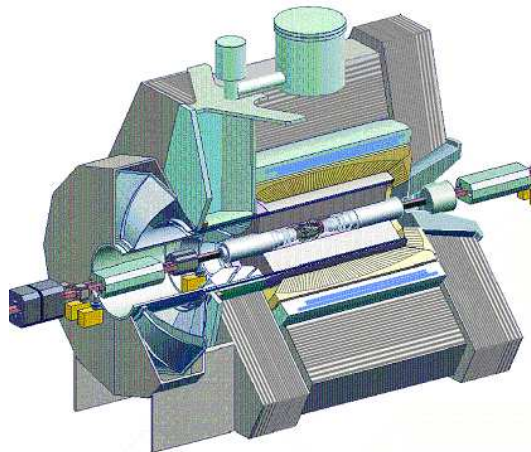


Figure 1: The BaBar Detector.

PEP-II is a two-ring  $e^+e^-$  storage ring, colliding 9 GeV electrons with 3.1 GeV positrons, energies chosen to maximize the production of  $B$  mesons. The c.m. energy corresponds to the mass of the  $\Upsilon(4S)$  resonance which decays 50% in  $B^+ B^-$ , 50% in  $B^0 \bar{B}^0$ . The energy asymmetry is necessary in order to boost the  $B$  mesons momentum, so that the decay length can be measured with the accuracy needed to prove the  $CP$  violation effects.

The BaBar Collaboration includes about 560 physicists, with contributions from about 80 Institutions in 10 countries in North America, Europe, and Asia. Approximately half of the group are physicists from U.S. Universities and Laboratories, with the largest foreign contribution coming from Italy, with 12 INFN Institutions and more than 90 people.

The BaBar detector has been designed primarily for  $CP$  studies, but it is also serving well for the other physics objectives of the experiment. The asymmetry of the beam energies is reflected in the detector design: the apparatus is centered 37 cm ahead of the collision point, along the direction of the high-energy beam, to increase forward acceptance. All services are placed on the opposite side of the detector, in order to minimize multiple scattering in the forward direction.

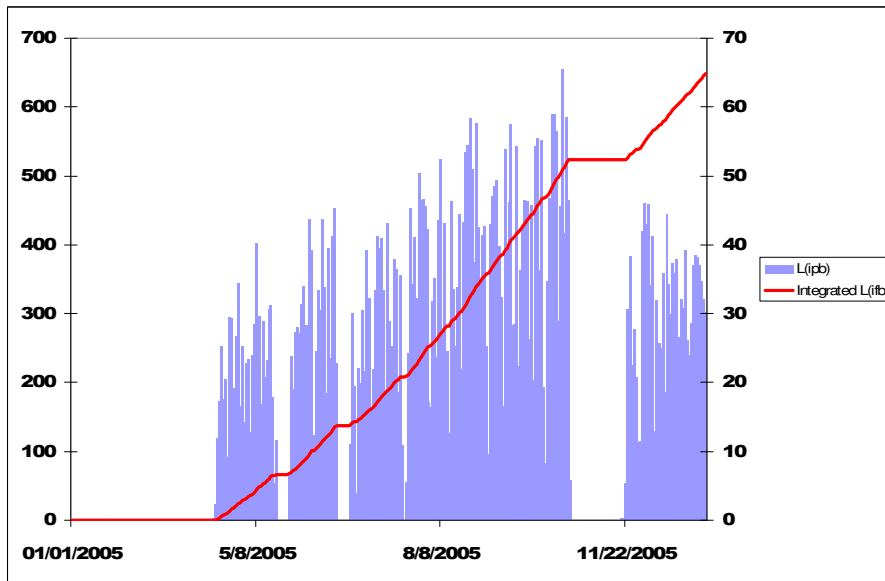


Figure 2: BaBar Luminosity in 2005.

The momentum of the charged tracks is obtained from the curvature in a solenoidal field of 1.5 T and is measured in a low mass Drift Chamber. Different species of hadrons are identified in the DIRC, a dedicated device of a novel kind, based on the detection of Čerenkov light. Excellent photon detection and electron identification is provided by a CsI crystals electromagnetic calorimeter.

Muons and neutral hadrons are identified in the iron magnet's yoke, where a total thickness of 65 cm of Fe plates has been segmented in 18 slabs of graded thickness (from 2 to 10 cm) and instrumented with Resistive Plate Counters and Limited Streamer Tubes. This system, made of a 6-sided barrel, 2 endcaps and a double cylindrical layer inside the magnet coil, is called Instrumented Flux Return, or IFR. In 2004 two barrel sextants were upgraded with addition of copper plates in six of the gaps, to increase the amount of absorber, and instrumented with LST (Limited Streamer Tubes).

The final ingredient in the  $CP$  asymmetry measurements, the distance between the two decay vertices, is measured by a state of the art vertex detector, with five layers of double sided silicon strips.

## 2 Activity

Data taking in 2005 was delayed 4 months due to a long and extremely severe safety review of all SLAC operating procedures. But finally, starting in mid-April, the machine turned up very fast and regularly, as seen in fig. 2. In October the record peak lminosity of  $10^{34} \text{ cm}^{-2}\text{sec}^{-1}$  was attained, more than 3 times the design value; and the daily integrated lumnosity were approximately  $.7fb^{-1}$ . This superb machine performance allowed a delivery of, approximately  $65fb^{-1}$  in 2005, bringing the total data sample recorded by BaBar to  $310fb^{-1}$ .

Data analysis activity by BaBar in 2005 continued regularly, covering results on  $\sin 2\beta$ ,  $\sin 2\alpha$ ,  $\sin 2\gamma$ ,  $\sin 2\beta + \gamma$ , systematic studies of many branching fractions for beauty and charmed mesons, and the most extensive systematic study up to now of low-energy meson spectroscopy in the energy

range between 1 and 4 GeV, possible at BaBar using the technique of Initial State Radiation (ISR). In 2005 BABAR was a major contributor at all HEP Conferences, for example, at the Lepton-Photon Symposium were presented 52 Journal papers, and 13 Conference papers. In the next sections the items of analysis in which the Frascati group is more directly involved are shortly described.

### 3 Measurement of $\sin 2\beta$ with partial reconstruction of $B$ mesons to the $D^{*+} D^{*-}$ decay

In 2005 this analysis has been advanced toward the final goal of publication. The main progress has been in the following areas:

- finalization of the event selection and a full review of the various part of the analysis, including tagging, vertexing etc.;
- finalization of the  $\sin 2\beta$  fitting procedure, including toy Monte Carlo validation studies of the fit;
- inclusion of the full data set collected until July 2004, corresponding to BaBar data taking runs 1 through 4;
- beginning of the study of the systematic errors;

The parameter  $\sin 2\beta$  is extracted from the  $CP$  and tag side vertices time difference  $\Delta t$  distribution of events selected using event topology and kinematic cuts.

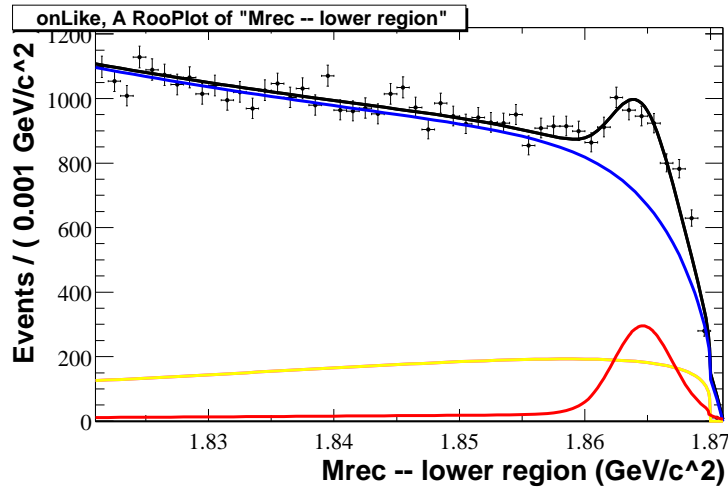


Figure 3: Missing mass for  $B \rightarrow D^{*\pm} \pi^\mp (X)$ . The curves represent the probability distribution functions (p.d.f.) for signal (red), continuum background (yellow),  $B\bar{B}$  background (blue) and their sum (black).

In fig. 3 we show the recoil mass distribution of real data from RUN 1 through 4 (solid histogram), corresponding to  $\approx 210 fb^{-1}$  of integrated luminosity. The presence of an excess of events in the signal region is evident, and a very preliminary fit to the data with a PDF (black

curve), made of a signal component (red) plus a continuum (yellow) and a  $B\bar{B}$  (blue) background component, has shown that the statistical power of this measurement is somewhat higher than that of the analysis made with the fully reconstructed sample. This is a very important result, as the two measurements of  $\sin 2\beta$  can be regarded as almost independent of each other.

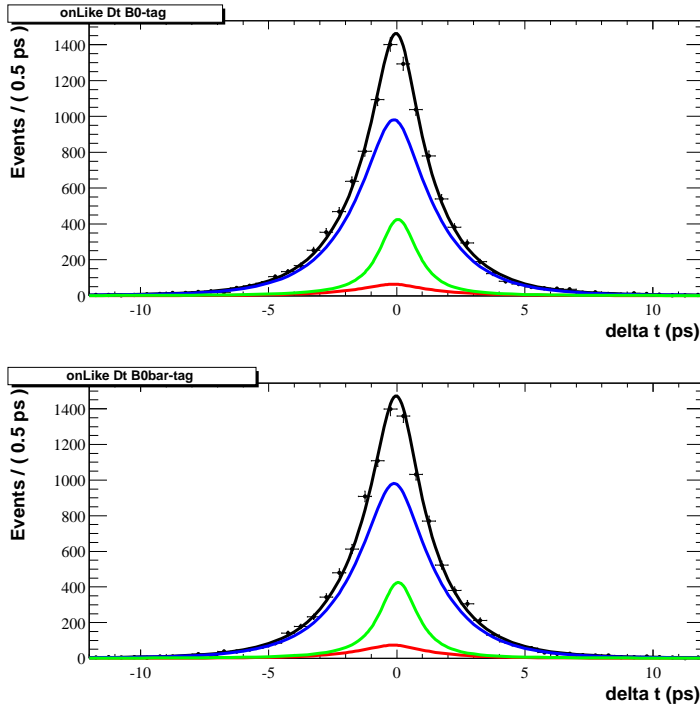


Figure 4:  $\Delta t$  fit to RUN 1-4 data. The curves represent the p.d.f.'s for signal (red), continuum background (green),  $B\bar{B}$  background (blue) and their sum (black).

We also fit the time distribution in the data, and in fig. 4 we show a fit to the time difference distribution of data events including signal and background, for the full RUN 1-4 statistics. As the study of the systematic errors is still ongoing, the analysis at this stage can not yet quote a result for the  $CP$  violating parameter  $\sin 2\beta$ .

#### 4 Measurement of $CP$ violation in mixing with partially reconstructed $B$ decays. (in collaboration with INFN-Padova and INFN-Perugia)

$CP$  violation in mixing can be measured reconstructing the time evolution of the neutral  $B$  pair produced at the  $\Upsilon(4S)$ .  $B$  flavour has to be assessed, in this kind of measurement, and, traditionally, the way to carry it out is to select events with two leptons in the final state, to study the time evolution of the various components of such sample and to extract the impurity parameter. A different way of performing this measurement would be to partially reconstruct one  $B$  with the  $D^{*-}\ell^+\nu$  decay (“Reco” side), using the lepton and the slow pion from the  $D^{*-}$  decay, and correlate the partially reconstructed  $B$  with the other  $B$  in the event, whose flavor can be tagged either by a lepton or by a kaon (“Tag” side). With respect to lepton pair technique, advantages of this method are that the background coming from charged  $B$  production is absent, as one would

positively require one  $B^0$ ; the reduced rate due to the  $B$  partial reconstruction and exclusive decay channel for the “Reco” side is somehow offset by the possibility of using Kaons as tag. At the moment, the Heavy Flavor Averaging Group reports for  $1 - \frac{q}{p}$  a value compatible with zero and an error of  $3.4 \times 10^{-3}$ . We expect with this analysis to reach a statistical error of  $\approx 2 \times 10^{-3}$ . The systematics associated to the measurement are currently under evaluation: we expect them to be lower than the statistical error. On this count, Monte Carlo studies are going on to test the behavior of Physics backgrounds and of the detector itself, as measuring asymmetries at the level of few permille is always a delicate experimental task.

## 5 Light hadron spectroscopy with initial state radiation events

Initial state radiation (ISR) events can be effectively used to measure  $e^+e^-$  annihilation at a high luminosity storage ring, such as the  $B$ -factory PEP-II. A wide mass range is accessible in a single experiment, contrary to the case of fixed energy colliders, which are optimized only in a limited energy region. In addition, the broad-band coverage may result also in greater control of systematic effects because only one experimental setup is involved.

Measurements of the main hadronic final states in the energy range between 1 and 4 GeV have been carried out at BaBar. We have been directly involved in the measurement of the cross section of the processes  $e^+e^- \rightarrow 3(\pi^+\pi^-)$ ,  $\pi^0\pi^0 2(\pi^+\pi^-)$  and  $K^+K^- 2(\pi^+\pi^-)$ , in collaboration with the Novosibirsk group.

Results for the processes with six pions in the final state are substantially in agreement with previous experiments, even if a somewhat lower cross section with respect to DM2 is observed for energies above 1.9 GeV in the channel  $e^+e^- \rightarrow \pi^0\pi^0 2(\pi^+\pi^-)$ , as shown in fig 5. A dip in the cross section distributions is seen around 1.9 GeV for both  $6\pi$  modes. A similar structure has been already observed by the DM2 and FOCUS experiments. Anyway, fitting BaBar data following the same procedure applied by the FOCUS Collaboration in order to extract the parameters of a possible resonant state at 1.9 GeV, we find that the peak position is compatible with the FOCUS result, but its width is substantially larger.

Our group is also involved, in collaboration with the Cincinnati University group, in the study of the  $KK\pi$  final states in the energy region from threshold up to the  $J/\psi$  region. Clear peaks around 1.65 GeV in the  $K^{*\pm}K^\mp$ ,  $K^{*0}K_S^0$  and  $\phi\eta$  channels are seen. These can be referred to decays of the resonance  $\phi(1680)$ , observed by the DM2 Collaboration in the  $K^*K$  channels, while the decay  $\phi(1680) \rightarrow \phi\eta$  has never been observed before. The very large statistics available at BaBar allows to disentangle the different isospin components contributing to these final states. A Dalitz plot analysis on these data is in progress and should be ready by Summer 2006.

## 6 Participation at conferences in 2005

- R. Baldini-Ferroli, “Preliminary BaBar Results on Proton Time-like Form Factors by Initial State Radiation”, presented at the *2005 International Europhysics Conference on High Energy Physics* Lisbon, Portugal, 21-27 July 2005.
- F. Anulli, “Measurement of Low Energy  $e^+e^-$  Interactions at BaBar with Initial State Radiation”, presented at the *XXIX International Conference of Theoretical Physics. Matter to the Deepest* Ustron, Poland, 8-14 September 2005.  
Proceedings published in *Acta Phys.Polon.B36*, 3389, 2005

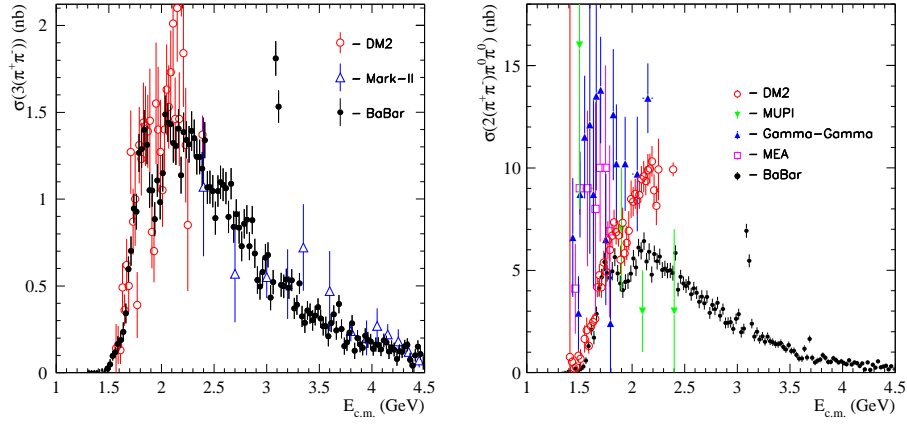


Figure 5:  $e^+e^- \rightarrow 3(\pi^+\pi^-)$  and  $e^+e^- \rightarrow \pi^0\pi^0 2(\pi^+\pi^-)$  cross section as a function of energy obtained with BaBar ISR data (black dots) in comparison with all previous  $e^+e^-$  data.

## 7 BaBar publications in 2005

- F. Anulli *et al.*, “Performance of 2nd generation BaBar Resistive Plate Chambers”, Nucl. Instr. and Meth. A552:276,2005.
- “BaBar forward endcap upgrade” Signed by the BaBar-IFR group, Nucl. Instr. and Meth. A539:155,2005.
- “Search for Radiative Penguin Decays  $B^+ \rightarrow \rho^+\gamma$ ,  $B^0 \rightarrow \rho^+\gamma$ , and  $B^0 \rightarrow \omega\gamma$ ”, Phys. Rev. Lett. 94:011801,2005.
- “Measurements of the Branching Fraction and  $CP$ -Violating Asymmetries in  $B^0 \rightarrow f_0(980)K_S^0$ ”, Phys. Rev. Lett. 94:041802,2005.
- “Search for the Decay  $B^+ \rightarrow K^+ \nu\bar{\nu}$ ”, Phys. Rev. Lett. 94:101801,2005.
- “Limit on the  $B^0 \rightarrow \rho^0\rho^0$  Branching Fraction and Implications for the Cabibbo-Kobayashi-Maskawa Angle  $\alpha$ ”, Phys. Rev. Lett. 94:131801,2005.
- “Measurements of Branching Fractions and Charge Asymmetries for Exclusive  $B$  Decays to Charmonium”, Phys. Rev. Lett. 94:141801,2005.
- “Improved Measurement of  $CP$  Asymmetries in  $B^0 \rightarrow (c\bar{c})K^{0(*)}$ ”, Phys. Rev. Lett. 94:161803,2005.
- “Search for Factorization-Suppressed  $B \rightarrow \chi_c K^{(*)}$  Decays”, Phys. Rev. Lett. 94:171801,2005.
- “Branching Fraction and  $CP$  Asymmetries in  $B^0 \rightarrow \pi^0\pi^0$ ,  $B^+ \rightarrow \pi^+\pi^0$ , and  $B^+ \rightarrow K^+\pi^0$  Decays and Isospin Analysis of the  $B \rightarrow \pi\pi$  System”, Phys. Rev. Lett. 94:181802,2005.

- “Measurements of Branching Fractions and Time-Dependent  $CP$ -Violating Asymmetries in  $B \rightarrow \eta' K$  Decays”,  
Phys. Rev. Lett. 94:191802,2005.
- “Search for Decays of  $B^0 \rightarrow e^+e^-$ ,  $B^0 \rightarrow \mu^+ \mu^-$ ,  $B^0 \rightarrow e^\pm \mu^\mp$ ”,  
Phys. Rev. Lett. 94:221803,2005.
- “Measurement of the ratio  $\mathcal{B}(B^- \rightarrow D^{*0}K^-)/\mathcal{B}(B^- \rightarrow D^{*0}\pi^-)$  and of the  $CP$  asymmetries of  $B^- \rightarrow D_{CP+}^{*0}K^-$  decays”,  
Phys. Rev. D71:031102,2005.
- “Measurement of  $B$  meson decays to  $\omega K^*$  and  $\omega\rho$ ”,  
Phys. Rev. D71:031103,2005.
- “Search for a charged partner of the  $X(3872)$  in the  $B$  meson decay  $B \rightarrow X^- K$ ,  $X^- \rightarrow J/\psi \pi^- \pi^0$ ”,  
Phys. Rev. D71:031501,2005.
- “Time-integrated and time-dependent angular analyses of  $B \rightarrow J/\psi K\pi$ : a measurement of  $\cos 2\beta$  with no sign ambiguity from strong phases”,  
Phys. Rev. D71:032005,2005.
- “ $e^+e^- \rightarrow \pi^+ \pi^- \pi^+ \pi^-$ ,  $K^+ K^- \pi^+ \pi^-$ , and  $K^+ K^- K^+ K^-$  cross sections at center-of-mass energy 0.5–4.5 GeV measured with initial-state radiation”,  
Phys. Rev. D71:052001,2005.
- “Study of the  $B^- \rightarrow J/\psi K^- \pi^+ \pi^-$  decay and measurement of the  $B^- \rightarrow X(3872)K^-$  branching fraction”,  
Phys. Rev. D71:071103,2005.
- “Search for  $CP$  violation and a measurement of the relative branching fraction in  $D^{*+} \rightarrow K^- K^+ \pi^+$  decays”,  
Phys. Rev. D71:091101,2005.
- “Measurement of  $CP$  asymmetries in  $B^0 \rightarrow \phi K^0$  and  $B^0 \rightarrow K^+ K^- K_s^0$  decays”,  
Phys. Rev. D71:091102,2005.
- “Search for  $B \rightarrow J/\psi D$  decays”,  
Phys. Rev. D71:091103,2005.
- “Measurement of the  $B^0 \rightarrow D^{*-} D_s^{*+}$  and  $D_s^+ \rightarrow \phi\pi^+$  branching fractions”,  
Phys. Rev. D71:091104,2005.
- “Evidence for the decay  $B^\pm \rightarrow K^{*\pm} \pi^0$ ”,  
Phys. Rev. D71:111101,2005.
- “Measurement of the branching fraction and the  $CP$ -violating asymmetry for the decay  $B^0 \rightarrow K_s^0 \pi^0$ ”,  
Phys. Rev. D71:111102,2005.
- “Measurement of time-dependent  $CP$ -violation asymmetries and constraints on  $\sin 2\beta + \gamma$  with partial reconstruction of  $B D^{*\mp} \pi^\pm$  decays”,  
Phys. Rev. D71:112003,2005.

- “Branching Fraction and  $CP$  Asymmetries of  $B^0 \rightarrow K_s^0 K_s^0 K_s^0$ ”,  
Phys. Rev. Lett. 95:011801,2005.
- “Search for Lepton Flavor Violation in the Decay  $\tau^\pm \rightarrow \mu^\pm \gamma$ ”,  
Phys. Rev. Lett. 95:041802,2005.
- “Search for the Rare Leptonic Decay  $B^- \rightarrow \tau^- \bar{\nu}_\tau$ ”,  
Phys. Rev. Lett. 95:041804,2005.
- “Improved Measurement of the Cabibbo-Kobayashi-Maskawa Angle  $\alpha$  Using  $B^0 (\bar{B}^0) \rightarrow \rho^+ \rho^-$   
Decays”,  
Phys. Rev. Lett. 95:041805,2005.
- “Measurement of the Branching Fraction of  $\Upsilon(4S) \rightarrow B^0 \bar{B}^0$ ”,  
Phys. Rev. Lett. 95:042001,2005.
- “Search for Strange-Pentaquark Production in  $e^+e^-$  Annihilation at  $\sqrt{s} = 10.58$  GeV”,  
Phys. Rev. Lett. 95:042002,2005.
- “Determination of  $|V_{ub}|$  from Measurements of the Electron and Neutrino Momenta in In-  
clusive Semileptonic  $B$  Decays”,  
Phys. Rev. Lett. 95:111801,2005.
- “Measurement of the Cabibbo-Kobayashi-Maskawa Angle  $\gamma$  in  $B^\mp \rightarrow D^{(*)} K^\mp$  Decays with  
a Dalitz Analysis of  $D \rightarrow K_s^0 \pi^- \pi^+$ ”,  
Phys. Rev. Lett. 95:121802,2005.
- “Measurement of Time-Dependent  $CP$  Asymmetries in  $B^0 \rightarrow D^{(*)\pm} D^\mp$  Decays”,  
Phys. Rev. Lett. 95:131802,2005.
- “Measurement of Branching Fractions and Charge Asymmetries in  $B^+$  Decays to  $\eta\pi^+$ ,  $\eta K^+$ ,  
 $\eta\rho^+$  and  $\eta/\pi^+$ , and Search for  $B^0$  Decays to  $\eta K^0$  and  $\eta\omega$ ”,  
Phys. Rev. Lett. 95:131803,2005.
- “Observation of a Broad Structure in the  $\pi^+ \pi^- J/\psi$  Mass Spectrum around 4.26 GeV/ $c^2$ ”,  
Phys. Rev. Lett. 95:142001,2005.
- “Production and Decay of  $\Xi_c^0$  at BaBar”,  
Phys. Rev. Lett. 95:142003,2005.
- “Improved Measurements of  $CP$ -violating Asymmetry Amplitudes in  $B^0 \rightarrow \pi^+ \pi^-$  Decays”,  
Phys. Rev. Lett. 95:151803,2005.
- “Measurement of Time-Dependent  $CP$  Asymmetries and the  $CP$ -Odd Fraction in the Decay  
 $B^0 \rightarrow D^{*+} D^{*-}$ ”,  
Phys. Rev. Lett. 95:151804,2005.
- “Search for Lepton-Flavor and Lepton-Number Violation in the Decay  $\tau^- \rightarrow \ell^\mp h^\pm h l^-$ ”,  
Phys. Rev. Lett. 95:191801,2005.
- “Evidence for  $B^+ \rightarrow \bar{K}^0 K^+$  and  $B^0 \rightarrow K^0 \bar{K}^0$ , and Measurement of the Branching Fraction,  
and Search for Direct  $CP$  Violation in  $B^+ \rightarrow K^0 \pi^+$ ”,  
Phys. Rev. Lett. 95:221801,2005.
- “Search for the rare decays  $B^+ \rightarrow D^{(*)} K_s^0$ ”,  
Phys. Rev. D72:011102,2005.

- “Search for the decay  $\tau^- \rightarrow 4\pi^- 3\pi^+(\pi^0)\nu_\tau$ ”,  
Phys. Rev. D72:012003,2005.
- “Measurement of double charmonium production in  $e^+e^-$  annihilations at  $\sqrt{s} = 10.6$  GeV”,  
Phys. Rev. D72:031101,2005.
- “Search for  $\rightarrow$  transitions in  $B^- \rightarrow D^0 K^-$  and  $B^- \rightarrow D^{*0} K^-$ ”,  
Phys. Rev. D72:032004,2005.
- “Measurement of the  $B^+ \rightarrow p \bar{p} K^+$  branching fraction and study of the decay dynamics”,  
Phys. Rev. D72:051101,2005.
- “Study of  $B \rightarrow \pi\ell\nu$  and  $B \rightarrow \rho\ell\nu$  decays and determination of  $|V_{ub}|$ ”,  
Phys. Rev. D72:051102,2005.
- “Measurement of the time-dependent  $CP$ -violating asymmetry in  $B^0 \rightarrow K_s^0 \pi^0 \gamma$  decays”,  
Phys. Rev. D72:051103,2005.
- “Search for the rare decay  $\bar{B}^0 \rightarrow D^{*0} \gamma$ ”,  
Phys. Rev. D72:051106,2005.
- “Amplitude analysis of the decay  $B^\pm \rightarrow \pi^\pm \pi^\mp \pi^\pm$ ”,  
Phys. Rev. D72:052002,2005.
- “Measurements of the  $B X_s \gamma$  branching fraction and photon spectrum from a sum of exclusive final states”,  
Phys. Rev. D72:052004,2005.
- “Precision measurement of the  $\Lambda_c^+$  baryon mass”,  
Phys. Rev. D72:052006,2005.
- “Dalitz plot analysis of  $D^0 \rightarrow \bar{K}^0 K^+ K^-$ ”,  
Phys. Rev. D72:052008,2005.
- “Measurement of the branching fraction and decay rate asymmetry of  $B^- \rightarrow D_{\pi^+\pi^-\pi^0} K^-$ ”,  
Phys. Rev. D72:071102,2005.
- “Measurement of  $CP$  observables for the decays  $B^\pm \rightarrow D_{CP}^0 K^{*\pm}$ ”,  
Phys. Rev. D72:071103,2005.
- “Study of  $\rightarrow c$  interference in the decay  $B^- \rightarrow [K^+\pi^-]_D K^{*-}$ ”,  
Phys. Rev. D72:071104,2005.
- “Dalitz-plot analysis of the decays  $B^\pm \rightarrow K^\pm \pi^\mp \pi^\pm$ ”,  
Phys. Rev. D72:072003,2005.
- “Measurement of the branching ratios  $\Gamma(D_s^{*+} \rightarrow D_s^{*+}\pi^0)/\Gamma(D_s^{*+} \rightarrow D_s^{*+}\gamma)$  and  $\Gamma(D^{*0} \rightarrow D^0\pi^0)/\Gamma(D^{*0} \rightarrow D^0\gamma)$ ”,  
Phys. Rev. D72:091101,2005.
- “Search for the radiative decay  $B^0 \rightarrow \phi\gamma$ ”,  
Phys. Rev. D72:091103,2005.
- “Search for the  $W$ -exchange decays  $B^0 \rightarrow D_s^{(*)-} D_s^{(*)+}$ ”,  
Phys. Rev. D72:111101,2005.

## BTeV

F. Bellucci<sup>4</sup> (Ass.), M. Bertani<sup>1</sup>, S. Bianco<sup>1</sup>, M.A. Caponero<sup>2</sup> (Ass.),  
D. Colonna<sup>3</sup> (Ass.), F.L.Fabbri<sup>1</sup> (Resp.), F. Felli<sup>3</sup> (Ass.),  
M. Giardoni<sup>1</sup>, A. La Monaca<sup>1</sup>, F. Massa<sup>3</sup> (Ass.), G. Mensitieri<sup>4</sup> (Ass.),  
B. Ortenzi<sup>1</sup> (Tecn.), M. Pallotta<sup>1</sup>, A. Paolozzi<sup>3</sup> (Ass.), L. Passamonti<sup>1</sup> (Tecn.),  
D. Pierluigi<sup>1</sup> (Tecn.), G. Saviano<sup>3</sup> (Ass.)

<sup>1</sup>*Laboratori Nazionali di Frascati*

<sup>2</sup>*Laboratori Nazionali di Frascati and ENEA Centro Ricerche, Frascati*

<sup>3</sup>*Laboratori Nazionali di Frascati and La Sapienza University, Rome*

<sup>4</sup>*Laboratori Nazionali di Frascati and Federico II University, Naples*

The BTeV experiment mission and the activity in BTeV of the Frascati group have been extensively described in the past Activity Reports. In February 2005, the US DOE cancelled the experiment because of budget cuts.

The Italian funding committee for HEP (CSN1) recognized quality and relevance of the R&D effort in progress by the Italian groups, and gave funding to close up the ongoing programs. The Frascati group finalized test beam results for the special module MOX<sup>1</sup>), completed analysis of the new tomographic method devised to assess the straw circularity<sup>2</sup>), and started a measurement campaign on the performance of the Omega-like device<sup>3</sup>), a repositioning novel concept for high-precision vertex detectors. The Omega-like device was shown to allow absolute repositioning of a movable structure with a 6 micron precision. The device was presented at the CMS collaboration for use with the pixel detector, finding good interest and feedback.

## References

1. E. Basile *et al.*, "A novel approach for an integrated straw tube - microstrip detector," arXiv:physics/0512257, IEEE Trans. Nucl. Sci. **53**, n.3, June 2006.
2. E. Basile *et al.*, "Two- and three-dimensional reconstruction and analysis of the straw tubes tomography in the BTeV experiment," arXiv:physics/0512256.
3. E. Basile *et al.*, "Micrometric position monitoring using fiber Bragg grating sensors in silicon detectors," arXiv:physics/0512255.

## CDF

A. Annovi (Art. 36), M. Cordelli (Resp.), P. Giromini,  
F. Happacher (Art. 23), I. Sfiligoi, S. Torre (Ass.)

### 1 Introduction

The TeVatron, with a  $p\bar{p}$  collision energy of 1.98 TeV in the centre of mass system, is running with a record instantaneous luminosity,  $L$ , delivered to the experiments of  $176 \times 10^{30} \text{ cm}^{-2}\text{s}^{-1}$ ; the designed high luminosity phase will have  $300 \times 10^{30} \text{ cm}^{-2}\text{s}^{-1}$  (*vs.*  $\sim 10^{31}$  of Run I). At the end of year 2005, the Tevatron has delivered to the experiments  $\sim 1600 \text{ pb}^{-1}$ ; CDF experiment has collected on tape  $\sim 1200 \text{ pb}^{-1}$  (see Figure 1); during the whole Run I we collected  $\sim 109 \text{ pb}^{-1}$ . The instantaneous luminosity is still increasing during the first months of data taking of the year 2006.

To reach high values of  $L$  it has been necessary to increase the number of  $p$  and  $\bar{p}$  bunches ( $N_b$ ); this reflects in the shortening of the time interval between two adjacent bunch crossings, thus requiring the upgrade of the CDF detector. The Run I sub-detectors that were able so to sustain this increase in luminosity without any major modification were the central calorimeters, electromagnetic and hadronic. They could work properly in the new Run after the renewal of all the front end electronics; indeed the integration time of charge signals has to be completed within the 132 ns window of the new machine clock (during Run I it was of 3.5  $\mu\text{s}$ ).

The CDF group of Frascati has built the hadronic calorimeter (the lead-scintillator based calorimeter in the central and end-wall region, CHA and WHA) and is responsible for its hardware maintenance and for its energy scale calibration.

We recall that to calibrate the calorimeter we profit of the following techniques:

- the  $^{137}\text{Cs}$  sources system determines the absolute energy scale; this procedure relies on the test beam of '83 - '85 that used  $\pi$ 's with energy greater than 10 GeV;
- in Run II we use also Minimum Ionizing Particles (Mip's) energy deposition in the hadronic calorimeter looking at muons from  $J/\Psi$ 's decays to cross-calibrate;
- the  $N_2$  laser system is often run to track the gains of the photomultipliers and it is a quick tool to check the functionality of the PM-ADMEM chain.

The group has also been involved in the calorimeter timing project, both for the hadron and electromagnetic compartments. The timing system in the hadronic calorimeters (CHA, WHA, PHA), is fully working since the beginning of year 2001. Our responsibility consisted in the design and realization of the fast discriminators VME boards, HADASD, the realization of the transition boards, TB, that connect the PM's cable signals to the backplane of the VME crates, and in the debugging and calibrations of the system. We fulfilled the boards installation and we keep calibrating the system determining the  $t_0$ 's, the dependence of the timing on the pulse-height (slewing corrections) together with the discriminators thresholds. All these calibrations taken regularly every  $\sim 10 \text{ pb}^{-1}$  go into database tables and are picked during the offline reprocessing of the data.

During year 2005 we completed the installation and commissioning of the time information in the central and plug electromagnetic calorimeters (CEM, PEM) for which the Frascati group designed and built the discriminator and transition boards. The system is working properly and it is calibrated using collision data the same way we calibrate the hadron timing system.

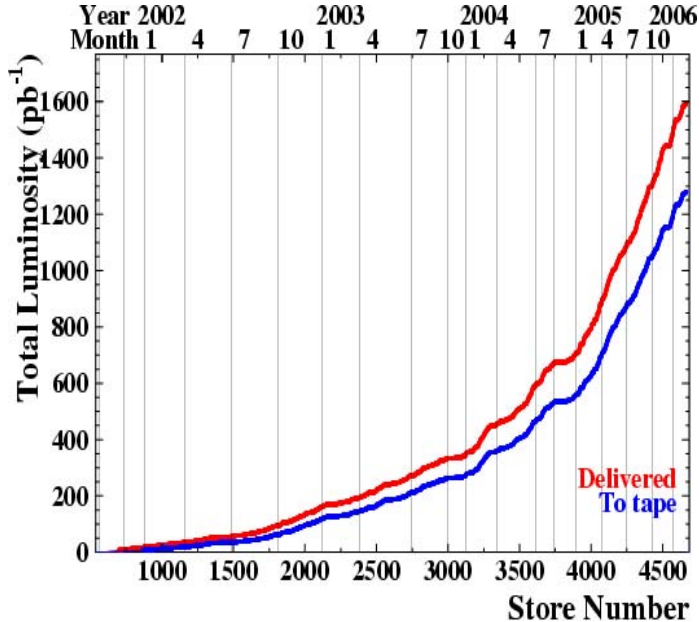


Figure 1: *Integrated Luminosity vs time*

## 2 Calibrating the central hadron calorimeter

The Frascati group plays a leading role in the calibration of the central hadron calorimeters, CHA/WHA. The procedure to monitor the energy response of the calorimeters has been well established during year 2003/2004.

For the WHA calorimeter the original Run I  $^{137}\text{Cs}$  Sources system is fully working and therefore it can be used to set the absolute energy scale for all the towers; we have taken two  $^{137}\text{Cs}$  Sources runs during April and September 2004 and we have accordingly computed two sets of Linear Energy Response:

$$LER = \frac{{}^{137}\text{Cs}(\text{test} - \text{beam})e^{-\Delta t/\tau}}{{}^{137}\text{Cs}(\text{today})}$$

that have been downloaded in the front end electronics to correct the raw ADMEM counts. This system effectively probes the behaviour of the calorimeter since the source runs in front of the inner scintillator plane of the wedges thus irradiating few of the scintillator/absorber layers of the calorimeter. In this way we monitor aging phenomena of the scintillator together with PM gain variations. Figure 2 shows the result of two different calibrations; the upper distributions are the LER calculated from the source runs taken in April and December 2005; the lower plots are the ratio of the correction factors that show the overall degradation of  $\sim 3.5\%$  (left) and the changes tower by tower (right).

We calibrate the CHA calorimeter looking at the energy deposition of Minimum Ionizing Particles (i.e. muons from  $J/\Psi$  decays).

We briefly recall the procedure to set the absolute calorimeter energy scale using Mip's. Looking at  $\mu$ 's from the  $\sim 81 \text{ pb}^{-1}$  dimuon trigger sample collected in Run Ib, we determined the necessary statistics to determine the peaks of  $\mu$ 's hadronic energy, HadE, distributions with

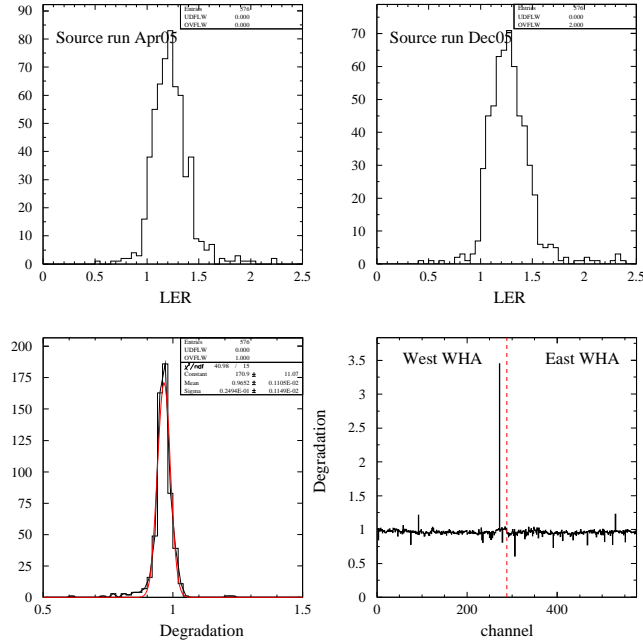


Figure 2: *WHA source calibrations. Upper plots are the LER distributions for two different source runs (Apr. - Dec. 2005); lower plots show the response degradation of the WHA calorimeter in this time interval.*

enough precision per every CHA tower. With a statistics of  $\sim 40 \text{ pb}^{-1}$  we find that the tower by tower peak is determined with a precision of  $\sim 1.5\%$ . The LER's correction factors are derived comparing tower by tower the HadE deposition for Run I and Run II mips every 30-40  $\text{pb}^{-1}$  of data; the LER at a given time  $t$  are defined as the previous set of LER ( $t-1$ ) multiplied by the observed ratio of the Mip's at a time  $t$  and in Run I:

$$LER(t) = LER^{t-1} \times \frac{MIP(\text{Run I})}{MIP(t)}$$

We look at Mip's response every  $\sim 100 \text{ pb}^{-1}$  and the typical response is shown in Figure 3 where we plot the ratio between the Run I and October-November 2005 Mip's peaks. The CHA calorimeter is pretty stable, we observe tiny 1.5% gain variations on average and few channels that drifted more than 5%.

## 2.1 $N_2$ Laser

The laser system represents a quick tool to follow the trend of the PM's gains. We have continuously acquired laser runs since year 2003 to monitor the gain variations of each photomultiplier. In Figures 4 and 5 we show the comparison of two laser runs taken in march and september 2004; we plot, per every arch and per every tower, the ratio of the mean ADC counts after fitting every tower distribution with a gaussian function. It can be seen that the CHA is stable within  $\sim 2\%$  and that the WHA moved a bit more. In Figure 6 we show the trend of the gain variations as measured with laser runs during the last two years.

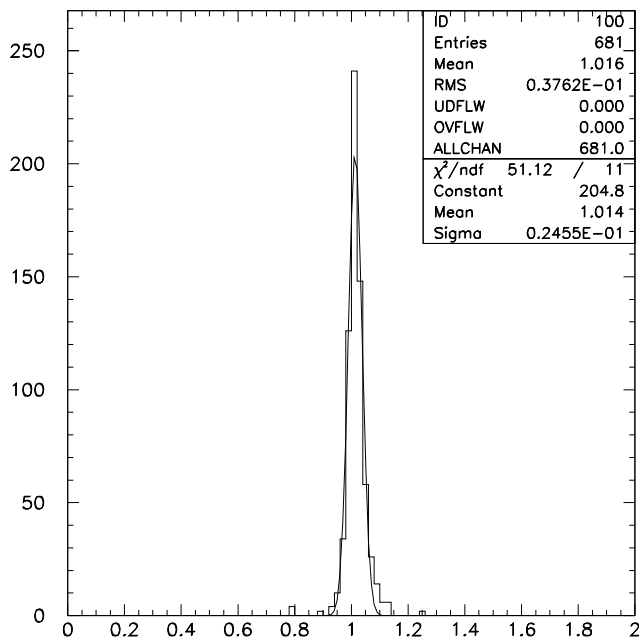


Figure 3: Tower by tower Mip's peaks ratio between Run I and October-November 2005 data.

### 3 ONLINE-OFFLINE energy scale calibration

At CDF with the current luminosity the data is being processed through the OFFLINE reconstruction every three months. Before producing the fully reconstructed events from the raw information of the detector we first produce small dedicated calibration samples to derive the calibrations constants for all the sub detectors. Every 6-8 weeks we run an executable called CalibExe which produces all the data entuples for different data sets, including the dimuon trigger data sample where we reconstruct  $J/\Psi$  events; then the various calibrators use these samples to derive the calibrations. All these procedure became automatic during the year 2005.

Usually for the Hadron calorimeters we produce two set of calibrations: ONLINE calibrations are directly downloaded in the ADMEM electronics and are intended to correct the energy response for data that have to be acquired afterwards; the OFFLINE calibrations attempts to propagate back to the data already acquired the needed corections. The calibration costants are then filled in appropriate ORACLE data base tables called CHALINERESPONSE and CHAOFFLER. To validate the OFFLINE calibrations, the same data sets are reconstructed again picking the right calibration tables for every run range they have been produed for and the calibrators have to repeat their analysis to check that the calibrations are correct.

With this procedure the calorimeter response is kept costant at  $\sim 2\%$  level over the running period.

### 4 SVT Upgrade

Since autumn 2005 the group has grown and we have been involved in the installation of the Silicon Vertex Trigger upgrade.

The Silicon Vertex Trigger (SVT) is part of the L2 trigger of CDF II. The SVT reconstructs

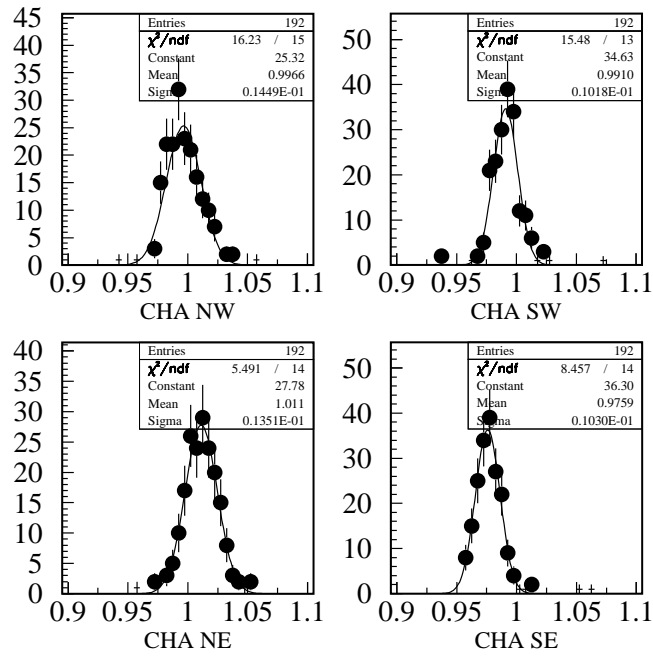


Figure 4: *Laser run. Comparison between two laser runs, for CHA arches.*

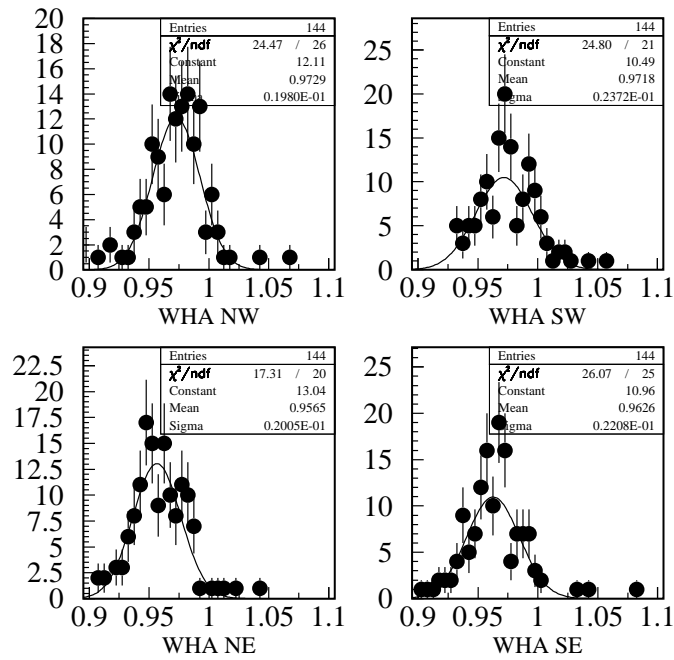


Figure 5: *Laser run. Comparison between two laser runs, for WHA arches.*

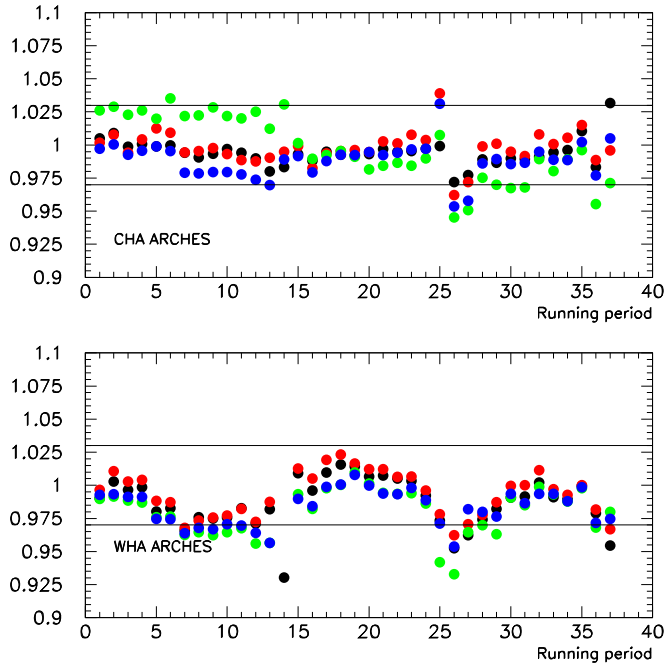


Figure 6: *Laser run. Trend of the gain scale determined using the laser during years 2003/2004.*

tracks by associating Silicon hits to Central Tracker (COT) tracks reconstructed by the L1 trigger.

The SVT required upgrade in order to perform track reconstruction within the allowed 20-40  $\mu\text{s}$ /per event at the highest expected Tevatron luminosity  $300 \times 10^{30} \text{ cm}^{-2} \text{ s}^{-1}$

In order to speed up the execution of SVT we took two actions:

- improve the resolution at the pattern recognition level. With higher resolution less track candidates are found and less fits have to be performed.
- increase the clock speed of the TrackFitter board and of other interface board. This allows for faster track fitting and faster IO speed.

The pattern recognition is performed within a custom Associative Memory (AM). In order to increase the clock speed of other boards in the system we re-implemented them with Pulsar boards.

We worked on the integration of the new boards within the existing system. This was mainly software development for the initialization of the boards, parasitic testing of the boards and development of simulation software. The other job we worked on was study on how to actually take advantage of the higher number of patterns available. We also worked to improve the monitoring of the system and its maintainability.

The system installation has been completed and the system is now fully operational.

## 5 CAF

The Frascati group is also responsible for developing and maintaining the CDF Analysis Farm (CAF) software. It has been developed as a simple-to-use graphical interface that allows the submission of jobs from any desktop to and pool, with output of the jobs written on a any disk

location worldwide. It also has extensive monitoring, both command line based and web based, plus it provides the user with a *quasi*-interactive access to the running job.

With time, the CAF software has moved from a single, dedicated farm at FNAL, to several farms around the globe, including one at INFN's CNAF. More recently it has started a migration to Grid resources, and indeed, approximately 25% of the current CDF computing power is obtained from Grid pools, the biggest being the Italian Tier1 at CNAF.

All the above has been achieved without any change to the user's habits.

Starting in 2005, Igor Sfiligoi is the responsible person for the CDF distributed computing and is presently located at FNAL. His duties encompass lying down the future path of the CAF development, supervision and contribution to the CAF development, interaction with the dedicated-CDF and Grid service providers, and coordination with the Grid entities, like EGEE in Europe and OSG in the US.

## 6 Publications 2005

1. A. Abulencia *et al.* [CDF Collaboration], "Measurement of the dipion mass spectrum in  $X(3872) \rightarrow J/\psi \pi^+ \pi^-$  decays," arXiv:hep-ex/0512074.
2. A. Abulencia *et al.* [CDF Collaboration], "Search for anomalous semileptonic decay of heavy flavor hadrons produced in association with a W boson at CDF II," arXiv:hep-ex/0512065.
3. A. Abulencia *et al.* [CDF II Collaboration], "Measurement of the inclusive jet cross section using the k(t) algorithm in p anti-p collisions at  $s^{*(1/2)} = 1.96$ -TeV," arXiv:hep-ex/0512062.
4. M. Goncharov *et al.*, "The timing system for the CDF electromagnetic calorimeters," arXiv:physics/0512171.
5. G. Apollinari *et al.*, "Phenomenological study of the atypical heavy flavor production observed at the Fermilab Tevatron," Phys. Rev. D **73**, 014025 (2006) [arXiv:hep-ex/0511053].
6. A. Abulencia *et al.* [CDF-Run II Collaboration], "Measurement of the helicity of W bosons in top-quark decays," arXiv:hep-ex/0511023.
7. A. Abulencia *et al.* [CDF Collaboration], Phys. Rev. Lett. **96**, 042003 (2006) [arXiv:hep-ex/0510065].
8. A. Abulencia *et al.* [CDF Collaboration], "A search for  $t \rightarrow \tau \nu q$  in t anti-t production," arXiv:hep-ex/0510063.
9. A. Abulencia *et al.* [CDF Collaboration], "Precision top quark mass measurement in the lepton + jets topology in p anti-p collisions at  $s^{*(1/2)} = 1.96$ -TeV," Phys. Rev. Lett. **96**, 022004 (2006) [arXiv:hep-ex/0510049].
10. A. Abulencia *et al.* [CDF Collaboration], "Top quark mass measurement using the template method in the lepton + jets channel at CDF II," arXiv:hep-ex/0510048.
11. . Bhatti *et al.*, "Determination of the jet energy scale at the Collider Detector at Fermilab," arXiv:hep-ex/0510047.
12. F. Happacher, P. Giromini and F. Ptohos, "Status of the observed and predicted b anti-b production at the Tevatron," Phys. Rev. D **73**, 014026 (2006) [arXiv:hep-ph/0509348].
13. A. Abulencia *et al.* [CDF Collaboration], "Direct search for Dirac magnetic monopoles in p anti-p collisions at  $s^{*(1/2)} = 1.96$ -TeV," arXiv:hep-ex/0509015.

14. A. Abulencia *et al.* [CDF Collaboration], “Search for neutral MSSM Higgs bosons decaying to tau pairs in p anti-p collisions at  $s^{**}(1/2) = 1.96\text{-TeV}$ ,” Phys. Rev. Lett. **96**, 011802 (2006) [arXiv:hep-ex/0508051].
15. A. Abulencia *et al.* [CDF Collaboration], “Search for  $B/s \rightarrow \mu^+ \mu^-$  and  $B/d \rightarrow \mu^+ \mu^-$  decays in p anti-p collisions with CDF II,” Phys. Rev. Lett. **95**, 221805 (2005) [Erratum-ibid. **95**, 249905 (2005)] [arXiv:hep-ex/0508036].
16. A. Abulencia *et al.* [CDF Collaboration], “Measurements of inclusive W and Z cross sections in p anti-p collisions at  $s^{**}(1/2) = 1.96\text{-TeV}$ ,” arXiv:hep-ex/0508029.
17. D. Acosta *et al.* [CDF Collaboration], “Measurement of b hadron masses in exclusive J/psi decays with the CDF detector,” arXiv:hep-ex/0508022.
18. A. Abulencia *et al.* [CDF Collaboration], “Measurement of the ratios of branching fractions  $B(B/s^0 \rightarrow D/s^- \pi^+)/B(B^0 \rightarrow D^- \pi^+)$  and  $B(B^+ \rightarrow \text{anti-}D^0 \pi^+)/B(B^0 \rightarrow D^- \pi^+)$ ,” arXiv:hep-ex/0508014.
19. A. Abulencia *et al.* [CDF Collaboration], “Search for new high mass particles decaying to lepton pairs in p anti-p collisions at  $s^{**}(1/2) = 1.96\text{-TeV}$ ,” Phys. Rev. Lett. **95**, 252001 (2005) [arXiv:hep-ex/0507104].
20. D. Acosta *et al.* [CDF Collaboration], “Search for  $\Lambda/b \rightarrow p \pi$  and  $\Lambda/b \rightarrow p K$  decays in p anti-p collisions at  $s^{**}(1/2) = 1.96\text{-TeV}$ ,” Phys. Rev. D **72**, 051104 (2005) [arXiv:hep-ex/0507067].
21. D. Acosta *et al.* [CDF Collaboration], “Search for W and Z bosons in the reaction anti-p  $p \rightarrow 2 \text{ jets} + \gamma$  at  $s^{**}(1/2) = 1.8\text{-TeV}$ ,” Phys. Rev. D **73**, 012001 (2006) [arXiv:hep-ex/0507051].
22. G. Apollinari *et al.*, “Search for narrow resonances below the Upsilon mesons,” Phys. Rev. D **72**, 092003 (2005) [arXiv:hep-ex/0507044].
23. G. Apollinari, I. Fiori, P. Giromini, F. Happacher, S. Miscetti, A. Parri and F. Ptohos, “Study of sequential semileptonic decays of b hadrons produced at the Tevatron,” Phys. Rev. D **72**, 072002 (2005) [arXiv:hep-ex/0507043].
24. D. Acosta *et al.* [CDF Collaboration], “Search for first-generation scalar leptoquarks in p anti-p collisions at  $s^{**}(1/2) = 1.96\text{-TeV}$ ,” Phys. Rev. D **72**, 051107 (2005) [arXiv:hep-ex/0506074].
25. D. Acosta *et al.* [CDF Collaboration], “A search for supersymmetric Higgs bosons in the di-tau decay mode in p anti-p collisions at  $s^{**}(1/2) = 1.8\text{-TeV}$ ,” Phys. Rev. D **72**, 072004 (2005) [arXiv:hep-ex/0506042].
26. D. Acosta *et al.* [CDF Collaboration], “Search for new physics using high mass tau pairs from 1.96-TeV p anti-p collisions,” Phys. Rev. Lett. **95**, 131801 (2005) [arXiv:hep-ex/0506034].
27. D. Acosta *et al.* [CDF Collaboration], “Measurement of the t anti-t production cross section in p anti-p collisions at  $s^{**}(1/2) = 1.96\text{-TeV}$  using lepton plus jets events with semileptonic B decays to muons,” Phys. Rev. D **72**, 032002 (2005) [arXiv:hep-ex/0506001].
28. D. Acosta *et al.* [CDF Collaboration], “Measurement of  $B(t \rightarrow W b)/B(t \rightarrow W q)$  at the Collider Detector at Fermilab,” Phys. Rev. Lett. **95**, 102002 (2005) [arXiv:hep-ex/0505091].

29. D. Acosta *et al.* [CDF Collaboration], “Evidence for the exclusive decay  $B/c^{+-} \rightarrow J/\psi \pi^{+-}$  and measurement of the mass of the  $B/c$  meson,” arXiv:hep-ex/0505076.
30. D. Acosta *et al.* [CDF Collaboration], “Study of jet shapes in inclusive jet production in p anti-p collisions at  $s^{*(1/2)} = 1.96\text{-TeV}$ ,” arXiv:hep-ex/0505013.
31. D. Acosta *et al.* [CDF Collaboration], “Measurement of the cross section for t anti-t production in p anti-p collisions using the kinematics of lepton + jets events,” Phys. Rev. D **72**, 052003 (2005) [arXiv:hep-ex/0504053].
32. D. Acosta *et al.* [CDF Collaboration], “ $K_0(S)$  and  $\Lambda_{b0}$  production studies in p anti-p collisions at  $s^{*(1/2)} = 1800\text{-GeV}$  and  $630\text{-GeV}$ ,” arXiv:hep-ex/0504048.
33. D. Acosta *et al.* [CDF Collaboration], “Measurement of the azimuthal angle distribution of leptons from W boson decays as a function of the W transverse momentum in p anti-p collisions at  $s^{*(1/2)} = 1.8\text{-TeV}$ ,” arXiv:hep-ex/0504020.
34. D. Acosta *et al.* [CDF Collaboration], “Search for Higgs bosons decaying into b anti-b and produced in association with a vector boson in proton antiproton collisions at  $s^{*(1/2)} = 1.8\text{-TeV}$ ,” Phys. Rev. Lett. **95**, 051801 (2005) [arXiv:hep-ex/0503039].
35. D. Acosta *et al.* [CDF Collaboration], “Search for long-lived doubly-charged Higgs bosons in p anti-p collisions at  $s^{*(1/2)} = 1.96\text{-TeV}$ ,” Phys. Rev. Lett. **95**, 071801 (2005) [arXiv:hep-ex/0503004].
36. D. Acosta *et al.* [CDF Collaboration], “First evidence for  $B/s_0 \rightarrow \Phi \Phi$  decay and measurements of branching ratio and  $A(\text{CP})$  for  $B^+ \rightarrow \Phi K^+$ ,” Phys. Rev. Lett. **95**, 031801 (2005) [arXiv:hep-ex/0502044].
37. D. Acosta *et al.* [CDF Collaboration], “Measurement of the moments of the hadronic invariant mass distribution in semileptonic B decays,” Phys. Rev. D **71**, 051103 (2005) [arXiv:hep-ex/0502003].
38. D. Acosta *et al.* [CDF Collaboration], “Measurement of the  $W^+ W^-$  production cross section in p anti-p collisions at  $s^{*(1/2)} = 1.96\text{-TeV}$  using dilepton events,” Phys. Rev. Lett. **94**, 211801 (2005) [arXiv:hep-ex/0501050].
39. D. Acosta *et al.* [CDF Collaboration], “Measurement of the forward-backward charge asymmetry from  $W \rightarrow e \nu$  production in p anti-p collisions at  $s^{*(1/2)} = 1.96\text{-TeV}$ ,” Phys. Rev. D **71**, 051104 (2005) [arXiv:hep-ex/0501023].
40. D. Acosta *et al.* [CDF Collaboration], “Search for Z Z and Z W production in p anti-p collisions at  $s^{*(1/2)} = 1.96\text{-TeV}$ ,” Phys. Rev. D **71**, 091105 (2005) [arXiv:hep-ex/0501021].

## KLOE

### The KLOE-LNF Collaboration

A. Antonelli, M. Antonelli, G. Bencivenni, S. Bertolucci, C. Bloise (Resp.), F. Bossi, P. Campana, G. Capon, P. Ciambrone, E. DeLucia (Art. 23), S. Dell’Agnello, P. De Simone, M. Dreucci (Art. 2222), G. Felici, M.L. Ferrer, G. Finocchiaro, C. Forti, C. Gatti (art. 36), S. Giovannella, G. Lanfranchi, J. Lee-Franzini, M. Martini (Dott.), S. Miscetti, M. Moulson, F. Murtas, M. Palutan, V. Patera (Ass.)\*, P. Santangelo, B. Sciascia (art. 23), A. Sciubba (Ass.)\*, I. Sfiligoi, T. Spadaro, G. Venanzoni

*\*Also Dipartimento di Energetica, “La Sapienza” University, Rome*

### The KLOE-LNF Technical Staff

M. Anelli, A. Balla, G. Fortugno, G. Paoluzzi, G. Papalino, R. Rosellini, M. Santoni

## 1 Overview of the activities

The KLOE Collaboration has been committed to guarantee smooth operations of the detector for data taking and to finalize the analyses mostly based on  $450 \text{ pb}^{-1}$  of integrated luminosity delivered during year 2001 and 2002.

Good detector performance and continuous operation of the computer farm have been maintained along all the year, allowing high efficiency and fine quality in data collection.

Hardware and software improvements in the offline environment are under development for the analysis of the new, five times bigger, data sample.

The LNF group made any effort to finalize data analyses, succeeding in the publication of new results relevant, among other issues, for solving the unitarity problem in the first row of the CKM matrix <sup>1, 2)</sup>, and for improving the sensitivity of the CPT test through the Bell-Steinberger relation <sup>3)</sup>.

### 1.1 KLOE data taking summary

The KLOE experiment in year 2005 has successfully completed its data taking at the  $\phi$ -peak, with a total integrated luminosity of about  $2.5 \text{ fb}^{-1}$ , as shown in fig.1. During the last data taking campaign, started in May 2004, DAΦNE delivered data with increasing performance reaching  $200 \text{ pb}^{-1}$  per month in the last three months and an overall average of  $3.5 \text{ pb}^{-1}/\text{day}$  in the whole 20-months period.

An energy scan around the  $\phi$  resonance has been accomplished by end of 2005, with  $40 \text{ pb}^{-1}$  collected for the measurement of the line shape of main final states.

Data collection will end in March 2006 after integrating a total of  $200 \text{ pb}^{-1}$  at 1 GeV for precision measurements of the hadronic cross section in the absence of the background coming at the  $\phi$ -peak from  $\phi \rightarrow \pi^+ \pi^- \pi^0$  decays.

KLOE has operated with excellent efficiency collecting more than 95% of the delivered luminosity. The efforts for ensuring good data taking conditions from both the DAΦNE and the KLOE teams have allowed the collection of a sample in steady conditions of machine background, beam energy as well as detector performance, trigger and DAQ operation, calibration quality.

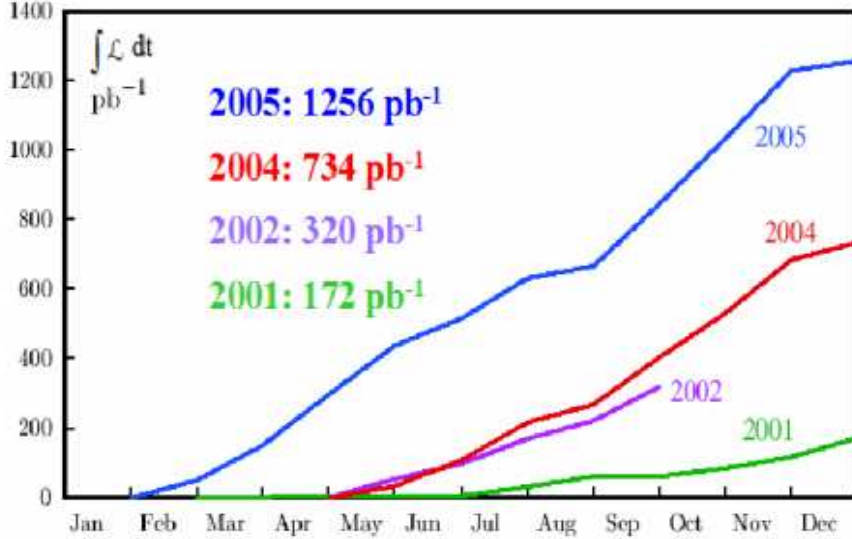


Figure 1: *Integrated luminosity per year at KLOE.*

Most sample (i.e.  $\geq 90\%$ ) has been reconstructed and archived according to the main event categories, namely neutral and charged kaons,  $\phi$  radiative decays, Bhabha's events. Data quality has been controlled, showing good time stability of basic features like the event yield for the major channels.

## 2 Results in Kaon physics

The main point of this section is that KLOE with the analysis of data obtained with a total integrated luminosity of about  $450 \text{ pb}^{-1}$  has been able to reach an accuracy of a fraction of one per cent on the measurements of the absolute kaon branching ratios and on the kaon lifetimes. The results remove a more than 30 year old problem with the unitarity of the quark mixing matrix.

Among other issues described in the following sections, for long lived neutral and charged kaons we have measured semileptonic branching ratios and lifetimes. We have isolated an almost background free sample of 13,000  $K_S \rightarrow \pi^\pm e^\mp \nu$  events, and separately measured the  $\pi^+ e^-$  and the  $\pi^- e^+$  final states. For charged kaons we have also obtained  $\text{BR}(\mu 2)$  to 0.3%.

### 2.1 The major $K_L$ decay channels

During year 2005 two results were published on  $K_L$  decays: a measurement of the main branching ratios (BR), with 0.5% accuracy on the semileptonic modes, and a measurement of the lifetime ( $\tau_{K_L}$ ) from the proper time distribution of  $K_L \rightarrow \pi^0 \pi^0 \pi^0$  decays, with 0.6% accuracy.

The measurement of the absolute  $K_L$  BR's through the tagging technique is a unique possibility of the  $\phi$ -factory. A pure sample of nearly monochromatic  $K_L$ 's is selected by the identification of  $K_S \rightarrow \pi^+ \pi^-$  decays. Events include  $K_L$ 's which decay to any possible final state in the detector volume, interact in the calorimeter or escape the detector. Starting from this sample, the  $K_L$  branching ratios are evaluated by counting the number of decays to each channel in the fiducial volume (FV) and correcting for the geometrical acceptance, the reconstruction efficiency, and the background contamination.

$K_L$  charged decays are identified by selecting a decay vertex in the FV matching the expected  $K_L$  flight direction, as defined by the tag. In order to discriminate among the different  $K_L$  charged modes the variable  $\Delta_{\mu\pi} = |p_{miss} - E_{miss}|$  is used, where  $p_{miss}$  and  $E_{miss}$  are the missing momentum

and missing energy at the  $K_L$  vertex, evaluated by assigning the pion mass to one track and the muon mass to the other (Fig. 2). Signal counting is thus achieved by fitting the  $\Delta_{\mu\pi}$  spectrum with a linear combination of four Monte Carlo shapes ( $K_L \rightarrow \pi e\nu, \pi\mu\nu, \pi^+\pi^-\pi^0, \pi^+\pi^-$ ).

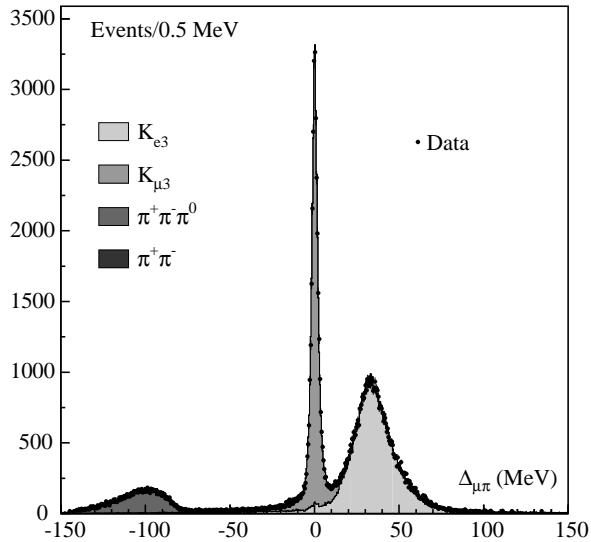


Figure 2: *Distribution of  $\Delta_{\mu\pi}$  for a data subsample, with fit to MC distributions for different decay channels.*

The shape of  $\Delta_{\mu\pi}$  spectrum is sensitive to the radiative corrections to  $K_L$  decay processes. The KLOE Monte Carlo includes very accurate generators for all of the radiative channels, which have been studied mostly in 2004 and are described in Ref. 4).

To count  $K_L \rightarrow \pi^0\pi^0\pi^0$  events decaying in the FV, we exploit the time-of-flight capability of the calorimeter to reconstruct the neutral vertex position. Such a vertex is assumed to be along the  $K_L$  line of flight. The arrival time of each photon identified in the calorimeter is thus used to give an independent determination of the path length of the  $K_L$ ,  $L_K$ . The final value of  $L_K$  is obtained from a weighted average of the different measurements coming from all of the photons.

The analysis of the  $K_L \rightarrow \pi^0\pi^0\pi^0$  sample is used not only to count events for BR measurement, but also to extract the  $K_L$  lifetime ( $\tau_{K_L}$ ) from a fit to the proper time distribution of neutral decay vertices. The KLOE environment is indeed very well suited for a direct measurement of  $\tau_{K_L}$ , because of the tagging technique which provides the value of the  $K_L$  momentum and allows to select a pure sample of  $K_L$  decays. The result is  $\tau_{K_L} = (50.92 \pm 0.17 \pm 0.25)$  ns. Control of systematic effects arising from vertex reconstruction efficiency and time scale calibration has been achieved by using the  $K_L \rightarrow \pi^+\pi^-\pi^0$  control sample.

A total of about  $13 \times 10^6$  tagged events have been analyzed for the measurement of the  $K_L$  BR's. Since the geometrical efficiency of the fiducial volume depends on the value of the  $K_L$  lifetime, fixing the sum of all of the decay modes to unity (BR's below 1% have been taken from PDG) we have removed the uncertainty on  $\tau_{K_L}$  and obtained a precise, indirect determination of the  $K_L$  lifetime itself.

Results for the main BR's are:

$$\text{BR}(K_L \rightarrow \pi e\nu) = 0.4007 \pm 0.0005_{\text{stat}} \pm 0.0004_{\text{syst-stat}} \pm 0.0014_{\text{syst}},$$

$$\begin{aligned}
\text{BR}(K_L \rightarrow \pi\mu\nu) &= 0.2698 \pm 0.0005_{\text{stat}} \pm 0.0004_{\text{syst-stat}} \pm 0.0014_{\text{syst}}, \\
\text{BR}(K_L \rightarrow \pi^0\pi^0\pi^0) &= 0.1997 \pm 0.0003_{\text{stat}} \pm 0.0004_{\text{syst-stat}} \pm 0.0019_{\text{syst}}, \\
\text{BR}(K_L \rightarrow \pi^+\pi^-\pi^0) &= 0.1263 \pm 0.0004_{\text{stat}} \pm 0.0003_{\text{syst-stat}} \pm 0.0011_{\text{syst}}.
\end{aligned}$$

The corresponding lifetime is  $\tau_{K_L} = (50.72 \pm 0.11_{\text{stat}} \pm 0.13_{\text{syst-stat}} \pm 0.33_{\text{syst}})$  ns, in agreement with the direct measurement. The two lifetime measurements are uncorrelated; their average is

$$\tau_{K_L} = (50.84 \pm 0.23) \text{ ns},$$

and has a fractional error of 0.45%. This represents an improvement of a factor of two with respect to previous measurements <sup>5)</sup>.

## 2.2 Semileptonic Form Factor slope from $K_L$ semileptonic decays

Semileptonic kaon decays,  $K_{L,S} \rightarrow \pi^\pm \ell^\mp \nu$ , offer possibly the cleanest way to obtain an accurate value of the Cabibbo angle,  $V_{\text{us}}$ . Only the vector part of the weak current has a non-vanishing matrix element between a kaon and a pion. The vector current is “almost” conserved. For a vector interaction, there are no  $SU(3)$ -breaking corrections to first order in the  $s$ - $d$  mass difference <sup>6)</sup>, making calculations of hadronic matrix elements more reliable. In the electron mode  $K_{L,S} \rightarrow \pi^\pm e^\mp \nu$ , only the vector form factor  $f_+(t)$  is involved, since extra terms in the matrix element depend on the electron mass. This form factor is usually parametrized as

$$f_+(t) = f_+(0) \left[ 1 + \lambda'_+ \frac{t}{m_{\pi^+}^2} + \frac{\lambda''_+}{2} \frac{t^2}{m_{\pi^+}^4} + \dots \right],$$

where  $f_+(0)$  is evaluated from theory and  $t$  is the lepton-pair invariant mass squared. We used about 2 million of  $K_L \rightarrow \pi e \nu$  decays from 2001-2002 data sample to measure the semileptonic form factor slopes. These have been extracted by fitting the spectrum of  $t/m_{\pi^+}^2$ . Fit procedure takes into account the efficiency of the selection cuts, the resolution effects and the background contamination as a function of  $t$ . Results from the two lepton charges have been first evaluated separately to control the reliability of the efficiency corrections. Using a linear parametrization of the form factor and combining the two charge results we obtain:

$$\lambda_+ = (28.6 \pm 0.5_{\text{stat}} \pm 0.4_{\text{syst}}) \times 10^{-3},$$

with  $\chi^2/ndf = 330/363$  ( $P(\chi^2) = 89\%$ ). The results obtained with a parametrization including the quadratic term are:

$$\lambda'_+ = (25.5 \pm 1.5_{\text{stat}} \pm 1.0_{\text{syst}}) \times 10^{-3}$$

$$\lambda''_+ = (1.4 \pm 0.7_{\text{stat}} \pm 0.4_{\text{syst}}) \times 10^{-3},$$

which gives a  $\chi^2/ndf = 325/362$  ( $P(\chi^2) = 92\%$ ).

We have also fit the data using a pole parametrization:  $f_+(t)/f_+(0) = M_V^2/(M_V^2 - t)$ . This assumes the form factor is dominated by the vector  $K-\pi$  resonances, the closest being the  $K^*(892)$ . We obtain  $M_V = (870 \pm 6_{\text{stat}} \pm 7_{\text{syst}})$  MeV ( $\chi^2/ndf = 326/363$ ), thus confirming the dominance of  $K^*$  meson, although contributions from other  $J^P = 1^-$  resonant and non-resonant  $K\pi$  scattering amplitudes are not negligible. Note that the quadratic parametrization of the form factor arises naturally as a Taylor expansion of the pole model, with the additional constraint  $\lambda''_+ = 2\lambda_+^2$ . This is nicely fulfilled by our result, which is competitive with other recent measurements <sup>8), 9)</sup> (Fig. 3). This measurement has been recently accepted for publication on PLB <sup>7)</sup>.

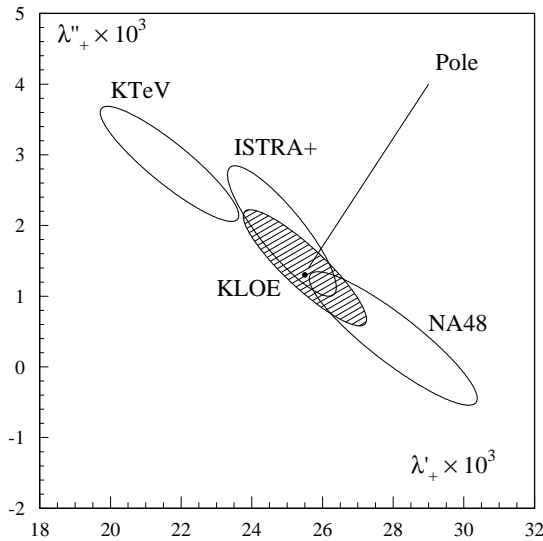


Figure 3: *KLOE* results on semileptonic form factor slopes compared with other recent measurements; the black dot represents the values of  $\lambda'_+$  and  $\lambda''_+$  obtained from the Taylor expansion of the pole parametrization.

### 2.3 The $K_S$ major decay modes

The ratio  $R_S^\pi = \Gamma(K_S \rightarrow \pi^+\pi^-(\gamma))/\Gamma(K_S \rightarrow \pi^0\pi^0)$  is a fundamental parameter of the  $K_S$  meson. It provides with almost no corrections the branching ratio (BR) for the two dominant decays of the short lived neutral kaon:  $K_S \rightarrow \pi^0\pi^0$  and  $K_S \rightarrow \pi^+\pi^-(\gamma)$ . The latter BR is a convenient normalization for the BR's of all other  $K_S$  decays to charged particles. In particular, it is used to obtain  $\text{BR}(K_S \rightarrow \pi e \nu)$  from the measurement of  $\text{BR}(K_S \rightarrow \pi e \nu)/\text{BR}(K_S \rightarrow \pi^+\pi^-(\gamma))$ , as explained in the Sec. 2.4. From  $R_S^\pi$  one can also derive phenomenological parameters of the kaon system such as the relative magnitude and phase of the  $I = 0, 2$   $\pi\pi$ -scattering amplitude<sup>10)</sup>. Finally,  $R_S^\pi$  enters into the double ratio that measures direct  $CP$  violation in  $K \rightarrow \pi\pi$  transitions. The most precise measurement of  $R_S^\pi$  was obtained from KLOE using data collected in 2000 for an integrated luminosity of  $\sim 20 \text{ pb}^{-1}$ , and has a fractional accuracy of 0.7%<sup>11)</sup>, dominated by systematic uncertainties. The present result is based on the analysis of  $410 \text{ pb}^{-1}$  of integrated luminosity acquired during the years 2001 and 2002, and improves on the total error by a factor of three, to 0.25%.

The data were divided into different samples following variations in the machine energy. The large number of events allowed us to get a statistical error at the per-mil level for each data period. Comparing the independent measurements from each data sample provides a stringent stability test (Fig. 4). The final result is obtained by averaging the results from each sample:

$$R_S^\pi = 2.2555 \pm 0.0012_{\text{stat}} \pm 0.0021_{\text{syst-stat}} \pm 0.0050_{\text{syst}},$$

where the first error is from the statistics of  $\pi^+\pi^-$  and  $\pi^0\pi^0$  events, the second is due to the statistical error in estimating all of the corrections, and the last is the systematic uncertainty.

This result is compatible with the previous published one; the two measurements can therefore be averaged, obtaining  $R_S^\pi = 2.2549 \pm 0.0054$ . Using this result, and taking into account also

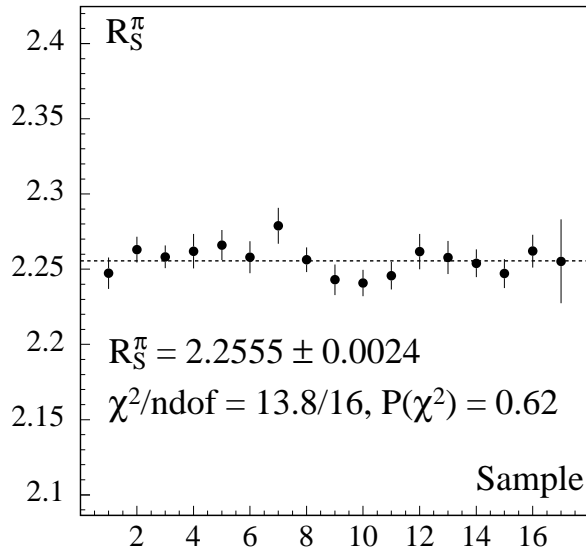


Figure 4: Measurement of  $R_S^\pi$  repeated on 17 independent subsamples, each corresponding to  $\sim 25 \text{ pb}^{-1}$ ; the error bars represent the total statistical error; the result of a fit of  $R_S^\pi$  to a constant and the associated  $\chi^2$  are also shown.

the measured  $\text{BR}(K_S \rightarrow \pi e \nu)/\text{BR}(K_S \rightarrow \pi^+ \pi^- (\gamma))$  ratio and the  $\text{BR}(K_S \rightarrow \pi \mu \nu)$  from lepton universality plus proper radiative and phase space corrections, we get:

$$\begin{aligned} \text{BR}(K_S \rightarrow \pi^+ \pi^- (\gamma)) &= (69.196 \pm 0.051) \times 10^{-2} \\ \text{BR}(K_S \rightarrow \pi^0 \pi^0) &= (30.687 \pm 0.051) \times 10^{-2}. \end{aligned} \quad (1)$$

The study of systematics has been completed, and a paper is in preparation <sup>12)</sup>.

#### 2.4 The $K_S$ semileptonic decays

At the  $\phi$  factory very large samples of tagged, monochromatic  $K_S$  mesons are available. From the analysis of 2001-2002 data sample, we were able to obtain a very pure sample of  $\sim 13\,000$   $K_S$  semileptonic decay events and thus to accurately measure for the first time the partial decay rates for transitions to each charged final state,  $\text{BR}(K_S \rightarrow e^+ \pi^- \nu)$  and  $\text{BR}(K_S \rightarrow e^- \pi^+ \bar{\nu})$ , as well as the charge asymmetry  $A_S$ :

$$A_S = \frac{\Gamma(K_S \rightarrow \pi^- e^+ \nu) - \Gamma(K_S \rightarrow \pi^+ e^- \bar{\nu})}{\Gamma(K_S \rightarrow \pi^- e^+ \nu) + \Gamma(K_S \rightarrow \pi^+ e^- \bar{\nu})}. \quad (2)$$

The comparison of  $A_S$  with the corresponding asymmetry  $A_L$  for  $K_L$  decays allows precision tests of the  $CP$  and  $CPT$  symmetries. If  $CPT$  symmetry is assumed, both  $K_S$  and  $K_L$  charge asymmetries are expected to be equal to  $2 \text{Re} \epsilon \simeq 3 \times 10^{-3}$ . The difference between the charge asymmetries,

$$A_S - A_L = 4 (\text{Re} \delta + \text{Re} x_-), \quad (3)$$

signals  $CPT$  violation either in the mass matrix ( $\delta$  term), or in the decay amplitudes with  $\Delta S \neq \Delta Q$  ( $x_-$  term). The sum of the asymmetries,

$$A_S + A_L = 4 (\text{Re} \epsilon - \text{Re} y), \quad (4)$$

is related to  $CP$  violation in the mass matrix ( $\epsilon$  term) and to  $CPT$  violation in the decay amplitude ( $y$  term).

The knowledge of both the  $K_L$  and the  $K_S$  semileptonic decay branching ratios and lifetimes allows the validity of the  $\Delta S = \Delta Q$  rule to be tested through the quantity

$$\text{Re } x_+ = \frac{1}{2} \frac{\Gamma(K_S \rightarrow \pi e \nu) - \Gamma(K_L \rightarrow \pi e \nu)}{\Gamma(K_S \rightarrow \pi e \nu) + \Gamma(K_L \rightarrow \pi e \nu)}. \quad (5)$$

In the SM,  $\text{Re } x_+$  is of the order of  $G_F m_\pi^2 \sim 10^{-7}$ , being due to second order weak transitions.

Finally, from the semileptonic decays of  $K_S$  a competitive measurement of  $V_{us}$  can be extracted, which also profits of a very precise knowledge of the  $K_S$  lifetime<sup>14</sup>).

The first measurement of  $\text{BR}(K_S \rightarrow \pi e \nu)$  was obtained from KLOE using data collected in year 2000, with a fractional accuracy of 5.4%<sup>13</sup>). The present BR measurement improves on the total error by a factor of four, to 1.3%. The  $K_S$  charge asymmetry has never been measured before.

Event counting is performed by fitting the  $E_{\text{miss}} - p_{\text{miss}}$  ( $\Delta E_{\pi e}$ ) spectrum with a combination of MC shapes for signal and background (Fig. 5). For each charge state we obtain the ratio

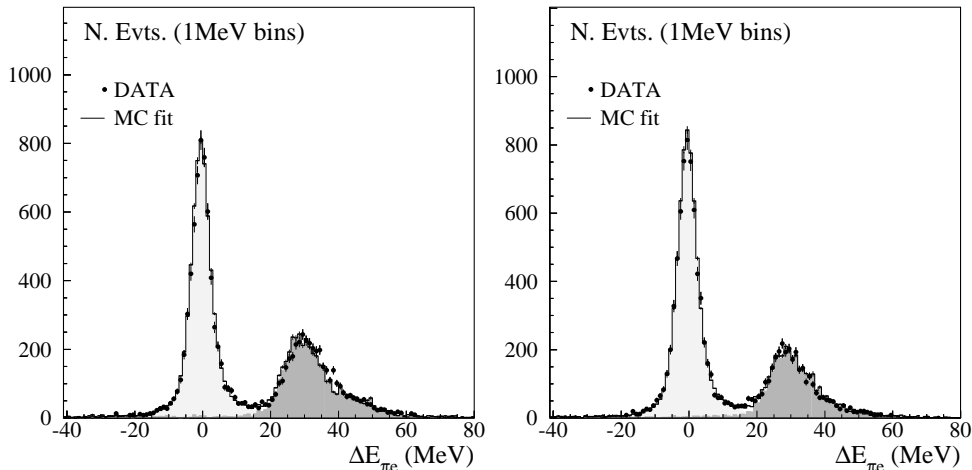


Figure 5:  $E_{\text{miss}} - p_{\text{miss}}$  spectrum for events selected as  $\pi^- e^+ \nu$  (left panel) and  $\pi^+ e^- \bar{\nu}$  (right panel); filled dots represent data from the entire data set; solid line is the result of a fit varying the normalization of MC distributions for signal (light gray) and background (dark gray), which are also shown.

$\text{BR}(K_S \rightarrow \pi^\mp e^\pm \nu(\bar{\nu})) / \text{BR}(K_S \rightarrow \pi^+ \pi^- (\gamma))$  by normalizing the number of signal events to the number of  $K_S \rightarrow \pi^+ \pi^- (\gamma)$  events and correcting for the overall selection efficiencies. In order to evaluate the absolute BR's for the semileptonic modes, we combine the measured ratios with the ratio  $R_S^\pi$  of the dominant  $K_S$  decays measured at KLOE as presented in Sec. 2.3. We obtain the following results:

$$\begin{aligned} \text{BR}(K_S \rightarrow \pi^- e^+ \nu) &= (3.528 \pm 0.062) \times 10^{-4} \\ \text{BR}(K_S \rightarrow \pi^+ e^- \bar{\nu}) &= (3.517 \pm 0.058) \times 10^{-4} \\ \text{BR}(K_S \rightarrow \pi e \nu) &= (7.046 \pm 0.091) \times 10^{-4}. \end{aligned} \quad (6)$$

The charge asymmetry of Eq. (2) is:

$$A_S = (1.5 \pm 9.6_{\text{stat}} \pm 2.9_{\text{syst}}) \times 10^{-3}.$$

From the total BR we test the validity of the  $\Delta S = \Delta Q$  rule in  $CPT$ -conserving transitions (Eq. 5). In the evaluation of  $\Gamma$ 's we used  $\tau_S = 0.08958(6)$  ns from the PDG <sup>14)</sup> and the KLOE results for  $\tau_L$  and  $\text{BR}(K_L \rightarrow \pi e \nu)$  reported in Sec. 2.1. The value of  $\text{Re } x_+$  is:

$$\text{Re } x_+ = (-0.5 \pm 3.6) \times 10^{-3}.$$

The error on this value represents an improvement by almost a factor of two with respect to the most precise previous measurement, from the CPLEAR experiment <sup>15)</sup>.

From the sum and difference of the  $K_L$  and  $K_S$  charge asymmetries one can test for possible violations of the  $CPT$  symmetry, either in the decay amplitudes or in the mass matrix (Eqs. 3 and 4). Using  $A_L = (3.34 \pm 0.07) \times 10^{-3}$  <sup>14)</sup>, and  $\text{Re } \delta = (3.0 \pm 3.3_{\text{stat}} \pm 0.3_{\text{syst}}) \times 10^{-4}$  from CPLEAR <sup>16)</sup>, we obtain from Eq. 3

$$\text{Re } x_- = (-0.8 \pm 2.5) \times 10^{-3}.$$

This result improves by a factor of ten the previous best result from CPLEAR <sup>16)</sup>.

Using  $\text{Re } \epsilon = (1.62 \pm 0.04) \times 10^{-3}$  <sup>14)</sup>, from Eq. 4 we obtain

$$\text{Re } y = (0.4 \pm 2.5) \times 10^{-3},$$

which has precision comparable to that ( $3 \times 10^{-3}$ ) obtained from the unitarity relation by CPLEAR <sup>17)</sup>.

Finally, we measured the form factor slope by fitting the ratio of data and MC distribution in  $t/m_{\pi^+}^2$ . The linear slope of the semileptonic  $K_S$  form factor is :

$$\lambda_+ = (33.9 \pm 4.1) \times 10^{-3}$$

with  $\chi^2/\text{dof} = 12.9/11$ , corresponding to a probability  $P(\chi^2) \simeq 30\%$ . This result is in agreement with the corresponding value for the linear slope of the semileptonic  $K_L$  form-factor.

This analysis has been completed, and all of the results are described in a dedicated paper <sup>18)</sup>.

## 2.5 Extraction of $V_{us}$

The CKM matrix element  $V_{us}$  can be extracted from the measurement of the semileptonic decay widths ( $\Gamma = \text{BR}/\tau$ ) and the most precise test of unitarity of the CKM matrix is performed from the first-row constraint:  $1 - \Delta = |V_{ud}|^2 + |V_{us}|^2 + |V_{ub}|^2$ . Using  $V_{ud}$  from nuclear beta decays, a test of the expectation  $\Delta = 0$  with a precision of one part per mil can be achieved,  $V_{ub}$  contributing only at the level of  $10^{-5}$ . Such a test has been performed by using both KLOE results on  $K_L$  semileptonic decays and  $\tau_{K_L}$  (Sec. 2.1), and the measurement of  $\text{BR}(K_S \rightarrow \pi e \nu)$  (Sec. 2.4) with  $\tau_{K_S}$  from Ref. <sup>14)</sup>.

$V_{us}$  is proportional to the square root of the partial width of semileptonic kaon decays and can be parametrized for neutral kaon decays as <sup>19)</sup> :

$$V_{us} \times f_+^{K^0 \pi^-}(0) = \left[ \frac{128 \pi^3 \Gamma}{G_\mu^2 M_K^5 S_{\text{ew}} I(\lambda'_+, \lambda''_+, \lambda_0, 0)} \right]^{1/2} \frac{1}{1 + \delta_{\text{em}}}, \quad (7)$$

where  $f_+^{K^0 \pi^-}(0)$  is the vector form factor at zero momentum transfer and  $I(\lambda'_+, \lambda''_+, \lambda_0, 0)$  is the result of the phase space integration after factorizing out  $f_+^{K^0 \pi^-}(0)$ . In the above expression, long-distance radiative corrections for both the form factor  $f_+^{K^0 \pi^-}$  and the phase space integral have been factorized out and are included in the parameter  $\delta_{\text{em}}$ , which amounts to  $5 - 8 \times 10^{-3}$  for

$K_{e3}$  and  $K_{\mu3}$  respectively <sup>20), 21)</sup>. The short-distance electroweak corrections are included in the parameter  $S_{\text{ew}} = 1.0232$  <sup>22)</sup>.  $\lambda'_+$  and  $\lambda''_+$  are the quadratic slopes of the vector form factor, and  $\lambda_0$  is the slope of the scalar form factor. Using the values  $\lambda'_+ = 0.0221 \pm 0.0011$ ,  $\lambda''_+ = 0.0023 \pm 0.0004$  and  $\lambda_0 = 0.0154 \pm 0.0008$  averaged from recent measurements by KTeV <sup>8)</sup> and ISTRA+ <sup>9)</sup> on  $K_L \rightarrow \pi^\pm e^\mp \bar{\nu}(\nu)$ ,  $\pi^\pm \mu^\mp \bar{\nu}(\nu)$  and  $K^+ \rightarrow \pi^0 e^+ \nu$  decays respectively, we obtain (Fig. 6):

$$\begin{aligned} f_+^{K^0 \pi^-}(0) \times V_{\text{us}} &= 0.2162 \pm 0.0014 \text{ from } K_S \rightarrow \pi e \nu, \\ f_+^{K^0 \pi^-}(0) \times V_{\text{us}} &= 0.21638 \pm 0.00067 \text{ from } K_L \rightarrow \pi e \nu, \\ f_+^{K^0 \pi^-}(0) \times V_{\text{us}} &= 0.21732 \pm 0.00087 \text{ from } K_L \rightarrow \pi \mu \nu. \end{aligned}$$

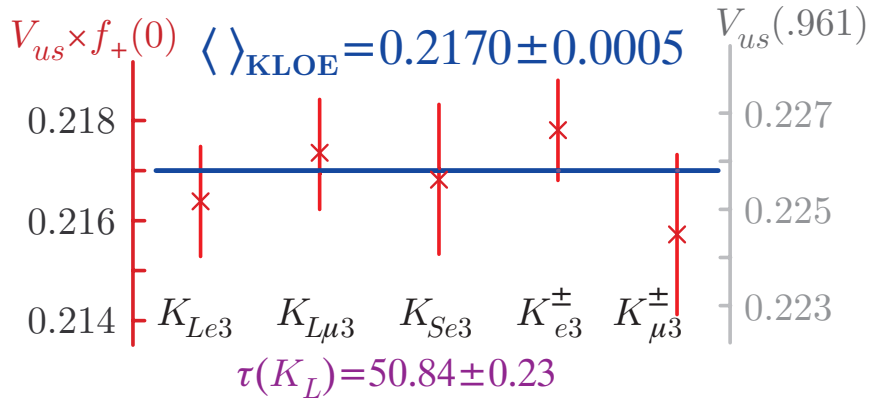


Figure 6: *KLOE* measurements of  $f_+^{K^0 \pi^-}(0) \times V_{\text{us}}$  for  $K_L$ ,  $K_S$  and charged kaon semileptonic modes.

Using  $V_{\text{ud}} = 0.9740 \pm 0.0005$  from Ref. <sup>23)</sup> and  $f_+^{K^0 \pi^-}(0) = 0.961 \pm 0.008$  from Ref. <sup>24)</sup>, also in agreement with a recent lattice calculation, <sup>25)</sup> the unitarity band is:

$$f_+^{K^0 \pi^-}(0) \times V_{\text{us}} = 0.2177 \pm 0.0028$$

in agreement with our results.

## 2.6 Measurement of $\text{BR}(K_L \rightarrow \pi^+ \pi^-)$

A measurement of the absolute BR for this decay is aimed at shedding light on the unclear experimental status: the result quoted by PDG <sup>14)</sup> differs by 6% (*i.e.* shows a  $4 - \sigma$  discrepancy) with respect to a recent 0.6% precise measurement from KTeV experiment. <sup>26)</sup> The analysis on 2001-2002 data sample has been recently finalized (Fig. 7), yielding a 1.1% precise measurement of the decay:

$$\text{BR}(K_L \rightarrow \pi^+ \pi^-) = (1.963 \pm 0.012_{\text{stat}} \pm 0.018_{\text{syst}}) \times 10^{-3},$$

that confirms the KTeV result. A paper is in preparation.

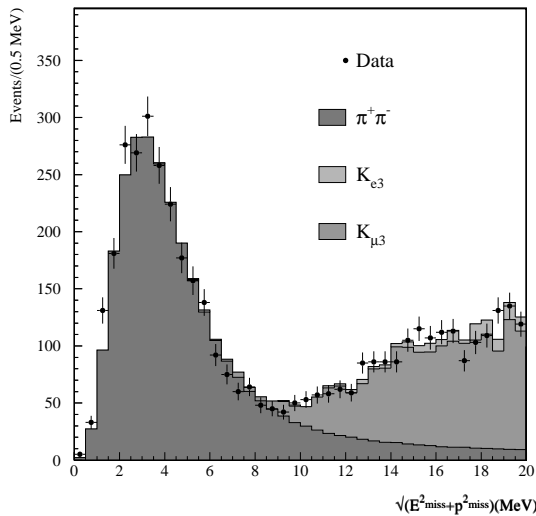


Figure 7: Spectrum of  $\sqrt{E_{miss}^2 + p_{miss}^2}$  for 2001-2002 data sample, with fit to MC distributions of  $K_L \rightarrow \pi^+\pi^-$  signal and background.

## 2.7 Direct search for the $K_S \rightarrow \pi^0\pi^0\pi^0$ decay

Observation of the decay  $K_S \rightarrow \pi^0\pi^0\pi^0$  signals  $\mathcal{CP}$  violation in kaon mixing and/or decay. The parameter  $\eta_{000}$ , defined as the ratio of  $K_S$  to  $K_L$  decay amplitudes, can be written as:  $\eta_{000} = A(K_S \rightarrow \pi^0\pi^0\pi^0)/A(K_L \rightarrow \pi^0\pi^0\pi^0) = \varepsilon + \varepsilon'_{000}$ , where  $\varepsilon$  quantifies the  $K_S$   $\mathcal{CP}$ -impurity and  $\varepsilon'_{000}$  is due to a direct  $\mathcal{CP}$ -violating term. The Standard Model (SM) prediction for this decay is  $\text{BR}(K_S \rightarrow \pi^0\pi^0\pi^0) \sim 1.9 \times 10^{-9}$  to an accuracy of a few %.

The best upper limit on  $\text{BR}(K_S \rightarrow \pi^0\pi^0\pi^0)$  from a direct search of the decay was obtained by the SND experiment at Novosibirsk. They found  $\text{BR}(K_S \rightarrow \pi^0\pi^0\pi^0) < 1.4 \times 10^{-5}$  with 90% confidence level (CL) <sup>27)</sup>. The NA48 collaboration recently reached a much higher sensitivity searching for the interference between  $K_S$  and  $K_L$  at small decay times. They find  $\text{BR}(K_S \rightarrow \pi^0\pi^0\pi^0) < 7.4 \times 10^{-7}$  at 90% CL <sup>28)</sup>. Apart from the interest in confirming the SM prediction, the knowledge of  $\eta_{000}$  allows to test the validity of  $CPT$  invariance using unitarity <sup>17)</sup>.

With the 2001-2002 data sample, we were able to reach a sensitivity at the  $\sim 10^{-7}$  level. At the end of the selection chain, we count 2 events for an expected background  $N_b = 3.13 \pm 0.82_{stat} \pm 0.37_{syst}$  and a total efficiency on signal events  $\varepsilon_{3\pi} = (24.36 \pm 0.11_{stat} \pm 0.57_{syst})\%$ . Folding the proper background uncertainty, we quote the number of  $K_S \rightarrow \pi^0\pi^0\pi^0$  decays to be below 3.45 at 90% CL. In the same sample we count  $37.8 \times 10^6$   $K_S \rightarrow \pi^0\pi^0$  events which are used for normalization, deriving:

$$\text{BR}(K_S \rightarrow \pi^0\pi^0\pi^0) \leq 1.2 \times 10^{-7} \text{ at } 90\% \text{ CL.}$$

This result improves by a factor of  $\sim 6$  the best previous limit, and has been published in year 2005 <sup>3)</sup>. We are presently analysing the sample acquired during years 2004 and 2005, aiming at a factor of ten improvement in our sensitivity.

## 2.8 Charged kaon analyses

For charged kaon decays, the measurement of the branching ratio of the  $K^+ \rightarrow \mu^+\nu$  decay has been completed in 2005 and published in January 2006<sup>29)</sup>. A preliminary measurement of the branching ratios of the semileptonic decays has been obtained during 2005 and presented at summer conferences. The status of the  $K^\pm$  lifetime analysis is well advanced.

Besides these analyses more technical activities related to the Monte Carlo simulation have been carried out, namely the digitization of the charge-signal from the ADC boards and the simulation of the observed spurious hits along the  $K^\pm$  tracks.

## 2.9 The $K^+ \rightarrow \mu^+\nu(\gamma)$ decays

As pointed out in Ref. 30), besides the traditional method of extracting  $|V_{us}|$  from  $K_{\ell 3}$  decays, one can obtain an independent and competitive estimate of  $|V_{us}|$  (or, to be more precise, of  $|V_{us}/V_{ud}|$ ) from the ratio of the inclusive decay widths of  $K^+ \rightarrow \mu^+\nu(\gamma)$  and  $\pi^+ \rightarrow \mu^+\nu(\gamma)$  decays. We have measured the fully inclusive  $K^+ \rightarrow \mu^+\nu(\gamma)$  absolute branching ratio using about  $175 \text{ pb}^{-1}$  of the total integrated luminosity in year 2002. The  $\phi$ -meson decays into quasi anti-collinear  $K^\pm$  pairs: the detection of a  $K^\pm$  tags the presence of a  $K^\mp$  of given momentum and direction. The decay chains of the  $K^\pm$  pair define two spatially well separated regions called the tag and the signal hemispheres. Identified  $K^\mp$  decays tag a  $K^\pm$  beam and provide an absolute BR. The branching ratio measurement is based on  $K^- \rightarrow \mu^-\nu$  decays for event tagging and on the search for the signal among all the  $K^+$  decays<sup>29)</sup>. The tagging selection is based on the presence of one two-tracks vertex in the DC which signals the  $K^-$  decay. The number of  $K^+ \rightarrow \mu^+\nu(\gamma)$  decays is obtained counting the events in the signal region of the distribution of the charged decay particle momentum computed in the kaon rest frame  $p^*$  assuming pion mass. The background is given by events with a  $\pi^0$  in the final state and its contribution to the  $p^*$  distribution is obtained directly from data. The efficiency of the analysis cuts has been determined directly on data using a control sample of  $K \rightarrow \mu\nu(\gamma)$  events selected exploiting their typical signature in the EMC. From some 865,283  $K^+ \rightarrow \mu^+\nu(\gamma)$  decays obtained from a sample of  $\sim 5.2 \times 10^8$   $\phi$ -meson decays, we find:

$$\text{BR}(K^+ \rightarrow \mu^+\nu_\mu(\gamma)) = 0.6366 \pm 0.0009_{\text{stat.}} \pm 0.0015_{\text{syst.}}$$

corresponding to an overall fractional error of 0.27%. The statistical error due to the event count is  $6 \times 10^{-4}$  and becomes  $9 \times 10^{-4}$  including the statistics of MC simulation and data used for the efficiency evaluation. Using the results of lattice QCD calculations of the ratio of the decay constants of pseudoscalar mesons  $f_K/f_\pi$ <sup>31)</sup>, we can obtain the CKM mixing matrix element  $|V_{us}| = 0.2223 \pm 0.0026$ . The preliminary result for the branching ratio, obtained at the beginning of 2005, has been presented at the CKM 2005 Workshop<sup>32)</sup>.

## 2.10 The $K^\pm$ semileptonic decays

The measurement of the branching ratios for the  $K^\pm$  semileptonic decays is based on four independent samples tagged by the following kaon decays:  $K_{\mu 2}^+$ ,  $K_{\pi 2}^+$ ,  $K_{\mu 2}^-$ , and  $K_{\pi 2}^-$ . Using 410  $\text{pb}^{-1}$  of total integrated luminosity of 2001 and 2002 data, about 60 million tag decays have been identified and divided into the four tag samples. To select a semileptonic decay on the signal side we ask for a decay vertex in the drift chamber and the charged decay particle track has to reach the calorimeter and to be associated to an energy deposit. Two-body decays are rejected applying a cut on the charged decay particle momentum computed in the kaon rest frame assuming pion mass. The lepton mass,  $m_{lept}^2$  is determined from the velocity of the lepton computed from time of flight. The

number of  $K_{e3}$  and  $K_{\mu3}$  decays is then obtained by fitting the  $m_{lept}^2$  distribution to a sum of MC distributions for the signals and proper background sources. The BR is separately evaluated for each tag sample, dividing by the number of tag counts and correcting for acceptances. The latter are obtained from MC simulations. Corrections are applied to account for data-MC differences in tracking and clustering. About 190 000  $K_{e3}^\pm$  and 100 000  $K_{\mu3}^\pm$  decays are selected. The resulting BR's are:

$$\text{BR}(K_{e3}^\pm) = 0.05047 \pm 0.00046_{\text{stat.}+\text{tag.}} \pm 0.00080_{\text{syst.}}$$

$$\text{BR}(K_{\mu3}^\pm) = 0.03310 \pm 0.00040_{\text{stat.}+\text{tag.}} \pm 0.00070_{\text{syst.}}$$

These have been obtained, for each channel, averaging over the four different tag samples carefully accounting for correlations. The error is dominated by the uncertainty on data/MC efficiency corrections. The evaluation of systematics coming from signal selection efficiency is still preliminary. These measurements have been presented at HEP 2005.

### 2.11 The $K^\pm$ lifetime

The  $K^\pm$  lifetime,  $\tau_\pm$ , is an experimental input to the determination of  $V_{us}$ . The present fractional uncertainty is about 0.2%, corresponding to 0.1% for  $V_{us}$ . However, data used so far by PDG show large discrepancies between “in-flight” and “at-rest” measurements. Moreover, the value of  $\tau_\pm$  affects, through the evaluation of the geometrical acceptance, also the BR measurements. Two different methods have been developed: one based on the measurement of the decay length, using charged decay vertices reconstructed in the drift chamber, and the other based on the decay time of the kaons. Both methods allow to reach accuracies at the few per mil level and their independency allows to assess part of the systematic uncertainty. The signal events are tagged by  $K_{\mu2}^-$  decays. In order to fit the proper time distribution of the charged kaon and measure the lifetime, we need to correct for the reconstruction efficiency of the decay vertex and to account for resolution effects. These efficiency and resolution functions are measured directly on data, using a control sample selected with calorimetric information only, and corrections have been applied to account for data-MC differences in tracking resolution. About 230  $\text{pb}^{-1}$  of data collected during 2002 are used:  $\sim 150 \text{ pb}^{-1}$  for the proper time distribution and  $\sim 80 \text{ pb}^{-1}$  for the efficiency evaluation.

## 3 Results in hadron physics

The program on the light scalars includes the measurements of the decay rates of  $f_0$ ,  $a_0$ , giving information on the structure of the giving information on the structure of the isoscalar and isovector states.

At present, KLOE is also the experiment with the highest statistics of  $\eta$  and  $\eta'$  decays, which are relevant to determine the free parameters and to test the predictions of  $\chi$ PT. Several decay modes are currently under study, including the  $\eta$  hadronic decays,  $\eta \rightarrow \pi\pi\pi$ .

Preliminary results recently presented to conferences are reported in the following sections.

### 3.1 $\eta$ mass measurement

The recent measurement of the  $\eta$  mass performed by the GEM collaboration <sup>33)</sup> provides a value about 500 keV below the previous NA48 measurement <sup>34)</sup>, both having an error of tens of keV. For this reason KLOE is performing a new measurement of the  $\eta$  mass, studying the decay  $\phi \rightarrow \eta\gamma$ , with  $\eta \rightarrow \gamma\gamma$ . To improve the energy response of the calorimeter a kinematic fit is performed, imposing energy-momentum conservation. A cut in the Dalitz plot of the  $3\gamma$ 's final state (Fig. 8.left),

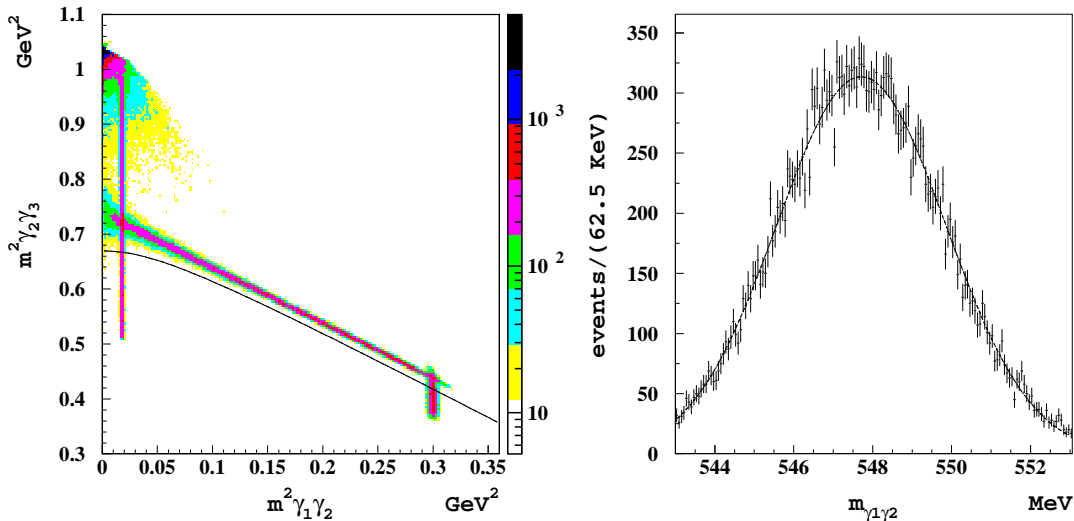


Figure 8: [**Left**] Dalitz plot of the  $3\gamma$  final state, obtained using 2001-2002 data. The cut chosen to reject the background is shown: only the events below the solid line are retained. [**Right**] Invariant mass of the two low energy photons of the event in the  $\eta$  mass region after the background rejection.

obtained by ordering photons with increasing energy, reduces the background to a negligible level. In Fig. 8.right the resulting invariant mass of the two low energy photons in the  $\eta$  mass region ( $M_{\gamma_1\gamma_2}$ ) is reported. The r.m.s. of the distribution is  $\sim 2$  MeV.

In order to study the stability of the measurement, the 2001-2002 data sample has been divided into eight periods, each corresponding to about  $50 \text{ pb}^{-1}$  of collected data. For all of them the  $\eta$  mass is obtained performing a Gaussian fit to the  $M_{\gamma_1\gamma_2}$  distribution. The  $\eta$  mass value and the corresponding statistical error are then computed by fitting all the measurements with a constant. A preliminary study of the systematics has been carried on, by taking into account the effect of energy, time, vertex position and  $\sqrt{s}$  miscalibration. The last effect gives the largest contribution, due to a 110 keV shift in the  $\phi$  mass calibration that has been conservatively taken as systematic error after the correction of the shift. All the eight measurements lie within the band defined by systematics. The preliminary result obtained is  $M_\eta = (547822 \pm 5_{\text{stat}} \pm 69_{\text{syst}}) \text{ keV}$ , in agreement with the NA48 measurement.

As a check of the method, we have also measured the  $\pi^0$  mass following the same procedure. The result,  $m_{\pi^0} = (134990 \pm 6_{\text{stat}} \pm 30_{\text{syst}}) \text{ keV}$ , is in very good agreement with the value reported by Particle Data Group <sup>35</sup>.

### 3.2 $f_0(980) \rightarrow \pi^+\pi^-$

At KLOE the nature of the lightest scalar mesons can be investigated through the radiative decays of the  $\phi$ . In particular, using  $350 \text{ pb}^{-1}$  from 2001-2002 data, a study of the decay chain  $\phi \rightarrow f_0(980)\gamma \rightarrow \pi^+\pi^-\gamma$  has been performed. The sample selection requires a vertex with two charged tracks in the interaction region and a photon matching the missing momentum of the track pair. Only events with a photon at large polar angle ( $45^\circ < \theta_\gamma < 135^\circ$ ) are retained to reduce the initial state radiation (ISR) background. The kinematics of the events, together with the time of flight signature, allows the rejection of the  $e^+e^- \rightarrow e^+e^-\gamma/\mu^+\mu^-\gamma$  and  $\phi \rightarrow \pi^+\pi^-\pi^0$  background events.

Parameter	KL	NS
$M_{f_0}$ (MeV)	980–987	973–981
$g_{f_0 K^+ K^-}$ (GeV)	5.0–6.3	1.6–2.3
$g_{f_0 \pi^+ \pi^-}$ (GeV)	3.0–4.2	0.9–1.1
$R = g_{f_0 K^+ K^-}^2 / g_{f_0 \pi^+ \pi^-}^2$	2.2–2.8	2.6–4.4
$g_{\phi f_0 \gamma}$ (GeV $^{-1}$ )	—	1.2–2.0

Table 1: Intervals of maximal variation of the  $f_0$  parameters for both kaon loop and “no structure” models.

We searched for the  $f_0$  signal in the  $\pi^+\pi^-$  invariant mass spectrum,  $M_{\pi\pi}$ , of  $\pi^+\pi^-\gamma$  events. The resulting distribution, characterized by the  $\rho^0$  peak and by the  $\rho$ - $\omega$  interference pattern, is dominated by ISR. Another relevant contribution comes from final state radiation events. The  $f_0(980)$  contribution appears as a small bump in the region  $M_{\pi\pi} \approx 980$  MeV, where the signal over background ratio is about 1/20. We fit the whole  $M_{\pi\pi}$  spectrum with two different theoretical descriptions of the  $f_0$  amplitude: the kaon loop model<sup>37, 38</sup> (KL), where the scalar is coupled to the  $\phi$  through a charged-kaon loop, and the “no structure” model<sup>39</sup> (NS). Here the scalar is described as a Breit-Wigner with a mass dependent width added to a polynomial complex function to allow an appropriate dumping of the resulting shape. In both cases the fit quality is good, with a  $\chi^2$  probability of 4.2% for KL and 4.4% for NS. The systematics have been evaluated by repeating the fit with the expected variation of several quantities such as luminosity, photon efficiency, expected background and bin size. The maximal variations of the parameters are reported in Tab. 1. There is a significant discrepancy between the two models, especially for the couplings  $g_{f_0 K^+ K^-}$  and  $g_{f_0 \pi^+ \pi^-}$ , while their squared ratio  $R$  is in good agreement, reinforcing the statement that  $f_0(980)$  is strongly coupled to  $KK$  rather than  $\pi\pi$ , as already stated by our previous work on the  $f_0(980) \rightarrow \pi^0\pi^0$  channel<sup>40</sup>.

### 3.3 Measurement of the hadronic cross section

After the publication of the measurement of  $\sigma(e^+e^- \rightarrow \pi^+\pi^-\gamma)$  with 2001 data (141 pb $^{-1}$ ), the activity has been focused to improve the analysis using  $\sim 300$  pb $^{-1}$  collected in year 2002, with better conditions in terms of machine background, stability of beam energy, and systematics from hardware cosmic veto, which has been enforced by a level-3 trigger capable to recover the efficiency loss using a *software* procedure to select particle tracks from the Interaction Region.

From the reconstruction point of view, mostly of the selection procedures have been redesigned to minimize the systematics errors. In particular:

- the error from the background filter (which was one of the biggest contribution to the total uncertainty), is expected to become negligible (was 0.6%);
- the error on  $\pi^+\pi^-\pi^0$  subtraction is expected to be reduced, due to a different selection, which allows the estimation of this contribution by data itself;
- the request on the reconstructed vertex has been released to reduce systematics coming from efficiency evaluation.

Moreover, relevant improvements in the measurement will come by the complementary analysis of the  $\pi^+\pi^-\gamma$  events with the photon at large angle, which allows to reach the 2-pion threshold, and by the study of the ratio of  $\pi^+\pi^-\gamma$  to  $\mu^+\mu^-\gamma$ , affected by different systematics since several effects cancel out in the ratio.

#### 4 Contributions to Conferences

*M. Antonelli* , “ $V_{us}$  and Rare  $K_S$  Decays at KLOE” , Les Rencontres de Physique de la Vallee d’Aoste, La Thuile, February 28, 2005.

*G. Lanfranchi* , “Measurement of kaon semileptonic decays and lifetimes at KLOE” , XL Rencontres de Moriond, Electroweak Interactions and Unified Theories, La Thuile, March 9, 2005.

*S. Giovannella* , “KLOE Results on  $f_0(980)$ ,  $a_0(980)$  scalars and  $\eta$  decays” , XL Rencontres de Moriond, QCD and Hadronic Interactions at high energy, La Thuile, March 14, 2005.

*C. Gatti* , “KLOE Results on kaon decays relevant to  $V_{us}$ ” , CKM Workshop, San Diego, March 16, 2005.

*M. Martini* , “Risultati recenti sui decadimenti dei mesoni K da KLOE” , IFAE - Incontri di Fisica delle Alte Energie, Catania, March 30, 2005.

*M. Martini* , “Recent KLOE results on neutral kaon decays” , LNF Spring School, May 20, 2005.

*M. Martini* , “Rare-decays program at KLOE” , K-Rare Workshop, LNF, May 26, 2005.

*P. De Simone* , “KLOE measurements of the charged kaon branching ratios and lifetime” , KAON 2005, Evanston, Illinois, June 14, 2005.

*C. Bloise* , “ $V_{us}$  extraction from KLOE measurements” , KAON 2005, Evanston, Illinois, June 14, 2005.

*T. Spadaro* , “Kshort Physics at KLOE” , KAON 2005, Evanston, Illinois, June 15, 2005.

*B. Sciascia* , “KLOE extraction of  $V_{us}$  from kaon decays and lifetimes” , HEP 2005, Lisbon, July 21, 2005.

*M. Moulson* , “KLOE results on neutral kaon decays and searches” , HEP 2005, Lisbon, July 23, 2005.

*S. Miscetti* , “Perspectives on hadronic physics with KLOE at DAΦNE” , HADRON05, Rio de Janeiro, August 23, 2005.

*C. Bloise* , “ $V_{us}$  determination from Kaon decays at KLOE” , FrontierScience 2005, Milan, September 13, 2005.

*C. Bloise* , “Perspectives on hadron physics with KLOE” , Eta05 Workshop, Cracow, September 17, 2005.

#### 5 Public notes in year 2005

*M. Martini and S. Miscetti* , “A direct search for  $K_S \rightarrow 3\pi^0$  decay with the KLOE detector at DAFNE” , KLOE Note **200**, May 2005.

*M. Martini and S. Miscetti* , “Determination of the probability of accidental coincidence between machine background and collision events and fragmentation of electromagnetic showers” , KLOE Note **201**, May 2005.

*G. Lanfranchi* , “Direct measurement of the Klong lifetime” , KLOE Note **203**, July 2005.

*M. Antonelli et al.* , “Measurement of the absolute branching ratios for dominant Klong decays, the Klong lifetime, and  $V_{us}$  with the KLOE detector” , KLOE Note **204**, August 2005.

*E. De Lucia and R. Versaci* , “Measurement of the branching ratio of the  $K^+ \rightarrow \mu^+\nu(\gamma)$  decay” , KLOE Note **205**, September 2005.

## 6 KLOE papers in year 2005

*F. Ambrosino et al.* , “Measurement of  $\sigma(e^+e^- \rightarrow \pi^+\pi^-\gamma)$  and extraction of  $\sigma(e^+e^- \rightarrow \pi^+\pi^-)$  below 1-GeV with the KLOE detector ”, Phys. Lett **606** (2005) 12.

*F. Ambrosino et al.* , “Upper Limit on the  $\eta \rightarrow \pi^+\pi^-$  branching ratio with the KLOE detector ”, Phys. Lett **B606** (2005) 276.

*F. Ambrosino et al.* , “Measurement of the leptonic width of the  $\phi$ -meson with the KLOE detector” Phys. Lett **B608** (2005) 199.

*F. Ambrosino et al.* , “A direct search for the CP-violating decay  $K_S \rightarrow 3\pi^0$  with the KLOE detector at DAFNE ”, Phys. Lett **B619** (2005) 61.

*F. Ambrosino et al.*, “Measurement of the Klong lifetime with the KLOE detector ”, Phys. Lett **B626** (2005) 15.

*F. Ambrosino et al.*, “Measurement of the absolute branching ratios for the dominant  $K_L$  decays, the  $K_L$  lifetime, and  $V_{us}$  with the KLOE detector”, Phys. Lett **B632** (2006) 43.

## References

1. KLOE Collaboration, “Measurement of the Klong lifetime with the KLOE detector ”, Phys. Lett.**B626**, 15 (2005).
2. KLOE Collaboration, “Measurement of the absolute branching ratios for the dominant  $K_L$  decays, the  $K_L$  lifetime, and  $V_{us}$  with the KLOE detector”, Phys. Lett.**B632**, 43 (2006).
3. KLOE Collaboration, “A direct search for the CP-violating decay  $K_S \rightarrow 3\pi^0$  with the KLOE detector at DAFNE ”, Phys. Lett.**B619**, 61 (2005).
4. C. Gatti, Eur. Phys. J.**C45**, 417 (2006) and references therein.
5. K. G. Vosburgh *et al*, Phys. Rev.**D6**, 1834 (1972).
6. M. Ademollo, R. Gatto, Phys. Rev. Lett. **13**, 264 (1964).
7. KLOE Collaboration, Measurement of the Form Factor Slopes for the Decay  $K_L \rightarrow \pi e \nu$  with the KLOE Detector, accepted in Phys. Lett.**B**, [hep-ph/0601038](#).
8. T. Alexopoulos *et al.*, KTeV collab., Phys. Rev. Lett. **93**, 181802 (2004).
9. O. P. Yushchenko *et al.*, ISTRA+ collab., Phys. Lett. **B589**, 111 (2004).
10. V. Cirigliano *et al.*, Eur. Phys. J.**C33**, 369 (2004).
11. KLOE Collaboration, Phys. Lett.**B538**, 21 (2002).
12. KLOE Collaboration, Precise measurement of  $\Gamma(K_S \rightarrow \pi^+\pi^-(\gamma))/\Gamma(K_S \rightarrow \pi^0\pi^0)$  with the KLOE detector at DAΦNE, [hep-ph/0601025](#).
13. KLOE Collaboration, Phys. Lett.**B535**, 37 (2002).
14. S. Eidelman, *et al.*, Particle Data Group, Phys. Lett.**B592**, 1 (2004).
15. CPLEAR Collaboration, Phys. Lett.**B444**, 38 (1998).
16. CPLEAR Collaboration, Phys. Lett.**B444**, 52 (1998).

17. CPLEAR Collaboration, Phys. Lett.**B456**, 297 (1999).
18. KLOE Collaboration, Measurement of the branching fraction and charge asymmetry for the decay  $K_S \rightarrow \pi e \nu$  with the KLOE detector, accepted in Phys. Lett.**B**, [hep-ph/0601026](#).
19. M. Battaglia *et al.*, Workshop on the CKM Unitarity Triangle, Geneva, Switzerland, February 13-16 2002, CERN report 2003-002, [hep-ph/0304132](#) (2003).
20. V. Cirigliano, H. Neufeld, H. Pichl, Eur. Phys. J.**C35** 53 (2004).
21. T. C. Andre, Radiative corrections to  $K_0(13)$  decays, [hep-ph/0406006](#).
22. A. Sirlin, Nucl. Phys. **B196**, 83 (1982).
23. A. Czarnecki, W. J. Marciano, A. Sirlin, Phys. Rev.**D70**, 093006 (2004).
24. H. Leutwyler, M. Roos, Z. Phys.**C25**, 91 (1984).
25. D. Becirevic *et al.*, Nucl. Phys.**B705**, 339 (2005).
26. T. Alexopoulos *et al.*, KTeV collab., Phys. Rev.**D70**, 092006 (2004).
27. M. N. Achasov *et al.*, SND collab., Phys. Lett.**B459**, 674 (1999).
28. A. Lai *et al.*, NA48 collab., Phys. Lett.**B610**, 165 (2005).
29. E. De Lucia, R. Versaci, *Measurement of the branching ratio of the  $K^+ \rightarrow \mu^+ \nu(\gamma)$  decay*, KLOE Note 205 (2005), <http://www.lnf.infn.it/kloe/pub/note/kn205.ps.gz>
30. W. J. Marciano, Phys. Rev. Lett. **93**, 231803 (2004).
31. C. Aubin *et al.* [MILC Collaboration], Phys. Rev. **D70**, 114501 (2004).
32. E. Blucher *et al.*, “Status of the Cabibbo Angle”, [hep-ph/0512039](#).
33. M. Abdel-Bary *et al.*, Phys. Lett.**B619**, 281 (2005).
34. A. Lai *et al.*, Phys. Lett.**B533**, 196 (2002).
35. S. Eidelman *et al.*, Phys. Lett.**B592** (2004).
36. F. Ambrosino *et al.*, [hep-ex/0511031](#), submitted to Phys. Lett.**B**.
37. N. N. Achasov and V. N. Ivanchenko, Nucl. Phys.**B315**, 465 (1989).
38. N. N. Achasov and V. V. Gubin, Phys. Rev.**D57**, 1987 (1998).
39. G. Isidori, L. Maiani, M. Nicolaci and S. Pacetti, private communication.
40. A. Aloisio *et al.*, Phys. Lett.**B537**, 21 (2002).

## LHCb

M. Alfonsi (Dott.), M. Anelli (Tecn.), G. Bencivenni, C. Bloise, F. Bossi, P. Campana, G. Capon, M. Carletti (Tecn.), P. Ciambrone, E. Dané, A. Di Virgilio (Tecn.), P. de Simone, C. Forti, G. Lanfranchi, F. Murtas, V. Patera (Ass.), M. Pistilli (Tecn.), M. Poli Lener (Dott.), R. Rosellini (Tecn.), M. Santoni (Tecn.), A. Sarti, A. Sciubba (Resp. Ass.), S. Valeri (Tecn.)

In collaboration with the “Servizio Supporto Costruzione Rivelatori”:  
A. Ceccarelli (Tecn.), A. Franceschi, A. Saputi (Tecn.)

In collaboration with the “Servizio di Elettronica”:  
A. Balla, G. Corradi, G. Felici, G. Paoluzzi, G. Papalino

### 1 Introduction

The LNF group of LHCb operates on the **muon subdetector** <sup>1, 2)</sup> with responsibilities on detectors (MWPC and GEM), electronics and mechanics. The detector production started in autumn 2003 and is expected to be completed within three years. The electronics production will start in 2005.

### 2 Multiwire Proportional Chambers

The LNF group of LHCb has the responsibility for the construction of  $\sim 1/4$  of the MWPCs of the muon detector. Depending on the position inside the detector, there are different chamber dimensions with different readout: anode pads, cathode pads, anode & cathode pads.

We designed, collaborating with the Ferrara group, all the details of 10 different chambers types (with active dimensions ranging from  $29 \times 35 \text{ cm}^2$  to  $31 \times 151 \text{ cm}^2$ ). With these characteristics 292 chambers will be assembled and tested in LNF. The same design is applied to the remaining 1170 chambers that will be built in Ferrara, Firenze, CERN and S.Petersbourg.

#### 2.1 Brief description of the LHCb MWPC

The MWPC chambers of the LHCb muon detector must fulfill stringent requirements on time response: for triggering purpose  $\sim 99\%$  minimum efficiency must be exploited in 20 ns. Each chamber is constituted by four layers assembled as two independent bigaps with hardwired-OR of the readout. In each 5 mm gap there are 30 microns gold-plated tungsten wires stretched at about 65 grams with a pitch of 2 mm. The filling mixture is Ar/CO<sub>2</sub>/CF<sub>4</sub> (40/40/20).

#### 2.2 Main goals reached in 2005

##### 2.2.1 Status of Production

In October 2004 we started the production of the chambers of region M5R3 of the Muon System. We completed the production (48 chambers + 11 spare) in October 2005.

Then, we started the production of the M5R4 chambers. We built 68 chambers. The other M5R4 chambers are being built by the Firenze INFN team.

### 2.2.2 Chamber Quality Control

All the chambers built are expected to pass successfully three main tests:

- Test of gas tightness: the chamber is inflated at an overpressure of 5 mbar and the pressure drop  $\Delta P$  is measured as a function of time. The requirement is  $\Delta P < 2$  mbar/hour.
- HV training: the chamber is slowly conditioned and is required to reach at least 2.85 kV of high voltage, drawing a negligible dark current.
- Test of gap gain uniformity: the gain fluctuation of each double-gap detector must be compatible with the plateau width measured at test beams (see below).

All the chambers tested up to now (57 M3R3, 58 M5R3 and 64 M5R4) satisfy the requirements on gas tightness and dark current ( $< 10$  nA/gap at 2.85 kV).

Uniformity of the gap gain is tested with a 40 mCi  $^{137}\text{Cs}$  source. The current drawn by each gap is monitored while the lead case containing the source is moved by means of a mechanical arm over the chamber surface. These measurements allow to check the gain uniformity within each gap and to compare different chambers among them. This system and the control software were designed and realized by the LHCb Rome-1 group.

Two different gas mixtures were used for the test. An Ar/CO<sub>2</sub>/CF<sub>4</sub> 40/40/20 was used for all the M3R3 chambers, 48 M5R3 and 13 M5R4 ones. Starting from chamber 14 M5R4 we decided to use the mixture which will be used in the experiment: Ar/CO<sub>2</sub>/CF<sub>4</sub> 40/55/5. The last 11 M5R3 chambers (49-59) were built after the M5R4 ones and thus they were tested with the new gas mixture. In the following the Ar/CO<sub>2</sub>/CF<sub>4</sub> 40/40/20 mixture will be indicated as the “old” one while the 40/55/5 as the “new” one. The presence of a single-gap reference chamber, below the tested chamber, made possible to compare the results obtained with different gas mixtures.

Criteria for the classification of the chambers As already described in <sup>3)</sup> and <sup>4)</sup> the chambers are classified on the basis of the results of the source scan.

Since each pair of adjacent gaps is hardware OR-ed into one Front End chip, the four-gap chamber can be considered as a couple of two independent double-gap detectors. For each double-gap of each chamber tested, we measured the spread of the current with respect to the average current of all double-gaps. In order to have the area of all the double-gaps inside the plateau the gas gain disuniformity translated in voltage should be lower than  $\pm 80$  V (corresponding to a factor 1.7 in the current).

So, each double-gap is classified, accordingly to the uniformity of the values of the current  $I_c^d(x,y)$ , in one of the following two categories:

$$\text{Category I : } \quad 1/1.5 \leq I_c^d(x,y)/I_0 \leq 1.5 \quad \forall x \text{ and } y \quad (1)$$

$$\text{Category II : } \quad 1/1.7 \leq I_c^d(x,y)/I_0 \leq 1.7 \quad \forall x \text{ and } y \quad (2)$$

where  $I_0$  is the current drawn by a double-gap at the nominal gain  $G_0$ . A chamber with no more than one double-gap exceeding the limits of category I and within the limits of category II is considered as *good*. A chamber having both double-gaps of category II is considered as *spare* and a chamber having at least one double-gap outside of category II is a *reserve* chamber.

### Results for M5R3 chambers

In Fig. 1 the mean values of  $\langle I \rangle$  for each double-gap of the 59 M5R3 chambers produced are reported, with the maximum spread found superimposed, once corrected for T and P by means of the single-gap data.

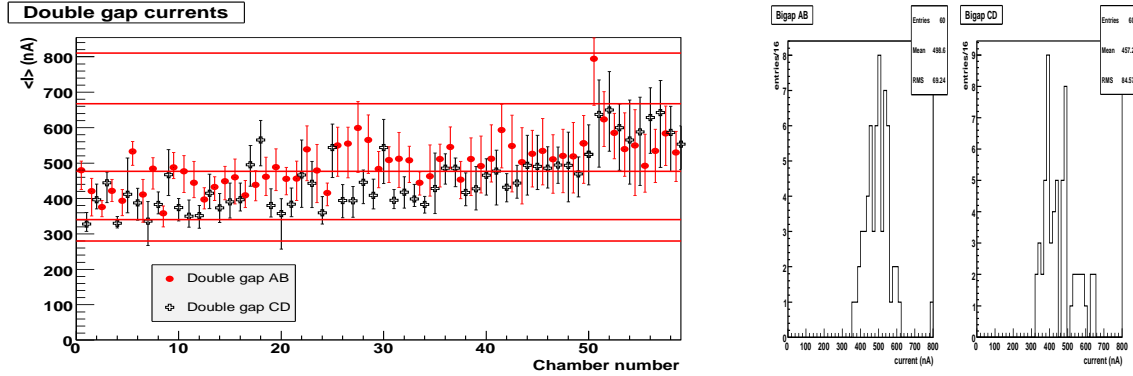


Figure 1: Average values of  $\langle I \rangle$  for the two double-gaps of the M5R3 chambers, with the maximum spread found superimposed, after the correction for the T and P effects.

From Fig.1 it is possible to see that up to chamber number 49, all chambers are “good” (apart chambers 7 and 20 which are “reserve”). Starting from chamber number 40 the maximum gain spread of all the double-gaps has increased and chambers from 50 to 58, have almost all at least one double-gap out from Category I. We found 3 “reserve”, 1 “spare” and 55 “good” chambers.

### Results for M5R4 chambers

The values of  $\langle I \rangle$  for the 65 M5R4 chambers produced are reported in Fig. 2, with the maximum spread found superimposed, once corrected for T and P by means of the single-gap data.

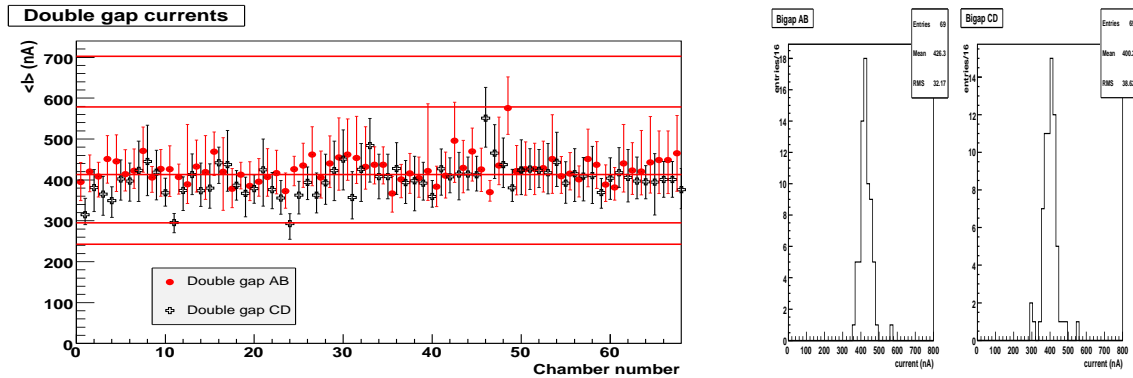


Figure 2: Values of  $\langle I \rangle$  for the double-gaps of the M5R4 chambers, with the maximum spread found superimposed, after the correction for the T and P effects.

No one M5R4 chamber has both the double-gaps with a gain outside from the Category I limits nor at least one double-gap outside from Category II. All the M5R4 chambers produced are “good”.

### 2.2.3 Chamber Test at CERN Gif Facility

In May 2005 we have tested two chambers at the Gamma Irradiation Facility <sup>5)</sup> at CERN (GIF source: <sup>137</sup>Cs, 662 keV).

The goal was to study the behavior of the MWPC related to the Malter effect. After a MWPC has been irradiated, the Malter effect gives rise to a self-sustained current (with HV on) even without radiation on the chamber. We tested two different types of chambers: M3R3 and M5R4. The M3R3 chambers have the cathode read-out and all panels are gold plated, instead the M5R4 that have anode read-out and panels are not gold plated.

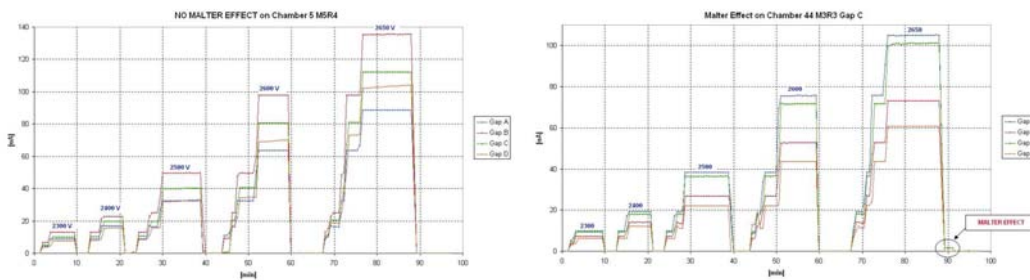
We performed the test following 4 steps for the two chambers:

- source on;
- set HV at 2300V;
- wait for current stability;
- source off and HV left turned on.

In the fourth step could appear residual current due to the Malter effect. We repeated this procedure increasing HV up to 2650 V.

In Fig. 3(a) the current drawn by each gap is plotted as a function of time for the chamber type M5R4. In this chamber no residual current is appeared.

In Fig. 3(b) the result for chamber type M3R3 is plotted.



(a) Chamber type M5R4 (Wire Pad).

(b) Chamber type M3R3 (Wire Cathode Pad).

Figure 3: Current drawn in each gap as a function of time for different HV settings.

In this chamber is appeared a residual current in gap C at 2650V. This residual current ( $\approx 2 \mu\text{A}$ ) is plotted in Fig. 4 and decrease to zero in about 20 minutes.

To better understand the Malter effect in our chambers, we disconnected the wire pad from the

HV one by one and we discovered that residual current was present only in one wire pad.

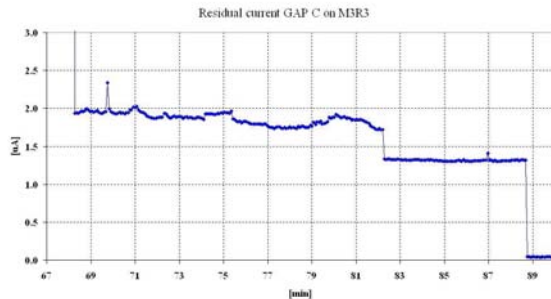


Figure 4: Residual current gap C on M3R3.

### 3 Triple GEM Detectors

For the innermost part (regions R1,  $\sim 0.6 \text{ m}^2$  area) of the first muon station (M1) of the LHCb experiment the LNF group, in collaboration with INFN-Cagliari, proposes a detector based on Gas Electron Multiplier (GEM) technology. The requirements <sup>1)</sup> for detectors in M1R1 are: a rate capability of  $\sim 500 \text{ kHz/cm}^2$ ; each station must have an efficiency of  $\sim 96\%$  in a 20 ns time window (two independent detector layers per station, logically OR-ed, are foreseen); a cluster size, i.e. the number of adjacent deetctor pads fired when a track crosses the detector, should not be larger than 1.2, for a  $10 \times 25 \text{ mm}^2$  pad size. In addition the detector must tolerate, without damages or large performance losses, an integrated charge of  $\sim 0.88 \text{ C/cm}^2$  in 10 years of operation at a gain of  $\sim 6 \times 10^3$  and an average particle flux of  $184 \text{ kHz/cm}^2$ , for an average machine luminosity of  $2 \times 10^{32} \text{ cm}^{-2} \text{ s}^{-1}$ .

The GEM <sup>6)</sup> consists of a thin ( $50 \mu\text{m}$ ) kapton foil, copper clad on each side, chemically perforated by a high density of holes having bi-conical structure, with external (internal) diameter of  $70 \mu\text{m}$  ( $50 \mu\text{m}$ ) and a pitch of  $140 \mu\text{m}$ . In safe condition, gains up to  $10^4$  are reachable using multiple structures, realized assembling more than one GEM at close distance one to each other.

After a long period of R&D, spent to qualify the GEMs as detectors suitable for the intense and radioactive environment around the beam pipe of LHCb, we chose to operate the detector with the  $\text{Ar/CO}_2/\text{CF}_4(45/15/40)$  gas mixture with an overall gain of  $\sim 8000$  (see the activity report of the 2004 for details).

In the 2005 the triple-GEM detectors were officially approved by LHC Committee to equip the M1R1 region of the Muon apparatus <sup>7)</sup>.

In the 2005 the major effort was the definition of the final detector design, the assembly procedure as well as the chamber quality controls, that have been revised by the Engineering Design Report (EDR) and the Production Readiness Review (PRR).

The pre-production has started and the first two detectors, built in agreement with the assembly procedure and check requirements, have tested at the T11-PS beam facility at CERN <sup>8)</sup>. Fig. 5 shows that a time resolution better than 3 ns (r.m.s.) has achieved with two OR-ed triple-GEM detectors, while Fig. 6 shows that the detector largely fulfills the M1R1 LHCb requirements on the pad cluster size and the efficiency in 20 ns time window. A large and safe working region

(defined as the gas gain range between the onset of the efficiency plateau and the gain at which the pad cluster size is 1.2) of about 80 V, is found with at electronic thresholds corresponding to 2-3 fC.

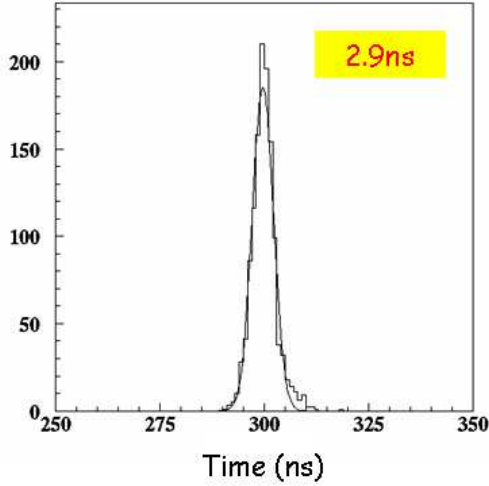


Figure 5: Time spectrum of the detector station for a gas gain of 18000.

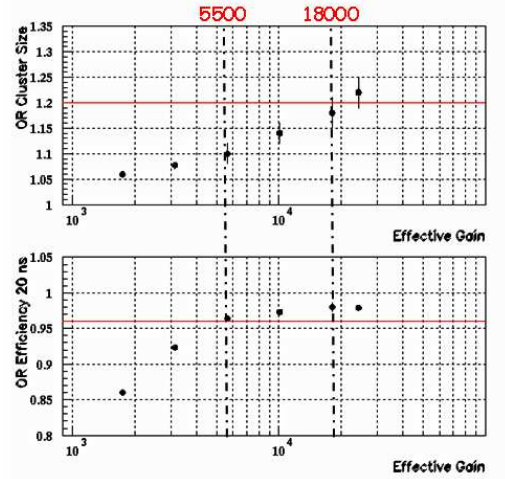


Figure 6: Detector station performances: the average pad cluster size (top) and the average efficiency within 20 ns time window (bottom) as a function of the gas gain.

The first prototype of the detector faraday cage (FC) has been designed and produced. The FC is made of 400  $\mu\text{m}$  thick brass which foresees the opening for the signals connector and the low voltage supply (LV) of the LHCb electronics. Due to the MIR1 space constraints, two high voltage plugs and gas pipe have also been designed and integrated in the FC (Fig. 7). The first prototype of the low voltage circuit for the front-end electronic chain (192 channels) and the high voltage divider for the detector supply have been produced and successfully tested.

The performances of each detector, composed by two triple-GEM chambers equipped with dedicated CARDIAC-GEM front-end electronics and all the final off-detector components, are measured with a cosmic ray telescope (Fig. 8). The CARDIAC-GEM, with respect to the chip designed for the LHCb-Muon MWPC, has been modified increasing the amplifier gain and removing the tail cancellation circuit, to take into account for the lower gas amplification and the purely electronic signal of the detector.

The trigger of the cosmic ray telescope is supply by the coincidence of two scintillator layers which cover the active area of the detector. They are 1 m apart and above the lower scintillator a 10 cm thick lead brick ( $\sim 18 X_0$ ) is used to select muons. To ensure the fine reconstruction of the impact parameter point on the GEM detector, two layers of drift tubes, placed above and below the detector, are used. The space resolution reachable with the drift tubes is better than  $\sim 150 \mu\text{m}$  (r.m.s.).



Figure 7: Top: Close view of the HV plug integrated on the faraday cage. Bottom: Picture of the final faraday cage of the detector station.



Figure 8: Picture of the cosmic ray setup used to measure the final station performances.

#### 4 Electronics

The LHCb muon trigger architecture relies on 1248 Trigger Sectors (TS) built by the first stage of the front-end electronic chain. About 122,112 physical channels are merged to generate about 26,000 logical channels both in the chamber front-end and in the Intermediate Boards (IB) system. The off detector front-end chain is mainly made of two components : the IB system and the ODE system.

The IB system is used to merge part of the physical channels and is made of 176 boards. Each IB board can manage up to 192 LVDS input signals and 60 LVDS output signals. To minimize the number of boards (because the chamber/TS geometries we have 5 different IB I/O configurations) the logic functions have been implemented using programmable devices. That choice allowed us to design a single PCB to match the whole detector geometry. The use of anti-fuse technology for programmable devices (ACTEL devices) gives also an intrinsic robustness in moderate radiation environment (like the levels foreseen near the LHCb detector).

In the Off Detector Electronics (ODE) boards, the logical channels are synchronized to the bunch crossing, arranged to implement the required TS, and, finally sent to the Level-0 (L0) trigger logic through 1248 optical links at 1.6 Gbit/s. The ODE board also provides a measure of signal arrival times (1.5 ns time resolution) and implements L0-pipelines and DAQ interface via a 1,6 Gbit/s optical link and ECS interface. Because the huge number of input channels per boards (192

LVDS) and the very strict requirements on timing performances for optical link connections (less than 100 ps peak to peak on clock jitter) the design of this board has been very challenging. To fully instrument the muon detector 152 ODE boards will be used.

Due to the huge number of I/O managed by each board both IB and ODE system use a passive Transition Board (TB) to arrange the different topologies of input logical channels. All boards are hosted in a mechanical standard 7U VME crate with custom backplane. The backplane allows to interconnect IB and TB boards and to distribute low voltage (+2.5V and + 3.3V) to the IB boards. Each crate can host up to 21 boards.

To minimize the cables length both IB and ODE systems are localized close to the detector. Then all boards have been implemented using radiation tolerant components, while critical components (anti-fuse and flash based FPGA) have been qualified (vs radiation) at the Louvain La Neuve irradiation facility with 70 MeV proton beam at a maximum fluence of  $6 \times 10^{11}$  p/cm<sup>2</sup>.

Two fundamental tests have been successfully performed: a full chain electronic test (including IB and ODE) with a fully instrumented chamber and the high speed data transmission from ODE to the L0 trigger and DAQ optical receivers. To measure the performance of the high speed serial links implemented on the ODE a dedicate instrumentation was provided that will be also used to qualify the final production.

The TB PCB have been already produced and assembled. IB design has been completed minimizing the channel to channel skew, mass production has been completed and boards qualification test are going on. A ten boards ODE pre-production has been completed and mass production will start after system qualification.

Besides the IB and ODE system the LNF group is also in charge for the main low voltage system distribution layout and for the on-chamber low voltage regulation. Because the low space availability on the platform a solution for the main low voltage power distribution based on high power generators and a high density distribution network including a fuse on each distributed line has been designed and implemented.

Finally, the low voltage regulation boards and high voltage filters to match all chambers geometries to match all chambers geometries have been designed and produced.

## 5 Chamber Supporting Structure

LHCb-LNF has the responsibility for the construction of the ten movable walls that will support the chambers in between the iron absorbers of the muon. Detailed studies were performed on the mechanical characteristics of the raw material and of the components that will be used to assemble large walls starting from 2 m height aluminium honeycomb panels. The chambers will be positioned on the wall over aluminium supports that will be attached to the wall by means of glue and rivets.

A partial prototype (1,5m×8m) has been assembled at LNF and loaded to simulate the chamber and cabling weight. The panel production started last year at COSPAL. The same company drills the precision holes to fix the chamber supports to the wall and produces a photogrammetric measurement that will be used to determine the final position of each chamber. Still some decision has to be taken about the procedure to align the chambers on the walls. Walls installation is foreseen for spring 2006. The main activity is now the project of the lifting system that will be used to assemble the structure following the CERN safety requirements.

Each chamber is fixed to the support lying on two feet that allow positioning and blocking by means of screws and spacers. The four corners of each chamber are closed by a thin brass Faraday cage with several holes to allow the insertion of signal, controls and low voltage connectors of the front end boards. The sides of the chamber house the low voltage regulating boards and high voltage filters. The production of the cages started in 2005 and will finish next months.

In the meanwhile the optimization of the dimensions and the positioning of the racks for the electronics and of the platforms around the detector was done since they must both move together with the supporting structure without interfere with some elements of the cryogenics and the RICH and the PS detectors. The adopted solution, worked out in collaboration with the CERN team, is a unique structure per side that moves together the walls of stations M2 to M5. The electronics of station M1 will be housed in the tunnel under the RICH. On M1 mechanical constraints for routing the cables (for signals, power supply and pulse and control signals), gas piping and air cooling are more stringent; system integration is under continuous and progressing study.

## 6 List of Conference Talks by LNF Authors in Year 2005

- D.Pinci and A.Sarti, "Production and test of the LHCb Muon Chambers", presented at Hadron Collider Physics Symposium (HCP05), Les Diablerets, Switzerland July 4-9, 2005.
- M. Poli Lener, "Triple-GEM detector for the innermost region of the LHCb apparatus", presented at Incontri di Fisica delle Alte Energie (IFAE05), Catania, Italy, March 30- April 2, 2005.
- G. Bencivenni, "The triple-GEM detector for the M1R1 muon station at LHCb", presented at Nuclear Science Symposium and Medical imaging (IEEE05), Wyndham El Conquistador Resort, Puerto Rico, October 23 - 29, 2005.

## References

1. LHCb Collaboration, "LHCb: muon system technical design report", CERN LHCC MUON 2001-010, LHCb TDR 4, 28 May 2001.
2. LHCb Collaboration, "LHCb: Addendum to muon system technical design report", CERN LHCC MUON 2003-002, LHCb TDR 4 Addendum 1, 15 January 2003.
3. M. Anelli *et al.* "Quality tests of the LHCb muon chambers at the LNF production site", Poster presented at the IEEE 2004 (Rome, Italy, October 16-22, 2004), and submitted to Transaction on Nuclear Science.
4. D.Pinci and A.Sarti, "Production and test of the LHCb Muon Chambers", presented at Hadron Collider Physics Symposium (HCP05), Les Diablerets, Switzerland July 4-9, 2005.
5. M. Anelli *et al.*, "Test of a MWPC for the LHCb Muon System at the Gamma Irradiation Facility at CERN", Public Note LHCb MUON-2005-003.  
<http://cdsweb.cern.ch/search.py?recid=815058&ln=en>
6. F. Sauli, Nucl. Instrum. Meth. **A386** (1997) 531.
7. LHCb Collaboration, "LHCb: Second addendum to muon system technical design report", CERN LHCC MUON 2005-012, LHCb TDR 4 Addendum 2, 9 April 2005.
8. A. Alfonsi *et al.*, presented at Puerto Rico 2005 IEEE conference (Oct. 23-29) and submitted to Transaction on Nuclear Science.
9. A. Balla *et al.*, Muon Off-Detector electronics: The IB system, LHCb note, LHCb 2003-023.

## BENE\_DTZ

F. Terranova

BENE-INFN is a study group closely related to the European initiative BENE (Beams for European Neutrino Experiments). The latter is aimed at developing novel sources for high intensity neutrino beams and is mainly focused on the conceptual design of Superbeams, Beta Beams and Neutrino factories <sup>1)</sup>. The activity in Frascati is focused on the Beta Beams, particularly in its medium <sup>2)</sup> and high gamma configuration <sup>3)</sup>. Moreover, studies have been carried out to assess the physics potential and technological challenges of laser-driven Superbeams <sup>4)</sup>. Finally, in 2005 LNF hosted the 7th International Workshop on Neutrino Factories and Superbeams (June 21-26).

### 1 List of Conference Talks by LNF Authors in Year 2005

1. F. Terranova “A european neutrino programme based on the machine upgrades of the LHC”, EPS-HEP2005 International Europhysics Conference on High Energy Physics, Lisbon, Portugal.
2. F. Terranova “Multi-GeV laser driven proton acceleration in the high current regime”, 7th International Workshop on Neutrino Factories and Superbeams, Frascati, Italy.
3. F. Terranova “Novel Acceleration Techniques for the Physics of Massive Neutrinos”, ICFA 38th Advanced Beam Dynamics and 9th Advanced and Novel Accelerators Joint Workshop on Laser-Beam Interactions and Laser and Plasma Accelerators, Taipei, Taiwan.
4. F. Terranova, “The experimental determination of three-family neutrino mixing and CP violation”, Seminar at Bologna Univ., Bologna, Italy.

### References

1. For a recent review see A. Guglielmi, M. Mezzetto, P. Migliozzi and F. Terranova, arXiv:hep-ph/0508034.
2. A. Donini, E. Fernandez, P. Migliozzi, S. Rigolin, L. Scotto Lavina, T. Tabarelli de Fatis and F. Terranova, arXiv:hep-ph/0511134, to appear in the proceedings of the LHC LUMI 2005 Workshop, Arcidosso, Italy.
3. F. Terranova, Nucl. Phys. Proc. Suppl. **149**, 185 (2005); F. Terranova, A. Marotta, P. Migliozzi and M. Spinetti, Eur. Phys. J. C **38**, 69 (2004).
4. S. V. Bulanov, T. Esirkepov, P. Migliozzi, F. Pegoraro, T. Tajima and F. Terranova, Nucl. Instrum. Meth. A **540**, 25 (2005); F. Terranova *et al.*, Nucl. Phys. Proc. Suppl. **143**, 572 (2005).

## ICARUS

### Resistive Chamber in Pure Noble GAS

G. Mannocchi, L. Periale, P. Picchi (Resp.), L. Satta, G. Trincherò

The ICARUS group (1994) <sup>1)</sup> was aimed to substitute a set of multiwires electrodes in the large liquid argon time projection chamber(TPC) by a more rigid and reliable construction. Basically, the idea was to use a printed circuit board with metal strips. Several designs were developed, some of them employing multilayer boards made of G10 with holes or grooves. Gas avalanche multiplication within small holes has been the subject of numerous studies in a large variety of applications. The most extensively studied hole multiplier is the Gas Electron Multiplier(GEM), made of  $50 - 70 \mu m$  diameter holes etched in a  $50 \mu m$  thick metallized kapton foil. The success of the GEM <sup>2)</sup> triggered the concept of a coarser structure(LEM) made by drilling millimeter sized holes in a  $\simeq 2 mm$  thick *Cu* plated G10 printed circuit board(PCB).

The Large Electron Multiplier(LEM) yields gains between  $10^3 - 10^4$  in pure noble gasses. These results are obtained without gas quencher because the G10 walls of the hole act as a “mechanical quencher” absorbing the *UV* photons produced in the electron avalanche that is thus localized in space and without sparks.

The optimization of the *LEM* parameters required a broad systematic study. In this year we concentrated on the *LEM* mechanism and on the possibility to increase the gain( $10^5 - 10^6$ ) without sparks. The mechanical quencher, we have simulated it by using blinded holes. . We made a *LEM* by using G10 plus a resistive material with well defined resistivity. The hole ends in a resistive plug.

Very high gain with noble gas can be obtained with resistive material that thanks to very high electrical fields and closed space allows to have limited streamer sparks by using noble gasses. The resistivity of the material must be chosen for two goals: disappearance of space charge and transparency of induced charge. If we have success we can detect the single electron in noble gas in double phase *TPC*. This new method will allow working with mixture of noble gasses and to photodopants with  $QE \simeq 1$ .

### References

1. P. Cennini *et al.*, Nucl. Instr and Meth in Phys. Res. **A346**, 50 (1994).
2. L. Periale *et al.*, Nucl. Instr and Meth in Phys. Res. **A478**, 377 (2002).

## LARES

G. Bellettini, (Ass.), A. Bosco (Laur.), C. Cantone (Bors.), S. Dell’Agnello (Resp.),  
 G. Delle Monache, M. A. Franceschi, M. Garattini (Laur.), T. Napolitano (Art. 23),  
 A. Paolozzi (Ass.), R. Tauraso (Ass.)

LARES is a satellite laser-ranging (SLR) space mission. The ancestor of the SLR technique was the Lunar Ranging RetroReflector (LRRR) experiment deployed by the Apollo 11. LRRR data have been used to measure the De Sitter effect, or *geodetic precession*, predicted by Einstein’s General Relativity (GR), to an accuracy of 0.35%. This shift arises from the effect of the gravitational field on the velocity of an orbiting gyroscope.

GR also predicts that a rotating central body like Earth will drag the local space-time around it (*frame dragging* or Lense-Thirring effect, LT). This will cause the precession of the *node* of an artificial Earth satellite and is a genuine rotation effect: currents of mass generate additional space-time curvature (gravitomagnetism). The LT effect has been measured with 10 % accuracy in 2004<sup>1)</sup> using two 6000 Km altitude laser-ranged satellites: LAGEOS I and LAGEOS II (Figure 1), whose node shift is just 33 mas/yr (mas = millisecond of arc), that is, 1.9 meter/yr.

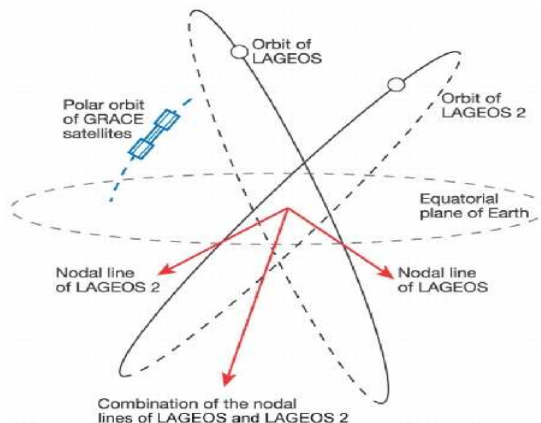


Figure 1: The LAGEOS (LAsEr GEOdynamics Satellite)

The main sources of experimental uncertainty are: (1) the deviation of the geo-potential from the perfect  $1/r$  behavior and (2) the asymmetric thermal thrusts (TTs) from direct solar radiation, Earth albedo and Earth IR radiation. The latter, the Yarkovsky-Rubincam effect, dominates the TT part of  $\sigma_{LT}$  and is driven by the uncertainty on the retro-reflector thermal relaxation time in the space climate,  $\tau_{CCR}$ . This constant has never been measured before and the spread of its calculated values in the literature is  $\sim 250\%$ , which gives  $\sigma_{LT}(TT) \sim 2 - 3\%$ .

A modern and improved satellite, called LARES (LAsEr RELativity Satellite) is being designed by the LNF and Lecce INFN groups to achieve  $\sigma_{LT} \leq 1\%$ , taking advantage of: (i) the recent high-accuracy EGMs (by the GRACE mission), (ii) exploiting a thorough mechanical and thermo-optical characterization of the satellite and (iii) a full re-design to reduce TTs.

The LNF group is building a Space Climatic Facility (SCF), a cryostat equipped with Solar

and Earth radiation simulators, to measure  $\tau_{CCR}$  of a LAGEOS prototype (see Figure 2) with an accuracy better than 10%. This would make  $\sigma_{LT}(TT) < 0.1\%$ . A commercial specialized software



Figure 2: The LAGEOS 3x3 retro-reflector (CCR) matrix prototype.

for satellite thermal simulation (Thermal Desktop, RadCad, Sinda-Fluint, by C&R Technologies) has been run extensively to estimate the expected value of  $\tau_{CCR}$  in various climatic conditions<sup>2)</sup>. For example, Figure 3 shows the CCR temperature profile in space at  $t = 2800$  sec, in the following conditions: the satellite Al body is held at the nominal 300 K, Sun and Earth radiations are turned off for at  $t \leq 0$  and the Sun is turned on for  $t > 0$ . Figure 4 shows the T variation of a FEM node on the center of the CCR outer face. An exponential fit provides an estimate of  $\tau_{CCR}$  with a statistical uncertainty of 2%.

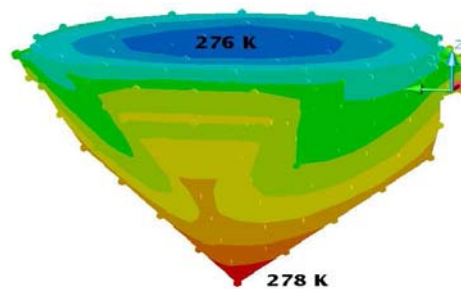


Figure 3: The LAGEOS CCR temperature profile: 276 K (outer face), 278 K (tip)

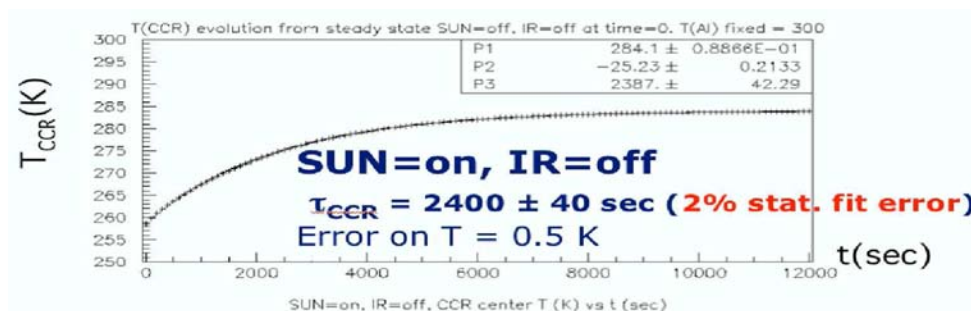


Figure 4: The LAGEOS thermal relaxation time.

The second goal of the SCF is the full characterization of LARES prototypes. A new satellite design has been conceived to strongly suppress TTs. The basic idea is to mount CCRs from the

inside on an outer Al shell, screwed on top an inner massive core and let a vacuum gap in between. The significant thermal radiation released inside the shell from the illuminated emisphere can thus propagate across the gap to the dark emisphere, making the overall CCR temperature more uniform than for the LAGEOS <sup>3)</sup>. This in turn will decrease TTs. A full thermal simulation is being performed and an actual prototype built at LNF to test the effectiveness of this new design at the SCF. Figure 5 shows the two half shells of a 1:2 scale prototype. Figure 6 shows the SCF, with the LAGEOS matrix inside the cryostat, the Sun simulator and, on the right, a tunnel to measure temperatures with an IR camera.



Figure 5: The outer half-shells of the new satellite design for the LARES space mission.

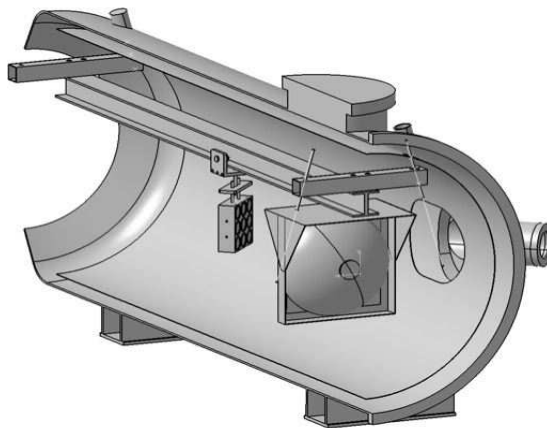


Figure 6: The LNF Space Climatic Facility.

A reliable control of TTs will make LARES the ideal test particle and could allow a precision measurement of its perigee shift, which is, in general, the observable most sensitive to new physics. For example, a recent brane-world theoretical model <sup>4)</sup> might imply perigee shifts observable after 5 years of ranging data with LARES. This possibility is currently under study.

## References

1. I. Ciufolini, E. C. Pavlis, *Nature*, Vol. **431**, 21 October 2004.
2. Arianna Bosco, Bachelor thesis (2004), University of Roma “Tor Vergata” (unpublished).
3. G. Delle Monache, talk at the ILRS Workshop, Oct. 2005, Eastbourne, UK.
4. G. Dvali, A. Gruzinov, and M. Zaldarriaga, *Phys. Rev. D* **68**, 024012 (2003).

## NEMO

M. Cordelli, A. Martini, H. Roberto (Ass.), L. Trasatti (Resp.)

### 1 Activity

The NEMO project (construction of a kilometer cube detector for neutrino astronomy) has continued studying the properties of possible sites in the Mediterranean sea, and produced several instruments to study the marine depths. During the year 2005 the pilot project, NEMO Phase 1, has been preparing the first tower, made up of 4 floors, that will be deployed at the Catania Test Site in May 2006. In 2007 the second tower, made up of 8 floors, will be deployed in the Capo Passero final site.

The experiment includes groups from: INFN Bari, Bologna, Catania, Genova, LNF, LNS, Messina, Roma1.

The LNF group is still working on NERONE, an instrument to measure with great accuracy the water transparency using measurements performed at several distances from the source. We are planning a deployment at the end of march 2006. The group has also developed the console software for the NEMO Phase 1 project.

## OPERA

F. Bersani Greggio (Ass.), A. Cazes (Ass.Ric.), C. Di Troia (Dott.),  
B. Dulach, G. Felici, A. Franceschi, F. Grianti (Ass.), A. Gambarara (Tecn.),  
F. Mastropietro (Laur.), A. Mengucci (Tecn.), T. Napolitano, A. Paoloni (Art.23),  
M. Spinetti (Resp.), F. Terranova, M. Ventura (Tecn.), L. Votano

In collaboration with

LNF-SEA: A. Balla, G. Corradi, U. Denni, A. Frani, M. Gatta, G. Paoluzzi, G. Papalino  
LNF-SPAS: A. Cecchetti, D. Orecchini  
LNF-SSCR: G. Catitti, E. Iacuessa, A. Tiburzi  
LNF Divisione acceleratori: M. Incurvati, F. Iungo, L. Pellegrino, C. Sanelli

### 1 The experiment

OPERA <sup>1)</sup> has been designed to provide a very straightforward evidence for  $\nu_\mu \rightarrow \nu_\tau$  oscillations in the parameter region indicated by Super-Kamiokande as the explanation of the zenith dependence of the atmospheric neutrino deficit. It is a long baseline experiment located at the Gran Sasso Laboratory (LNGS) and exploiting the CNGS neutrino beam from the CERN SPS. The detector is based on a massive lead/nuclear emulsion target. The target is made up of emulsion sheets interleaved with 1 mm lead plates and packed into removable “bricks” (56 plates per brick). The bricks are located in a vertical support structure making up a “wall”. Nuclear emulsions are used as high resolution tracking devices for the direct observation of the decay of the  $\tau$  leptons produced in  $\nu_\tau$  charged current interactions. Electronic detectors positioned after each wall locate the events in the emulsions. They are made up of extruded plastic scintillator strips read out by wavelength-shifting fibers coupled with photodetectors at both ends. Magnetised iron spectrometers measure charge and momentum of muons. Each spectrometer consists of a dipolar magnet made of two iron walls interleaved with pairs of precision trackers. The particle trajectories are measured by these trackers, consisting of vertical drift tube planes. Resistive Plate Chambers (RPC) with inclined strips, called XPC, are combined with the precision trackers to provide unambiguous track reconstruction in space. Moreover, planes of RPCs (Inner Tracker) are inserted between the magnet iron plates. They allow a coarse tracking inside the magnet to identify muons and ease track matching between the precision trackers. They also provide a measurement of the tail of the hadronic energy leaking from the target and of the range of muons which stop in the iron. A block of 31 walls+scintillator planes, followed by one magnetic spectrometer constitutes a “super-module”. OPERA is made up of two supermodules located in the Hall C of LNGS (see Fig. 1). The total number of bricks amounts to 206,336 resulting in a target mass of 1766 tons. Bricks are automatically produced in situ by a “brick assembly machine” (BAM) and inserted into the wall support structure through a dedicated robot (BMS).

OPERA is able to observe the  $\nu_\tau$  signal with an impressively low background level. The direct and unambiguous observation of  $\nu_\mu \rightarrow \nu_\tau$  appearance will constitute a milestone in the study of neutrino oscillations. Moreover, OPERA has some sensitivity to the sub-dominant  $\nu_\mu \leftrightarrow \nu_e$  oscillations in the region indicated by the atmospheric neutrino experiments. It has been shown <sup>2)</sup>

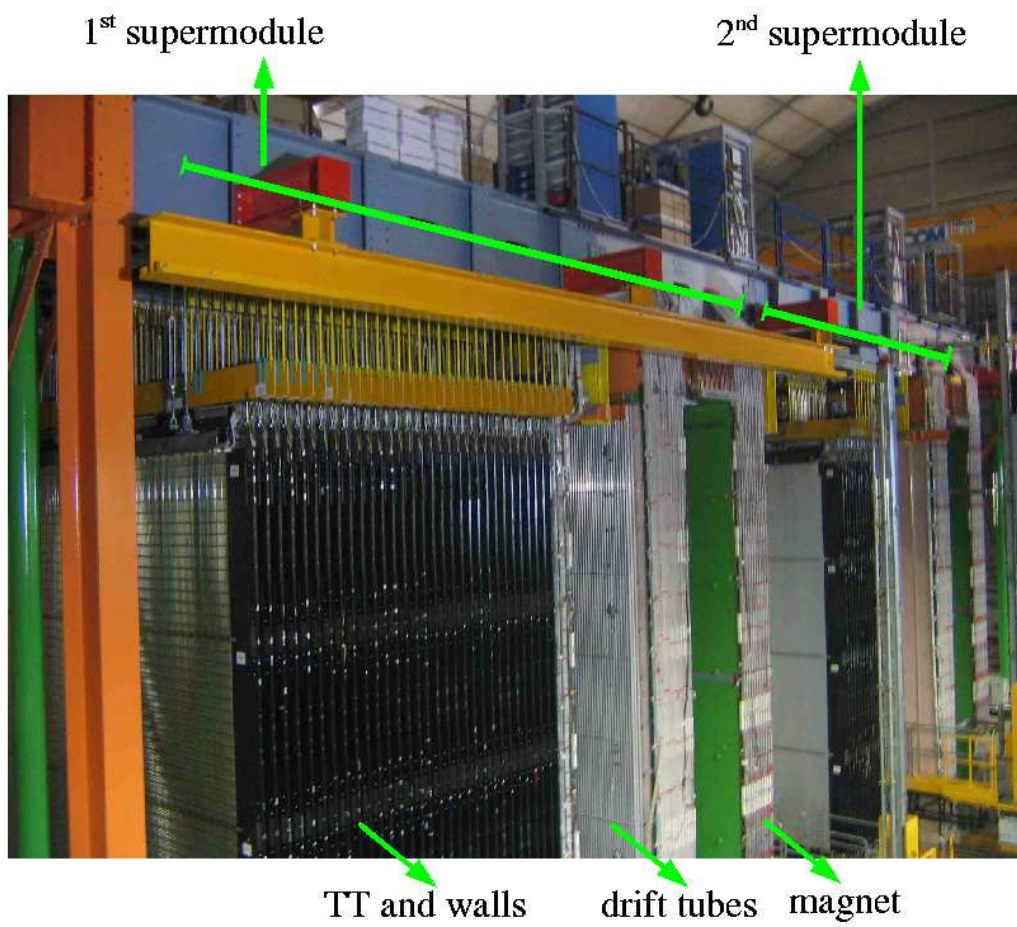


Figure 1: OPERA as in February 2006.

that the CNGS beam optimized for  $\nu_\tau$  appearance, will improve significantly (about a factor of three) the current limit of CHOOZ.

Opera is an international collaboration (Belgium, China, Croatia, France, Germany, Israel, Italy, Japan, Russia, Switzerland, and Turkey) and the INFN groups involved are Bari, Bologna, LNF, LNGS (Gran Sasso), Naples, Padova, Rome and Salerno. The Technical Coordinator of the experiment (M. Spinetti), the Chairperson of the Collaboration Board (L. Votano) and two of the OPERA project leaders (M. Spinetti for the magnets and A. Franceschi for the wall construction) are LNF researchers.

## 2 Overview of the OPERA activities in 2005

In 2005 most of the electronic detectors have been installed and a large part of the LNF commitments has been successfully carried out. The installation of the instrumented magnets was completed in April and the general structure (rails and platforms among the two magnets, and the support structure at the back of the experiment) was ended up in summer. The underground BAM site is ready since November 2005. In the meanwhile, all the wall support structures and scintillators for the first supermodule have been installed (see below). About 25 microscopes are under commissioning in Europe. Several components of the Japanese scanning system are ready (mechanics, CMOS camera, optics) while the track recognition part (system-embedded through FPGA's) is in progress.

## 3 Activities in Frascati

The Frascati group is responsible for the design and construction of the dipolar magnets and the general support structure for the subdetectors. It shares responsibility with INFN Padova and LNGS for the construction and installation of the bakelite RPC planes (Inner Tracker). Frascati and Naples also designed and prototyped the wall support structures housing the lead/emulsion bricks and LNF is responsible for their production and installation. Moreover, the group contributes to software development and to the analyses aimed at assessing the performance of the experiment after the completion of the CNGS programme. Since 2002 LNF is involved in the construction of the Brick Assembly Machine (BAM) and will contribute to the emulsion scanning with two dedicated microscopes located in Frascati.

### 3.1 OPERA General layout

The overall support structure for the OPERA subdetectors has been designed by LNF-SPAS in collaboration with external firms. Its installation started in 2004 after the completion of the first spectrometer: the support rails, upper floor and the seismic dumping structure for the first supermodule were positioned. In spring 2005 (completion of the second magnet) the rails among the two magnets have been installed together with the support structure at the back of the experiment (see Fig.2). As for 2004, LNF-SPAS follows closely the installation procedure at LNGS; together with LNGS staff, it coordinates material transportation and logistics and validates the installation operations done by the external firms. Moreover, LNF-SPAS played a crucial role in the design of the mechanics for the drift tubes, it took care of the installation and alignment of the rails for the



Figure 2: Seismic support structure at the back of OPERA.

BMS and, in general, it has been dealing with the coordination and interference handling of all operations in Hall C. Due to this special role, the overall technical coordination of the experiments is under responsibility of Frascati (M. Spinetti).

### 3.2 Magnets

The installation of the iron slabs and the active detectors (see next section) for the OPERA instrumented magnets has run in parallel. The first magnet was completed in 2004 while the second in March 2005 (see Fig.3). Thereafter, the upper return yoke, the coil and the coil cooling system was mounted (April 2005). In the meanwhile, the devices for field monitoring (pickup coils and Hall probes) was installed, too. The water cooling system for the spectrometers has been designed in 2004 in collaboration with L. Pellegrino (LNF-Div.Acc.) and R. Adinolfi Falcone (LNGS) but the tender was completed only in Sep 2005 due to delays related to LNGS safety procedures during non-INFN works at Gran Sasso: since 2003 modifications of the LNGS and Gran Sasso highway infrastructures have been planned by the Commissioner appointed by the Italian government (July 2003) after the Borexino accident (see <sup>3)</sup>) and works are still in progress. In particular, in 2005 all works in Hall C have been completed while the Gran Sasso highway tunnel has been partially closed from Sep 2005 until Feb 2006. The tender for the high current power supplies driving the magnet coils has been made in 2004 and the devices were completed in Dec 2005. Follow-up of the construction and tests of these devices have been carried out in collaboration with LNF Acc. Div. (M. Incurvati, C. Sanelli) and INFN Padova (A. Bergnoli).

### 3.3 Inner Trackers

The mass production of the Resistive Plate Chambers ended at the beginning of 2005 and, as mentioned above, the installation of RPCs inside the second magnet was completed in March, following the same procedures as for the first spectrometer <sup>3)</sup>. Before the installation, extensive quality tests have been carried out at the LNGS external laboratory <sup>3)</sup>. The large number of tested RPCs (>1000) allowed a detailed assessment of the main parameters <sup>4)</sup>. In particular, it

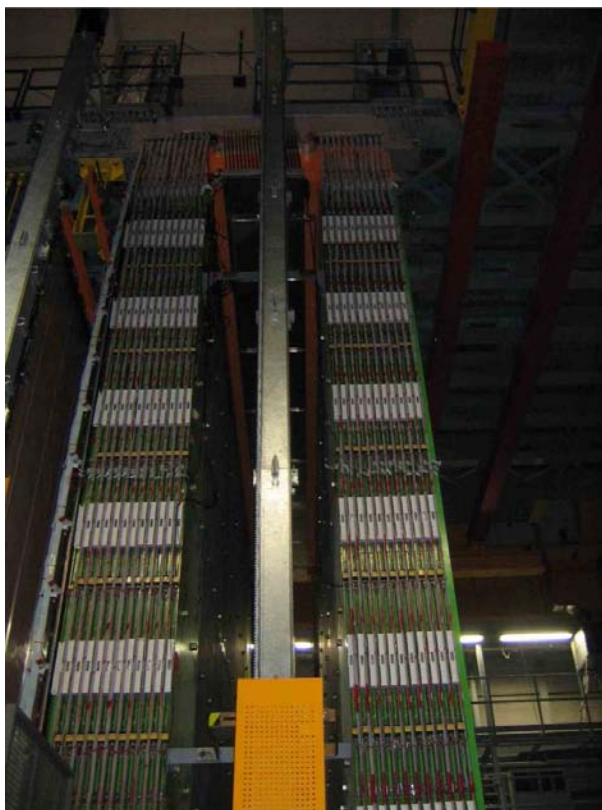


Figure 3: The second instrumented magnet.

was demonstrated that the ohmic current, the operating current and the intrinsic noisiness decrease with the electrode resistivity.

In order to study the time evolution of detectors showing up local noisy areas (hot spots), long term operation tests <sup>5)</sup> have been performed on six RPCs, which were rejected by the quality control (QC) tests. After eight months of operation at surface, equivalent to 13 years of operation underground, the detectors show stable currents (lower than  $1 \mu\text{A}$ ) and counting rates (around  $300 \text{ Hz/m}^2$ ), with no efficiency loss. The test also showed that the local intrinsic noise increases with the temperature, while it is damped by high resistivity electrodes ( $> 10^{12} \Omega\text{cm}$ ).

A realistic test of the RPCs installed in OPERA was performed during spring 2005. Four RPC layers of the first spectrometer (84 chambers) were instrumented to reconstruct cosmic muon tracks. The test was performed in absence of magnetic field using  $\text{Ar}/\text{C}_2\text{H}_2\text{F}_4/i - \text{C}_4\text{H}_{10}/\text{SF}_6 = 75.4/20.0/4.0/0.6$  premixed gas bottles <sup>6)</sup>. In figure 4 the efficiency of a chosen layer is shown as a function of the voltage.

At 5.6 kV average currents of 260 nA for one row composed of three RPCs were measured. Counting rates of  $17 \text{ Hz/m}^2$  were also measured and are shown in figure 5. The rate of cosmic muons crossing the four layers (about 16 muons/h) was found to be consistent with a MC simulation tuned on MACRO data. In figure 6 the angular distribution of the reconstructed muons is shown; events with multiple muons were also observed.

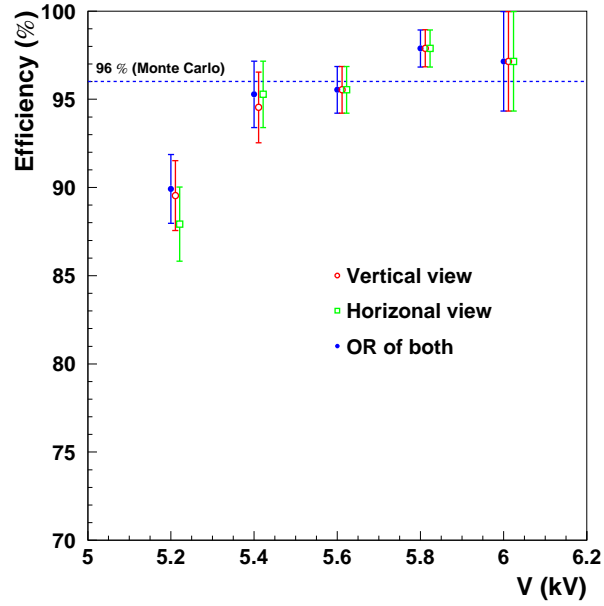


Figure 4: RPC layer efficiency as a function of the operating voltage.

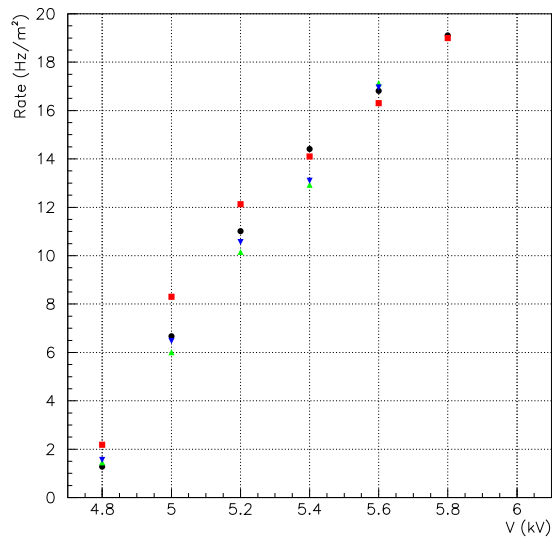


Figure 5: Counting rates as a function of the operating voltage for the four tested RPC layers.

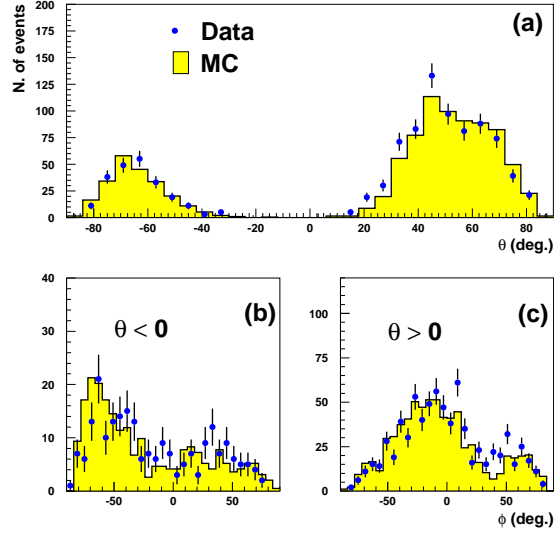


Figure 6: Cosmic angular distributions. The top plot (a) shows the distribution of the muon angle with respect to the horizon projected in the vertical plane containing the  $\nu$  beam axis ( $\theta$ ). The lower plots (b,c) show the azimuthal angle ( $\phi$ ) distribution for muons coming along or opposite the  $\nu$  beam ( $\theta <, > 0$ ).

The tasks concerning the design and construction of the RPC electronics are shared among LNF-SEA (strip boards, current monitoring, timing boards), Padova (front-end boards) and Napoli (controller boards interfaced to DAQ) and coordinated by LNF-SEA. In 2005 the cabling of the signal and HV was completed for both magnets and all current-meters have been installed. The timing board design has been finalized according to the results of cosmic ray tests performed at LNF on small size RPCs operated with the OPERA gas mixture. The timing system is described in <sup>8)</sup>. During 2005 the production of 260 timing boards and of their control electronics has been completed. The LNF OPERA group also contributed to the design of the Precision Trackers trigger, performed separately in each spectrometer with 9 RPC layers <sup>9)</sup>.

### 3.4 Wall support structure

The wall support structure (“walls”) is made of thin stainless steel vertical bands welded to light horizontal trays where the bricks are positioned with a precision of one millimeter. The structure is suspended through rods and joints from the general support structure and tensioned from the bottom through a spring system. The walls are installed in parallel with the plastic scintillators (Target Trackers, TT). During 2004 the production cycle has been finalized by LNF-SSCR and the external firm in charge of the mass production. Since the end of the year, the production cycle has been running well within specifications with a production rate of about 1.2 walls per week. During 2005 all walls of the first supermodule were installed (May-Nov, see Fig.7) after a three month delay. The latter was due to difficulties in the mounting of the scintillators, which was cured

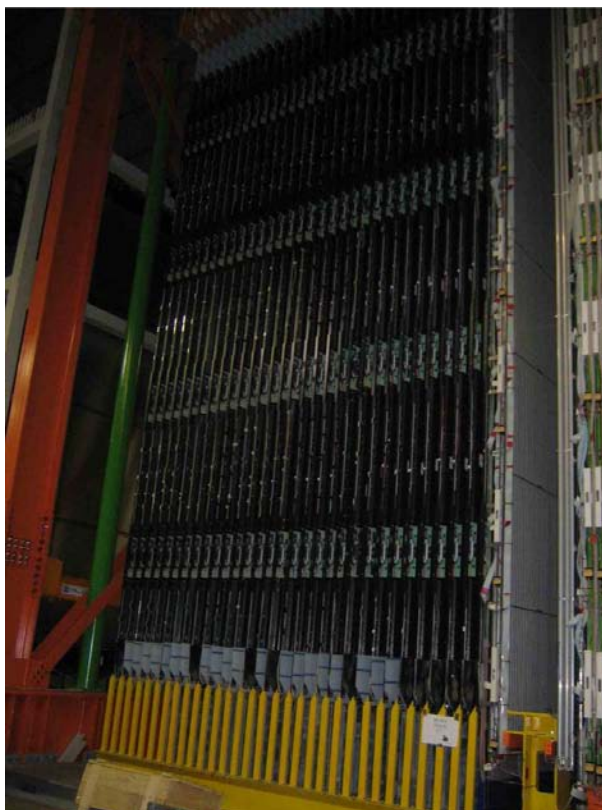


Figure 7: The target of the first supermodule (walls and TT's).

through a change of the pitch between walls and TT's and, hence, a modification of the supporting rails. Installation of the second supermodule is in progress and completion is expected by spring 2006. The installation rate has exceeded the expectations and the quality of the wall alignment is well within specs.

### 3.5 Brick Assembly Machine

The basic design of the Brick Assembly Machine (BAM) has been fixed in 2004 after the endorsement of the new mechanical packaging for the bricks. LNF has contributed significantly to the studies that brought to this novel solution <sup>3)</sup>. In 2005, the activities the LNF-BAM group has mainly been focused on the optimization of the materials for packing and the follow-up of the construction in firm. In particular, the aluminum structure ("spider") that compacts and exerts a well-tuned pressure over the lead-emulsion bulk has been optimized. The design of the lead containers was tuned and finalized, as well. LNF follows continuously the progress in the construction at firm site and validates the solutions proposed during the production phase; commissioning at LNGS is foreseen in spring 2006. Finally, LNF is involved with the definition and implementation of the database that records the number and components of the bricks and that interfaces these information to the BMS and the general OPERA database.

### 3.6 Software and analysis

LNF contributes to the simulation of the magnetic spectrometers, the embedding of the magnetic field maps and the development of reconstruction algorithms for charged particles in the new offline framework for OPERA. In 2005 a very detailed map of the field has been embedded in the new OPERA simulation package, accounting for the magnet properties of the steels used for the slab and yoke production<sup>10</sup>). Moreover, track momentum reconstruction algorithms, based on the Kalman filter and using both RPC's and drift tubes has been developed in collaboration with Univ. of Hamburg. A topic that has been recently investigated at LNF is the monitoring of the CNGS beam through the identifications of muons emerging from the rock in coincidence with the CNGS spill. This channel offers the opportunity to tag in real-time (i.e. employing only the electronic detectors of OPERA) misalignments and time variations both during the commissioning phase of CNGS and during data taking. The analysis has been completed in autumn 2005<sup>11</sup>). Finally, LNF contributes to the development of the spectrometer slow control (SC) and in particular handles the interface with the overall OPERA DAQ/SC through a dedicated CORBA server.

### 4 List of Conference Talks by LNF Authors in Year 2005

1. A. Paoloni "Tests on OPERA Resistive Plate Chambers", The VIII Workshop on Resistive Plate Chambers and Related Detectors, Seoul, Korea.
2. F. Terranova, "Long-baseline neutrino oscillation experiments in Europe," AIP Conf. Proc. **794**, 211 (2005).
3. F. Terranova, "The CNGS physics programme", Frontier Science 2005: New frontiers in subnuclear physics, Milano, Italy.
4. F. Terranova, "The OPERA experiment", SLAC Experimental Seminar, Stanford, CA.

### References

1. M. Guler *et al.*, OPERA proposal, CERN/SPSC 2000-028, SPSC/P318, LNGS P25/2000.
2. M. Komatsu, P. Migliozzi, F. Terranova, J. Phys. **G29**, 443 (2003);  
P. Migliozzi, F. Terranova, Phys. Lett. **B563**, 73 (2003).
3. See "LNF 2004 Annual Report", E. Nardi ed., LNF-05/5 (IR), p.70; "LNF 2003 Annual Report", S. Dell'Agnello ed., LNF-04/08 (IR), p.64.
4. E. Carrara, A. Mengucci, A. Paoloni, M. Ventura, "Electrical tests on OPERA RPCs", OPERA note, 2004.
5. F. Mastropietro, "Tests on Resistive Plate Chambers for the OPERA experiment", Diploma Thesis, Univ. della Calabria, 2005.
6. A. Paoloni, "Commissioning of RPCs with cosmic ray muons", Talk at the OPERA General Meeting, May 26-28, 2005, LNGS.

7. A. Paoloni *et al.*, “Studies about mechanical deformations of RPCs installed the OPERA magnet gaps”, OPERA note, 2005.
8. G. Corradi *et al.*, “A 16 ch. Timing Board for the OPERA RPCs”, OPERA note, 2005.
9. G. Felici *et al.*, “Concept of the Trigger System for the Precision Tracker”, OPERA note, 2005.
10. A. Cecchetti, B. Dulach, D. Orecchini, G. Peiro, F. Terranova, “Chemical and Magnetic Characterization of the Steels for the Opera Spectrometers”, LNF-04/28(IR) and OPERA note, 2004.
11. C. Di Troia, “Lo spettrometro e la segnatura muonica in OPERA”, Ph.D. Thesis, Univ. of Naples, 2005.

## PVLAS-DTZ

E. Zavattini<sup>1</sup>, G. Zavattini<sup>2</sup>, G. Ruoso<sup>3</sup>, E. Polacco<sup>4</sup>,  
E. Milotti<sup>5</sup>, M. Karuza<sup>1</sup>, U. Gastaldi<sup>3</sup>, G. Di Domenico<sup>2</sup>, F. Della Valle<sup>1</sup>,  
R. Cimino (Resp. loc)<sup>6</sup>, S. Carusotto<sup>4</sup>, G. Cantatore<sup>1</sup>, M. Bregant<sup>1</sup>

<sup>1</sup>Dipartimento di Fisica and INFN, Trieste;   <sup>2</sup>Dipartimento di Fisica and INFN, Ferrara;  
<sup>3</sup>INFN, Laboratori Nazionali di Legnaro;   <sup>4</sup>Dipartimento di Fisica and INFN, Pisa;  
<sup>5</sup>Università di Udine and INFN Trieste;   <sup>6</sup>INFN, Laboratori Nazionali di Frascati;

The PVLAS collaboration is conducting experimental studies of vacuum magnetic birefringence and dichroism by operating a high-sensitivity ( $10^{-7}$  1/ $\sqrt{\text{Hz}}$ ) optical ellipsometer, located at the INFN Legnaro National Laboratory, Legnaro, Italy. This instrument is capable of detecting, using the heterodyne technique, both ellipticities and rotations in an independent way, down to levels below  $10^{-8}$  rad, for about one hour of data taking time. In 2005 we reported the first experimental observation of a light polarization rotation in vacuum in the presence of a transverse magnetic field <sup>1, 2, 3</sup>). The measured signal is generated within the PVLAS Fabry-Perot cavity when the magnet is energized. Assuming that data distribution is Gaussian, the average measured rotation is  $(3.9 \pm 0.5) 10^{-12}$  rad/pass, at 5 T with 44000 passes through a 1 m long magnet, with  $\lambda = 1064$  nm. The apparatus is described in the literature and in other annual reports. Here we show in fig. 1 a typical measured signal with and without magnetic field.

The observed rotation of the polarization plane of light propagating through a transverse magnetic field has the following characteristics: i) it depends on the presence of the magnetic field; ii) it is localized within the Fabry-Perot cavity; iii) it has the proper phase with respect to the magnetic field instantaneous direction. Experimentally, then, we find that vacuum induces a rotation of the polarization plane in the presence of a magnetic field. The possibility that this effect is due to an unknown, albeit very subtle, instrumental artifact has been investigated at length without success. Speculations on the physical origin of the measured signal suggest the possible presence of new physics. In fact, a possible explanation for the observed source of apparent rotation could be associated to a neutral, light boson produced by a two-photon vertex. In this photon-boson oscillation framework, both induced rotation and induced ellipticity can be expressed as functions of the particle mass  $m_b$  and of the inverse coupling constant to two photons  $M_b$ . Analysis performed by considering our data in combination with previously published limits, indicate that only one allowed segment of the the  $M_b$  vs.  $m_b$  curve is consistent with the PVLAS signal. Such allowed segment is contained in the intervals  $2 \cdot 10^5$  GeV  $< M_b < 6 \cdot 10^5$  GeV, and  $1$  meV  $< m_b < 1.5$  meV. Our results were presented in two international workshops and published, in 2005, in the related proceedings <sup>2, 3</sup>). Let us finally note here that a crucial check of these speculations could come from a photon-regeneration experiment of the type already attempted with laser light, but can certainly benefit from the use of an intense, very high flux soft X ray laser like the SPARXINO / SPARX FEL project of the LNF.

Also, during 2005, the Cotton-Mouton effect in neon <sup>4</sup>) has been measured. Using the highly sensitivity of our apparatus, we were able to precisely measure the specific birefringence value of  $\Delta\nu = (5.9 \pm 0.2)10^{16}$  at the wavelength of 1064 nm (for  $B = 1$  T and atmospheric pressure) and

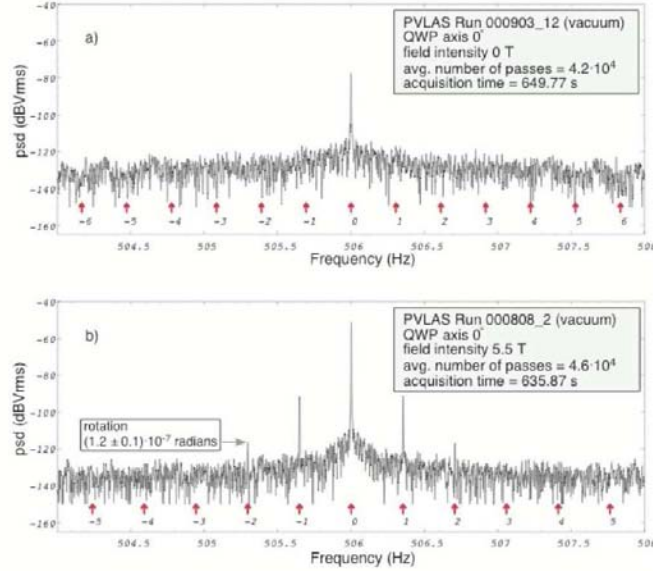


Figure 1: *Typical Fourier amplitude spectra from vacuum rotation data ( $P = 10^{-8}$  mbar) with and without magnetic field. Both spectra were taken with the magnet rotating. Arrows and numbers below the curves indicate the expected position of sidebands with frequency shifts that are integer multiples of  $\nu$ ; the relevant signal peaks correspond to frequency shifts of  $2\nu$ .*

$T = 290$  K. The results obtained are in agreement with theory, while the only previous precise measurement differs significantly. The experiments performed by injecting gas into the cavity are also of interest to cross-check the physical origin of our “in vacuum” signal <sup>2)</sup>.

## References

1. “Experimental observation of optical rotation generated in vacuum by a magnetic field”, PVLAS coll., Physical Review Letters, **96**, 110406 (2006).
2. “Experimental observation of magnetically induced linear dichroism of vacuum”, PVLAS coll., presented at the “XI International Workshop on Neutrino Telescopes”, Venezia, Italia, 22-25 febbraio 2005, Proceedings (Papergraf, Padova, 2005), p. 433.
3. “PVLAS results on laser production of axion-like dark matter candidate particles”, PVLAS coll., Proceedings of the Fifth International Workshop on the Identification of Dark Matter, by N.J.C. Spooner e V. Kudryavtsev, (World Scientific, Singapore, 2005).
4. “A precise measurement of the CottonMouton effect in neon”. PVLAS coll., Chem. Phys. Lett. **410** (2005) 288292.

## RAP

S. Bertolucci, B. Buonomo (Bors.), G.O. Delle Monache, G. Ceccarelli (Tecn.),  
R. Ceccarelli (Tecn.), M. De Giorgi (Tecn.), D. Di Gioacchino, V. Fafone, C. Ligi (Art.23),  
R. Lenci (Tecn.), A. Marini (Resp. Naz.), G. Mazzitelli, G. Modestino,  
G. Pizzella (Ass. Ric.), L. Quintieri (Art.23), F. Ronga (Resp.),  
P. Tripodi (Osp.)

### 1 Aim and description of the experiment

The primary scope of the experiment RAP is to measure the longitudinal vibrations of cylindrical test masses, impinged by the electrons provided by the DAΦNE Beam Test Facility (BTF), in order to investigate if a higher efficiency mechanism for the particle energy loss conversion into mechanical energy takes place when the bar is in the superconducting state.

The motivation of the experiment is related to the fact that the gravitational wave antenna Nautilus has detected high energy cosmic rays at a rate higher than the expectations when the bar was operated at  $T = 0.14$  K, that is in the superconductive ( $s$ ) state. On the contrary, the observed rate of high energy cosmic rays was in agreement with the expectations when the bar was operated at  $T = 1.5$  K, that is in the normal ( $n$ ) state.

The expectations rely on the thermo-acoustic model (TAM), which accounts for the excitations of the longitudinal modes of vibration of a cylinder due to the energy lost by particles in the interaction, inducing a local heating of the material with a consequent thermal expansion. According to TAM applied to a thin cylinder, if a particle normally impinges on the middle point of the generatrix then the maximum amplitude of the first longitudinal mode of oscillation (FLMO) is given by:

$$B_0 = \frac{2\alpha LW}{\pi c_v M},$$

where  $L$  and  $M$  are length and mass of the cylinder,  $W$  is the total energy lost by the particle in the cylinder,  $\alpha$  and  $c_v$  are respectively the linear thermal expansion coefficient and the specific heat at constant volume of the material. The expected FLMO maximum amplitude,  $X_{exp}$ , is given by  $X_{exp} = B_0(1 + \epsilon)$ , where  $\epsilon$  is estimated by a realistic montecarlo simulation, which takes into account the solutions at the 2nd order for the modes of oscillation of a cylinder, the transverse dimension of the beam at the impact point and the angles with the cylinder axis of the secondary particles showering in the bar. To evaluate  $B_0$  at different temperatures and for each beam pulse,  $\alpha$  and  $c_v$  are computed by interpolating data available on literature, while  $W$  is given by the product  $N_e \times \Delta E$ . The number of electrons per pulse,  $N_e$ , is measured by the BTF beam monitor facility, while the average energy lost by each electron in the interaction,  $\Delta E$ , is estimated by the montecarlo simulation. In order to assess TAM,  $X_{exp}$  is compared with the values of the measured FLMO maximum amplitude, which is given by  $X_{meas} = V_{meas}/(G\lambda)$ , where  $\lambda$  is the electro-mechanical conversion factor of the piezoelectric transducers (PZ),  $G$  is the amplifier gain and  $V_{meas}$  is the maximum amplitude of the signal component at the FLMO frequency, which is obtained by Fast Fourier Transform algorithms applied to the digitized Pz signals.

The experimental setup (*viz.* the beam, the test mass, the suspension system, the cryogenic and vacuum system, the mechanical structure hosting the cryostat, the readout and the data acquisition system) is described in the the paper listed in the bibliography.

INFN and Physics Department Università di Roma Tor Vergata and Kamerlingh Onnes Laboratory, Leiden University (The Netherlands) are participating institutions to the experiment.

## 2 Activities in the year 2005

Two lines of activity were performed in the past year: a) completion of the analysis of the data collected on the Al5056 bar and b) data taking with a Nb bar.

a) Data collected in the year 2004 with an Al5056 bar, the same aluminum alloy of Nautilus, have been analyzed for assessing the TAM predictions in the temperature range 270-4 K. The assessment is made by the parameter  $m$  fitting the relation  $X_{meas} = mX_{exp}$ . Table 1 shows the results obtained at different temperatures and Fig. 1 shows the values of  $X$  normalized to the total energy lost per pulse. A systematic error of 7%, quadrature of the beam monitor (3%) and the

$T[K]$	$m$	$\Delta m$
264	0.96	0.01
71	0.98	0.03
4.5	1.16	0.03

Table 1: *Al5056* - Values of  $m$  fitting  $B_{meas} = m B_{exp}$ .

PZ calibration (6%) accuracies, affects the measurements. This is the first time that, using this technique, TAM is assessed for an Al5056 bar operated below the room temperature. The results have been published on Astroparticle Physics.

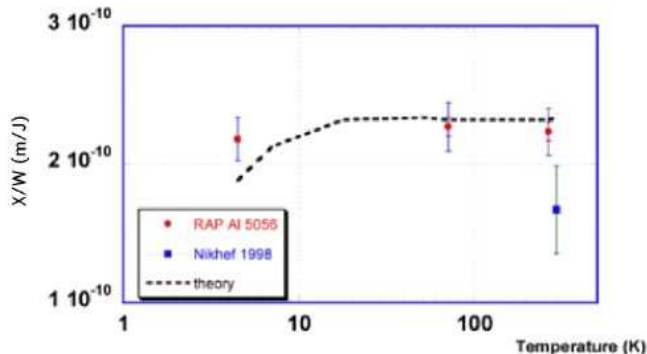


Figure 1: *Al5056* - Normalized FLMO maximum amplitudes vs. temperature. Dots: measured by RAP; square: measured by a past experiment at room temperatures; broken line: expected.

b) A dilution refrigerator is needed to perform measurements below the temperature of transition to ( $s$ ) state ( $T_c \sim 1K$ ) for Al5056. In waiting for the delivery of the dilution refrigerator a Nb ( $T_c \sim 10K$ ) bar has been used to have a first insight of TAM for a material in  $s$  state. Preliminary values of the  $m$  fitting parameter are given in Table 2 for the  $n$  state, showing a good agreement with the TAM predictions. Fig. 2 shows the measured FLMO maximum amplitudes normalized to  $W$  above and below  $T_c$ , together with the expectations computed by taking the values of the ratio  $\alpha/c_V$  in the  $n$  and  $s$  state respectively. The residual respect to the thermal contribution in the  $s$  state is under study in order to investigate possible local transitions effects.

$T[K]$	$m$	$\Delta m$
275	1.01	0.01
81	1.08	0.01
12.5	1.01	0.02

Table 2: Nb - Values of  $m$  fitting  $B_{meas} = m B_{exp}$ .

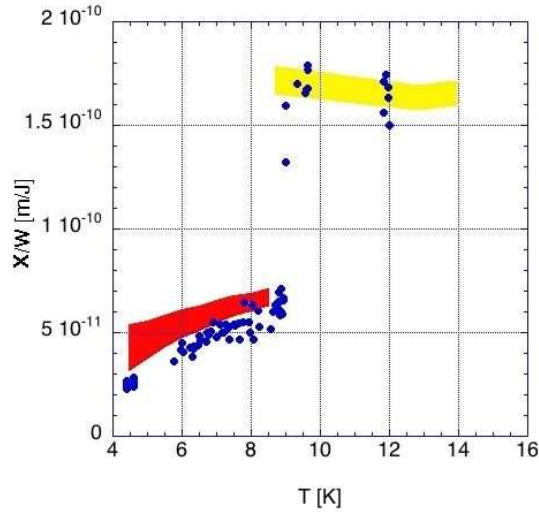


Figure 2: Nb - Normalized FLMO maximum amplitudes vs. temperature. Dots: measured; bands: expected from thermal effects.

### 3 Activities in the year 2006

The dilution refrigerator will be tested in the first quarter of the year. After this step the execution of measurements at  $T < 1$  K on the Al5056 bar is planned. Nb data analysis will be completed.

### 4 List of Conference Talks by LNF Authors in the Year 2005

1. G. Mazzitelli, First Results in Low Temperature Regime of the RAP Experiment, Amaldi 6 Conference, Okinawa (Japan).
2. L. Quintieri, RAP Collaboration: Acoustic Detection of Particles-The RAP Experiment Present Status and Result, TAUP 2005, Zaragoza (Spain).
3. C. Ligi, Rivelazione Acustica di Particelle in Cilindri di Alluminio e Niobio, SIF 2005, Catania (Italy).

### References

1. B. Buonomo *et al*, *Astropart. Phys.*, **24**, 65 (2005).
2. C. Ligi *et al*, *Int. J. Mod. Phys. A*, **20**, 7054 (2005).

## ROG

D. Babusci, V. Fafone (Resp.), G. Giordano, M. Iannarelli (Tecn.),  
R. Lenci (Tecn.), A. Marini, G. Modestino, G.P. Murtas (Ass.), G. Pizzella (Ass.),  
L. Quintieri (Art. 23), F. Ronga (Resp.), E. Turri (Tecn.)

Collaboration with INFN Roma 1, INFN Roma 2, LNGS, INFN Genova,  
University of Rome La Sapienza, University of Rome Tor Vergata,  
Geneva University, Leiden University

### 1 Introduction

The ROG group is currently operating two cryogenic gravitational wave (GW) bar detectors: EXPLORER (at CERN) and NAUTILUS (in Frascati)<sup>1)</sup>. The main goal of this search is the direct detection of the GW's that could be emitted by astrophysical sources (such as Supernovae or Coalescent Binaries). Such detection could be of enormous interest for general relativity and for astrophysics.

Both detectors consist of an aluminum cylindrical bar having a mass of 2.3 tons. The principle of operation of these detectors is based on the idea that the GW excites the first longitudinal mode of the bar (at about 1 kHz), which is cooled to cryogenic temperatures to reduce thermal noise, and is isolated from seismic and acoustic disturbances. To measure the strain of the bar, a capacitive resonant transducer, tuned to the excited mode, is mounted on one bar face, followed by a very low noise superconducting amplifier.

When searching for impulsive signals, the data are filtered with a adaptive filter matched to a delta-like signal. This search for bursts is suitable for any transient GW which shows a nearly flat Fourier spectrum at the two resonance frequencies of each detector.

Resonant-mass detectors are now in the continuous observational mode with a duty cycle near 100%.

The sensitivity of a GW detector can be expressed in terms of the so called spectral density  $\tilde{h}(f)$ . It represents the sum of the noise sources (the Brownian noise and the electronic noise) referred to the input of the detector (as if it was a GW spectral density). In the case of a resonant-mass detector, this function has a resonant behaviour and can be characterized by its value at the detector resonance frequencies and by its half height width, which gives the detection bandwidth. Another parameter which is used to describe the sensitivity to GW bursts is the noise temperature  $T_{eff}$ . It is obtained when the data are filtered to have the maximum signal to noise ratio in the case of delta-like signals and represents the minimum detectable energy innovation.

Thanks to the upgrades of the read-out systems, a significant increase in the detection bandwidth has been achieved. The present spectral amplitude is  $\tilde{h} \equiv \sqrt{S_h} \simeq 2 \cdot 10^{-21} \text{Hz}^{-1/2}$  with a bandwidth at the level of  $10^{-20} \text{Hz}^{-1/2}$  of about 40 Hz corresponding to a burst sensitivity  $h \simeq 3.4 \cdot 10^{-19}$ <sup>2)</sup>. Such a sensitivity should allow the detection of the strongest sources in our Galaxy and in the Local group.

Developments in bar detectors can be achieved improving the readout system and working at ultracryogenic temperatures, but much better sensitivities could be achieved developing new acoustic detectors. The near future evolution of resonant detectors is considered in the direction of a sphere design: a sphere allows isotropic sky coverage, determination of the source direction and wave polarization. The needed technology is defined and is currently under test in MiniGrail and

Schenberg <sup>3)</sup>, the 68 cm diameter spherical detectors being developed at the Leiden University and in Brasil. These evolutions of the current resonant antennas could permit to these devices to complement, in specific frequency ranges, the interferometers, allowing a precise reconstruction of the GW signal.

The LNF group has major responsibilities in the maintenance and running of NAUTILUS (including the production of liquid helium), in the maintenance, building and running of the cosmic ray detectors, in the development of a new nearly quantum limited signal read-out, in the data acquisition, in many items of data analysis and in the studies for the development of spherical GW detectors.

## 2 NAUTILUS and EXPLORER

The ultra-cryogenic detector NAUTILUS <sup>4)</sup> is operating at the Frascati INFN National Laboratory since December 1995. It is equipped with a cosmic ray detector.

The present data taking started in 2003, with a new bar tuned at 935 Hz, where a pulsar, remnant of the SN1987A, is supposed to emit GW's <sup>5)</sup>, with a more sensitive readout chain (the same as for EXPLORER), and a new suspension cable, to provide a more stable position setting. At present, the temperature of the bar is 3.5 K. The resulting strain noise (the minimum detectable spectral density) is  $\tilde{h} \simeq 1 \div 2 \cdot 10^{-21} / \sqrt{Hz}$  around 935 Hz, and  $\tilde{h} \leq 10^{-20} / \sqrt{Hz}$  over about 30 Hz. The noise temperature is less than 2 mK, corresponding to an adimensional amplitude of GW bursts  $h = 3.4 \cdot 10^{-19}$  <sup>2)</sup>. Better results in terms of sensitivity are expected when the system will be cooled down to 0.1 K during 2006. Thanks to a careful optimization of the working parameters of the detector, its duty cycle is now very high (about 90%), mainly limited by the cryogenic maintenance operations. The high duty cycle and the stationary behaviour are very important to realize a GW observatory and collect the data needed to perform coincidence analysis with EXPLORER and the other GW detectors.

The EXPLORER antenna is located at CERN and is very similar to NAUTILUS, but can operate only down to 2.6 Kelvin <sup>6)</sup>. The present data taking started in February 2004. Also the duty cycle of EXPLORER is very high (of the order of 90%) and the noise temperature of the order of 2 mK <sup>2)</sup>, with a strain sensitivity  $\tilde{h} \simeq 2 \div 3 \cdot 10^{-21} / \sqrt{Hz}$  around the two resonances at 904 Hz and 927 Hz, and  $\tilde{h} \leq 10^{-20} / \sqrt{Hz}$  over about 30 Hz. Also EXPLORER is equipped with a cosmic ray detector. Thanks to the larger bandwidth obtained with the read-out installed in 2001 on EXPLORER and in 2003 on NAUTILUS, a good time resolution (less than 10 ms) in the determination of the events due to the passage of cosmic rays has been reached <sup>7)</sup>.

Both EXPLORER and NAUTILUS will be upgraded during next year with a new nearly quantum limited read-out which will provide a noise temperature one order of magnitude better than present on EXPLORER and more than two orders of magnitude on NAUTILUS.

## 3 Read-out developments

The read-out of all the resonant-mass GW detectors is based on an electromechanical transducer (capacitive or inductive) and a d.c. SQUID amplifier.

In most practical applications the sensitivity of a SQUID with a standard electronics is usually good enough. However GW detectors require the highest possible sensitivity of a d.c. SQUID. In this case the standard read-out may not be the best solution, because the overall sensitivity can be limited by the room-temperature preamplifier noise. With this standard setup the typical energy resolution measured by the detector is about  $20000\hbar$ .

The sensitivity of a resonant-mass detector is limited by three sources of noise which, referred to the output are: the narrowband thermal noise, due to the input wideband brownian motion of the resonant masses, which appears at the output after passing through the mechanical transfer function of the system; the wideband amplifier noise, which appears directly at the output and the narrowband back-action noise, originated from the back-energy flow from the amplifier, which excites the resonant masses.

The useful bandwidth of such detectors is by no means limited to the very narrow width of the high  $Q$  mechanical resonance. Rather, it is the amplifier noise that limits the bandwidth. The lowest spectral noise is found in the frequency region where the narrowband (thermal plus back action) noises dominate the amplifier noise, and there the noise level is the sum of the two. As a consequence, any reduction in the amplifier noise and/or increase in transducer coupling, increases the antenna bandwidth.

In the last years, it has been shown <sup>8)</sup> that a double-SQUID system can reach quantum limit energy resolution and that a double-SQUID system can be arranged in a stable configuration when connected to a high- $Q$  resonant circuit.

The double-SQUID amplifier of the ROG Collaboration is made of a sensor d.c. SQUID, developed by the Institute of Photonic and Nanotechnologies of CNR, while the preamplifier SQUID is a commercial Quantum Design d.c. SQUID. The performances of the device are very good: with open input and open loop it exhibited <sup>8)</sup> energy resolutions equal to  $28\hbar$  at 4.2 K and  $5.5\hbar$  at 0.9 K. The system has been successfully tested with a high- $Q$  resonant input load in the temperature range 2 K-4.2 K. The device showed very good stability and an energy resolution of about  $(70 \pm 8)\hbar$  at 2 K has been measured <sup>9)</sup>.

With this new device, the expected NAUTILUS sensitivity at 0.1 K is around  $3 \cdot 10^{-22} \text{Hz}^{-1/2}$  and the bandwidth, at the level of  $10^{-21} \text{Hz}^{-1/2}$ , is about 35 Hz. The noise temperature of the detector should be around  $7\mu\text{K}$  corresponding to a sensitivity to 1ms bursts  $h = 2.1 \cdot 10^{-20}$ .

#### 4 Cosmic rays

The cryogenic resonant GW detectors EXPLORER and NAUTILUS are able to detect cosmic ray showers <sup>10)</sup>. The experimental result leads to classify the responses in two categories: many small signals, in most cases with small multiplicity, obeying the thermoacoustic model, and few large signals, usually associated to large multiplicity, which exceed the thermo-acoustic model by orders of magnitude, and whose understanding is still under investigation with the RAP experiment at LNF.

The cosmic ray showers, observed by EXPLORER and NAUTILUS, have already been used to estimate the time uncertainty of the events employed for the search of coincidences <sup>12)</sup>.

During 2005, the same measurements have been investigated to calibrate the detectors in energy. Using the low multiplicity showers, we can make a relative calibration of the apparatuses, comparing the response of EXPLORER with that of NAUTILUS. This comparison turns out useful when searching for coincidences between GW detectors <sup>13)</sup>.

A more accurate calibration of the two detectors also allowed to reduce the discrepancy of about a factor ten observed in 2004 between the response of NAUTILUS and EXPLORER to high multiplicity cosmic rays to about a factor 2 (the observed rate of EXPLORER is higher than that of NAUTILUS). This residual discrepancy might be due to the different cosmic ray detectors: plastic scintillators in EXPLORER and streamer tubes in NAUTILUS. In order to investigate this hypothesis we plan to install in 2006 two modules of plastic scintillators above the streamer tubes of NAUTILUS.

## 5 Data analysis

- **Search for coincidences between resonant bar detectors.** The analysis of the EXPLORER-NAUTILUS 2003 data has been completed (11, 12). During 2003, NAUTILUS and EXPLORER operated with a common time of 148.7 days. The energy sensitivity was of the order of 3 mK, corresponding to the detection with SNR=1 of a conventional GW burst of amplitude  $h \simeq 4 \cdot 10^{-19}$ , which was the best sensitivity ever reached for long data taking runs. Furthermore, the improvement in the bandwidth of NAUTILUS, with respect to the previous 2001 run, allowed us to lower the coincidence window from about 0.5 s to about 30 ms, lowering significantly the number of accidental coincidences.

The coincidence analysis gives 24 coincidences against 18.8 expected and the sidereal time analysis is not showing a significant departure from the background distribution, even if one can notice that in the sidereal hours where there was an excess in the 2001 data, again now there are more coincidences than accidentals.

The interpretation of the result of the 2001 run in terms of a possible continuous and uniform (in time) arrival of bursts signals at  $h \simeq 10^{-18}$  level is excluded by the present result at 95% confidence level. We report in Figure 1 the upper limit derived from the 2003 data in terms of a uniform flux. We must stress however that the number of the observed coincidences was not uniformly distributed in time (see Fig. 2).

EXPLORER and NAUTILUS are well operating, better than in 2003, without significant interruptions since the beginning of 2004, and we expect to complete this long run at the end of 2005.

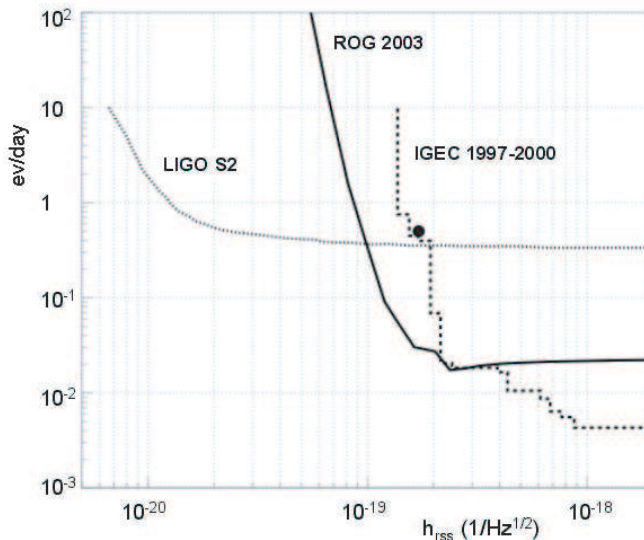


Figure 1: Upper limit at 95% on the rate of events arriving on Earth as a function of  $h_{rss}$ . The value of  $h_{rss}$  is numerically related to the adimensional  $h$  we use more commonly by  $h_{rss} \equiv 6.86 \cdot 10^{-2} h$ . The upper limits fixed by the second scientific run of LIGO and by the IGEC analysis are also reported. The large point represents roughly what could have been the rate (in terms of a uniform flux) deduced by our 2001 results (14).

- **IGEC analysis.** The bar detectors distributed worldwide operated for a few years as a network, giving for the first time significant upper limits to the yearly rate of GW burst events in the

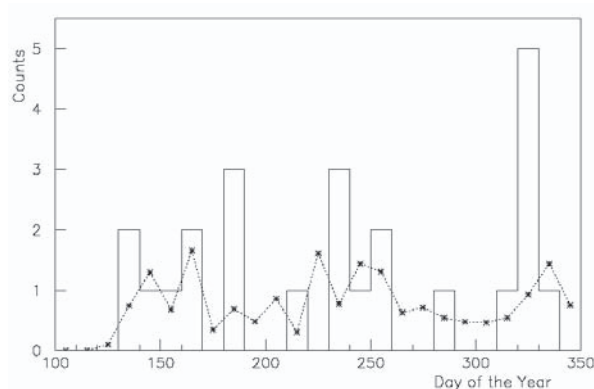


Figure 2: Number of coincidences (solid line) and the average number of accidentals (dashed line) as a function of the day of the year, in 10-days bin.

Galaxy <sup>15)</sup> (see Fig. 1). In 2003 and 2004 EXPLORER and NAUTILUS have been the only two detectors in data taking over long time periods. Since May 2005 both Auriga at LNL and Allegro at the Louisiana State University are taking data. We plan to perform in 2006 a coincidence analysis among all the four detectors.

In November 2005 LIGO started a one-year long data taking run. The data collected during this period will be analyzed for the search of impulsive signals from astrophysical sources in coincidences with the INFN bars in operation.

**- Search for coincidences with gamma ray bursts and other astrophysical events.** The statistical association between the output of the GW detectors EXPLORER and NAUTILUS and a list of Gamma Ray Bursts (GRBs) detected by the satellite experiments BATSE and BeppoSAX has been analyzed using cumulative algorithms. GW detector data collected between 1991 and 1999 have been searched for an energy excess in a 10 s interval around the GRB flux peak times. The cumulative analysis of the data relative to a large number of GRBs (387) allows to push the upper bound for the corresponding GW burst amplitude down to  $h = 2.5 \cdot 10^{-19}$  <sup>16)</sup>.

The analysis of the correlation of the EXPLORER and NAUTILUS data with different astrophysical sources, such as magnetars <sup>17)</sup> is in progress.

**- Search for monochromatic signals.** We have analysed three data sets, each two days long, of the EXPLORER resonant bar detector <sup>18)</sup>. We have searched for continuous gravitational-wave signals from spinning neutron stars. Our data analysis technique was based on the maximum likelihood detection method. The main outcome of our analysis is an upper limit of  $1 \cdot 10^{-22}$  for the dimensionless amplitude of a continuous GW signal. The upper limit is for any source location in the sky, any polarization of the wave and for signals of frequency from 921.00 Hz to 921.76 Hz and with spin down from  $-2.36 \cdot 10^{-8}$  Hz/s to  $+2.36 \cdot 10^{-8}$  Hz/s.

## 6 Advanced detectors

The LNF group is involved in the development of resonant-mass detectors of spherical shape. A single sphere is capable of detecting GW's from all directions and polarizations and is capable of determining the direction information and tensorial character of the incident wave.

A sphere will have a larger mass than the present bars (with the same resonance frequency), turning into an increased cross section and improved sensitivity. Omnidirectionality and source direction finding capability make a spherical detector a unique instrument for GW astronomy

with respect to all present detectors. At present, two small spheres (about 1 ton) are being developed: one in Brasil and one (MiniGRAIL) in Holland. The ROG group is collaborating with the Leiden University group for the development of MiniGRAIL, mainly on new read-out chains, data acquisition and of cosmic ray effect .

The results obtained with the MiniGRAIL detector <sup>19)</sup>, allowed to test techniques useful for a large spherical antenna. MiniGRAIL is large enough to develop techniques applicable to a large antenna, but is of a sufficiently manageable size to allow for rapid measurements and design changes. It has been important to address issues such as the design and construction of a complete cryogenic system, mechanically decoupled from the suspension system and the detector, the operation of the cryogenic system at a very low acoustic noise level, the possibility of rapidly cooling a 1 meters diameter sphere to low temperatures, the design and construction of a suspension system with at least -350 dB of attenuation, without appreciable upconversion mechanisms, the investigation of the problems of data acquisition and processing by observing the 5 quadrupole modes of a sphere.

The proposal for the construction of a GW resonant-mass spherical detector 2 meters in diameter, with a mass of 33 tons, is at present under discussion <sup>20)</sup>. The expected sensitivity of this detector will be equal to or even better than that of a large scale interferometer such as VIRGO or LIGO, over the frequency range 900-1100 Hz, thus making the observatory very powerful in terms of GW signals identification and characterization.

## 7 List of Conference Talks by LNF Authors in Year 2005

1. G. Pizzella, Inizio della ricerca di onde gravitazionali in Italia: attività del gruppo di Roma, Convegno di Gravitazione e Cosmologia dell'Accademia Nazionale delle Scienze detta dei Quaranta, Roma, Italy.
2. V. Fafone, Developments in Resonant-Mass Detectors, 6th Edoardo Amaldi Conference on Gravitational Wave, Okinawa, Japan.
3. F. Ronga, Detection of gravitational waves with resonant antennas, IX International Conference on Topics in Astroparticle and Underground Physics, Zaragoza, Spain.
4. V. Fafone, SFERA: the new spherical gravitational wave detector, IX International Conference on Topics in Astroparticle and Underground Physics, Zaragoza, Spain.

## References

1. [www.lnf.infn.it/esperimenti/rog](http://www.lnf.infn.it/esperimenti/rog)
2. P. Astone *et al.*, (ROG Collaboration), "Status report on the EXPLORER and NAUTILUS detectors and the present science run ", in: Proc. 6th Edoardo Amaldi Conference on Gravitational Waves, Class. Quantum Grav., in press.
3. [www.minigrail.nl](http://www.minigrail.nl), [www.das.inpe.br/~graviton/](http://www.das.inpe.br/~graviton/)
4. P. Astone *et al.*, (ROG Collaboration), *Astropart. Phys.* **7**, 231 (1997).
5. J. Middleditch *et al.*, *New Astronomy* **5**, 243 (2000).
6. P. Astone *et al.*, (ROG Collaboration), *Phys. Rev. D* **47**, 362 (1993).
7. P. Astone *et al.*, (ROG Collaboration), *Phys. Rev. Lett.* **91**, 111101 (2003).

8. P. Carelli *et al.*, Appl. Phys. Lett. **72**, 115 (1998).
9. M. Bassan *et al.*, “A new capacitive read-out for EXPLORER and NAUTILUS”, in: Proc. 6th Edoardo Amaldi Conference on Gravitational Waves, Journal of Phys. Conference Series, in press.
10. P. Astone *et al.*, (ROG Collaboration) Phys. Rev. Lett **84**, 14 (2000).
11. G. Pizzella, “Coincidences between the gravitational wave detectors EXPLORER and NAUTILUS ”, Nuovo Cimento B **120**, 591 (2005).
12. P. Astone *et al.*, (ROG Collaboration), “The 2003 run of the EXPLORER-NAUTILUS gravitational wave experiment”, in: Proc. 6th Edoardo Amaldi Conference on Gravitational Waves, Class. Quantum Grav., in press.
13. G. Modestino, G. Pizzella, F. Ronga, “Calibration of the resonant gravitational wave detectors EXPLORER and NAUTILUS in 2003 and 2004 using cosmic rays”, LNF05/ 27 (IR) 20 Dicembre, 2005.
14. P. Astone *et al.*, (ROG Collaboration), Class. Quantum Grav. **19**, 5449 (2002).
15. P. Astone *et al.*, (IGEC Collaboration), Phys. Rev. D **68**, 022001 (2003).
16. P. Astone *et al.* (ROG Collaboration), “Cumulative analysis of the association between the data of the gravitational wave detectors NAUTILUS and EXPLORER and the gamma ray bursts detected by BATSE and BeppoSAX”, Phys. Rev. D **71**, 042001 (2005).
17. L. Stella *et al.*, Astrophys. Journal **634**, L165 (2005).
18. P. Astone *et al.*, (ROG Collaboration), “An all-sky search of EXPLORER data ”, Classical Quantum Grav. **22**, S1243 (2005).
19. V. Fafone *et al.*, “MiniGRAIL progress report 2004”, Classical Quantum Grav. **22**, S215 (2005).
20. ROG Collaboration, SFERA: Proposal for a Spherical Gravitational Wave Detector, LNF-06-08 (IR) 28 Febbraio, 2006.

## WIZARD

G.Basini, F.Bongiorno (Ass.), L.Bongiorno (Ass.Ric.),  
G.Mazzenga (Tecn.), M.Ricci (Resp.)

Participant Institutions:

ITALY: INFN Bari, LNF, Firenze, Napoli, Roma Tor Vergata, Trieste;  
CNR Ist. Fisica Applicata “Nello Carrara” Firenze;  
ASI (Italian Space agency);  
Electronic Engineering Department, University of Roma 2 “Tor Vergata”;  
RUSSIA: MePhi Moscow;  
FIAN Lebedev Moscow;  
IOFFE St Petersburg;  
TsSKB-Progress Samara;  
SWEDEN: KTH Stockholm;  
GERMANY: Siegen University;  
USA: NASA Goddard Space Flight Center;  
New Mexico State University.

### 1 Experimental Program and Scientific Objectives

The WIZARD experimental program is devoted to the extensive study of cosmic ray spectra (particles, antiparticles, isotopes, abundances and search for antimatter) in several energy ranges achievable through different instruments on board stratospheric balloons and long duration satellite missions. WIZARD is an International Collaboration between several Universities and Research Institutions from Russia, Sweden, Germany, USA together with the Space Agencies NASA, RSA (Russia), SNSB (Sweden), DLR (Germany) and ASI. The experimental activities have been and are carried out through three main programs:

- Balloon flights;
- Satellite missions NINA-1 and NINA-2;
- Satellite mission PAMELA.

We refer to previous editions of this report for the description of the activities related to the balloon flights and to the two NINA missions.

#### 1.1 The satellite mission PAMELA

PAMELA is a cosmic ray space experiment that will be installed on board a Russian satellite (Resurs-DK1) whose launch is foreseen in the first half of 2006 from the cosmodrome of Baikonur, Kazakhstan, by a Soyuz TM2 rocket. The satellite will fly for at least 3 years in a low altitude, elliptic orbit (300-600 km) with an inclination of 70.4 degrees. The PAMELA telescope consists of a magnetic spectrometer composed of a permanent magnet coupled to a silicon tracker, an electromagnetic silicon-tungsten calorimeter, a time-of-flight system, an anticoincidence system, a shower tail catcher scintillator and a neutron detector <sup>1, 2</sup>). A sketch of the PAMELA instrument is shown in fig.1.

The total height of PAMELA is 120 cm, the mass is 450 kg and the power consumption is 360 W.

The observational objectives of the PAMELA experiment are to measure the spectra of antiprotons, positrons and nuclei over an extended range of energies, to search for antimatter and

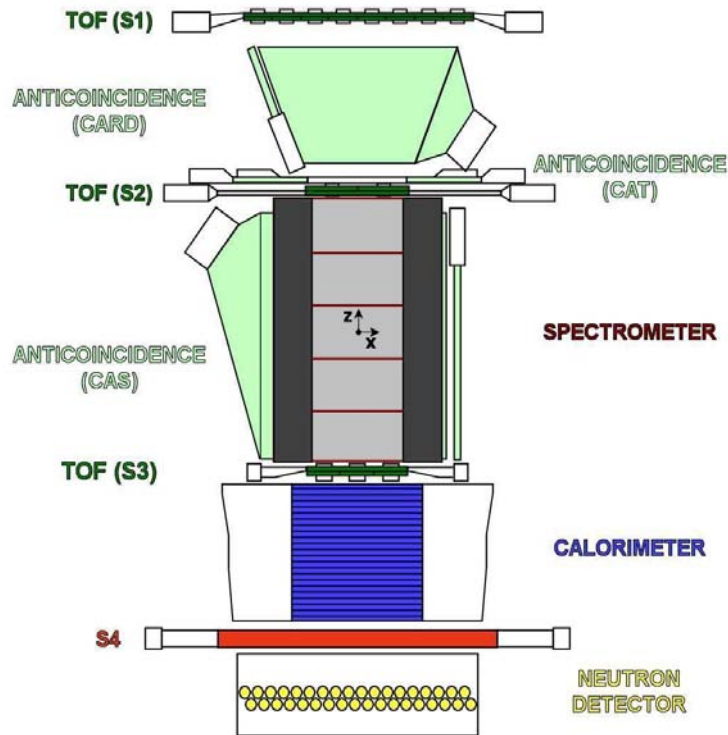


Figure 1: Sketch of the PAMELA telescope.

for indirect signatures of dark matter and to study cosmic ray fluxes over a portion of the Solar cycle.

The main scientific goals can be schematically listed as the following:

- a) measurement of the antiproton spectrum in the energy range 80 MeV-190 GeV;
- b) measurement of the positron spectrum in the energy range 50 MeV-270 GeV;
- c) search for antinuclei with a sensitivity of  $\sim \times 10^{-8}$  in the  $\overline{He}/He$  ratio;
- d) measurement of light nuclei spectra (up to  $Z=6$ ) at energies 100 MeV/n - 200 GeV/n;
- e) measurement of the electron spectrum up to 2 TeV.

In addition, the PAMELA experiment will be able to measure the light nuclear component of cosmic rays and investigate phenomena connected with Solar and Earth physics.

Activity in the year 2005 has covered the following items:

- Completion of PAMELA Flight Model, integration and ground tests with cosmics in Roma Tor Vergata assembly facility and clean rooms.
- Establishment of the PAMELA data network and Data Center (through CNAF, Bologna).
- Shipment and delivery of Flight Model to TsSKB Progress plant (Samara, Russia).
- Tests and integration with spacecraft Resurs DK1.

## 2 Activity of the LNF group during year 2005

The LNF WIZARD group has been fully involved in all the previous balloon and present satellite programs.

During the year 2005 the activity for the PAMELA experiment has been carried on as follows:

- Responsibility of the Mechanical Ground Support Equipment (MGSE) for the assembly and integration of the whole apparatus.
- Preparation, assembly and tests of the Flight Model.
- Completion and equipment of the transport container for the Flight Model.
- Definition and organization of the data base of the command-control procedures from ground.

## 3 Planned activity in 2006

- Pre-launch readiness tests and launch from Baikonur Cosmodrome (Kazakhstan).
- Additional Beam tests of detectors of the Technological/Engineering Model at GSI/Darmstadt (nuclei) and CERN/SPS (protons).
- Data taking in flight: first phase and establishment of downlink procedures.
- Final set-up and operation of the main (Russia) and peripheric (Roma Tor Vergata) ground control and data receiver centers.

## 4 List of Publications in 2005

1. R.Sparvoli *et al.*, "Launch in orbit of the Space Telescope PAMELA and Ground Data Results" , Proc. 9th ICATPP Conf. on Astroparticle, Particle, Space Physics and Medical Physics Applications (Como, Italy, 2005)
2. A. Basili *et al.*, "The PAMELA Data Acquisition System", Proc. 9th ICATPP Conf. on Astroparticle, Particle, Space Physics and Medical Physics Applications (Como, Italy, 2005)
3. V.Malvezzi *et al.*, "Performance of neutron detector and bottom trigger scintillator of the space experiment PAMELA", Proc. 9th ICATPP Conf. on Astroparticle, Particle, Space Physics and Medical Physics Applications (Como, Italy, 2005)
4. S.Russo *et al.*, "The Time of Flight detector and trigger for the PAMELA experiment in space", Proc. 9th ICATPP Conf. on Astroparticle, Particle, Space Physics and Medical Physics Applications (Como, Italy, 2005)
5. A.Leonov *et al.*, "Pitch angle distribution of trapped energetic protons and helium isotope nuclei measured along the Resurs-01 N0.4 LEO satellite", *Ann.Geophysicae*, **23**, 1 (2005)

## References

1. M.Boezio *et al.*, "The PAMELA Space Experiment" , Proc. 29th International Cosmic Ray Conference (Pune, India 2005) **OG 1.5** p.101.
2. R.Sparvoli *et al.*, "Launch in orbit of the Space Telescope PAMELA and Ground Data Results" , Proc. 9th ICATPP Conf. on Astroparticle, Particle, Space Physics and Medical Physics Applications (Como, Italy, 2005).

## AIACE

E. De Sanctis (Dir.), M. Mirazita (Art.23), J. de Oliveira Echeimberg (Dott.), A. Orlandi (Tech.),  
S. A. Pereira (Ass.), W. Pesci (Tech.), E. Polli, F. Ronchetti (Ass. Ric.),  
P. Rossi (Resp. Naz.), A. Viticchié (Tech.)

### 1 Introduction

AIACE stands for Attività Italiana A CEbaf. It is the collaboration of the INFN groups of Frascati and Genova which participate into the physics program carried in the Hall B at the 6 GeV Continuous Electron Beam Accelerator Facility (CEBAF) at the Jefferson Laboratory (JLab). The Hall B collaboration counts about 140 physicists from 35 Institutions from seven Countries.

The scientific program of Hall B, which is equipped with the CLAS detector, is the precision study of the structure of the nucleon and the nature of the strong interaction.

This scientific program can be summarized in the following main topics: search for exotic mesons and baryons, dynamics of the strong interactions, spin structure functions in the resonance region, nucleon tomography, baryon resonances.

In the period covered by this report the Frascati group has carried out:

- the publication on Physical Review Letters of the paper on the onset of asymptotic scaling in the deuteron photodisintegration cross section.
- The publication of the paper “*Comparative Regge analysis of  $\Lambda, \Sigma^0, \Lambda(1520)$  and  $\Theta^+$  production in  $\gamma p, \pi p$  and  $pp$  reaction*”.
- The completion of the analysis of the data taken in spring 2004 for the search of the pentaquark  $\Theta^+$  in the reaction  $\gamma d \rightarrow \Theta^+ \Lambda$ .
- The write-up of the paper “*Search for the  $\Theta^+$  pentaquark in the  $\gamma d \rightarrow \Lambda n K^+$ ” to be submitted to Physical Review Letter.*
- The start-up of the data analysis of the reaction  $\gamma n(p) \rightarrow K^+ \Sigma^-(p)$  and  $\gamma p(n) \rightarrow K^+ \Lambda(n)$ .
- The elaboration of a Letter of Intent to measure the nucleon form factor in the time-like region with DAΦNE.
- The organization of the “*N05 international workshop on the nucleon form factors*”.
- The presentation of the results at conferences, workshops and seminars.

### 2 Onset of asymptotic scaling in exclusive photoreactions

**2.1 Deuteron photodisintegration (Experiment E93-017):** Deuteron photodisintegration at high energies is a very suited reaction to study the transition from hadronic picture to quark-gluon picture in nuclear reactions due to the relatively large amount of momentum transferred to the nucleons for a relatively low incident photon energy. One possible signature for this transition is the scaling of reaction cross sections above some incident photon energy. In particular, simple Constituent Counting Rules predict an asymptotic  $s^{-11}$  dependence of  $d\sigma/dt$  of the process at all proton angles. Here  $s$  and  $t$  are the invariant Mandelstam variables.

To give a clearer answer to this important question, the CLAS experiment E93-017 at Jefferson Lab performed an extensive measurement of the deuteron photodisintegration cross section between 0.5 and 3.0 GeV and over an almost complete proton angular range ( $\vartheta_p^{\text{CM}} = 10^\circ - 160^\circ$ ). These recent, extensive cross section data <sup>1)</sup> (together with all previous data) offered the unique opportunity for a detailed study of the energy dependence of the  $d(\gamma, p)n$  differential cross section at fixed angles to looking for the onset of cross section scaling at some incident photon energy.

The obtained results show that the  $s^{-11}$  scaling is reached for proton transverse momentum above about 1.1 GeV/c and for  $\vartheta_p^{CM}$  between  $50^\circ$  and  $130^\circ$  <sup>2)</sup>.

**2.2 Single pion photoproduction:** Single pion photoproduction reactions are essential probes of the transition from meson-nucleon degrees of freedom to quark-gluon degrees of freedom in exclusive processes. The cross sections of these processes are also advantageous, for investigation of the oscillatory behavior around the quark counting prediction, since they decrease relatively slower with energy ( $s^{-7}$ ) compared with other photon-induced processes. Recent data from JLab Hall A show dramatic change in the scaled differential cross section from the  $\gamma n \rightarrow \pi^- p$  and  $\gamma p \rightarrow \pi^+ n$  processes in the c.m. energy between 1.8 GeV to about 2.4 GeV and for  $\theta_{CM} = 90^\circ$ . The Frascati group has started the analysis of the g10 data on the  $\gamma n \rightarrow \pi^- p$  to investigate this behavior in much finer photon energy bins and for a wide angular range and to study the angular dependence of the scaling behavior. The analysis is in progress and the results will be released soon.

### 3 Search of the pentaquark baryon state $\Theta^+$

In the year 2003 the LEPS Collaboration at SPring-8 announced the observation of the new state  $\Theta^+$  with mass 1.54 GeV and width less than 25 MeV with a minimum quark content  $qqqq\bar{q}$  <sup>3)</sup>. After that, experiential evidences for this exotic state in both its decaying channels  $\Theta^+ \rightarrow pK^0$  and  $nK^+$  have been reported by several other experimental groups analyzing previously obtained data [for a complete review see <sup>4)</sup>]. The reported masses in some cases vary by more than the uncertainties given for the individual experiments, ranging from 1522 to 1555 MeV, with the masses obtained from processes involving  $nK^+$  signals in the initial or final states giving on average 10-15 MeV higher values than those in the  $pK^0$  channel.

The relatively small statistical significance in every measurement, possibly explained by the fact that all the results come from the analysis of data taken for other purposes, and the discrepancy in mass determination, are not the only problems to face to overcome the reticence to accept the existence of the pentaquark. In fact, a major problem frequently mentioned, is that several experiments at high statistic and high energies reported negative results in searches for the  $\Theta^+$  [for a complete review see <sup>4)</sup>]. However the different kinematical and experimental conditions between the low energy exclusive experiments and the high energy semi-inclusive experiments do not allow a direct comparison so that the null results do not prove that the positive ones are wrong.

To find a definite answer to the question of existence of the  $\Theta^+$  a broad experimental program has been approved in the Hall B. The new dedicated experiments, whose main features are summarized in Table 1, aim to improve the statistical accuracy of the measurements by at least one order of magnitude.

Table 1: Summary table of the new dedicated experiments in Hall B at JLab for the search of exotics baryons.

EXP.	SEARCH	TARGET	RUNNING PERIOD	E (GeV)
E03-113 ( <i>g10</i> )	$\Theta^+$	$LD_2$	3/13 - 5/16/04	$E_\gamma = 0.8 - 3.6$
E04-021 ( <i>g11</i> )	$\Theta^+, \Theta^{+*}, \Theta^{++}$	$LH_2$	5/22 - 7/25/04	$E_\gamma = 0.8 - 3.8$
E04-010 ( <i>eg3</i> )	$\Xi_5$	$LD_2$	11/20/04 - 1/31/05	$E_{e^-} = 5.7$
E04-017 ( <i>super g</i> )	$\Theta^+, \Xi_5$	$LH_2$	2 <sup>nd</sup> half 2006	$E_\gamma = 1.5 - 5.4$

The Frascati group is deeply involved in this program: two new approved proposals are signed by the members of the group which also participated to the construction of the new Start Counter of the CLAS detector, necessary to run the new experiments at higher rates. Moreover they served as run coordinators during the data taking of both g10 and g11 runs and they performed the analysis for the  $\Theta^+$  search in the reaction channel  $\gamma d \rightarrow \Theta^+ \Lambda(1115)$ .

Searching for  $\Theta^+$  through photoproduction on the deuteron together with a  $\Lambda$  hyperon has various positive aspects. The main advantage of this reaction channel is that it allows identification of the final state without the need of removing competing channels, while at the same time it excludes kinematical reflections of heavy mesons in the  $NK$  invariant mass spectrum, possible in other channels, like  $pK^+K^-(n)$  or  $pK^+K^0(p)$ . Moreover, the presence of the  $\Lambda$  allows a “strangeness tag” ( $S_\Lambda = -1$ ) in both the  $nK^+$  and the  $pK^0$  decay modes.

After selecting the  $\Lambda K^+(n)$  events, the  $\Theta^+$  has been searched for calculating the invariant mass of the  $nK^+$  system. The result obtained is shown in the top plot of Fig. 1. Since the  $nK^+$  mass spectrum does not show any evident structure, kinematical cuts on non-spectator-neutron and on photon-energy, according to the model <sup>5)</sup> have been applied. Several cuts on the neutron momentum ( $p_n$ ) and on the photon energy ( $E_\gamma$ ) have been tested. However, also under these stringent kinematic conditions, no narrow peaks having statistical relevance was observed in the mass region around 1.54 GeV/c<sup>2</sup>. An example is given in the bottom plot of Fig. 1, where the kinematic requirements  $p_n > 0.2$  GeV/c and  $E_\gamma < 1.6$  GeV are applied.

An upper limit on the cross section has been then calculated.

The results will be reported in a paper which is under the collaboration review and which will be soon submitted to Physical Review Letter.

#### 4 Strangeness photoproduction

The long-standing question of “missing resonances”, i.e. experimentally not established baryon states which are predicted by SU(6) x O(3) symmetric quark models but not expected by the diquark model, can only be settled if experiments unambiguously identify some of these resonances. Symmetric quark models predict several “missing” baryon states to couple strongly to  $\gamma p$  as well as  $K\Lambda$  or  $K\Sigma$  but not significantly to  $\pi N$ . Thus, resonances with these properties would not have been observed in pion experiments on which most of the data analyses are based.

The electromagnetic strangeness production is an important part of the JLab’s experimental program and several experiments have been approved to run in all the three halls.

The Frascati group, taking advantage of the high quality of the g10 data collected for the pentaquark search, have started the analysis of the  $\gamma n(p) \rightarrow K^+\Sigma^-(p)$  and  $\gamma p(n) \rightarrow K^+\Lambda(n)$  reactions in the invariant mass range from 1.54 to 2.76 GeV where data are not available, in order to study the baryon resonance spectrum to emphasize resonances not otherwise revealed.

#### 5 Nucleon form factor in the time-like region

The possibility to fully measure nucleon form factors in the time-like region at Frascati in the proposed high energy upgrade of DAΦNE storage ring is under investigation by the AIACE group. Differential  $e^+e^- \rightarrow p\bar{p}$  and  $e^+e^- \rightarrow n\bar{n}$  cross section should be measured, in order to extract the moduli of proton and neutron form factors. The relative phase between electric and magnetic form factors (never measured yet) can be obtained by measuring the polarization of the outgoing nucleon in the normal direction to the scattering plane. A Letter of Intent has been written and signed by 80 physicists from 24 institutions in 7 countries and presented to the LNF Scientific Committee. An international workshop attended by 85 physicists has also been organized to discuss recent and new data on the form factors and their strangeness contribution as well as their theoretical

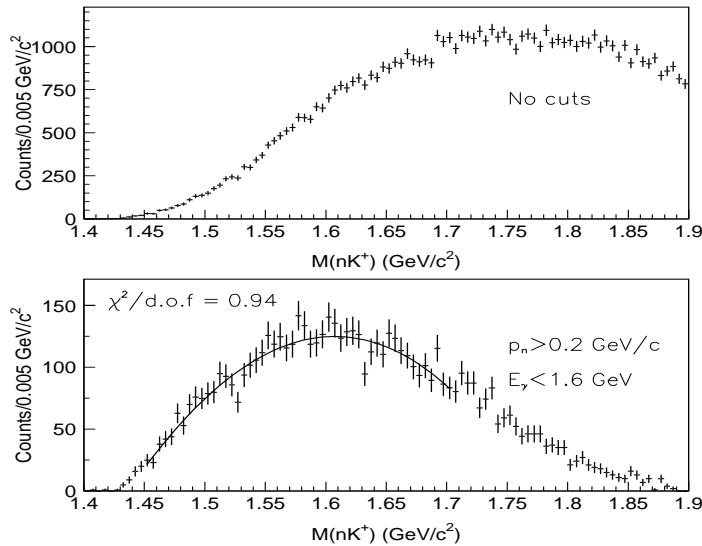


Figure 1: Invariant mass of the  $nK^+$  system, after channel selection. Top plot: no kinematical cuts are applied. Bottom plot: the  $E_\gamma < 1.6$  GeV and  $p_n > 0.2$  GeV/c kinematical cuts are applied. No statistically significant structure is visible in the mass range around  $1.54$  GeV/c<sup>2</sup>. The third-order polynomial fit used for the upper limit estimate is shown.

interpretation and connection to GPD's. A special attention was devoted to fostering current and future measurements.

## 6 List of Publications

1. "Onset of asymptotic scaling in deuteron photodisintegration."  
P. Rossi *et al.* and CLAS collaboration, Phys. Rev. Lett. 94 (2005), 012301; hep-ph/0405207.
2. "The experimental search for pentaquark."  
P. Rossi, Nucl. Phys. A752 (2005), 111.
3. "The pentaquark search at Jefferson Laboratory."  
P. Rossi, Czech. Jour. Phys. 55, (2005), A131.
4. "The experimental search for the  $\Theta^+$  in the  $\gamma d \rightarrow \Lambda \Theta^+$  reaction with CLAS."  
P. Rossi, Nucl. Phys. A755 (2005), 371.
5. "Comparative Regge analysis of  $\Lambda$ ,  $\Sigma^0$ ,  $\Lambda(1520)$  and  $\Theta^+$  production in  $\gamma p$ ,  $\pi p$  and  $pp$  reaction."  
V.Yu Grishina, L.A. Kondratyuk, W. Cassing, E. De Sanctis, M. Mirazita, P. Rossi, Eur. Phys. Jour. A25 (2005), 141; nucl-th/0506053.
6. "Survey of  $A_{LT'}$  asymmetries in semi-exclusive electron scattering on He4 and C12."  
D. Protopopescu *et al.* and CLAS collaboration, Nucl. Phys. A748 (2005), 357; nucl-ex/0405021.
7. "Exclusive  $\rho^0$  meson electroproduction from hydrogen at CLAS."  
C. Hadjidakis *et al.* and CLAS collaboration, Phys. Lett. B605 (2005), 256 ; nucl-ex/0408005.
8. "Exclusive photoproduction of the cascade ( $\Xi$ ) hyperons."  
J. Price *et al.* and CLAS collaboration, Phys. Rev. C71 (2005), 058201; nucl-ex/0409030.

9. “Radiative decays of the  $\Sigma^0(1835)$  and  $\Lambda(1520)$  hyperons.”  
S. Taylor *et al.* and CLAS collaboration, Phys. Rev. C71 (2005), 054609; hep-ex/0503014.
10. “Deeply virtual and exclusive electroproduction of omega mesons.”  
L. Morand *et al.* and CLAS collaboration, Eur. Phys. Jour.A24 (2005), 445; hep-ex/0504057.
11. “Measurement of the polarized structure function  $\sigma_{LT'}$  for pion electroproduction in the Roper resonance region.”  
K. Joo *et al.* and CLAS collaboration, Phys. Rev. C72 (2005), 058202; nucl-ex/0504027.
12. “Beam-helicity asymmetries in double-charged-pion photoproduction on the proton.”  
S. Strauch *et al.* and CLAS collaboration, Phys. Rev. Lett. 95 (2005), 162003 ; hep-ex/0508002.
13. “Search for  $\Theta^+(1540)$  pentaquark in high statistics measurement of  $\gamma p \rightarrow \bar{K}^0 K^+ n$  at CLAS.”  
M. Battaglieri *et al.* and CLAS collaboration, Phys. Rev. Lett. 96 (2006), 042001; hep-ex/0510061.
14. “The CLAS electromagnetic calorimeter at large angles.”  
M. Anghinolfi *et al.*, Nucl. Instr. Meth. A537 (2005), 562.
15. “Electron scattering from high-momentum neutrons in deuterium.”  
A. Klimenko *et al.* and CLAS collaboration, accepted by Phys. Rev. C ; nucl-ex/0510032.
16. “Measurement of 2 and 3 nucleon short range correlation probabilities in nuclei.”  
K. Egiyan *et al.* and CLAS collaboration, accepted by Phys. Rev. Lett.; nucl-ex/0508026.
17. “ $\eta'$  photoproduction on the proton for photon energies from 1.527 to 2.227 GeV.”  
M. Dugger *et al.* and CLAS collaboration, accepted by Phys. Rev. Lett.; nucl-ex/0512019.
18. “Differential cross section for  $\gamma p \rightarrow K^+ + Y$  for  $\Lambda$  and  $\Sigma^0$  hyperons.”  
R. Bradford *et al.* and CLAS collaboration, accepted by Phys. Rev. C; nucl-ex/0509033.
19. “Measurement of the deuteron structure function F2 in the resonance region and evaluation of its moments.”  
M. Osipenko *et al.* and CLAS collaboration, Submitted to Phys. Rev. D; nucl-ex/0506004.

## 7 Presentation at Conferences

1. “*Exclusive reactions: a tool to understand the way from quarks to nuclei*”  
Patrizia Rossi - Invited talk at the “XLIII International winter meeting on nuclear physics”  
- Bormio (Italy), March 13-20, 2005.
2. “*The high energy program at DAΦNE.*”  
Marco Mirazita - “X LNF Spring School in Nuclear, Subnuclear and Astroparticle Physics”  
- Frascati (Italy), May 16-20, 2005.
3. “*Onset of scaling in exclusive processes.*”  
Marco Mirazita - Invited talk at the “First workshop on quark-hadron duality and the transition to pQCD” - Frascati (Italy), June 6-8, 2005.
4. “*Pentaquark results from JLAB.*”  
Patrizia Rossi - Invited talk at the “QCD 05” - Montpellier (France), July 4-9, 2005
5. “*Recent pentaquark results.*”  
Patrizia Rossi - Invited talk at the “Resonances in QCD” - ECT Trento (Italy), July 11-15, 2005.

6. *“Exclusive reactions at JLab.”*  
Patrizia Rossi - Invited talk at the “Probing microscopic structure of the lightest nuclei in electron scattering at Jlab energies and beyond ” - ECT Trento (Italy), July 25-30, 2005.
7. *“Proposta per la misura dei Fattori di Forma del nucleone a DAΦNE.”*  
Marco Mirazita - “Incontro sul futuro dei Laboratori Nazionali di Frascati” - Frascati (Italy), September 16, 2005.
8. *“Large angle processes.”*  
Patrizia Rossi - Plenary review talk “Electromagnetic Interactions with Nucleons and Nuclei (EINN 2005)” - Milos (Greece), September 21-24, 2005.
9. *“Ricerca della produzione di  $\Theta^+$  nella reazione  $\gamma d \rightarrow \Lambda KN$ ”*  
Marco Mirazita - Contributed talk at the “XCI Congresso Nazionale SIF” - Catania (Italy), September 26 - October 1, 2005.
10. *“Exclusive reactions.”*  
Patrizia Rossi - Invited talk at the “XCI Congresso Nazionale SIF” - Catania (Italy), September 26 - October 1, 2005.

## 8 Seminars

1. *Pentaquark: Fact or Fancy.*  
Patrizia Rossi - Laboratori Nazionali di Frascati-INFN, March, 2005
2. *The search for exotic pentaquark baryons*  
Marco Mirazita - University of Virginia, Charlottesville (USA), April 15, 2005
3. *Pentaquark search at JLab.*  
Patrizia Rossi - Duke University (USA), September 1, 2005
4. *Pentaquark search at JLab.*  
Patrizia Rossi - Mainz University (Germany), December 14, 2005

## References

1. M. Mirazita *et al.*, Phys. Rev. C **70**, (2004) 014005.
2. P. Rossi *et al.*, Phys. Rev. Lett. **94** (2005), 012301.
3. T. Nakano *et al.*, Phys. Rev. Lett. **91**, (2003) 012002.
4. P. Rossi, Nucl. Phys. A **752**, (2004) 111.
5. V. Guzey, Phys. Rev. C **69**, (2004) 173.

## FINUDA

L. Benussi (Art. 23), M. Bertani, S. Bianco, M. A. Caponero (Ass.), F. L. Fabbri, P. Gianotti (Resp.), M. Giardoni, V. Lucherini, E. Pace, M. Pallotta, S. Tomassini, L. Passamonti (Tecn.), D. Pierluigi (Art. 15), F. Pompili (Art. 23), A. Russo (Art. 15)

### 1 Introduction

FINUDA (Fisica NUcleare a DAΦNE) is an experiment devoted to hypernuclear physics studies. Hypernuclei are nuclear systems in which one or more nucleons are replaced by a hyperon. This feature adds explicit strangeness to the nuclear system allowing to study, in a more general environment, the baryon-baryon interaction.

At FINUDA, hypernuclei are produced via the reaction:



stopping  $K^-$  from  $\phi(1020)$  decay almost at rest into a thin ( $\sim 0.2 \text{ g cm}^{-2}$ ) target. The spectroscopy of the hypernuclear levels produced is performed by measuring the momentum of the outgoing  $\pi^-$ . Therefore, it is crucial to determine this quantity very precisely. FINUDA has been designed to reach a momentum resolution of 0.4% corresponding to an energy resolution, of the hypernuclear level, of  $\sim 840 \text{ keV}$  ( $FWHM$ ). Moreover, the products of the sub-subsequent decay of the  $\Lambda$  embedded in the nucleus can be detected by FINUDA, allowing to investigate the decay mechanisms of hypernuclei together with the production reaction, a feature never reached by any other experiment.

The FINUDA detector is a large acceptance magnetic spectrometer housed inside a superconducting solenoid (2.7 m length and 2.4 m diameter) providing a field of 1 T. The apparatus can be sub-divided in two distinct areas: the interaction-target region and the outer tracking zone. The former, surrounding the DAΦNE beam pipe, consists of a barrel of plastic scintillators, a layer of double-sided silicon microstrips, and the target station, which can house up to 8 different materials. The latter consists of several layers of tracking detectors: a double-sided silicon microstrips array, two layers of planar drift chambers, and six layers of straw tubes. The outermost detector of the whole complex is a second barrel of plastic scintillators, for trigger purposes and neutron detection. The whole FINUDA tracking volume ( $\sim 8 \text{ m}^3$ ) is filled with helium to reduce multiple-Coulomb scattering that is the main factor limiting the momentum resolution.

The FINUDA Collaboration consists of 60 physicists coming from LNF, several INFN sections and Italian universities (Torino, Bari, Trieste, Pavia, Brescia) plus foreign researchers from the TRIUMF laboratory of Vancouver, Canada, the KEK laboratory of Tsukuba, Japan, the Seoul National University, South Korea, and the Joint Institute for Nuclear Research of Dubna, Russia.

### 2 FINUDA activity in 2005

The activity of the LNF FINUDA group during 2005 has been devoted to the analysis of the data in order to produce scientific results.

FINUDA has performed the first data taking from October 2003 up to March 22, 2004. A first sample of data, corresponding to an integrated luminosity of about  $50 \text{ pb}^{-1}$ , has been collected both for machine and detector calibration purposes. Further  $200 \text{ pb}^{-1}$  have been acquired for the scientific analyses. The set of targets mounted in this first data taking was composed by: three  $^{12}\text{C}$ , two  $^6\text{Li}$ , one  $^7\text{Li}$ , one  $^{27}\text{Al}$ , one  $^{51}\text{V}$ . With the two  $^6\text{Li}$  targets FINUDA can access light hypernuclear systems;  $^6_{\Lambda}\text{Li}$  is unstable for proton emission and it decays into  $^5_{\Lambda}\text{He} + \text{p}$ , or it may transform into  $^4_{\Lambda}\text{He} + \text{p} + \text{n}$ , or into  $^4_{\Lambda}\text{H} + \text{p} + \text{p}$  via a Coulomb assisted mechanism.

Furthermore,  ${}^6\text{Li}$  data are used to look for neutron rich hypernuclei and deeply bound kaonic systems.  ${}^7_\Lambda\text{Li}$  is the hypernucleus most extensively studied from the  $\gamma$ -spectroscopy point of view by using Ge detectors, but its decays are not known. FINUDA can therefore complete the knowledge of this system adding the missing information. The choice of installing three  ${}^{12}\text{C}$  targets is motivated by the fact that  ${}^{12}_\Lambda\text{C}$  is the most studied hypernucleus. Therefore, it has been used as a reference system to tune FINUDA detector performance. Furthermore, since the spectrometer characteristics are better than those available in previous experiments, some improvements on the resolution of hypernuclear levels and in the knowledge of the decay modes have been also obtained.  ${}^{27}\text{Al}$ , and  ${}^{51}\text{V}$  targets have been selected to perform a first study of medium-heavy hypernuclei. For  ${}^{27}_\Lambda\text{Al}$  there are old data taken with a very coarse energy resolution (6 MeV *FWHM*). The excitation spectrum of  ${}^{51}_\Lambda\text{V}$  has been measured at KEK (using a different production mechanism) with an energy resolution of 1.65 MeV *FWHM*. Fig.1 shows the trend of hypernuclear capture rate measured by FINUDA per stopped  $K^-$  as a function of the mass number of the target.

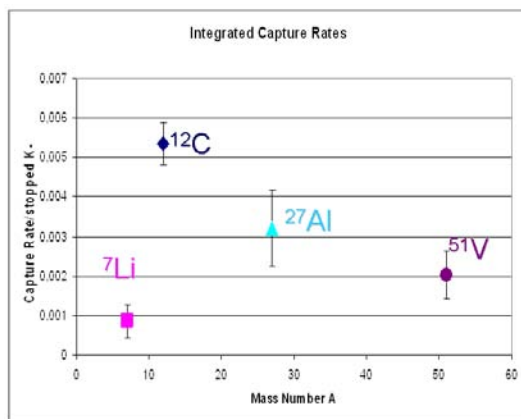


Figure 1: *Hypernuclear capture rate per  $K^-_{stop}$  (integrated over the bound region) measured by FINUDA as a function of the target mass number.*

## 2.1 Data analysis

### 2.1.1 ${}^{12}_\Lambda\text{C}$ hypernuclear system

The main analysis task of LNF FINUDA group has been the spectroscopy of  ${}^{12}_\Lambda\text{C}$ . Hypernuclear event candidates have been identified via  $\pi^-$  tracks emitted from the  $K^-$  stopping point inside the nuclear target. In addition, hypernuclear decays can be studied by reconstructing the  $\Lambda$  charged decay products. Two hypernuclear peaks, corresponding to the  $\Lambda$  hyperon in the *s* and *p* shell respectively, are visible in this spectrum of fig.2.

The  $\Lambda$  binding energy distribution ( $-B_\Lambda$ ) shown in fig. 3 is obtained from the  $\pi^-$  momentum distribution after background subtraction. The curve, drawn over the histogram, is the result of the best fit performed using seven gaussians for the hypernuclear states. The obtained energy resolution of 1.250 MeV (*FWHM*) represents an improvement with respect to the best previous measurement performed by the E369 collaboration at KEK (1.450 MeV<sup>1</sup>).

FINUDA can study not only the hypernuclei formation reaction, but also their decays or, more generally, all the processes that follow  $K^-$  nucleus interaction. Inside the nucleus, due to the Pauli blocking mechanism, the  $\Lambda$  decay into pion-nucleon pairs is inhibited. This effect increases with mass number, and therefore hypernuclei decay via different weak interactions involving four baryons:  $\Lambda + N \rightarrow n + N$ ,  $N$  being a neutron or a proton. FINUDA is able to detect both the

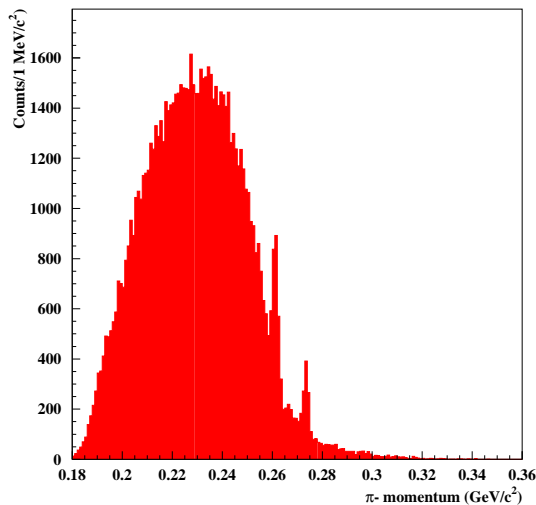


Figure 2: *Inclusive  $\pi^-$  momentum spectra of  $^{12}\text{C}$  targets.*

protons and the neutrons from hypernuclear decay, and hence to measure these reaction channels. This allow to obtain experimental information on weak interaction between four baryons involving strangeness. Fig. 4 shows the energy spectra of the protons and of the neutrons measured in coincidence with negative pions with momentum in the region expected for the hypernuclear states.

### 2.1.2 Search for kaon-nucleus bound systems

After the theoretical prediction by Akaishi and Yamazaki in 2002 <sup>2)</sup>, the E471 collaboration at KEK claims to have observed two  $S = -1$  tribaryon states formed by  $K^-$  stopped on  $^4\text{He}$ . Nevertheless, the above mentioned experimental results have been obtained with the missing-mass method looking to the TOF spectrum of the nucleon ejected from the reaction  $K^-_{stop} ^4\text{He} \rightarrow XN$ , and hence they are not clear and direct observations of the supposed  $K^-$ -bound states.

FINUDA, being able to fully detect all the products of the  $K^-$  interaction, is ideally suited to look for these signals by using the direct method of the invariant-mass of the decay particles. In FINUDA, a kaonic bound state like  $K^-pp$  would decay via  $\Lambda p$ , with the  $\Lambda$  then transforming into  $p \pi^-$ . The data sample used for this analysis is that with two protons and a  $\pi^-$  in the final state; the  $\Lambda$  is reconstructed via its decay  $p\pi^-$  and finally a  $p$  emitted back-to-back with respect to the  $\Lambda$  is requested. The invariant mass of  $\Lambda p$  events suggests the existence of a  $K^-pp$  bound system with  $B = 115^{+6}_{-5} \text{stat } ^{+3}_{-4} \text{sys MeV}$  and a width  $\Gamma = 67^{+14}_{-11} \text{stat } ^{+2}_{-3} \text{sys MeV}$  <sup>3)</sup>.

Similar analyses have been performed to search for other deeply bound kaonic systems in events with a  $p$ , a  $n$  and a  $\pi^-$  in the final state. Two sets of data have been selected corresponding to:

$$\begin{aligned} K^-pn &\rightarrow \Lambda n, & \Lambda &\rightarrow p\pi^-; \\ K^-pn &\rightarrow \Sigma^- p, & \Sigma^- &\rightarrow n\pi^-. \end{aligned}$$

The angular correlation between the  $\Lambda$  and the  $n$  and the  $\Sigma^-$  and the  $p$  has been studied and only the events where the two particles are emitted back-to-back are retained. Indications of the existence of  $K^-pn$  states have been found. Fig. 5 shows the preliminary plot of the invariant mass distributions of the final  $\Lambda n$  and  $\Sigma^- p$  events. Again the events accumulated below the threshold of the unbound three-body system, but the lack of statistics prevents from drawing firm conclusions. The set of target that FINUDA will mount for the next data taking ( $2 ^6\text{Li}$ ,  $2 ^7\text{Li}$ ,  $2 ^9\text{Be}$ ,  $1 ^{13}\text{C}$ ,  $1 \text{D}_2\text{O}$ ) will allow high statistic measurements on this topic.

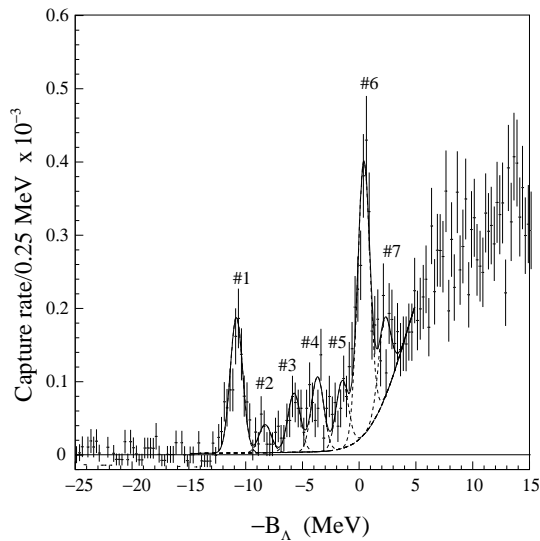


Figure 3: *The hypernuclear levels of  ${}_{\Lambda}^{12}\text{C}$ .*

### 3 Talks to international conferences by LNF authors in year 2005

- L. Benussi *6th International Conference on Nuclear Physics at Storage Rings*, 23-26 May 2005, Jlich - Bonn, Germany.
- M. Bertani, *31st Meeting of the LNF Scientific Committee*, 28-30 November 2005, LNF-Frascati, Italy.

### 4 Talks to international conferences by FINUDA authors in year 2005

- A. Filippi, *XI International conference on hadron spectroscopy - HADRON 05*, 21-26 August 2005, Rio de Janeiro, Brazil.
- H. Fujioka *Second Joint Meeting of the Nuclear Physics Divisions of the APS and JPS*, September 18-22, 2005, Ritz-Carlton, Kapalua Maui, Hawaii.
- M. Palomba, *Particles and Nuclei International Conference*, October 24-28, 2005, Santa Fe, New Mexico, USA.
- H. Fujioka, *Particles and Nuclei International Conference*, October 24-28, 2005, Santa Fe, New Mexico, USA.
- S. Piano, *High Performance Computing Symposium (HPC 2005)*, April 3-7, 2005, San Diego, California, USA.
- T. Nagae, *EXA05 International Conference on Exotic Atoms and Related Topics*, February 21 - 25, 2005, Vienna, Austria.
- P. Camerini, *XLIII International winter meeting on nuclear physics*, March 13-20, 2005, Bormio, Italy.
- S. Piano, *International Workshop on Chiral Restoration in Nuclear Medium*, February 15-17, 2005, Okochi hall, RIKEN, Japan.

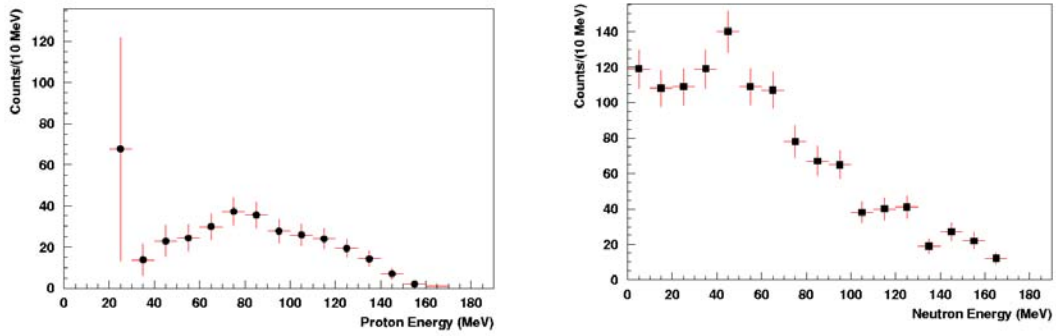


Figure 4: Energy spectrum of protons (left) and of neutrons (right), emitted in coincidence with hypernuclear bound states formation in  $^{12}\text{C}$ .

## References

1. M. Agnello *et al.*, Phys. Lett. B 622 (2005) 35.
2. Y. Akaishi and T. Yamazaki, Phys. Rev. C 65 (2002) 044005.
3. M. Agnello *et al.*, Phys. Rev. Lett. 94 (2005) 212303.

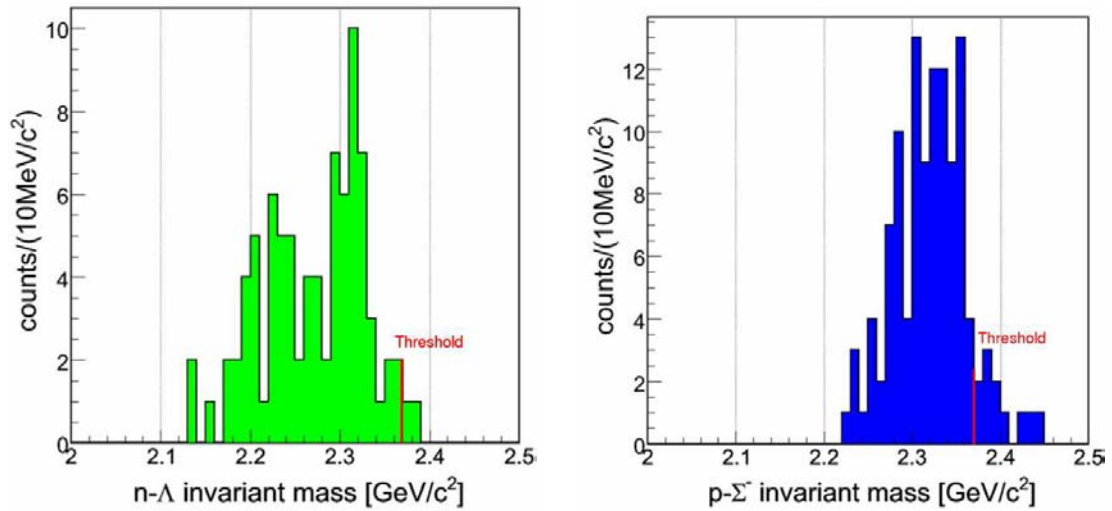


Figure 5: a)  $n\text{-}\Lambda$  invariant mass distributions. b)  $\Sigma^- p$  invariant mass distribution. The threshold of the unbound  $K^- n p$  system is also indicated.

## GRAAL

P. Levi Sandri (Resp.), D. Pietreanu

### 1 Introduction

The Graal experiment aims at a more detailed knowledge of the baryon spectrum via the precise measurement of cross sections and polarisation observables in photo-induced reactions on the nucleon.

The use of the electromagnetic probe and of its polarisation, coupled to large acceptance detectors with cylindrical symmetry and high efficiency in the detection of all final state particles, is the technique chosen in many laboratories to perform the ambitious program of a full determination of the scattering amplitude of a given photonuclear reaction. Such determination requires, for each reaction channel, the measurement of the cross section, of the three single polarisation observables and of four appropriately chosen double polarisation observables.

The Graal experiment is performed in collaboration between 6 INFN Sections (Roma2, LNF, Catania-LNS, Roma1, Genova and Torino), LPSC-Grenoble and INR-Moscow. The Frascati group is responsible of running and maintaining the  $\Delta E/\Delta x$  scintillator barrel detector, the Montecarlo simulation program LAGGEN, the off-line reconstruction of events in the BGO calorimeter, the data analysis for coherent  $\eta$  photoproduction off the deuteron and contributes to the data analysis of  $\pi^0$  and  $\eta$  photoproduction from the neutron bound in a deuteron in the quasi-free kinematics regime.

### 2 The Graal Beam and the Lagran $\gamma$ e apparatus

The Graal facility provides a polarised and tagged photon beam by the backward Compton scattering of laser light on the high energy electrons circulating in the ESRF storage ring<sup>1)</sup>. Using the UV line (350 nm) of an Ar-Ion laser we have produced a gamma-ray beam with an energy from 550 to 1550 MeV. Its polarisation is 0.98 at the maximum photon energy and the energy resolution has been measured to be 16 MeV (FWHM).

The Lagran $\gamma$ e detector is formed by a central part surrounding the target and a forward part. Particles leaving the target at angles from  $25^\circ$  to  $155^\circ$  are detected by two cylindrical wire chambers with cathode readout, a barrel made of 32 strips of plastic scintillator parallel to the beam axis, used to determine the  $\Delta E/\Delta x$  of charged particles, and the BGO rugby-ball made of 480 crystals of BGO scintillator.

The BGO ball is made of crystals of pyramidal shape with trapezoidal basis which are 21 radiation lengths long (24 cm). This calorimeter has an excellent energy resolution for photons<sup>2)</sup>, a good response to protons<sup>3)</sup>, a high detection efficiency for neutrons<sup>4)</sup> and is very stable in time due to a continuous monitoring and to the calibration slow control system<sup>5)</sup>.

Particles moving at angles smaller than  $25^\circ$  encounter two plane wire chambers, (xy and uv) two walls of plastic scintillator bars, 3 cm thick, located at 3 m from the target point, that provide a measurement of the time-of-flight for charged particles (700 ps FWHM resolution) followed by a shower wall made by a sandwich of four layers of lead and plastic scintillators, 4 cm thick, that provides a full coverage of the solid angle for photon detection (with 95 percent efficiency) and a 20 percent efficiency for neutron detection<sup>6)</sup>.

Finally, two disks of plastic scintillator separated by a disk of Lead complete the solid angle coverage in the backward direction.

The beam intensity is continuously monitored by a flux monitor, composed by three thin plastic scintillators and by a lead/scintillating fibre detector that measures energy and flux <sup>7)</sup>.

### 3 2005 activity

During the year 2005 the Graal experiment has restarted the data taking after one year dedicated to the tentative installation of a polarised HD target. The data taking was successfully resumed and was focused in the measurements of photoproduction processes from the neutron bound in the deuterium nucleus, in the quasi-free kinematics regime where the proton acts as a spectator.

#### 3.1 Proton target

The data analysis activity was mainly focused upon completion of the study  $\pi^0$  photoproduction from the proton from 550 to 1500 MeV: the results obtained significantly improve the database for beam asymmetry (446 data points, wherein 240 cover the unexplored 1100-1500 MeV region) and of the differential cross section (1564 high precision data points). Of particular interest, besides the constraints that such a complete and coherent data base offers to modern partial waves analysis, is the cross section in the region  $W = 1910 - 1950$  MeV corresponding to  $E_\gamma = 1480 - 1560$  MeV (fig 1): the necessary contribution of a new  $D_{15}$  (2070)  $N^*$  resonance is clearly, for the first time, evidenced.

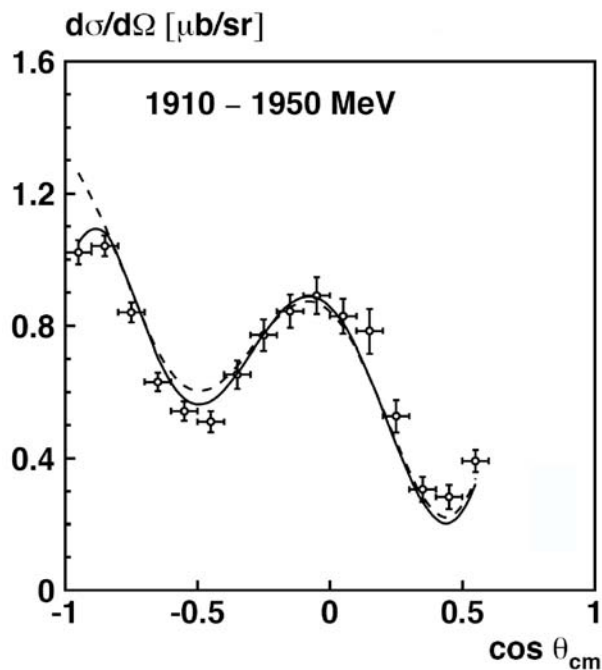


Figure 1: *Differential cross section for  $W=1910-1950$  MeV. The partial waves analysis with a new  $N(2070)D_{15}$  is shown as a solid line. The dashed line shows the result of the PWA when the  $5/2^-$  state is replaced by a  $7/2^-$  state.*

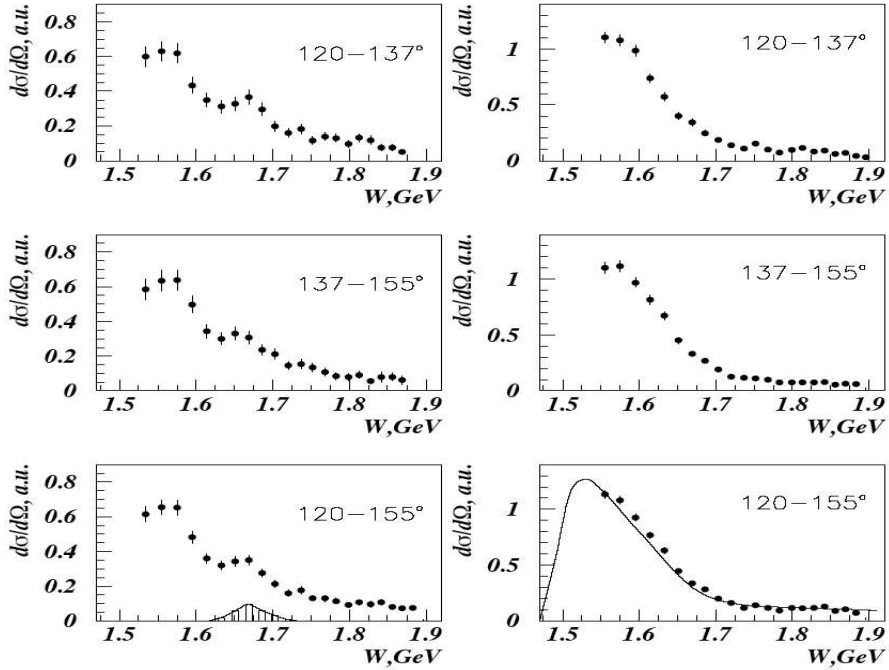


Figure 2: Preliminary  $\eta n$  (left) and  $\eta p$  (right) photoproduction cross sections. Dashed area simulates the contribution of a narrow state at  $W=1.675$  GeV.

Also the data analysis for the reactions with strangeness photoproduction with  $K^+\Lambda$  and  $K^+\Sigma^0$  final states has produced the conclusive values and the results are under theoretical interpretation.

### 3.2 Deuteron target

The deuteron was used at Graal as a target of quasi-free neutrons. Following the announced results coming from SPRING-8<sup>8)</sup>, a search for pentaquark states ( $\theta^+$  and non-strange antidecuplets members) was performed and some preliminary results were presented in international conferences. The  $S=+1$  narrow resonance was searched in the reaction

$$\gamma + D \rightarrow \theta^+ + \Lambda$$

while the possible signal of non strange members of the antidecuplet was searched for in the cross section of  $\eta$  photoproduction. The preliminary results of the cross section for  $\eta$  photoproduction on the quasi-free neutron are shown in figure 2. A clear peak is evident in the cross section on the quasi-free neutron and absent in the cross section on the quasi-free proton as predicted by Diakonov et al.<sup>9)</sup>: this peak could be ascribed to a narrow baryon resonance at  $W=1.675$  GeV and could be an indication of a non strange antidecuplet pentaquark member (crypto-pentaquark)<sup>10)</sup>. Further investigations (i.e. beam asymmetry) have been performed and indicate a different behaviour of the  $\Sigma$  beam asymmetry as measured from the proton and from the neutron (fig. 3) at the same c.m. energy where the peak shows up..

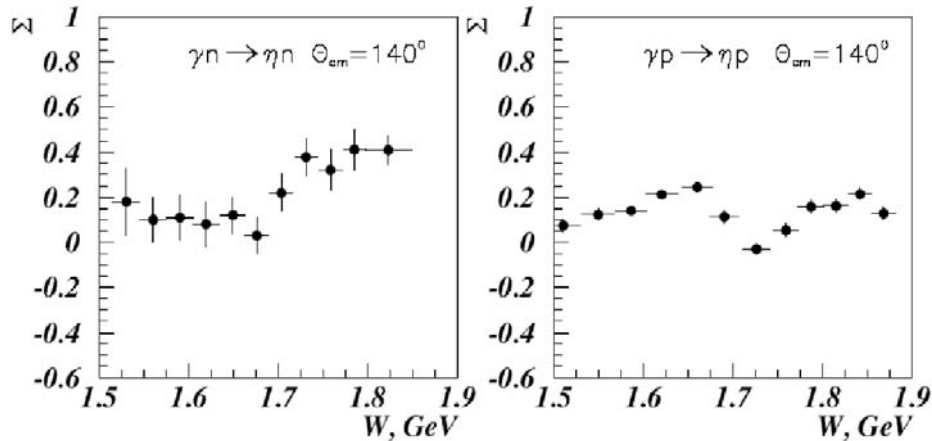


Figure 3: Preliminary  $\eta n$  (left) and  $\eta p$  (right)  $\Sigma$  beam asymmetry. The difference between proton and neutron indicates clearly that a different resonant state contributes to the neutron- $\eta$  asymmetry around 1650-1700 MeV.

#### 4 A serendepic result

The excellent stability of the ESRF electron beam and, consequently, of the Graal photon beam and in particular of its Compton edge, has allowed to study, during many years of Graal data taking, the fluctuations in the speed of light with respect to the apex of the dipole of the Cosmic Microwave Background radiation. The results have enabled to obtain a conservative constraint on the anisotropy in the light speed variations

$$\Delta c(\theta)/c < 3 \cdot 10^{-12}$$

improving the existing limit by two orders of magnitude.

#### 5 Activity in 2006 and conclusions

The Graal experiment started data taking in 1997. It was run both with the green laser line giving rise to a photon beam of maximum energy of 1100 MeV and with UV multi-line with the corresponding gamma-ray beam of 1550 MeV maximum energy. The typical intensity was  $2 \cdot 10^6 s^{-1}$  for the UV line and  $5 \cdot 10^6 s^{-1}$  for the green line, reaching the design intensity. The detector was found very stable during the eight years of operation, with only minor maintenance problems.

Proton and deuteron targets of different lengths were used and asymmetry data and cross sections have been produced for  $\eta$ ,  $\pi^0$ ,  $\pi^+$ ,  $2\pi^0$  and  $\omega$  photoproduction channels providing, for these reactions, the most extended and coherent data base available until now. Also the strangeness photoproduction from the proton with  $K^+\Lambda$  and  $K^+\Sigma^0$  final states has been analysed and the final results will be submitted for publication in the next months. The analysis of the Compton process on the proton, and of all the mentioned photoreactions on the quasi-free neutron of the deuteron target are underway.

During the year 2006 Graal will continue the data taking with deuteron (and eventually other medium nuclei) in order to increase the available statistics for the  $\theta^+$  signal and to study the behavior of  $\eta$  photoproduction cross section as a function of the atomic number A.

## 6 Main recent publications

- V. G. Gurzadyan *et al.*, Mod. Phys. Lett. A 20, (2005),19.  
O. Bartalini *et al.*, Eur. Phys. J. A26, (2005), 349.  
V. Kuznetsov *et al.*, arXiv:hep-ex/0409032v4 (24-12-2005).

## References

1. Graal Collaboration, Nucl. Phys. A622, (1997) 110c.
2. P. Levi Sandri *et al.* Nucl. Inst. and Meth. in Phys. Research A370, (1996), 396.
3. A. Zucchiatti *et al.*, Nucl. Inst. and Meth. in Phys. Research A321, (1992), 219.
4. O. Bartalini *et al.*, to be published in Nucl. Instr. and Meth. in Phys. Research A.
5. F. Ghio *et al.*, Nucl. Inst. and Meth. in Phys. Research A404, (1998), 71.
6. V. Kouznetsov *et al.*, Nucl. Instr. and Meth. in Phys. Research A487 (2002), 396.
7. V. Bellini *et al.*, Nucl. Inst. and Meth. in Phys. Research A386, (1997), 254.
8. T. Nakano *et al.* Nucl. Phys. A721, (2003), 112c.
9. D.Diakonov, V. Petrov and M. Polyakov, Z. Phys. A359 (1997) 305.
10. Ki-Seok Choi *et al.* arXiv:hep-ph/0512136v1 (12/12/2005).

## HERMES

E. Avetisyan (Ass.), N. Bianchi (Resp. Naz.), G.P. Capitani (Resp. Loc.),  
E. De Sanctis, P. Di Nezza, A. Fantoni, A. Funel (Dott.), C. Hadjidakis (Ass.),  
D. Hasch (Ass.), V. Muccifora, A. Orlandi (Tecn.), W. Pesci (Tecn.),  
E. Polli, A.R. Reolon, C. Riedl (Ass.), A. Viticchié (Tecn.)

### 1 Introduction

HERMES (HERa MEasurement of Spin) is an experiment at DESY mainly dedicated to study the spin structure of the nucleon. Nucleons (protons and neutrons) are the basic ingredients of the matter of the known universe and their most important quantum number is the spin 1/2. The nucleon is a composite object which can be described in terms of moving quarks of different flavors (up, down and strange) in different configurations (valence and sea) and gluons. Up to year 2000, HERMES collected data with a longitudinally polarized positron beam of 27.5 GeV on longitudinally polarized H, D and  $^3\text{He}$  internal gas targets. From these runs HERMES provided the most accurate and complete data set for the polarized structure function  $g_1$  and allowed for the first time a direct flavor decomposition of the nucleon spin. The use of a tensor polarised deuteron gas target with only a negligible residual vector polarization enabled the first measurement of the tensor asymmetry  $A_{zz}^d$  and of the tensor structure function  $b_1^d$  (Fig. 1). Runs on several unpolarized nuclear gas targets have been also collected.

In 2005 data taking with a transversely polarized hydrogen target have been completed and data from 2002-2204 have been analysed. The extracted Fourier components as a function of the azimuthal angle of the pion  $\phi$  and the target spin axis  $\phi_S$  about the virtual photon direction and relative to the lepton scattering plane are interpreted as a signal of the previously unmeasured quark transversity distribution in conjunction with the Collins fragmentation function and an asymmetry arising from a correlation between the transverse polarization of the target nucleon and the intrinsic transverse momentum of the quark, are represented by the previously unmeasured Sivers distribution function. Evidence for both signals is observed (Fig. 2). The average Collins moment for  $\pi^+$  is found to be positive, whereas it is negative for  $\pi^-$ . Although the sign of these transversity densities resembles the helicity densities ( $\delta u, \Delta u > 0$  and  $\delta d, \Delta d > 0$ ), the  $\pi^-$  asymmetry magnitude is unexpectedly large, which could point towards the importance of the disfavored fragmentation function entering with opposite sign compared to the favored one. The Sivers distribution function is related to the still unknown orbital angular momentum of quarks. The average Sivers moment for  $\pi^+$  is positive, which may provide the first evidence for a T-odd parton distribution in leptonproduction. The  $\pi^-$  Sivers moment is consistent with zero. The transversity distribution  $h_1(x)$  is the missing function in the leading twist description of the nucleon, together with the better known momentum  $f_1(x)$  and helicity  $g_1(x)$  distributions.

In 2005 a search for an exotic baryon resonance with S=-2 and Q=-2 has been performed in quasi-real photoproduction on a deuterium target and no evidence for a previously reported  $\Xi^{--}(1860)$  resonance is found in the  $\Xi^- \pi^-$  invariant mass spectrum. An upper limit for the photoproduction cross section of 2.1 nb is found at the 90% C.L. In addition, the well established  $\Xi^0(1530)$  is clearly identified and its photoproduction cross section is found to be between 9 and 24 nb.

### 2 The LNF HERMES group

HERMES is a Collaboration of about 180 physicists from 31 Institutions from 12 Countries. Italy participates with 4 groups and more than 30 physicists from Bari, Ferrara, Frascati and Rome. A Frascati physicist (P. Di Nezza) is the deputy spokesman and run-coordinator of the experiment. A Frascati physicist (D. Hasch) is the analysis coordinator of the experiment. The Frascati group

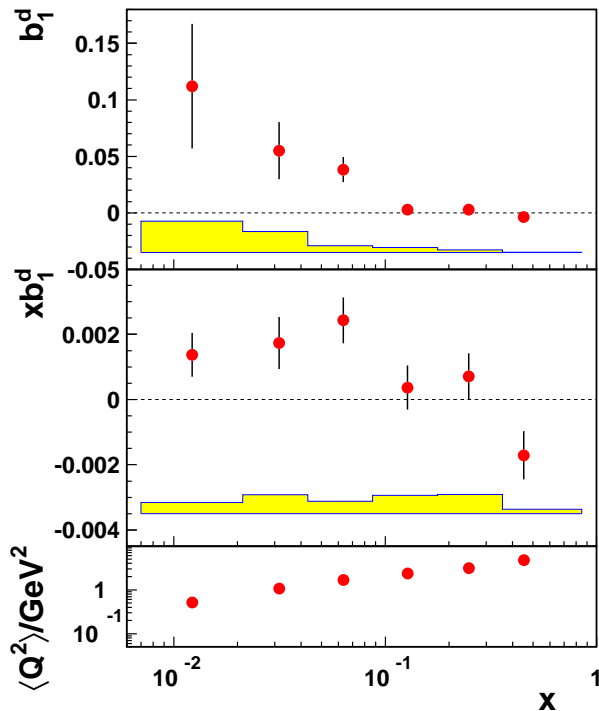


Figure 1: The tensor structure function presented as  $b_1^d(x)$  (top) and  $xb_1^d(x)$  (middle). The error bars are statistical and the shaded bands show the systematic uncertainty. The bottom panel shows the average value of  $Q^2$  in each  $x$ -bin.

is responsible for the electromagnetic calorimeter and has participated in the project and in the construction of two dual RICH detectors. It has been involved in the project and in the construction of Photon Detector, a part of the new Recoil Detector, installed at the end of 2005. A Frascati physicist (C. Hadjidakis) has the responsibility of the analysis working groups of azimuthal asymmetries in semi-inclusive processes and of the pseudoscalar meson exclusive production. A Frascati physicist (P. Di Nezza) has the responsibility of the nuclear physics analysis working group. Frascati physicists are involved in the analysis of many other physics processes. In addition they are playing a major role in the physics paper draftings and in the editorial process being the leading authors of about one third of the HERMES Collaboration physics publications.

### 3 Experimental activity of the LNF group in 2005

#### 3.1 Calorimeter and TOF

In the period of data taking 2006-2007 with Recoil detector, one of the most important physics goals of HERMES is the investigation of the properties of the Deeply Virtual Compton scattering, a process where a virtual photon is transforming to a real one. For the detection of real photons the HERMES electromagnetic calorimeter, consisting of 840 lead-glass blocks, is used. Its basic purposes are the first level trigger on leptons and offline separation of charged hadrons from leptons by comparing their momentum from the energy of the electromagnetic showers deposited in the clusters of the calorimeter. In addition it allows to measure the energy and the angle of single photons from DVCS as well as double photons from  $\pi^0$  and  $\eta$  meson decays. The responsibility for the calorimeter required the online monitoring of the status of the detector for the whole period of

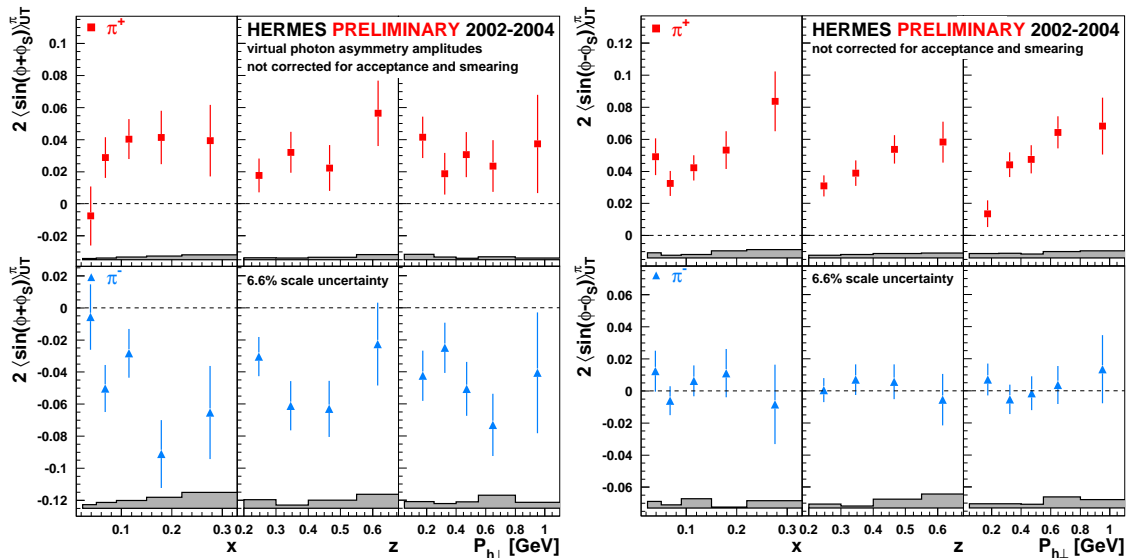


Figure 2: Collins moments (left panel) and Sivers moments (right panel) for charged pions as a function of  $x$ ,  $z$  and  $P_{h\perp}$ . The error bands represent the systematic uncertainties due to acceptance and detector smearing effects and due to a possible contribution from the  $\cos\phi$  moment in the unpolarised cross section. The common overall 6.6% scaling uncertainty is due to the target polarization uncertainty.

data taking. During 2005 all the data collected in the past has been reprocessed with recalibration of many detectors, including the calorimeter. During the long shutdown at the end of 2005 the key components of the calorimeter (the high voltage power supplies and the readout electronics) were tested and maintained to assure their reliable service for the high intensity running of next years. A precise energy and position reconstruction of electromagnetic showers allowed to separate leptons and hadrons with high efficiency by comparing their energy with momentum measured in the tracking system. An improved method of the energy reconstruction accounting for the losses in the preshower lead layer allowed to improve the resolution of the measured energy by  $\sim 25\%$  (Fig. 3-left).

HERMES has two sets of scintillator hodoscope paddles which were mainly designed for charge particle triggering and lepton/hadron separation. The second one is also working as a preshower detector. Nevertheless, it turned out that they can be used also as a time-of-flight system to distinguish different hadron types from each other by their mass extracted from speed and momentum. A method was therefore developed to allow a nice separation of pions from protons in the momentum range of 0.6-3 GeV/c with total efficiency of 98% and pion contamination in proton sample of less than 5% (Fig. 3-right). This momentum range is complementary to the one provided by the HERMES dual RICH detector.

### 3.2 Recoil detector

The recent proof of factorization for exclusive processes and their interpretation in terms of Generalized Parton Distributions to describe the nucleon structure, suggested the detailed investigation of these processes in which a fast meson or a photon is emitted in the forward direction while the slow nucleon is recoiling intact at large angle. Several exclusive processes have been already investigated by HERMES with the missing mass technique. To better identify these processes, a compact Recoil Detector has been constructed and installed around the target in autumn 2005.

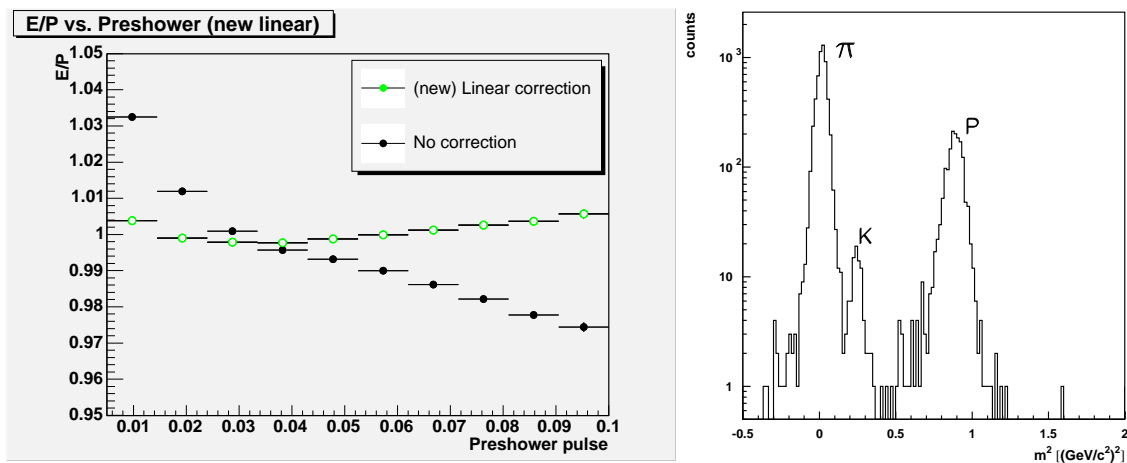


Figure 3: Left : Reconstruction of positron energy in the calorimeter with the improved algorithm. Right : Identification of charged pions, protons and kaons of low momenta with Time of Flight.

It consists of three part: an inner Silicon Detector inside the beam vacuum, a SciFi (Scintillating Fibre) Detector that is situated concentrically outside the beam pipe and an outer Photon Detector that is made of scintillator blocks, with the purpose to reconstruct the paths of protons involved in DVCS reactions from a hydrogen target cell located at the center of the detector. The Frascati group has built the Photon Detector, used to detect photons from the  $\pi^0$  decay. It consists of three layers of scintillating strips with a WLS fiber system readout. Multi-anode photomultipliers are used with specially designed fan-in/preamplifiers to ensure capable transmittance of the signal. The Photon detector (Fig. 4) has been assembled in Frascati, transported to DESY and tested with cosmic rays with different trigger configurations. The cosmic rays have been used to test the full readout of the detector, using the Photon Detector as a trigger and a stand-alone tracking system, since the magnet was not included in the test. The reconstruction algorithm, the event display and the wire maps were developed, ensuring effective data acquisition, data processing and interpretation for standard HERMES software analysis tools. The Gain Monitoring System (GMS) of the detector was also successfully tested. The value of GMS signal was at the level of 4 MIPs. The efficiency of the Photon Detector has been calculated in three different conditions, looking if the hit in the strip of the Photon Detector is according to the tracking based on SciFi, or in 1 neighbouring strip in each side, or in 2 neighbouring strips on each side (Fig. 5-left) in all three layers. The Recoil Detector has been installed at the end of 2005 and it will enter in the data taking of next years.

### 3.3 Technical software

LNF members were main responsible for Particle Identification (PID). In particular they worked on the maintenance and code development of the PID library function, on the PID calibration, on the new data productions of 2004 and 2005, on the flux corrections to PID for different physics analyzes, mainly dedicated to the transversity group. LNF has also the responsibility of the online data quality. At the end of 2005 the code has been developed for taking into account the Recoil detector in the upcoming data and the display of the online data quality chain has been implemented.

The LNF group acted also as HERMES Linux administrator and represented HERMES on DESY

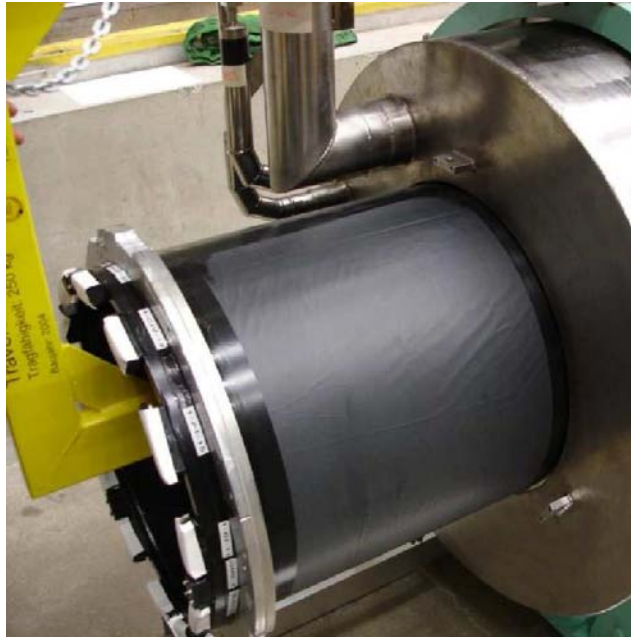


Figure 4: A picture of the Photon Detector during the installation in the HERMES experimental area in November 2005.

Linux user meeting, where user requirements and future strategy for Linux support were discussed. HERMES has a powerful Linux-based PC-farm with 2 work-groups servers, 4 file-servers and 30 batch nodes for various types of analysis. In 2005 there were 16 more batch nodes purchased with new powerful 64-bit AMD Dual Opteron CPUs. A suitable Linux distribution for this cluster has been set up to meet the growing demands of the users on data analysis and Monte-Carlo productions. The maintenance of the computers is provided through SNMP protocol plugged through an SMS gateway, which allows immediate knowledge in case of failures. In addition, there are about 40 desktop PCs acting as terminals for users and about 20 notebook computers for working use.

## 4 Data analysis and physics results of the LNF group in 2005

### 4.1 Inclusive spin structure functions

The cross-check of the moments of the polarised structure function  $g_1$  have been performed, as well as the checks for the compatibility of the HERMES and SLAC measurements of  $g_1$  for the deuteron, performing also studies on the parameterisation of the unpolarised structure function  $F_2$ . All these studies will be reported in a long paper on the precise determination of the spin-dependent structure function  $g_1$  of the proton, deuteron and neutron in preparation.

Deep inelastic scattering from a polarised spin-1 target yields qualitative new information which is not available in the spin 1/2 case, like the tensor structure function  $b_1$ . It describes the difference in the quark distributions between the helicity-0 and the averaged non-zero helicity states of the deuteron. It is sensitive only to the spin of the hadron embedding the quarks, in contrast to the spin structure  $g_1$  which probes the helicity of the quarks. The measurement of  $b_1$  therefore

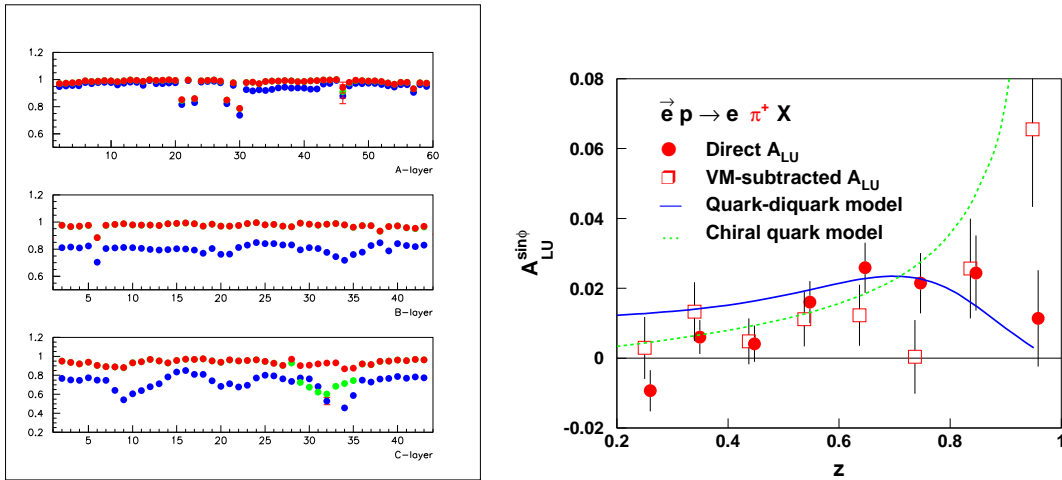


Figure 5: *Left: The Photon Detector efficiency in three different combinations: the reconstructed track crosses exactly the strips fired in each side (blue) according to the tracking based on the SciFi detector, with  $\pm 1$  neighbouring strip on each side (green) and with  $\pm 2$  neighbouring strips on each side (red symbols). A,B,C correspond to the three layers of the Photon Detector. Right: Beam spin asymmetry for semi-inclusive  $\pi^+$  production as function of the pion relative energy. The HERMES data, with and without subtraction of contribution from vector meson production, are compared with two theory model predictions, based on different assumptions.*

represents the opportunity to obtain new information on nuclear binding effects at the parton level. Because the deuteron is a weakly-bound state of spin-1/2 nucleons,  $b_1^d$  was predicted to be negligible. The first measurement, done by HERMES (Fig. 1), shows that  $b_1^d$  is different from zero and its magnitude rises for decreasing  $x$  and, for  $x \leq 0.03$  becomes even larger than that of  $g_1^d$  at the same value of  $Q^2$ .

#### 4.2 Beam-spin asymmetry in SIDIS

Single-spin asymmetries in semi-inclusive deep-inelastic-scattering (SIDIS) are known as a powerful tool for probing the structure of the nucleon. They give access to transverse momentum dependent parton distributions and time-reversal-odd fragmentation functions with prominent examples like the transversity  $h_1$  and Sivers  $f_{1T}^\perp$  distributions and Collins  $H_1^\perp$  fragmentation functions. These quantities have been studied so far with unpolarized beam and both transverse and longitudinally polarized targets. Recently, the analyzing power for a beam spin asymmetry with unpolarized beam has been also investigated (Fig. 5-right). This asymmetry can be related to the twist-3  $p_T$  dependent unpolarized distribution  $e(x)$  and requires a non-zero Collins fragmentation function.

#### 4.3 Exclusive production of single pion

The interest in the hard exclusive electroproduction of mesons has grown since a QCD factorization theorem was proved in the case of longitudinal photon at large  $Q^2$ . The amplitude for such reactions can be factorized into a hard lepton scattering part and two soft parts which parametrize the produced meson by a distribution amplitude and the target nucleon by four Generalized Parton Distributions (GPDs). In the case of exclusive electroproduction of pion, the reaction provides

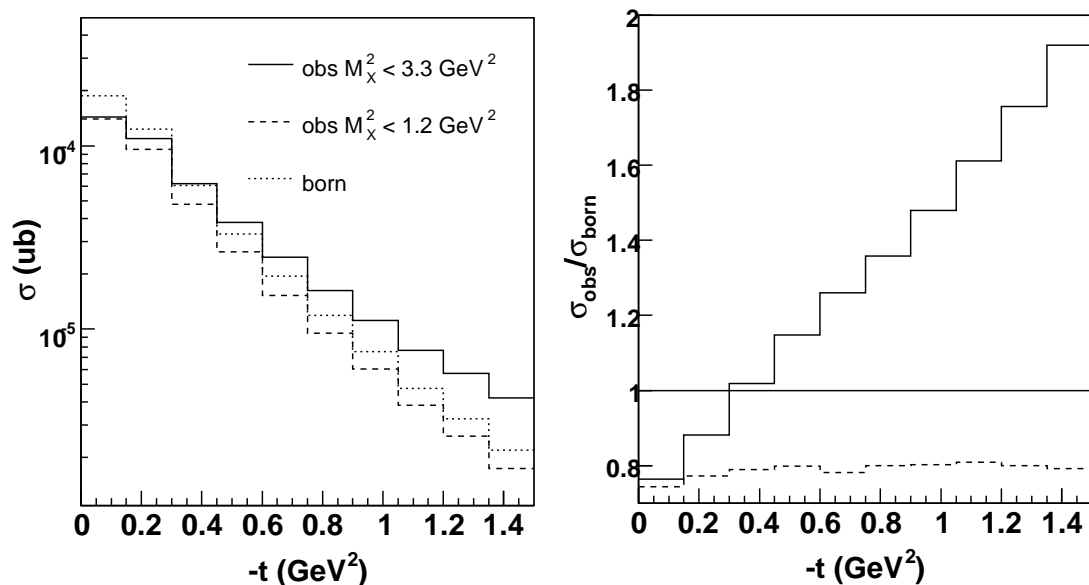


Figure 6: Left : Observed and born cross sections as a function of  $-t$ . Right: Radiative correction as a function of  $-t$  for two different inelasticity cuts corresponding to the cut applied on the data  $M_X^2=1.2 \text{ GeV}^2$  (dashed line) and to the cut applied on the data  $+3\sigma M_X^2=3.3 \text{ GeV}^2$  (full line).

essential information of the largely unknown space-like pion form factor and of the polarized GPDs ( $\tilde{H}$  and  $\tilde{E}$ ). First preliminary results for the unpolarized  $ep \rightarrow en\pi^+$  has been extracted in a wide  $Q^2$ - and  $x$ -ranges. For the total cross section determination a Monte Carlo based on GPD has been developed to account for detector acceptance and efficiency. The radiative corrections has been implemented event by event in the Monte Carlo in order to extract the Born cross section from the data and to estimate the radiative effect to the detector acceptance and efficiency (Fig. 6). Futhermore, SSA on a transversally polarized target are now in the stage of the analysis. This observable is expected to be less sensitive to corrections to QCD leading order and will be directly compared to GPD's predictions.

#### 4.4 Exclusive production of $\pi^+\pi^-$ pairs

Hard exclusive electroproduction of  $\pi^+\pi^-$  pairs is sensitive the interference between isospin  $I = 1$  (P-wave) and  $I = 0$  (S, D-wave) channels and provides new constrains on certain combination of GPDs. By studying the angular distribution of charged pion pair at high  $x_{Bj}$  and by evaluating the relevant Legendre moments  $P_n$ , it has been already shown that these results constrain models for GPDs. In particular this observable showed high sensibility for the separation of the contributions of two-gluon and  $q\bar{q}$  exchange mechanism, which are connected to the quark and gluon content of the nucleon. New results came by studying the low  $x_{Bj}$  region where  $P_n$  would shown contributions from the higher-twist 3-gluon exchange mechanism giving possible signature of the elusive *odderon*. The results show that the first moment of the Legendre polynomial associated to the hadron pair gets flattened to zero as  $x_{Bj}$  decreases. However, no signature of a possible contribution to  $P_1$  from odderon is visible within the experimental accuracy reached.

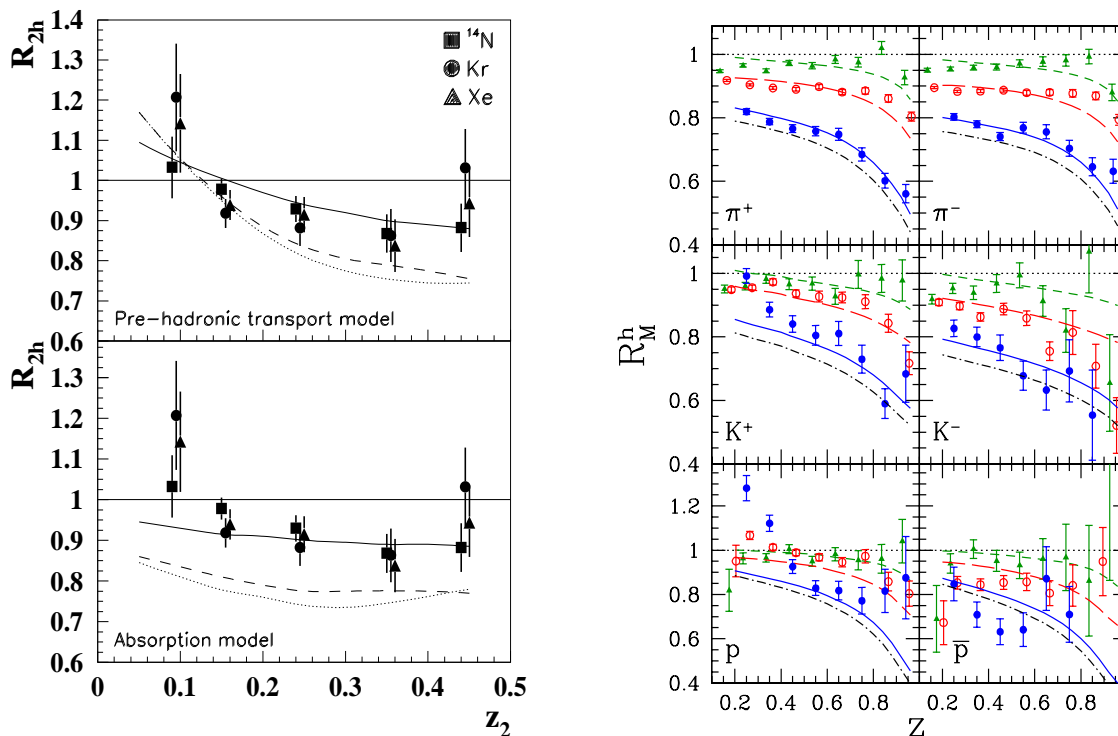


Figure 7: *Left* : The two hadron suppression on nuclei for  $^{14}\text{N}$ , Kr and Xe. In the upper panel the curves (solid for  $^{14}\text{N}$ , dashed for Kr, dotted for Xe) are calculated within a BUU transport model. In the bottom panel the same data are shown with calculations that assume only absorption for the three nuclei (same line types as in the upper plot). *Right* : Computed multiplicity ratios for pions, kaons, protons and antiprotons as a function of  $z$  for He (dashed line), Ne (long-dashed line), Kr (solid line) and Xe (dot-dashed line) compared with the HERMES data on Kr (solid circles) and the preliminary HERMES data on He (closed triangles) and on Ne (open circles).

#### 4.5 Nuclear effects in two hadron electroproduction

Medium modification of dihadron fragmentation function has been studied by considering the relative yield of two hadrons (leading and sub-leading) over the leading one in nuclei with respect to deuterium. In parallel with the jet correlation measurements in heavy-ion collisions, double hadron leptonproduction offers a way to disentangle hadronization occurring inside versus outside the nucleus. In Fig. 7-left the HERMES data show an effect which is substantially smaller in magnitude and reduced in the  $A$ -dependence compared to the previously measured single hadron multiplicity ratio. The solid curves are model theoretical prediction which use the quark concept for the prehadronic cross section and a hadron formation time  $\tau_f = 0.5$  fm/c. The data do not support naïve expectations for pre-hadronic and hadronic final-state interactions that are purely absorptive. Models that interpret modifications to fragmentation as being due to pre-hadronic scattering or partonic energy loss are also inconsistent with the data. In fact the latter predict an even larger  $A$ -dependence, while the data show little.

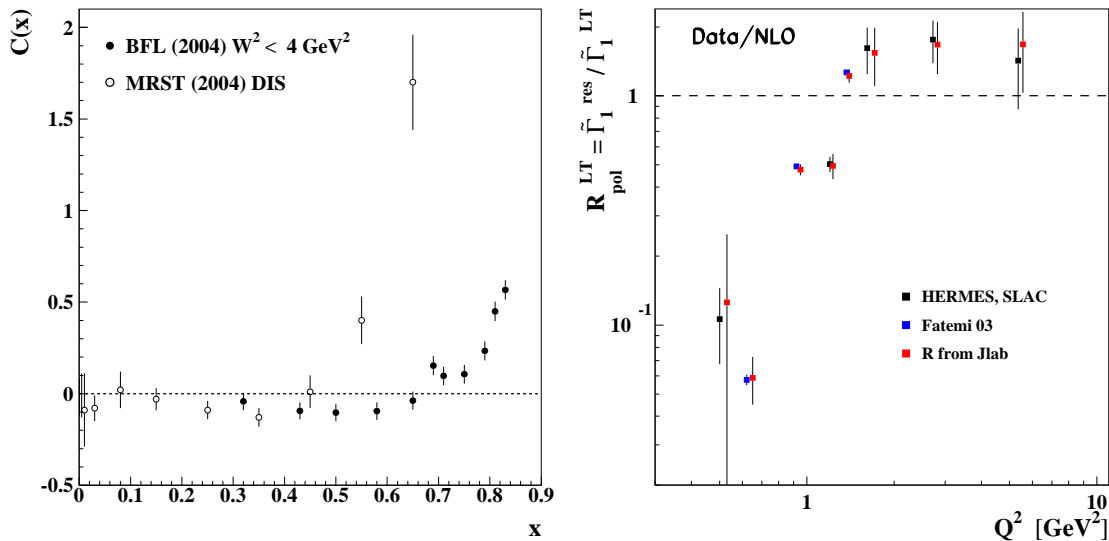


Figure 8: *Left: Comparison of HT contributions for the structure function  $F_2$  in the DIS and resonance regions, respectively. The full circles are the values of HT obtained in the resonance region, the empty ones are from MRST parameterization. Right: Ratio of the experimental data on  $g_1$  and the PQCD extrapolation to the resonance region. Notice that the new Fatemi results agree with the trend of the Hermes data.*

## 5 Phenomenology on HERMES physics of the LNF group in 2005

### 5.1 Nuclear medium effects in fragmentation

Hadron production in lepton-nucleus scattering is studied in an absorption model in which hadronization in the nuclear medium is dominated by pre-hadron formation and absorption. The hadron formation length is shown to be flavor dependent. The model correctly describes pion and kaon multiplicity ratios, while model computations disagree with proton data, especially at low  $z$ , suggesting a non-negligible diquark fragmentation contribution (Fig. 7-right).

### 5.2 Quark-hadron duality

Parton-hadron duality is generally defined as the similarity between hadronic cross sections in the Deep Inelastic Scattering region and in the resonance region. It encompasses therefore a range of phenomena where one expects to observe a transmutation from partonic to hadronic degrees of freedom, a question, the latter, at the very heart of Quantum Chromodynamics. A perturbative QCD NLO analysis including target mass corrections and large  $x$  re-summation effects has been extended to the integrals of both unpolarized and polarized structure functions in the resonance region. Both effects have been quantified and disentangled for the first time. A different behavior for unpolarized and polarized structure functions has been found. The discrepancy of the ratio from unity has been interpreted in terms of higher twists (HTs). The extraction of the dynamical HT terms from the resonance region for the unpolarised structure function  $F_2$  is shown in Fig. 8 (left panel), where a clear discrepancy is seen for  $F_2$ , marking perhaps a breakdown of the twist expansion at low values of  $W^2$ . A comparison with other results obtained in the DIS region

is also shown. Compared to previous analysis, new data from JLab have been added for the polarized structure function  $g_1$  and the experimental values of the ratio  $R = \sigma_L/\sigma_T$  from recent JLab measurements in the resonance region have been used (Fig. 8-right). The latter introduce an oscillation around the original result of about 2%, well within the error bars. The new data introduced confirm a large violation of duality at  $Q^2 \approx 1 \text{ GeV}^2$  in the polarised case. A complete analysis of these results in comparison with other HT extractions is under study.

## 6 Outlook

The data taking with Recoil Detector installed will start at the beginning of 2006 and it will continue until the shutdown, scheduled in autumn. New precision data on hard exclusive reactions will be collected and analyzed. The ongoing physics analysis and the phenomenological investigations will be completed.

## 7 Conferences by LNF Authors in Year 2005

### 7.1 Conference Talks

1. E. Avetisyan, Beam Single Spin Asymmetry measurements at HERMES, International Workshop on Semi-inclusive Reactions and 3-D Parton Distributions (SIR05), JLab (USA).
2. E. Avetisyan, Transverse spin effects in single and double hadron production at Hermes, International Europhysics Conference on High Energy Physics (EPS2005), Lisboa (Portugal).
3. N. Bianchi, Nuclear Medium Effects in Fragmentation Functions, X Workshop on Nuclear Physics (WONP05), Havana (Cuba).
4. N. Bianchi, Review of Transversity Measurements, XLIII Winter Meeting, Bormio, (Italy).
5. P. Di Nezza, Spin Physics Overview, International Workshop on Quantum Chromodynamics: Theory and Experiments (QCD@Work2005), Conversano (Italy).
6. P. Di Nezza, What we can learn from DIS on nuclei, 47th Workshop of the INFN Eloisatron Project, Erice (Italy).
7. A. Fantoni, Quark-Hadron Duality and Higher Twist Contributions in Structure Functions, XLIII Winter Meeting, Bormio, (Italy).
8. A. Fantoni, The transition from pQCD to non perturbative QCD, First Workshop on Quark-Hadron Duality and the Transition to pQCD, Laboratori Nazionali di Frascati (Italy).
9. A. Fantoni, The transition from QCD to perturbative QCD: duality and higher twist effects, 6th Research Conference on Electromagnetic Interactions with Nucleon and Nuclei (EINN2005), Milos (Greece).
10. A. Fantoni, Recenti risultati dell'esperimento HERMES, XCI Congresso Nazionale Società Italiana di Fisica (SIF), Catania (Italy).
11. A. Fantoni, Test of Time Invariance in Electromagnetic Interactions, International Workshop on Nucleon Form Factors, Laboratori Nazionali di Frascati (Italy).
12. C. Hadjidakis, Hard exclusive production at HERMES, XLIII Winter Meeting, Bormio, (Italy).
13. C. Hadjidakis, Hermes overview on diffractive and exclusive physics, XVII Rencontre de Blois: XI International Conference on Elastic and Diffractive Scattering (EDS05), Blois (France).
14. C. Hadjidakis, Deeply Virtual Meson Production, 6th Research Conference on Electromagnetic Interactions with Nucleon and Nuclei (EINN2005), Milos (Greece).
15. D. Hasch, Flavour separation from Semi-Inclusive Data, Annual meeting on Particle Physics and Hadron Structure of the German Physics Society (DPG), Berlin (Germany).

16. D. Hasch, Future Measurements of Transverse Momentum Dependent Distributions and Fragmentation Functions, International Workshop on Semi-inclusive Reactions and 3-D Parton Distributions (SIR05), JLab (USA).
17. D. Hasch, Experimental Overview on Exclusive Processes, First Workshop on Quark-Hadron Duality and the Transition to pQCD, Laboratori Nazionali di Frascati (Italy).
18. D. Hasch, Future Transverse Momentum Distribution Measurements, Advanced Studies Institute on Symmetries and Spin, Prague (Czech Republic).
19. V. Muccifora, Introduction to the experimental results on in-medium hadron production, Workshop on Parton propagation through Strongly Interacting Systems, ECT\* Trento (Italy).
20. C. Riedl, Precision results on the spin structure  $g_1$  of the proton, the deuteron and the neutron from the HERMES experiment, XCI Congresso Nazionale Società Italiana di Fisica (SIF), Catania (Italy).

## 7.2 Conference organization and advisory, Projects, Seminars, Lectures, Editors

1. N. Bianchi, (Member) JLab Scientific Committee.
2. N. Bianchi, (International Advisory Committee) International Workshop on Semi-inclusive Reactions and 3-D Parton Distributions (SIR05), JLab (USA).
3. N. Bianchi, (Chair International Organizing Committee) First Workshop on Quark-Hadron Duality and the Transition to pQCD, Laboratori Nazionali di Frascati (Italy).
4. N. Bianchi, (International Organizing Committee) International Workshop on Nucleon Form Factors, Laboratori Nazionali di Frascati (Italy).
5. E. De Sanctis, (Organizer) Workshop on New Hadrons: Facts and Fancy, Milos (Greece).
6. E. De Sanctis, (Organizer) Workshop on Physics and Technology frontiers of facilities for hadron physics, Milos (Greece).
7. E. De Sanctis, (International Organizing Committee) 6th Research Conference on Electromagnetic Interactions with Nucleon and Nuclei (EINN2005), Milos (Greece).
8. E. De Sanctis, (International Organizing Committee) International Workshop on Nucleon Form Factors, Laboratori Nazionali di Frascati (Italy).
9. E. De Sanctis, (Convener) N7-Transversity: Exploring the unknown transverse spin structure of the nucleon, I3HP Project.
10. E. De Sanctis, (Convener) Misura della Trasversalità del Nucleone, Cofinanziamento MIUR.
11. E. De Sanctis, (Convener) HERMES-LNF TARI at DESY.
12. P. Di Nezza (Seminar), Hadron propagation in nuclear matter, CERN (Switzerland).
13. P. Di Nezza, (Convener Spin Physics) 13th International Workshop on Deep Inelastic Scattering and QCD (DIS05), Madison (USA).
14. P. Di Nezza (Organizing Committee) First Workshop on Quark-Hadron Duality and the Transition to pQCD, Laboratori Nazionali di Frascati (Italy).
15. P. Di Nezza (Seminar), Overview on the Deep Inelastic Scattering, Hamburg (Germany).
16. P. Di Nezza (Seminar), Overview on the Deep Inelastic Scattering, Zeuthen (Germany).
17. P. Di Nezza (Lectures), The spin of the nucleon, DESY Summer school, Hamburg (Germany).
18. P. Di Nezza (Lectures), The spin of the nucleon, DESY Summer school, Zeuthen (Germany).
19. A. Fantoni, (Chair International Organizing Committee) First Workshop on Quark-Hadron Duality and the Transition to pQCD, Laboratori Nazionali di Frascati (Italy).
20. A. Fantoni, (Local Organizing Committee), International Workshop on Nucleon Form Factors, Laboratori Nazionali di Frascati (Italy).

21. A. Fantoni, (Seminar) From DAΦNE to DAFNE2, University of Virginia (USA).
22. A. Fantoni, (Editor Proceedings) First Workshop on Quark-Hadron Duality and the Transition to pQCD, Laboratori Nazionali di Frascati (Italy).
23. A. Fantoni, (Editor) Future Research Activities at LNF: Working Group Report, LNF-05/33.
24. D. Hasch, (Local Organizing Committee), International Workshop on Transverse Polarisation Phenomena in Hard Processes (Transversity 2005), Como, Italy.
25. D. Hasch, (Lectures) Exploring the Structure of the Nucleon, Graduate College of the Albert-Ludwigs-University, Freiburg (Germany).
26. D. Hasch, (Lectures) Spin physics at Hermes, Workshop on Hard Processes of the Joint Graduate College of the University Bochum and University Dortmund, Dortmund (Germany).
27. V. Muccifora, (Organizing Committee) First Workshop on Quark-Hadron Duality and the Transition to pQCD, Laboratori Nazionali di Frascati (Italy).
28. V. Muccifora, (Organizer) Workshop on Parton propagation through Strongly Interacting Systems, ECT\* Trento (Italy).
29. V. Muccifora, (Local Organizing Committee), International Workshop on Nucleon Form Factors, Laboratori Nazionali di Frascati (Italy).

## 8 Publications of LNF Authors in Year 2005

1. A. Accardi, D. Grunewald, V. Muccifora and H.J. Pirner, “Atomic Mass Dependence of Hadron Production in Deep Inelastic Scattering on Nuclei”, Nuclear Physics **A761** (2005) 67.
2. A. Airapetian *et al.*, “Quark Helicity Distributions in the Nucleon for up-, down-, and strange-quarks from Semi-inclusive Deep-inelastic Scattering”, Phys. Rev. Lett. **71** (2005) 012003.
3. A. Airapetian *et al.*, “The HERMES Polarized Hydrogen and Deuterium Gas Target in the HERA Electron Storage Ring”, Nucl. Instr. and Meth. **A540** (2005) 68.
4. A. Airapetian *et al.*, “Single-Spin Asymmetries in Semi-Inclusive Deep-Inelastic Scattering on a Transversely-Polarized Hydrogen Target”, Phys. Rev. Lett. **94** (2005) 012002.
5. A. Airapetian *et al.*, “Search for an exotic S=-2, Q=-2 baryon resonance at a mass near 1862 MeV in quasi-real photoproduction”, Phys. Rev. **D71** (2005) 032004.
6. A. Airapetian *et al.*, “First Measurement of the Tensor Structure Function  $b_1$  of the Deuteron”, Phys. Rev. Lett. **95** (2005) 242001.
7. A. Airapetian *et al.*, “Subleading twist effects in single-spin asymmetries in semi-inclusive deep-inelastic scattering on a longitudinally polarized hydrogen target”, Phys. Lett. **B622** (2005) 14.
8. A. Airapetian *et al.*, “Double hadron leptonproduction in the nuclear medium, submitted to Phys. Rev. Lett., hep-ex/0510030.
9. A. Airapetian *et al.*, “The time-of-flight technique for the HERMES experiment”, Nucl. Instr. and Meth., **A540** (2005) 305.
10. N. Bianchi, “Experimental Review of Transversity”, Nucl. Phys. **A755** (2005), 91.
11. A. Fantoni, N. Bianchi and S. Liuti, “Quark-hadron duality in structure functions”, Eur. Phys. J. **A24S1** (2005) 35.

## $\bar{\text{P}}\text{ANDA}$ - $\bar{\text{p}}$ Annihilation at Darmstadt

B. Dulach, P. Gianotti (Resp. Naz.), C. Guaraldo, O.N. Hartmann (Art. 23),  
M. Iliescu (Art. 2222), V. Lucherini, D. Orecchini, E. Pace,  
L. Passamonti, D. Sirghi (Art. 2222), F. Sirghi (Bors. UE)

### 1 Introduction

$\bar{\text{P}}\text{ANDA}$ , one of the bigger future experiments in nuclear and hadron physics at the Facility for Antiproton and Ion Research (FAIR <sup>1</sup>), is dedicated to study annihilations of antiprotons on nucleons and nuclei up to a maximum center-of-mass energy in  $\bar{\text{p}}\text{p}$  of 5.5 GeV. For more details, refer to <sup>2, 3</sup>.

The LNF are particularly involved in the planning and construction of the central tracker (s.a. <sup>4</sup>) of the  $\bar{\text{P}}\text{ANDA}$  detector.

### 2 The $\bar{\text{P}}\text{ANDA}$ Central Tracker

The central tracking detector of  $\bar{\text{P}}\text{ANDA}$  is a cylindrical device surrounding the interaction point, with an inner radius of 15 cm and an outer boundary at  $r = 42$  cm. Two options for this detector are discussed, a straw tube tracker (STT) and a time projection chamber (TPC). The LNF group is working especially on the first option.

#### 2.1 Detector Design

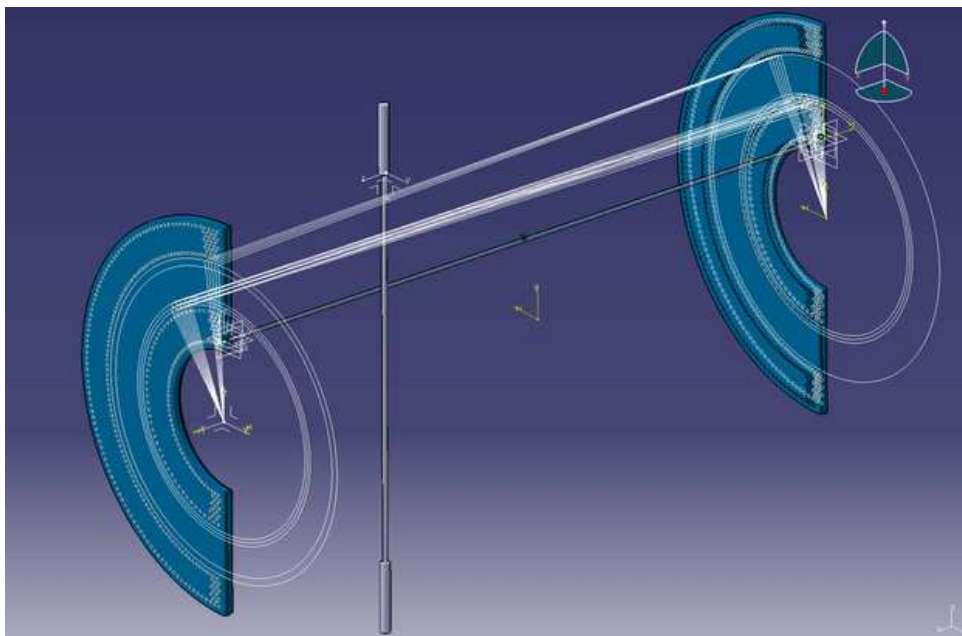


Figure 1: A support solution for the STT. Details in the text.

One work carried out at the LNF is a the overall design of the STT. The straw tubes, preferentially in two diameters (6 and 8 mm), have to be arranged and supported.

The tubes have a nominal length of 150 cm, the introduction of skewed (stereo) layers might be necessary to resolve ambiguities in the reconstruction of the  $z$  coordinate. The mechanical support could be incurred by two flanges at the upstream and the downstream end, respectively. Fig. 1 shows the principle.

In the figure, two half-flanges with the appropriate drillings for the single tubes are shown, together with the target pipe; the intersection of target- and beam pipe ( $z$  axis) denotes the interaction point. The tubes are oriented parallel to the  $z$  axis, or, as also indicated, skewed by a small angle ( $2^\circ \dots 3^\circ$ ).

A small scale prototype (15 tubes) has been constructed at the LNF to allow further R&D on mechanics, electronics, gas feed, power supply, readout etc. Fig. 2 shows a photograph of that prototype.



Figure 2: Photograph of the straw tube prototype constructed at the LNF.

## 2.2 Simulation Studies

The  $\overline{\text{P}}\text{ANDA}$  central tracker will operate in the magnetic field of a solenoid. Following the design of the magnet, it could not easily be avoided to have a non-uniform magnetic field especially at the borders of the tracking region. To study the influence of the magnetic field on the major properties of a single straw tube, the Garfield/Magboltz<sup>5)</sup> programs have been used. Here, a tube of 6 mm diameter with a  $20 \mu\text{m}$  wire at 2 kV high voltage and a gas mixture of Argon and  $\text{CO}_2$  (9:1, 300 K, atmospheric pressure) is traversed by a 500 MeV  $\pi^+$ . The magnetic field has been varied by  $\pm 10\%$  in  $B_z$  and by adding a  $B_r$  component. The influence on the drift velocity and the time-space-correlation has been investigated. Fig. 3 shows the  $x(t)$  plot. The data points correspond to the minimum drift time which has been found and the integrated diffusion for the fastest driftline. The dataset with the non-uniform field ( $B_r > 0$ ) lies nearly on top of the uniform one. Also for the drift velocity, a small influence has been found only outside the working region (plateau). In conclusion, with the given magnetic field values for the  $\overline{\text{P}}\text{ANDA}$  solenoid, a single straw tube is not significantly affected in its functionality.

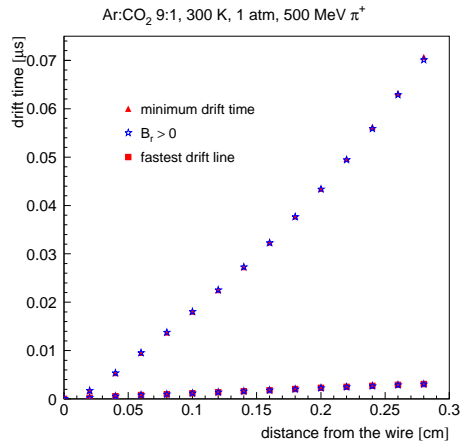


Figure 3: The space-time-correlation plot for a single straw tube. Details in the text.

### 3 Acknowledgments

We appreciate the support from the European Community-Research Infrastructure Activity under the FP6 “Structuring the European Research Area” program (HadronPhysics, contract number RII3-CT-2004-506078).

### 4 List of Conference Talks by LNF members in the year 2005

1. Hartmann, O.N.: “Nuclear and Hadron Physics with Antiprotons: PANDA@FAIR”; 6th International Conference on Nuclear Physics at Storage Rings, May 23-26, Jülich-Bonn, Germany.
2. Gianotti, P.: “Perspectives with PANDA”; 1st Workshop on Quark-Hadron Duality and the Transition to pQCD, June 6-8, LN Frascati, Italy.
3. Hartmann, O.N.: “Tracking in Antiproton Annihilation Experiments”; Workshop on Tracking in High Multiplicity Environments, October 3-7, Zürich, Switzerland.

### References

1. <http://www.gsi.de/fair/>
2. <http://www.gsi.de/panda/>
3. PANDA Letter of Intent, 2004; PANDA Technical Progress Report, 2005.
4. TIME’05 Proceedings, to be published in NIM A, LNF-06/3(P), nucl-ex/0602001.
5. <http://consult.cern.ch/writeup/garfield/>
6. STORI’05 - Proceedings of the 6th International Conference on Nuclear Physics at Storage Rings, Schriften des FZ Jülich, Reihe Materie und Material, Band 30, ISBN 3-89336-404-8.

## SIDDHARTA

M. Bragadireanu (Bors. UE), M. Catitti (Ass. Ric.), C. Curceanu Petrascu (Co-Resp. Naz.),  
C. Guaraldo (Co-Resp. Naz.), M. Iliescu (Art. 2222), P. Levi Sandri, V. Lucherini,  
F. Lucibello (Tecn.), D. Pietreanu (Bors. PD), D. Sirghi (Art. 2222), F. Sirghi (Bors. UE)

### 1 The SIDDHARTA scientific program

The objective of the SIDDHARTA (Silicon Drift Detector for Hadronic Atom Research by Timing Application) experiment is to continue, to deepen and enlarge the successful scientific line, initiated by the DEAR experiment in performing precision measurements of X-ray transitions in exotic (kaonic) atoms at DAΦNE.

The eV precise determination of the shift and width of the  $1s$  level with respect to the purely electromagnetic calculated values, in kaonic hydrogen and kaonic deuterium, generated by the presence of the strong interaction, through the measurement of the X-ray transitions to this level, will allow the first precise experimental determination of the isospin dependent antikaon-nucleon scattering lengths.

The shift  $\epsilon$  and the width  $\Gamma$  of the  $1s$  state of kaonic hydrogen are related to the real and imaginary part of the complex  $s$ -wave scattering length,  $a_{K^-p}$ , through the Deser formula:

$$\epsilon + i\Gamma/2 = 2\alpha^3 \mu^2 a_{K^-p} = (412 \text{ eV } fm^{-1}) \cdot a_{K^-p} \quad (1)$$

where  $\alpha$  is the fine structure constant and  $\mu$  the reduced mass of the  $K^-p$  system. In the isospin limit, i.e. in the absence of the electromagnetic interaction and at  $m_d = m_u$ ,  $a_{K^-p}$  can be expressed directly in terms of the scattering lengths for isospin  $I=0$  and  $I=1$ :

$$a_{K^-p} = \frac{1}{2}(a_0 + a_1) \quad (2)$$

A similar relation applies to the case of kaonic deuterium and to the corresponding scattering length  $a_{K^-d}$ :

$$\epsilon + i\Gamma/2 = 2\alpha^3 \mu^2 a_{K^-d} = (601 \text{ eV } fm^{-1}) \cdot a_{K^-d} \quad (3)$$

An accurate determination of the  $K^-N$  isospin dependent scattering lengths will place strong constraints on the low-energy  $K^-N$  dynamics, which, in turn, constraints the SU(3) description of chiral symmetry breaking in systems containing the strange quark, contributing to the determination of the so-called kaon-nucleon sigma terms. These sigma terms are also important inputs for the determination of the strangeness content of the proton. This quantity depends on both kaon-nucleon and pion-nucleon sigma terms, being more sensitive to the first ones.

The DEAR measurement on kaonic hydrogen, performed in 2002 (Phys. Rev. Lett 94 (2005), 212302), has triggered new interest and results from the theoretical groups working in the low-energy kaon-nucleon interaction field, as well related to non-perturbative QCD tests.

The new experiment SIDDHARTA, aims to improve the precision obtained by DEAR by an order of magnitude and to perform the first measurement ever of kaonic deuterium. Other measurements (kaonic helium, sigmonic atoms, precise determination of the charged kaon mass) are as well considered in the scientific program.

### 2 The SIDDHARTA experiment features

SIDDHARTA (Silicon Drift Detector for Hadronic Atom Research by Timing Application) represents a new phase in the study of kaonic atoms at DAΦNE. The DEAR precision was limited by a

signal/background ratio of about 1/70. In order to significantly improve this ratio a breakthrough is necessary. An accurate study of the background sources present at DAΦNE was re-done. The background includes two main sources:

- synchronous background: coming together with the  $K^-$  - related to  $K^-$  interaction in the setup materials and also to the  $\phi$ -decay process; it can be defined hadronic background;
- asynchronous background: final products of electromagnetic showers in the machine pipe and in the setup materials originated by particles lost from primary circulating beams either due to the interaction of particles in the same bunch (Touschek effect) or due to the interaction with the residual gas.

Accurate studies performed by DEAR showed that the main background source in DAΦNE is of the second type, which shows the way to reduce it. A fast trigger correlated to the negative kaon entrance in the target would cut the main part of the asynchronous background.

While DEAR used for the X rays detection the CCD (Charge Coupled Device) detectors - excellent X-ray detectors, with very good energy resolution (about 140 eV FWHM at 6 keV), but having the drawback of being non-triggerable devices (since the read-out time per device is at the level of 10 s), a recently developed device, which preserves all good features of CCDs (energy resolution, stability and linearity) but additionally is triggerable - i.e. fast (at the level of  $1\mu\text{s}$ ) was implemented. This new detector is represented by large area Silicon Drift Detector (SDD), specially designed for spectroscopic application. The development of the new  $1\text{ cm}^2$  SDD device is partially performed in the framework of an European Joint Research Activity (JRA10) within the FP6 program, the HadronPhysics I3.

Successful tests of SDD prototypes were performed in 2003 and 2004 at the Beam Test Facility of Frascati (BTF), in realistic (i.e. DEAR-like) conditions. The results of this tests were very encouraging: a trigger rejection factor of  $5 \cdot 10^{-5}$  was measured. Extrapolated to SIDDHARTA conditions, this number translates into a S/B ratio in the region of interest about 20/1. By triggering the SDDs, the asynchronous e.m. background (mainly due to Touschek effect) can therefore be eliminated.

### 3 Activities in 2005

In what follows, we present the main 2005 SIDDHARTA activities performed at LNF.

#### 3.1 Long term stability tests on SDD prototypes with final electronics configuration and 1 mV stabilized power supply

Long term stability tests were performed in the laboratory all along 2005 on SDD chip prototypes, equipped with the final-like readout electronics chip. The tests were done using a specially designed and LNF built 1 mV stabilized power supply, shown in Fig. 1.

The results of the tests were very encouraging, showing a stability for one month of run of better than 2-3 eV at 4.5 keV - titanium peak position (Figure 2).

#### 3.2 SDD ceramics design

The 200  $1\text{ cm}^2$  SDD chip production ended within 2005; in parallel, the design of the ceramics proceeded in a collaboration between SMI-Vienna and LNF-Frascati. The first prototype of the new ceramics adapted to the SDD geometry used in SIDDHARTA is ready (Fig. 3) and will be tested in 2006.

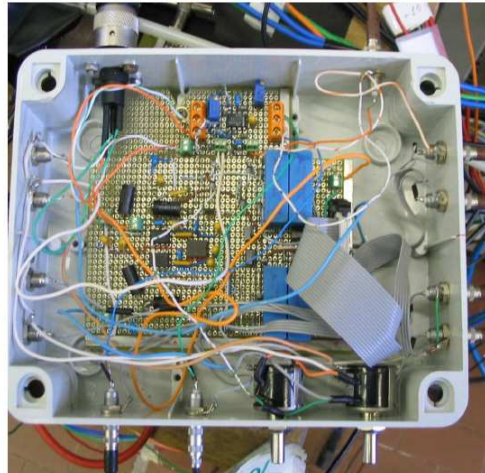


Figure 1: *The stabilized power supply specially designed for tests for SIDDHARTA.*

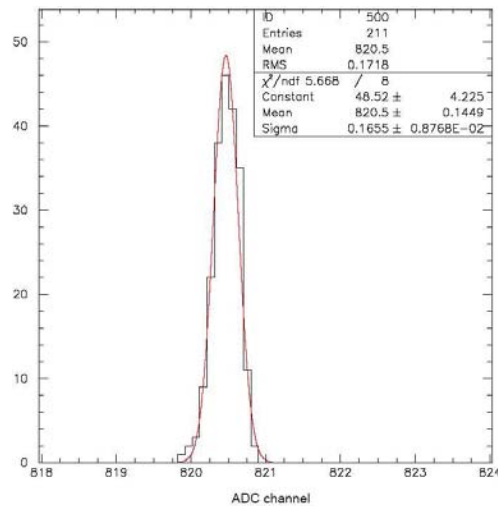


Figure 2: *Stability of the Titanium peak position for one month of run.*

### 3.3 Trigger tests for SIDDHARTA

The new trigger system for SIDDHARTA, using BC420 scintillator and Hamamatsu R4998 PMs, was tested in the laboratory and on BTF beam at LNF. In Fig. 4 a picture of the test trigger prototype, as installed at BTF, is shown, while in Fig. 5 the results, compared with previous kaon monitor system used in DEAR are presented. As seen from the figure, the system resolution in SIDDHARTA is a factor about 3 better than in the DEAR system.

### 3.4 General SIDDHARTA layout design

The design of the general SIDDHARTA layout, including platforms and supports to be installed at DAΦNE in the KLOE Interaction Region, started in 2005. A first drawing of the layout was realized and is discussed with DAΦNE staff and LNF mechanical workshop.



Figure 3: *The ceramics for SDD chips in SIDDHARTA.*

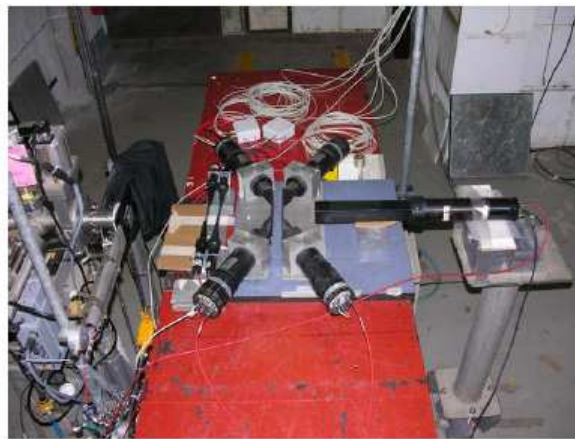


Figure 4: *The SIDDHARTA trigger prototype as installed in 2005 at BTF facility in Frascati.*

#### 4 Activity in 2006

The LNF activity of SIDDHARTA in 2006 is focussed in the following directions:

- intensive testing of the of front-end electronics; participation in the design of the final production run and testing;
- test of the DAQ system in parallel with final electronics;
- construction of the final trigger system;
- measurements in the lab and on BTF of 1 cm<sup>2</sup> SDD test setup;
- construction of a multi-channel high voltage control system and biasing of the SDD detectors;
- finalize the SIDDHARTA various setup components and start integration and testing;

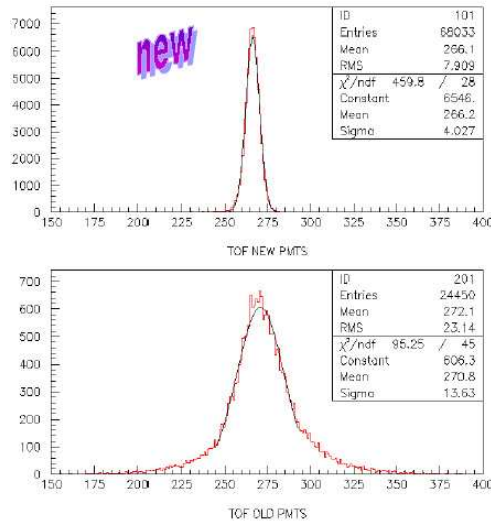


Figure 5: *The results of the test performed in parallel on the new SIDDHARTA trigger system (upper) and on the old DEAR system (lower).*

- finalize the general SIDDHARTA layout (platforms, supports) and start construction of components;
- Monte Carlo simulation of the system performance.

## 5 Publications 2005

### 5.1 List of Conference Talks given by LNF Authors in Year 2005

1. C. Curceanu (Petrascu), “Latest results from DEAR (Dafne Exotic Atom Research)”, Workshop on Exotic Hadrons, ECT\*, Trento, Italy, 21-25 February 2005.
2. D. Sirghi, “The physics of Kaonic Atoms at DAΦNE”, LNF Spring School in Nuclear, Sub-nuclear and Astroparticle Physics, Frascati (Italy), May 16 - 20, 2005.
3. F. Sirghi, “The SIDDHARTA experiment at DAΦNE”, LNF Spring School in Nuclear, Sub-nuclear and Astroparticle Physics, Frascati (Italy), May 16 - 20, 2005.
4. D. Sirghi and F. Sirghi, “Kaonic atoms measured by DEAR experiment at DAΦNE”, “Annual meeting of Bucharest University Phys. Department, 2005”, Bucharest, Romania, May 27, 2005.
5. C. Curceanu (Petrascu), “The SIDDHARTA experiment”, XCI Congresso Nazionale Societa’ Italiana di Fisica, Catania, 26 September - 1 October 2005.
6. C. Curceanu and C. Guaraldo, “AMADEUS - LOI for DAFNE2”, Austrian-Japanese Workshop on “Antikaon Mediated Bound Systems - Doorway to Kaon Condensation in Neutron Stars”, SMI Vienna (Austria, 21-22 December 2005.

## 5.2 Papers and Proceedings

1. M. Cargnelli *et al.*, “Kaonic hydrogen measurement with DEAR at DAΦNE”, *Int. J. Mod. Phys A* **20** (2005), 341.
2. H. Zmeskal *et al.*, “The DEAR experiment: first results on kaonic hydrogen”, *Nucl. Phys. A* **754** (2005), 369.
3. G. Beer *et al.*, “Measurement of the kaonic hydrogen X-ray spectrum”, *Phys. Rev. Lett.* **94** (2005), 212302..
4. C. Curceanu *et al.*, “Precision measurements on kaonic hydrogen and kaonic deuterium: present and future”, *AIP Conf. Proc.* **768** (2005), 291.
5. D. Sirghi and F. Sirghi *et al.*, “Kaonic atoms measured by DEAR experiment at DAΦNE”, *Romanian Reports in Physics Vol.* **57**, No. 3 (2005), 320.
6. M. Cargnelli *et al.*, “Silicon drift detectors for hadronic atom research - SIDDHARTA”, *Proceedings of EXA 05 - International Conference on Exotic Atoms and related topics, Vienna, Austria, 21-25 February, Austrian Academy of Sciences Press, Eds. A. Hirtl, J. Marton, E. Widmann and J. Zmeskal*, p. 313.
7. J. Zmeskal *et al.*, “Precision measurements with kaonic atoms: from DEAR to SIDDHARTA”, *Proceedings of EXA 05 - International Conference on Exotic Atoms and related topics, Vienna, Austria, 21-25 February, Austrian Academy of Sciences Press, Eds. A. Hirtl, J. Marton, E. Widmann and J. Zmeskal*, p. 139.
8. J. Marton *et al.*, “Precision measurements with kaonic atoms”, *Proceedings of HadAtom05 International Workshop, 15-16 February 2005, Univ. of Bern, Switzerland.*
9. M. Cargnelli *et al.*, “The SIDDHARTA project - Experimental Study of kaonic deuterium and helium”, *Proceedings of the conference Hadron Structure 2004, Smolenice Castle, Slovakia, Acta Physica Slovaca* **55**, No. 1 (2005), 7.
10. J. Marton *et al.*, “DEAR: Results on Kaonic Hydrogen”, *Proceedings of the conference Hadron Structure 2004, Smolenice Castle, Slovakia, Acta Physica Slovaca* **55**, No. 1 (2005), 69.
11. J. Marton *et al.*, “Kaonic Atoms at DAFNE: DEAR and SIDDHARTA”, *Proceedings of the 6th International Conference on Nuclear Physics at Storage Rings, Eds. D. Childze, A. Kacharava and H. Stroehel, Forschungszentrum Juelich* (2005), 190.
12. J. Marton *et al.*, “ Experimental Studies of Exotic Atoms at DAFNE: recent results and perspectives”, *Proceedings of Particle and Nuclei International Conference, PANIC05, Santa Fe, USA, October 22-28, 2005.*

## 5.3 Technical Notes

1. C. Curceanu (Petrascu), “Towards the definition of the SIDDHARTA setup: Monte Carlo simulations for 3 selected configurations”, *SIDDHARTA Note-IR-8, May 15, 2005.*

## VIP

S. Bartalucci, S. Bertolucci, M. Catitti (Ass. Ric.), C. Curceanu Petrascu (Resp. Naz.),  
S. Di Matteo (Art. 23), C. Guaraldo, M. Iliescu (Art. 2222), F. Lucibello (Tecn.),  
D. Sirghi (Art. 2222), F. Sirghi (Bors. UE), L. Sperandio (Dott.)

### 1 The VIP scientific case and the experimental method

The Pauli Exclusion Principle (PEP) represents a fundamental principles of the modern physics and our comprehension of the surrounding matter relies on it. Even if today there are no compelling reasons to doubt its validity, it still spurs a lively debate on its eventual limits, as testified by the abundant contributions found in the literature and in many topical conferences and it is still possible to speculate that it is only an approximation of a more fundamental law, and that there may be tiny violations. The indistinguishability and the symmetrization (or antisymmetrization) of the wave-function should be then checked independently for each particle, and accurate tests were and are being done.

The VIP (VIolation of the Pauli Exclusion Principle) experiment, an international Collaboration among 5 Institutions of 4 countries, has the goal to improve the current limit on the violation of the Pauli Exclusion Principle (PEP) for electrons, ( $P < 1.7 \times 10^{-26}$  established by E. Ramberg e G. A. Snow: *Experimental limit on a small violation of the Pauli principle*, Phys. Lett. **B 238** (1990) 438) by four orders of magnitude ( $P < 10^{-30}$ ), exploring a region where new theories might allow for a possible PEP violation.

The experimental method consists of introducing new electrons into a copper strip and to look for X-rays resulting from the  $2p \rightarrow 1s$  anomalous X-rays transitions emitted if one of the new electrons would be captured by a Cu atom and cascades down to the 1s state already filled with two electrons of opposite spin. The energy of this transition would differ from the normal  $K\alpha$  transition by about 400 eV (7.64 keV instead of 8.04 KeV), providing an unambiguous signal of the PEP violation. The measurement alternates periods with no current in the Cu strip, in order to evaluate the X-ray background in conditions where no PEP violating transitions are expected to occur, to periods in which current is flown in the conductor, thus providing “fresh” electrons, which might possibly violate PEP. The rather straightforward analysis consists on the evaluation of the statistical significance of the normalized subtraction of the two spectra in the region of interest.

The experiment is going to be performed at the LNGS Laboratories, where the X-ray background, generated by cosmic rays and natural radioactivities, is reduces, as will be shown in Section 3.1.

### 2 The VIP experimental setup

The VIP setup was built in 2005, starting from the DEAR setup, reutilizing the CCD (Charge Cpuoled Devices) X-ray detectors, and consists of a copper cylinder, acting as target, 4.5 cm in radius, 50  $\mu\text{m}$  thick, 8.8 cm high, surrounded by 16 equally spaced CCDs of type 55. The CCDs are at a distance of 2.3 cm from the copper cylinder, grouped in units of two chips vertically positioned. The setup is enclosed in a vacuum chamber, and the CCDs are cooled to about 165 K by the use of a cryogenic system, as shown in Fig. 1.

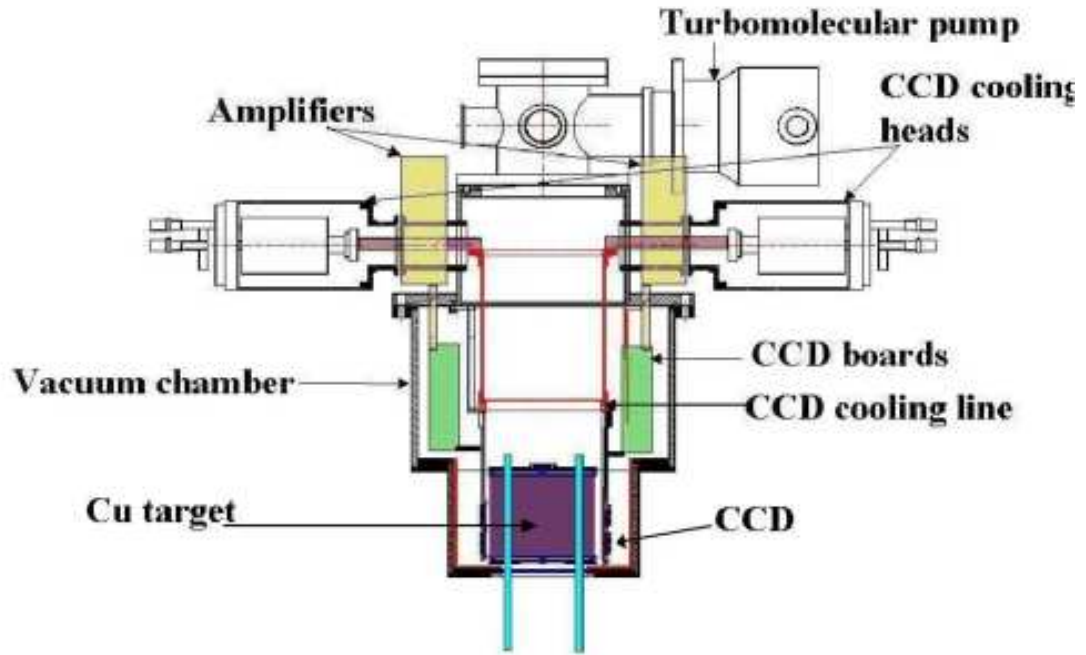


Figure 1: *The VIP setup. All elements of the setup are identified in the figure.*

### 3 Activities in 2005

#### 3.1 Preliminary X-ray background measurement at LNGS

In the first months of 2005, from 21 February to 28 March, an X-ray background measurement was performed at the LNGS laboratories, with a test setup consisting of 2 CCDs of the same type of those present in the VIP setup, with and without shielding. In Fig. 2 the 2 CCD test setup with lead and copper shielding, during its installation at LNGS, is shown.

A background reduction factor of about 50 was then obtained at LNGS, with respect to the preliminary measurements performed at Neuchatel. We recall that the VIP proposal asked for a reduction factor of about 100 (with respect to Neuchatel) by performing the measurement at LNGS. The factor 100 or more is then feasible by designing a special VIP shielding at LNGS and using specially treated, low activity, lead and copper.

#### 3.2 Test of the VIP setup in laboratory and preliminary PEP violation measurement

The VIP setup was mounted in the LNF laboratory, Fig. 3, after having built all the components, in autumn 2005. During the last two months of 2005 a VIP run was done at LNF, to test the setup performance and to obtain a preliminary limit on PEP violation.

The new limit on the probability that PEP is violated by electrons, as obtained from analyzing the data taken in the LNF laboratories with the VIP setup, gives a value, about  $4 \times 10^{-28}$  for the probability that PEP is violated for electrons, improving the existing limit by almost two orders of magnitude. This new value is going to be submitted for publication.

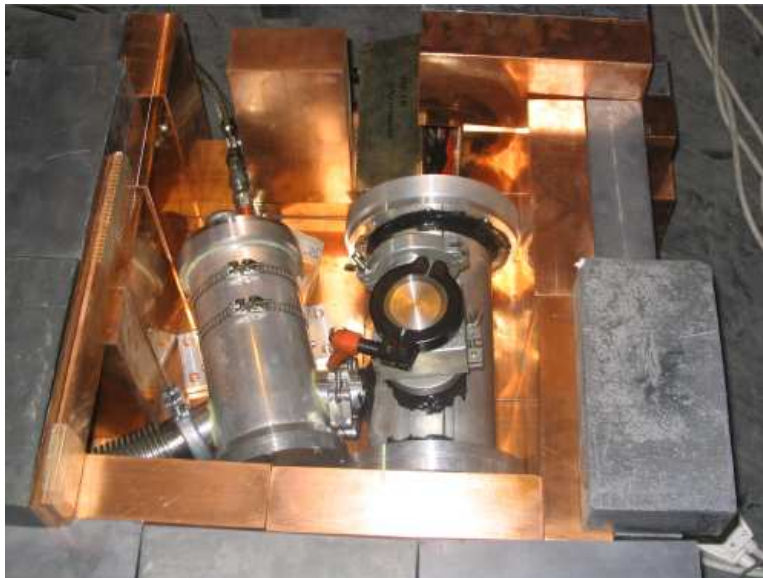


Figure 2: *The 2 CCD test setup while mounted with shielding of copper and lead at LNGS.*



Figure 3: *The VIP setup mounted in the LNF laboratories.*

## 4 Activities in 2006

In January 2006 the barrack allocated to VIP at LNGS was prepared to receive the setup and, then, in February the VIP setup was transported and installed at LNGS. The activities which will take place for VIP in 2006 are the following:

- commissioning of the VIP setup at LNGS;
- start data taking, alternating periods of DAQ with and without circulating current;
- data analysis and continuous update of the PEP violation limit.

## 5 Publications 2005

### 5.1 List of Conference Talks given by LNF Authors in Year 2005

1. S. Di Matteo, “The VIP experiment”, LNF Spring School in Nuclear, Subnuclear and Astroparticle Physics, Frascati (Italy), May 16- 20, 2005.
2. D. Sirghi and F. Sirghi, “The VIP experiment”, Annual meeting of Bucharest University Phys. Department, 2005, Bucharest, Romania, May 27, 2005
3. E. Milotti, “The VIP experiment”, Proceedings of Quantum Theory: reconsideration of foundations -3, Vaxjo (Sweden), June 6-11, 2005.
4. L. Sperandio, “The VIP experiment”, XCI Congresso Nazionale Societa’ Italiana di Fisica, Catania, 26 September - 1 October 2005.

### 5.2 Papers and Proceedings

1. D. Sirghi and F. Sirghi *et al.*, “The VIP experiment”, Romanian Reports in Physics Vol. **57**, No. 3 (2005), 306.
2. S. Bartalucci *et al.*, “New experimental limit on the Pauli exclusion principle violation by electrons”, sent for publication in Phys. Lett. B.

### 5.3 Technical Notes

1. S. Di Matteo and L. Sperandio, “Evaluation of the anomalous X-ray energy in VIP experiment”, VIP Note-IR-03, April 21, 2005.
2. S. Di Matteo and L. Sperandio, “Evaluation of the anomalous X-ray energy in VIP experiment: values from Dirac-Fock method”, VIP Note-IR-04, April 26, 2005.
3. The VIP Collaboration , “Background measurement for VIP with a 2-CCD test setup (in the DEAR laboratory and at LNGS)”, VIP Note-IR-05, April 26, 2005.

**FA51**  
**Astroparticle Physics**

E. Nardi (Resp.)

## 1 Description of the 2005 activity

The main research activities of the project during the year 2005 have been: (1) the conclusion of the analysis of the effects of neutrino masses on a neutrino signal from a future Galactic core-collapse supernova; <sup>1)</sup> (2) the study of the effects of spectator processes <sup>2)</sup> and of lepton flavor dynamics <sup>3)</sup> during the leptogenesis era.

*Supernova neutrinos.* The results of a comprehensive statistical analysis of a large set of synthetic neutrino data generated according to Monte Carlo simulations of different types of supernova explosions have been published in. <sup>1)</sup> The analysis is based on a Bayesian approach, and takes into account non-Gaussian statistical effects as well as several sources of systematics. The main results obtained are:

- i)* A limit  $m_\nu \lesssim 1$  eV is within the reach of the method;
- ii)* The limit is almost independent of the specific location of the supernova within our Galaxy.

*Spectator processes in Leptogenesis.* The effects of various processes that can be active during the leptogenesis era, like QCD and electroweak sphalerons, Yukawa interactions and the presence of a non-vanishing Higgs asymmetry, have been studied. Depending on the specific temperature ranges in which leptogenesis occurs, the final baryon asymmetry can be enhanced or suppressed by factors of order 20%–40% with respect to the case when these effects are altogether ignored. <sup>2)</sup>

*Flavor effects in Leptogenesis.* We have studied leptogenesis in the medium (low) temperature regime,  $T \lesssim 10^{12}$  GeV ( $10^{10}$  GeV), where the rates of processes mediated by the  $\tau$  (and  $\mu$ ) Yukawa coupling are non negligible, implying that lepton flavor effects must be taken into account in the dynamics controlling the generation of a cosmic lepton asymmetry. <sup>3)</sup> Important quantitative and qualitative differences with respect to the case where flavor effects are ignored have been found:

- i)* The cosmic baryon asymmetry can be enhanced by up to one order of magnitude;
- ii)* The sign of the asymmetry can be opposite to what one would predict from the sign of the total lepton asymmetry;
- iii)* Successful leptogenesis is possible even when the total asymmetry parameter  $\epsilon_1$  is vanishing.

## References

1. Enrico Nardi and Jorge I. Zuluaga, “Constraints on neutrino masses from a Galactic supernova neutrino signal at present and future detectors”, Nucl. Phys. **B 731** (2005) 140.
2. Enrico Nardi, Yosef Nir, Juan Racker and Esteban Roulet, “On Higgs and sphaleron effects during the leptogenesis era”, JHEP **0601**, (2006) 068; [arXiv:hep-ph/0512052].
3. Enrico Nardi, Yosef Nir, Esteban Roulet and Juan Racker, “The importance of flavor in leptogenesis”, JHEP **0601**, (2006) 164; [arXiv:hep-ph/0601084].

**LF21**  
**Phenomenology of Elementary Particle**  
**Interactions at Colliders**

G. Isidori (Resp.), F. Mescia (Art. 23), S. Pacetti (Ass. Ric), G. Pancheri (Resp. Naz.),  
O. Shekhovstova (Bors. PD), C. Smith (Bors. PD), D. Temes (Ass. Ric.), S. Trine (Bors. PD)

## 1 Summary of the project

The research topics investigated by this project can be divided into two main areas:

- Flavour physics.
- Hadronic form factors and total hadronic cross-sections.

The first area, discussed in Section 2, concerns the possibility to perform new low-energy precision tests about the mechanism of quark- and lepton-flavor mixing. The second area, discussed in Section 3, is in itself divided into two sections, one related to precision studies of hadronic processes relevant to electron-positron colliders at low energy, the other related to the QCD description of hadronic and photonic total cross-sections at high energies.

## 2 Flavour Physics

One of the strategies to obtain additional clues about the nature of New Physics (NP) is by means of precision tests of the Standard Model (SM) at low energies. These are particularly interesting in processes which are not mediated by tree-level SM amplitudes, such as flavour-changing neutral current (FCNC) transitions, both in the quark and in the lepton sector. Up to now there is no evidence for deviations from the SM in such rare processes, and this leads to the so-called *flavour problem*: if we insist with the theoretical prejudice that NP has to emerge in the TeV region, we have to conclude that the new theory possesses a highly non-generic flavour structure. Interestingly enough, this structure has not been clearly identified yet, mainly because the SM, *i.e.* the low-energy limit of the new theory, doesn't possess an exact flavour symmetry. The attempt to clarify this structure, both at the phenomenological level (with the help of precision data on rare decays) and at a more fundamental level (with the help of new symmetry principles), is one of the main activity of our group.

A closely related subject –which is also one of the primary research objectives of our group– is a better understanding of the SM itself, fixing his fundamental couplings (quark masses, CKM angles, non-perturbative condensates, ...) by means of precise calculations within the framework of effective field theories and Lattice QCD.

Within this general scenario, last year we have performed a series of works on:

*Minimal Lepton Flavour Violation.* We have extended the notion of Minimal Flavor Violation to the lepton sector, namely we have introduced a symmetry principle which allows us to express lepton flavor violation in the charged lepton sector in terms of neutrino masses and mixing angles. The phenomenological consequences of this hypothesis for radiative FCNC decays ( $\ell_i \rightarrow \ell_j \gamma$ ) and  $\mu$ -to- $e$  conversion in nuclei have been investigated. <sup>1)</sup>

*Rare K decays.* The experimental evidence of the  $K^+ \rightarrow \pi^+ \nu \bar{\nu}$  transition and the recent proposal to measure it at CERN has implied a great deal of attention for rare kaon decays. Their

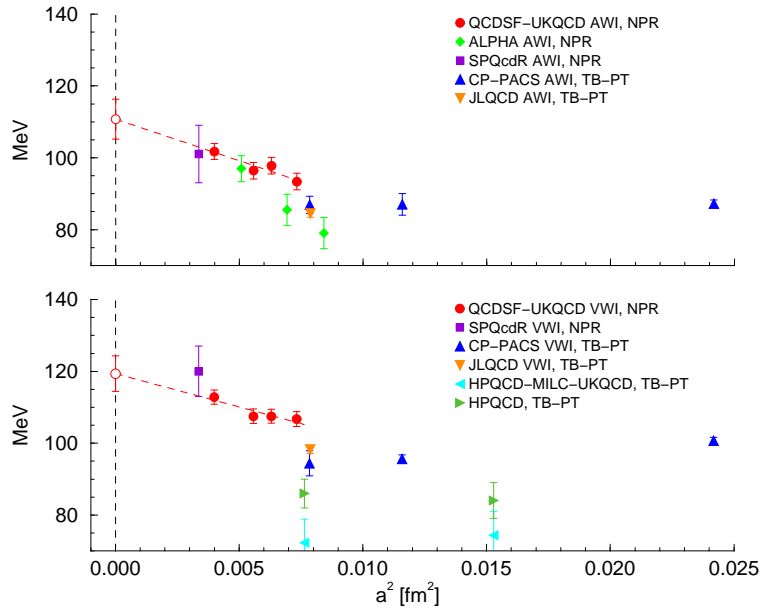


Figure 1: Results for  $m_s^{MS}(2\text{ GeV})$  versus  $a^2\text{ fm}^2$  using the Axial Ward Identity (upper plot) and Vector Ward Identity (lower plot) methods. Our points are in diamonds NPR denotes non-perturbative renormalisation, while TB-PT denotes tadpole-improved boosted perturbation theory.

theoretical determination is quite clean and thus offer a good test of the Standard Model. We have estimated for the first time the long distance contributions of  $K^+ \rightarrow \pi^+ \nu \bar{\nu}$  and shown that further reduction of the theory error can be obtained by means of Lattice QCD. Our work has allowed to increase the sensitivity to potential effects of New Physics of this channel. 2, 3, 4)

*Effective field theories for non-rare K decays.* The issue of extracting  $\pi\pi$  phase shift in  $K \rightarrow 3\pi$  decays and the role the  $\Delta I = 1$  rule in radiative  $K$  decays have been investigated. 5, 6)

*B decays.* We have presented for the first time complete analytic expressions to evaluate at  $O(\alpha)$  the effects of soft-photon emission, and the related virtual corrections, in non-leptonic decays of the type  $B, D \rightarrow P_1 P_2$ , where  $P_{1,2}$  are scalar or pseudoscalar particles. 7)

*Lattice QCD.* Determination of the light quark masses 8, 9) and the kaon B-parameter from unquenched simulations with Wilson fermions; 10) in Fig. 1, we show our value for the strange mass with respect other groups. Evaluation of the quark condensate using non-perturbative renormalization in the x-space. 11, 12) Studies of semileptonic form factors, where we have shown that introducing twisted boundary condition in a finite lattice, we can estimate hadronic matrix elements with arbitrary momenta. 13)

### 3 Hadronic form factors and total hadronic cross-sections

#### 3.1 Studies of $\sigma(e^+e^- \rightarrow \pi^+\pi^-\gamma)$ close to the $\phi$ peak

We have considered the possibility to test the final state radiation (FSR) model in the reaction  $e^+e^- \rightarrow \pi^+\pi^-\gamma$  at DAΦNE. <sup>21)</sup> We propose to consider the low  $Q^2$  region ( $Q^2$  is the invariant mass squared of the di-pion system) to study the different models describing  $\gamma^* \rightarrow \pi^+\pi^-\gamma$  interaction. Final state radiation (FSR) is the main irreducible background in radiative return measurements of the hadronic cross section which is important for the anomalous magnetic moment of the muon. Besides being of interest as an important background source, this process could be of interest in itself, because a detailed experimental study of FSR allow us to get information about pion-photon interaction at low energies.

We have compared in particular the scalar QED and Resonance Perturbation Theory (RPT) prediction for the  $e^+e^- \rightarrow \pi^+\pi^-\gamma$  cross section. The model parameters for the RPT pion form factor was fitted to Novosibirsk experimental data CMD-2. For our numerical calculation of  $e^+e^- \rightarrow \pi^+\pi^-\gamma$  cross section we wrote Monte Carlo code that is based on the Monte Carlo EVA structure We also consider the contribution coming from the  $\phi$  direct decay ( $\phi \rightarrow \pi^+\pi^-\gamma$ ). To estimate the  $\phi \rightarrow \pi^+\pi^-\gamma$  decay we apply the Achasov four quark parametrization with the parameters taken from the fit of the KLOE data for  $\phi \rightarrow \pi^0\pi^0\gamma$  with only the  $f_0$  intermediate state. We study on-peak ( $s = m_\phi^2$ , where  $s$  is the total initial energy squared) and off-peak ( $s = 1\text{GeV}^2$ ) energies.

We have found that for on-peak kinematics the  $\phi$  resonant contribution to cross section is quite large and the FSR contribution, that are not included in the sQED\*VMD model, can be revealed only in the case of the destructive interference between the  $\phi \rightarrow \pi\pi\gamma$  amplitude and FSR one.

According to our numerical results the low  $Q^2$  region is sensitive to FSR model. Thus the inclusion of additional FSR contribution of RPT both for on-peak and off-peak energies changes the cross section about 20% compare with sQED prediction (see Fig. 2). The new data on  $e^+e^- \rightarrow \pi^+\pi^-\gamma$  from KLOE especially for low  $q^2$  region will certainly help us to test FSR model prediction.

#### 3.2 Light mesons transition form factors

We have defined a general procedure based on analyticity, vector meson dominance, power law asymptotic behavior and dispersion relations, to connect the amplitudes of the crossed processes:  $e^+e^- \rightarrow \phi M$ ,  $\phi \rightarrow e^+e^- M$  and  $\phi \rightarrow \gamma M$ , where  $M$  is a generic light scalar or pseudoscalar meson.

We have considered explicitly two cases, i.e.  $M = \eta$  and  $M = f_0$ , and with the help of the BaBar data on the corresponding annihilation cross sections  $e^+e^- \rightarrow \phi\eta$  and  $e^+e^- \rightarrow \phi f_0$ , the  $\phi\eta$  and  $\phi f_0$  transition form factors (tff) have been reconstructed in the whole  $q^2$ -complex plane. Since the procedure is sensitive to the number of final hadronic fields, we can use it to test different hypotheses about the still controversial nature of the scalar meson  $f_0$ . In the case of the  $\eta$  meson, we can reproduce the low energy behaviour of the tff, in agreement with the PDG value, under the usual hypothesis of a  $q\bar{q}$  pseudoscalar meson. The same procedure, under the hypothesis of  $q\bar{q} f_0$ , gives, for the low energy  $\phi f_0$  tff, values which are 30 times lower than the data. However, if we upgrade the procedure, in order to account for a more exotic  $[qq][\bar{q}\bar{q}] f_0$ , we obtain, in the low energy region, values for the tff which are still lower than the data, but the discrepancy is reduced to a factor of 2. In addition, this result is in agreement with a recent and updated re-analysis of Kloe data.

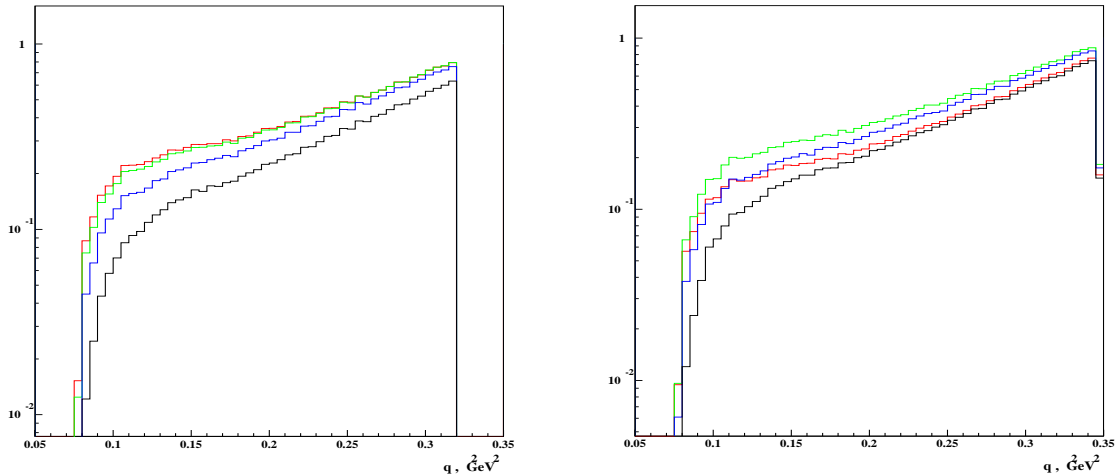


Figure 2: The cross section  $e^+e^- \rightarrow \pi^+\pi^-\gamma$  low  $q^2$  region. The black line corresponds only to ISR. The blue one corresponds FSR in the framework of the sQED\*VMD model and does not include the  $\phi$  direct decay. The green line is the same but FSR is within RPT. The red line is the cross section that includes all contributions, FSR is calculated in RPT. The left figure is for  $s = m_\phi^2$ , the right one is for  $s = 1\text{GeV}^2$ .

### 3.3 Total hadronic cross-sections in QCD

The energy behavior of total proton and photon cross-sections is the focus of this line of research and its description through QCD is the ultimate goal of this project. QCD indeed provides various mechanisms to explain the energy dependence, although quantitatively rigorous studies are yet to come. The goal would be to obtain a QCD description of the initial decrease and the final increase of total cross-sections through soft gluon summation and QCD calculable jet x-sections, also known as mini-jets in this context. The resulting physical picture includes multiple parton collisions, whose number increases with energy, and soft gluon emission dressing each collision, with a reducing effect.

#### 3.3.1 The Eikonal Minijet Model for protons and photons

In the Eikonal Minijet Model (EMM) the rise can be obtained using the QCD calculable contribution from the parton-parton cross-section, whose total yield increases with energy. For a unitary description, the jet cross-sections are embedded into the eikonal formalism, where the eikonal function contains both the energy and the impact parameter distribution in b-space. The simplest formulation, with minijets to drive the rise and hadronic form factors for the impact parameter distribution, can be applied to all the available x-sections. One finds that, with a single set of parameters, the simple eikonalized mini-jet model cannot describe both the early rise, which in proton-antiproton scattering takes place around  $10 \div 50 \text{ GeV}$ , and the Tevatron data.

A possible way to decrease the uncertainty in the predictions is to refine the QCD analysis, through resummation of soft gluon emission from the initial state partons, a feature absent from most simple EMM.

During a number of years, a model for the impact parameter space distribution of parton in the hadrons has been developed and applied to the proton and photon cross-sections in order to obtain a better description of total cross-section. The physical picture underlying this model is

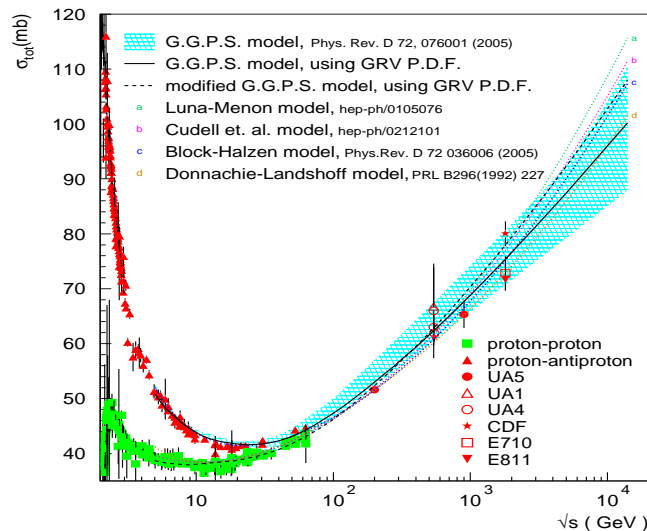


Figure 3: Predictions for total  $pp$  and  $p\bar{p}$  total cross-section in various models. The shaded area gives the range of results in the Eikonised Mini-jet model with soft gluon resummation <sup>19)</sup>. The long-dashed dotted curve (*d*), indicates the predictions for the Donnachie and Landshoff Regge-Pomeron parametrization.

that the fast rise due to mini-jets and the increasing number of gluon-gluon collisions as the energy increases, can be reduced if one takes into account that soft gluons, emitted mostly by the initial state valence quarks, determine an acollinearity between the partons which reduces the overall parton-parton luminosity. This model can describe very well all available data for proton collisions as we show in <sup>19)</sup>.

During the year 2006, the model has been applied to show the range of predictions at LHC, obtained by varying the model parameters, as shown in Fig. 3, from a contribution to the Les Houches Workshop 2005.

#### 4 Work Program for the year 2006

Most of the activity previously described will be continued into the year 2006.

#### References

1. V. Cirigliano, B. Grinstein, G. Isidori and M. B. Wise, Nucl. Phys. B **728**, 121 (2005) [hep-ph/0507001].
2. G. Isidori, F. Mescia and C. Smith, Nucl. Phys. B **718**, 319 (2005) [hep-ph/0503107].
3. G. Isidori, G. Martinelli and P. Turchetti, Phys. Lett. B **633**, 75 (2006) [hep-lat/0506026].
4. D. Bryman, A. J. Buras, G. Isidori and L. Littenberg, Int. J. Mod. Phys. A **21**, 487 (2006) [hep-ph/0505171].

5. N. Cabibbo and G. Isidori, JHEP **0503**, 021 (2005) [hep-ph/0502130].
6. J. M. Gerard, C. Smith and S. Trine, Nucl. Phys. B **730**, 1 (2005) [hep-ph/0508189].
7. E. Baracchini and G. Isidori, Phys. Lett. B **633**, 309 (2006) [hep-ph/0508071].
8. D. Becirevic *et al.*, Nucl. Phys. B **734**, 138 (2006) [hep-lat/0510014].
9. D. Becirevic *et al.*, PoS **LAT2005**, 079 (2005) [hep-lat/0509091].
10. F. Mescia, V. Gimenez, V. Lubicz, G. Martinelli, S. Simula and C. Tarantino, PoS **LAT2005**, 365 (2005) [hep-lat/0510096].
11. V. Gimenez, V. Lubicz, F. Mescia, V. Porretti and J. Reyes, PoS **LAT2005**, 081 (2005) [hep-lat/0510090].
12. V. Gimenez, V. Lubicz, F. Mescia, V. Porretti and J. Reyes, Eur. Phys. J. C **41**, 535 (2005) [hep-lat/0503001].
13. D. Guadagnoli, F. Mescia and S. Simula, submitted to Phys. Lett. B [hep-lat/0512020].
14. E. Blucher *et al.*, “Status of the Cabibbo angle”, [CKM2005 - WG 1], hep-ph/0512039.
15. F. Mescia, AIP Conf. Proc. **794** (2005) 157.
16. F. Mescia, hep-ph/0512142.
17. C. Smith, hep-ph/0505163.
18. G. Pancheri, Y. Srivastava and N. Staffolani, Eur. Phys. J. C **42**, 303 (2005).
19. R. M. Godbole, A. Grau, G. Pancheri and Y. N. Srivastava, Phys. Rev. D **72**, 076001 (2005).
20. G. Pancheri, R. M. Godbole, A. Grau and Y. N. Srivastava, Nucl. Phys. Proc. Suppl. **146**, 177 (2005).
21. G. Pancheri, O. Shekhovtsova and G. Venanzoni, hep-ph/0506332.

**LF61**  
**Synchrotron Radiation Spectroscopies and the Physics of**  
**Strongly Correlated Electron Systems**

M. Benfatto, S. Di Matteo (Art. 23), R. Gunnella (Ass.), Y. Joly (Visit.), K. Hatada (Ass),  
K. Hayakawa (Ass), C.R. Natoli (Resp.), N. Perkins (Visit.), D. Sebilliau (Visit.),  
A. Tenore, Wu Ziyu (Visit.)

## 1 The Project

The aim of this project is the theoretical analysis of strongly correlated electron systems, in the light of their fundamental as well as technological interest. When appropriate methods borrowed from field theory and statistical mechanics are used to bear on the description of the essential physics of such systems. At the same time in-depth theoretical studies of significant synchrotron radiation spectroscopies (like absorption, dichroism, elastic and inelastic resonant x-ray scattering, etc..) that can shed light on charge and magnetic correlations in such systems are carried out. To this aim a peculiar analysis in terms of electromagnetic quadrupoles is developed

## 2 Physics of strongly correlated electron systems

In 2005 research in this field has developed along the following directions:

- Analysis of synchrotron radiation experiments (resonant x-ray scattering, absorption and dichroism) in  $V_2O_3$ ,  $LuVO_3$ , actinides ( $NpO_2$ ) and pyrochlore materials ( $MgTi_2O_4$ ,  $CdV_2O_4$ ,  $ZnV_2O_4$ ).
- Classification of the electromagnetic multipoles in matter, with an eye to chiral systems and the identification of the axial toroidal moment in the x-ray natural circular dichroism.
- Investigation of the physics of the complex magnetic oxides like  $MgTi_2O_4$ ,  $ZnV_2O_4$ ,  $LuVO_3$ ,  $NpO_2$ ,  $V_2O_3$ , and perovskites.
- Fitting of X-ray Absorption Near Edge Structure (XANES) by a full multiple scattering procedure
- An application of the nuclear scissors mode in condensed matter
- Implementation of Multichannel Multiple Scattering Theory into a computer code for the interpretation of various SR spectroscopies in strongly correlated systems

### 2.1 Analysis of synchrotron radiation experiments

We have extended the tensor analysis derived for circular and linear dichroism in photoemission and photoabsorption to Bragg-forbidden reflections in anomalous diffraction. In Ref. <sup>1)</sup> we present a unitary cluster approach to the calculation of several electron spectroscopies, ranging from core and valence level photoelectron diffraction and absorption to electron, Auger and anomalous diffraction. Electron energy loss and Auger-photoelectron coincidence spectroscopies can also be treated in the same frame. This approach is based on multiple scattering theory with a complex optical potential of the Hedin-Lundqvist type and is valid for all photoelectron kinetic energies. Similarities and differences between these diffraction techniques are examined and cluster size convergence is discussed in connection with the electron mean free path. Applications to selected problems are presented to illustrate the method, both for structural and electronic analysis. Such

a review article may represent a good starting point towards further improvement in each specific spectroscopy.

On the specific subject of  $V_2O_3$ , we solved the question regarding the nature of the magnetic space group in its monoclinic phase. All experiments performed before 2000 had shown that the system admitted a different magnetic space group than that suggested by a recent dichroic experiment at vanadium K edge (Goulon *et al.* Phys. Rev. Lett. 85, 4385 (2000)). The authors of this latter work found that the system allows non-reciprocal effects, implying that time-reversal and inversion symmetries are broken and only their product conserved, contrary to previous findings. This situation led to a further experiment to resolve this inconsistency (S. Di Matteo, A.G.M. Jansen, Phys. Rev. B 66, R100402 (2002)): however no magnetic-electric effect was detected in the system, and this finding is not compatible with the presence of a non-reciprocal gyrotropic linear dichroism. This result solved a problem but raised another question: the correct interpretation of the dichroic experiment at the vanadium K edge. For this reason we have analyzed this experiment in more detail, in order to give a consistent interpretation of all the recent x-ray resonant scattering and dichroic experiments in  $V_2O_3$  <sup>2)</sup>. Moreover, we have performed numerical simulations based on the multiple scattering theory for both dichroic and resonant scattering spectra, analysing the experimental implications related to the different magnetic space symmetries. We have shown in this way the paradoxical consequences of the interpretation proposed by Goulon *et al.* quoted above on the physics of this system and suggested how to perform unambiguously the dichroic experiment in order to dissipate any doubt on the properties of the system. Following this suggestion a new linear dichroism experiment has been performed, which confirms our previous interpretation: the results are analyzed in Ref. <sup>3)</sup>.

The fruitful interplay between synchrotron radiation experiments and theory of strongly correlated electron systems found many other applications in several domains: in  $LuVO_3$  resonant x-ray spectroscopies, both Templeton and magnetic, allowed to detect a crossing of  $V^{3+}$  electronic levels, which in turn radically changed the ground-state properties, by allowing a finite value of the magnetic orbital moment. The case of actinides, in particular  $NpO_2$  is emblematic as an example of multipolar order, in that the magnetic order is not determined by a magnetic dipole, as usual, but by an magnetic octupole order parameter. This gives rise to a so-called triple- $k$  structure which could not be resolved through neutron diffraction and only the sensitivity determined by the highly brilliant synchrotron radiation allowed to disentangle the various multipolar contributions. Two articles are now ready to be submitted on these arguments. <sup>4, 5)</sup>

In section (2.3) below we show how the analysis of resonant x-ray scattering can shed light on the ground state properties in frustrated spinels, like  $MgTi_2O_4$  and  $ZnV_2O_4$ .

## 2.2 Analysis of the magnetic and non-magnetic anomalous scattering

The second direction of research is concerned with the analysis of the polar (magnetic) and axial (non-magnetic) toroidal multipoles of a system by means of x-ray dichroism and resonant scattering. In this field a lot has been done, especially in russian literature, but very little has been said in connection with the detection of toroidal moments by means of resonant scattering. For this reasons, a general discussion of (magnetic and non-magnetic) toroidal multipolar expansion in condensed matter systems is needed in the community, with the aim of applying it to the theory of anomalous x-ray resonant scattering. The idea turned out to be fruitful, and the main results of such a work regard the possibility to detect the toroidal moment and its multipoles in centrosymmetric magnetic systems by means of RXS and to separate in a similar way all the parity and time-reversal odd multipolar components. With this aim, in Ref. <sup>6)</sup>, following a brief discussion on electromagnetic multipole expansion, we provide a link between several multipole moments and the measurable quantities of some x-ray spectroscopies, like resonant x-ray scattering or dichroism

in absorption. A general classification is given, accompanied by some specific examples and a geometrical interpretation of the axial toroidal nonmagnetic quadrupole, related to the x-ray natural circular dichroism. In order to provide a physical example for the detection of magnetic parity-odd multipoles, like the toroidal moment, we performed a numerical simulation for x-ray nonreciprocal directional dichroism, at the Fe K edge, in the polar ferrimagnet GaFeO<sub>3</sub>. Our calculations described quite well the reported experimental profile, with the correct order of magnitude for dichroism/absorption intensity ratio and a signal which is limited to pre-edge. Moreover, in order to highlight some theoretical aspects related also to the resonant x-ray scattering, we analyzed also the main features of the experiments of resonant x-ray scattering, through quantitative numerical calculations: such a work is currently submitted to J. Phys. Soc. Jpn. <sup>7)</sup>.

### 2.3 Investigation of the physics of the complex magnetic oxides

The third direction of research concerns the investigation of the physics of complex magnetic oxides such as MgTi<sub>2</sub>O<sub>4</sub>, ZnV<sub>2</sub>O<sub>4</sub>, and the manganites which exhibit a whole variety of interrelated phenomena such as metal-insulator transitions, orbital and magnetic ordering, double exchange, geometrical frustration, heavy fermion behaviour and colossal magnetoresistance.

The interest in frustrated systems lies in the fact that their ground state is highly degenerate and can evolve in a variety of ways: they can freeze on cooling forming ice, remain liquid down to the lowest temperature due to quantum effects or, finally, lift their geometrical degeneracy through a phase transition that lowers the local symmetry. MgTi<sub>2</sub>O<sub>4</sub> is a spinel, which recently has attracted much attention because of its tendency to dimerize. It undergoes a metal-insulator transition on cooling below  $T = 260\text{K}$ , which is accompanied by strong lattice distortion leading to the formation of helical chains of short and long bonds running along the tetragonal  $c$  axis, a unique example of chiral ordering of the spinel structure. In order to study the low temperature phase of MgTi<sub>2</sub>O<sub>4</sub>, we have derived an effective spin-1/2, pseudospin-1 Hamiltonian and demonstrated that the orbital degrees of freedom can remove the infinite spin-degeneracy of the "pyrochlore" structures and induce a spin dimerization. Moreover, we have shown that the residual orbital degeneracy can be lifted by the spin-lattice interaction forcing a tetragonal distortion to the chiral structure actually observed. We propose to investigate such a low-symmetry phase by means of x-ray natural circular dichroism. The work had been published in Phys. Rev. Lett. in 2004. We have then extended the previous idea of spin-lattice interaction to a quantitative model taking into account all the normal modes of the tetragonal low-temperature lattice: this has led us to a better description of the experimental data, and has been published in Phys. Rev. B. <sup>8)</sup>.

Moreover, we have found out that the introduction of a spin-orbit interaction, that does not modify the situation with Ti<sup>3+</sup> ion, strongly affects the physics of V<sup>3+</sup> ion, as in ZnV<sub>2</sub>O<sub>4</sub>. Here the interplay of superexchange, spin-orbit, and spin-lattice interactions is so deep that the ground state of the system with V<sup>3+</sup> ion is completely different from that of the Ti<sup>3+</sup> ion, the former being a one dimensional antiferromagnet, while the latter was a dimerized singlet state. Thus, spin-orbit coupling can exert a strong influence on these systems, even though its magnitude is much smaller than the typical superexchange energies (20 meV vs. 80 meV). Remarkably, we have found that it is possible to single out all orbital and magnetic orderings that appear in the phase diagram of this system by means of resonant x-ray scattering, with different polarization conditions and/or exchanged wave vectors. This last work has been published as a rapid communication in Phys. Rev. B. <sup>9)</sup>

### 2.4 Fitting of XANES spectra by a full multiple scattering procedure

During this year my scientific activity has been devoted to both the develop of the MXAN method, already described in the previous reports, and its application to biological problems and significant

test cases. The computer code has been adapted to parallel processing by distributing different parts of the calculation across multiple processors of a PC cluster. This approach, based on the MPI protocol, entails a gain in computing speed by an order of magnitude or more. We have modified the potential generator of the MXAN method to modify the net charge over the atomic species and we have also started the extension of the MXAN method to the analysis of systems containing different no-equivalent absorbing sites. At the same time, in collaboration with several groups, we have used the MXAN method to get an accurate determination of the coordination geometry around the absorbing atom, from the coordination geometry of Cu<sup>2+</sup> ion at different chemical condition to the photolyzed carbonmonoxy myoglobin. 10, 11, 12, 13, 14, 15, 16)

## 2.5 An application of the nuclear scissors mode in condensed matter.

We have suggested that in an anisotropic crystal there should be a new mechanism of dichroism related to a scissors mode, a kind of excitation observed in several other many-body systems. Such an effect should be found in crystals, amorphous systems and also metallo-proteins. Its signature is a strong magnetic dipole transition amplitude, which is a function of the angle between the momentum of the photon and the anisotropy axis of the cell. 17)

## 2.6 Implementation of Multichannel multiple scattering theory into a computer code for the interpretation of various SR spectroscopies in strongly correlated systems

It is known that one of the major problems in present day condensed matter science is the introduction of electron correlation effects in extended systems, in order to understand and predict ground state features of new materials. This line of research aims at interpreting SR experiments in strongly correlated systems, like magnetic and non magnetic oxides of transition metals, in order to derive from them information on their ground state. Important applications to systems of biological interest are also envisaged 18). Development of the related computer code is under way.

## List of Conference Talks by LNF Authors in Year 2005

1. S. Di Matteo, "Resonant X-ray scattering as a tool to detect electromagnetic multipoles in condensed matter" Congresso Annuale della Societa' Italiana di Luce di Sincrotrone (SILS) Modena 07/07/2005.
2. C.R. Natoli, "Multichannell Multiple Scattering Theory for Electron Spectroscopies in correlated systems" International Workshop on X-ray Spectroscopy of Magnetic Solids - XRMS 05 Villigen, Switzerland 18/10/2005.

## References

1. D. Sebilliau, R. Gunnella, Z.-Y. Wu, S. Di Matteo, and C.R. Natoli, "Multiple Scattering approach with complex potential in the interpretation of electron and photon spectroscopies" (Topical Review), *J. Phys.: Condens. Matter* **18**, R175 to R230 (2006).
2. S. Di Matteo, "On the nature of the magnetic space group in the monoclinic phase of V<sub>2</sub>O<sub>3</sub>", *Physica Scripta* **71**, CC1-6 (2005).
3. C. Meneghini, S. Di Matteo, C. Monesi, C.R. Natoli *et al.*, "Structural dichroism in the anti-ferromagnetic insulating phase of V<sub>2</sub>O<sub>3</sub>", *Physical Review B* **72**, 033111-1 to 4 (2005).

4. S. Di Matteo, S. Wilkins, C. Mazzoli, *et al.*, “Level crossing in the electronic configuration of  $V^{3+}$ -ion in  $\text{LuVO}_3$ ”, submitted to Phys. Rev. B.
5. S. Di Matteo, R. Caciuffo, P. Santini, *et al.* - “Ground state properties of  $\text{NpO}_2$ ”, submitted to Phys. Rev. B as a brief report.
6. S. Di Matteo, Y. Joly, C.R. Natoli, “Detection of electromagnetic multipoles by resonant x-ray spectroscopies”, Physical Review B **72**, 144406-1 to 7 (2005).
7. S. Di Matteo, Y. Joly, “Parity and time-reversal breaking effects detected by resonant x-ray scattering: the case of  $\text{GaFeO}_3$ ”, submitted to Jour. Phys. Soc. Jpn.
8. S. Di Matteo, G. Jackeli, N.B. Perkins, “Valence-bond crystal and lattice distortions in a pyrochlore antiferromagnet with orbital degeneracy”, Physical Review B **72**, 024431-1 to 15 (2005).
9. S. Di Matteo, G. Jackeli, N.B. Perkins, “Orbital order in vanadium spinels”, Physical Review B **72**, R020408-1 to 4 (2005).
10. J Li, ZC Zhou, WS Chu, WM Gong, M. Benfatto, TD. Hu, YN Xie, DC Xian, ZY Wu, “Investigation of zinc-containing peptide deformylase from *Leptospira interrogans* by X-ray absorption near-edge spectroscopy”, Journal of Synchrotron Radiation **12**, 111-114 (2005).
11. ZY Wu, Y. Tao, M. Benfatto, DC. Xian, JZ Jiang, “XANES quantitative structural determination of the sandwich bis(naphthalocyaninato) cerium complex”, Journal of Synchrotron Radiation **12**, 98-101 (2005).
12. OM Roscioni, P. D’Angelo, G. Chillemi, S. Della Longa, M. Benfatto “Quantitative analysis of XANES spectra of disordered systems based on molecular dynamics”, Journal of Synchrotron Radiation **12**, 75-79 (2005).
13. P. Frank, M. Benfatto, RK Szilagyi, P. D’Angelo, S. Della Longa, KO Hodgson “The solution structure of  $\text{Cu}(\text{aq})_2^+$  and its implications for rack-induced bonding in blue copper protein active”, Inorganic Chemistry **44** **6**, 1922-1933 (2005).
14. A. Arcovito, DC Lamb, GU Nienhaus, JL Hazemann, M Benfatto, SD Longa “Light-induced relaxation of photolyzed carbonmonoxy myoglobin: A temperature-dependent x-ray absorption near-edge structure (XANES) study”, Biophysical Journal **88**, 2954-2964 (2005).
15. C. Monesi, C. Meneghini, F. Bardelli, M. Benfatto, S. Mobilio, U. Manju, DD. Sarma “Local structure in  $\text{LaMnO}_3$  and  $\text{CaMnO}_3$  perovskites: A quantitative structural refinement of Mn K-edge XANES data”, Physical Review B **72**, 174104 (2005).
16. R. Sarangi, M. Benfatto, K. Hayakawa, L. Bubacco, EI Solomon, KO Hodgson, B. Hedman, “MXAN analysis of the XANES energy region of a mononuclear copper complex: Applications to bioinorganic systems”, Inorganic Chemistry **44**, 9652-9659 (2005).
17. Hatada K, Hayakawa K, Palumbo F “Scissors mode and dichroism in an anisotropic crystal”, Physical Review B **71**, 092402 (2005).
18. P. Kruger, C.R. Natoli, “Theory of Ca  $L_{2,3}$ -edge XAS using a novel multichannel multiple-scattering method”, J. Synchrotron Rad. **12**, 80-84 (2005).

MI11  
**Lattice QCD and the Quark Gluon Plasma**

Maria Paola Lombardo (Resp.)

## 1 Preamble: Symmetries and a-Symmetries of the Strong Interactions

My current research focusses on Quantum Chromodynamics, the basic theory of Strong Interactions, and the symmetry I am mostly concerned with is the chiral symmetry. Chiral symmetry is spontaneously broken in ordinary conditions: because of this a-symmetry proton and neutron gain their masses. A chirally symmetric world would then be completely different from ours: the proton and the neutron - hence the nuclei - will be much lighter, just to mention one effect directly related to our everyday life. This exotic world did actually exist at the very early stages of the Universe, and experiments at the RHIC and LHC aim at recreating it - the higher the energy, the closer we get to the Big Bang.

Symmetry and a-Symmetry are two faces of the same physics, which are both described by the same fundamental Lagrangian: a-Symmetry characterising our world, Symmetry the beginning of the Universe. Lattice QCD theorists aim at understanding both in a unified fashion, starting from the fundamental theory, Quantum Chromodynamics, and using powerful computers to handle the complicated mathematics involved.

## 2 Results

This said, my last year activity was basically twofold: on one side, studies of strong interactions at extreme conditions to provide a sound framework for the upcoming LHC experiments, using the same Lattice QCD formalism of the last two years; on the other side, the development of new Lattice Tools, namely a better setup for calculations based on the so-called Wilson Fermions with a twisted mass term.

### 2.1 Strong Interactions at Extreme Conditions

I have computed the critical line by suggesting and exploring a new extrapolation scheme. T. Alles, M. D'Elia and I have completed the first lattice study of topology at nonzero baryon density. M. D'Elia, F. Di Renzo and I have presented a conclusive evidence of the non-perturbative nature of the plasma above  $T_c$  - confirming the RHIC observations - and we are now contrasting the results with what expected of a strongly interactive QGP: we want to assess the hadronic contents of the system.

### 2.2 New Methods

Karl Jansen and I have begun a study of the thermal transition with twisted mass Wilson fermions, which so far were applied only to the study of QCD in ordinary conditions. We believe this Action has a very good promise at finite temperature as well, because of its good chiral behaviour which should make it ideal for the symmetry studies discussed above. This project is running on apeNEXT. We produced the first results on this machine, which were reported at the apeNEXT Laboratory official opening in Rome by the spokesperson of the apeNEXT collaboration. Recently, new collaborators from the Humboldt and Muenster University have joined this project.

### 3 Nearest Neighbors: the Experimental Side and the European Context

Over the past five years - beginning from the GISELDA project proposed in 2001 by Wanda Alberico, Marzia Nardi and myself - a deliberate effort was made to link this research with the ongoing experimental activities at RHIC and upcoming at CERN. Our natural reference is the ALICE Collaboration, and indeed we have already a tradition of meetings and common events with ALICE members.

Our latest step in this was taken by Luciano Maiani, Francesco Becattini, Marzia Nardi, Fulvio Piccinini and myself: we have proposed the new IS RM31, Ultrarelativistic Heavy Ion Collisions and Quark Gluon Plasma, whose startup meeting was held at the LNF in June 2005.

On the European side, I am the coordinator of the Frascati node of the I3 Hadron Physics Network “Strongly Interacting Matter in Ultrarelativistic Heavy Ion Collisions”, and the coordinator of the first plenary meeting of the same Network, to be held at the European Center for Theoretical Studies in Nuclear Physics during June 2006.

### 4 Conference Talks

1. "Imaginary Chemical Potential", at 'Modern Challenge in Lattice Gauge Theory' KITP Program, Santa Barbara, March 2005.
2. "Quark Gluon Plasma and the Hadronic Gas on the Lattice", at 'First Workshop on Quark-Hadron Duality and the Transition to pQCD', LNF, June 2005.
3. "QCD thermodynamics : lattice results and new possibilities" at 'QCD@Work 2005, International Workshop on Quantum Chromodynamics: Theory and Experiment', Conversano, June 2005.
4. "Series representation, Pade' approximants, and critical behaviour in QCD" at 'Lattice2005, 23rd International Symposium on Lattice Field Theory', Dublin, Jul 2005.
5. "Lattice QCD at finite temperature" at 'Supercomputing Relativistic Heavy-Ion Collision Physics' TIFR. Mumbai, December 2005.

### 5 Publications

1. B. Alles, M. D'Elia and M. P. Lombardo, "Behaviour of the topological susceptibility in two colour QCD across the finite density transition," arXiv:hep-lat/0602022.
2. M. D'Elia, F. Di Renzo and M. P. Lombardo, "QCD at high temperature: Results from lattice simulations with an imaginary AIP Conf. Proc. **806** (2006) 245.
3. M. P. Lombardo, "Series representation: Pade approximants and critical behavior in QCD at nonzero T and  $\mu$ ," PoS **LAT2005** (2005) 168.
4. G. Akemann, E. Bittner, M. P. Lombardo, H. Markum and R. Pullirsch, "Density profiles of small Dirac operator eigenvalues for two color QCD at Nucl. Phys. Proc. Suppl. **140** (2005) 568.
5. M. P. Lombardo, "Lattice QCD at finite temperature and density," arXiv:hep-lat/0509180.

## MI12

S. Bellucci (Resp.), P.-Y. Casteill (Osp.), M. Cini (Ass.), A. Cordelli (Ass.),  
S. Ferrara (Ass.), E. Latini (Dott.), A. Marrani (Bors.), P. Onorato (Ass. Ric.),  
E. Orazi (Dott.), E. Perfetto (Ass. Ric.), R. Raimondi (Ass.)

### 1 Research Activity

Supersymmetric theories, supergravity, superstrings and M-theory are the subject of extensive investigation by us. More specifically, the group in Frascati focuses on supersymmetry breaking in string and M-theory compactification, relation of non-commutative supersymmetric theories with strings in different backgrounds, effective actions of bulk supergravity coupled to branes in the presence of fluxes, gauged supergravity, non-commutative superspaces and their occurrence in string theory.

We made important contributions to gauged supergravity and duality symmetry, supersymmetry algebras in diverse dimensions, super Higgs effect, supersymmetric theories in non-commutative superspaces, classification of operators in the AdS/CFT correspondence, supergravity interpretation of flux compactification, supersymmetric Born-Infeld actions.

The main lines of research for our group concern the following topics:

- AdS/CFT correspondence
- Supersymmetric Yang-Mills theory and supergravity
- Non-commutative supersymmetric field theories
- Spontaneous supersymmetry breaking
- Effective actions for brane dynamics
- Transport proprieties in low-dimensional systems and spin Hall effect

The main active collaborations include:

- JINR-Dubna, Russia
- Tomsk Univ. Russia
- Univ. Hannover, Germany
- Turin Polytechnic, Italy
- CERN, Switzerland
- Annecy, LAPTH, France
- Valencia U., Spain
- CSIC, Madrid, Spain
- Univ. Roma Tor Vergata, Italy
- Univ. Roma Tre, Italy

We also organized recently a Winter School on Supersymmetric Mechanics Frascati (Italy), 7 - 12 March 2005 with the participation of fair amount of collaborators, both as lecturers and as students.

A related noteworthy event was the RTN Winter School on Strings, Supergravity and Gauge Theories, held at S.I.S.S.A (Trieste), January 31 - February 4 2005, with the participation of students from our group.

Finally, a really important related event was organized by Frascati and Tor Vergata, in order to honour a member of MI12, Prof. S. Ferrara: The Legacy of Supergravity Villa Mondragone (Roma), 6-8 June 2005. Moreover the same member of MI12 was awarded the E. Fermi prize by the SIF (September 2005) and designated for the "Dannie Heineman prize for Mathematical Physics" of the APS in October 2005.

## 2 Non-commutative field theory

We considered the problem of noncommutative elastic scattering in a central field. General formulas for the differential cross-section for two cases were obtained. For the case of high energy of an incident wave it is shown that the differential cross-section coincides with that on the commutative space. For the case in which noncommutativity yields only a small correction to the central potential it is shown that the noncommutativity leads to the redistribution of particles along the azimuthal angle, although the whole cross-section coincides with the commutative case. We have also constructed the appropriate Hamiltonian of the noncommutative coulombic monopole (i.e. the noncommutative hydrogen atom with a monopole). The energy levels of this system have been calculated, discussed and compared with the noncommutative hydrogen atom ones. The main emphasis is put on the ground state. In addition, the Stark effect for the noncommutative coulombic monopole has been studied.

## 3 Construction of new superstring and superparticle models and their quantization

Superstring theory possesses a very rich structure of vacuum states which can be studied considering the string models coupled to background fields. Another way to study the various aspects of superstring theory is to construct one-dimensional superparticle models having properties analogous to superstrings. The results we found point to the many interesting links between supersymmetric field theory and one dimensional quantum mechanics and allow one to clarify the aspects of superstring theory with help of simplified models.

We proposed the Hamiltonian model of  $N = 8$  supersymmetric mechanics on  $n$ -dimensional special Kähler manifolds (of the rigid type).

We demonstrated that a two-dimensional  $N=8$  supersymmetric quantum mechanics which inherits the most interesting properties of  $N = 2, d = 4$  SYM can be constructed if the reduction to one dimension is performed in terms of the basic object, i.e. the  $N = 2, d = 4$  vector multiplet. In such a reduction only complex scalar fields from the  $N = 2, d = 4$  vector multiplet become physical bosons in  $d = 1$ , while the rest of the bosonic components are reduced to auxiliary fields, thus giving rise to the **(2, 8, 6)** supermultiplet in  $d = 1$ . We constructed the most general action for this supermultiplet with all possible Fayet-Iliopoulos terms included and explicitly demonstrated that the action possesses duality symmetry extended to the fermionic sector of theory. In order to deal with the second-class constraints present in the system, we introduced the Dirac brackets for the canonical variables and find the supercharges and Hamiltonian which form a  $N=8$  super Poincaré algebra with central charges. Also, we explicitly presented the generalization of two-dimensional  $N=8$  supersymmetric quantum mechanics to the  $2k$ -dimensional case with a special Kähler geometry in the target space.

In addition, we constructed  $N=8$  supersymmetric mechanics with four bosonic and eight fermionic physical degrees of freedom. Starting from the most general  $N=4$  superspace action in harmonic superspace for the  $(4, 8, 4)$  supermultiplet we found conditions which make it  $N=8$  invariant. We introduced in the action Fayet-Iliopoulos terms which give rise to potential terms. We presented the action in components and give explicit expressions for the Hamiltonian and Poisson brackets. Also, we discussed the possibility of  $N=9$  supersymmetric mechanics. Then, we constructed a two-dimensional  $N=8$  supersymmetric quantum mechanics which inherits the most interesting properties of  $N=2$ ,  $d=4$  supersymmetric Yang-Mills theory. After dimensional reduction to one dimension in terms of field-strength, we showed that only complex scalar fields from the  $N=2$ ,  $d=4$  vector multiplet become physical bosons in  $d=1$ . The rest of the bosonic components are reduced to auxiliary fields, thus giving rise to the  $(2, 8, 6)$  supermultiplet in  $d=1$ . We constructed the most general superfields action for this supermultiplet and demonstrate that it possesses duality symmetry extended to the fermionic sector of theory. We also explicitly present the Dirac brackets for the canonical variables and construct the supercharges and Hamiltonian which form a  $N=8$  super Poincarè algebra with central charges. Finally, we discuss the duality transformations which relate the  $(2, 8, 6)$  supermultiplet with the  $(4, 8, 4)$  one.

Recently, we were able to construct  $N=4$  supersymmetric mechanics using the  $N=4$  nonlinear chiral supermultiplet. The two bosonic degrees of freedom of this supermultiplet parameterize the sphere  $S(2)$  and go into the bosonic components of the standard chiral multiplet when the radius of the sphere goes to infinity. We construct the most general action and demonstrate that the nonlinearity of the supermultiplet results in the deformation of the connection, which couples the fermionic degrees of freedom with the background, and of the bosonic potential. Also a non-zero magnetic field could appear in the system. We have been able to show that the Witten-Dijkgraaf-Verlinde-Verlinde equation underlies the construction of  $N=4$  superconformal multi-particle mechanics in one dimension, including a  $N=4$  superconformal Calogero model.

The  $N=8$ , 1D analytic bi-harmonic superspace was shown by us to provide a natural setting for  $N=8$  supersymmetric mechanics associated with the off-shell multiplet  $(4, 8, 4)$ . The latter was described by an analytic superfield  $q^{1,1}$ , and we constructed the general superfield and component actions for any number of such multiplets. The set of transformations preserving the flat superspace constraints on  $q^{1,1}$  constitutes  $N=8$  extension of the two-dimensional Heisenberg algebra  $\mathfrak{h}(2)$ , with an operator central charge. The corresponding invariant  $q^{1,1}$  action is constructed. It is unique and breaks 1D scale invariance. We also find a one-parameter family of scale-invariant  $q^{1,1}$  actions which, however, are not invariant under the full  $N=8$  Heisenberg supergroup. Based on preserving the bi-harmonic Grassmann analyticity, we formulate  $N=8$ , 1D supergravity in terms of the appropriate analytic supervielbeins. For its truncated version we construct, both at the superfield and component levels, the first example of off-shell  $q^{1,1}$  action with local  $N=8$ , 1D supersymmetry. This construction can be generalized to any number of self-interacting  $q^{1,1}$ .

We constructed also a new two-dimensional  $N=8$  supersymmetric mechanics with nonlinear chiral supermultiplet. Being intrinsically nonlinear this multiplet describes 2 physical bosonic and 8 fermionic degrees of freedom. We constructed the most general superfield action of the sigma-model type and proposed its simplest extension by a Fayet-Iliopoulos term. The most interesting property of the constructed system is a new type of geometry in the bosonic subsector, which is different from the special Kahler one characterizing the case of the linear chiral  $N=8$  supermultiplet.

Moreover, we proposed to consider the  $N=4$ ,  $d=1$  supermultiplet with  $(4, 4, 0)$  component content as a “root” one. We elaborated a new reduction scheme from the “root” multiplet to supermultiplets with a smaller number of physical bosons. Starting from the most general sigma-model type action for the “root” multiplet, we explicitly demonstrated that the actions for the rest of linear and nonlinear  $N=4$  supermultiplets can be easily obtained by reduction. Within the proposed reduction scheme there is a natural possibility to introduce Fayet-Iliopoulos terms. In the

reduced systems, such terms give rise to potential terms, and in some cases also to terms describing the interaction with a magnetic field. We demonstrated that known  $N=4$  superconformal actions, together with their possible interactions, appear as results of the reduction from a free action for the “root” supermultiplet. As a byproduct, we also constructed an  $N=4$  supersymmetric action for the linear  $(3,4,1)$  supermultiplet, containing both an interaction with a Dirac monopole and a harmonic oscillator-type potential, generalized for arbitrary conformally flat metrics.

Last, but not least, we showed that the nonlinear chiral supermultiplet allows one to construct, over a given two-dimensional bosonic mechanics, a family of two-dimensional  $N=4$  supersymmetric mechanics parameterized by a holomorphic function  $\lambda(z)$ . We show, that this family includes, as a particular case, the  $N=4$  superextensions of two-dimensional mechanics with magnetic fields, which have factorizable Schrödinger equations.

#### 4 $N=4$ supersymmetric Yang-Mills theory and spin bits

Large  $N$  physics gained noticeable interest in the past few years, owing to the AdS/CFT conjecture enlightenment and, more recently, to the consideration of various limits of this correspondence. Initially formulated in the  $N \rightarrow \infty$  limit, the conjecture in its strong form extends to finite  $N$ . It relates the strongly coupled regime of  $N=4$  SYM to the weakly coupled string theory and viceversa. This property, which makes out of this correspondence a very strong and efficient predictive tool, appeared to be an obstacle in proving the duality in itself.

At  $N \rightarrow \infty$  the spin Hamiltonian is a local and integrable operator. The Hamiltonian and the total spin generator represent the first two charges, in the tower of commuting ones, predicted by integrability. Higher charges are given in terms of higher powers of next-to-nearest spin generators summed up over the chain. Corrections in  $\frac{1}{N}$  spoil locality and integrability. The Hamiltonian and its higher spin analogs, which can be interpreted as broken symmetries of the would-be integrable system, can still be defined in terms of powers of spin generators. However, now there is no more restriction to next-to-nearest generators and the corresponding charges are no longer commuting among themselves. The role of these broken charges in the theory near the “integrable” point  $N \rightarrow \infty$  remains to be understood.

If the non-planar contributions are considered, the single-trace sector is not conserved anymore, and one ends up with trace splitting and joining in the operator mixing. Even in this case one can still consider a one-to-one map, the so-called spin-bit map, between local g.i. operators and a spin system. In this case one has to introduce a set of new degrees of freedom, beyond the spin states, which describes the linking structure of the sites in the spin-chain. This can be encoded in a new field, taking values in the spin-bits permutation group and introducing a new gauge degree of freedom.

We derived the coherent state representation of the integrable spin chain Hamiltonian with symmetry group  $SL(2, \mathbb{R})$ . By passing to the continuum limit, we found a spin chain sigma model describing a string moving on the hyperboloid  $SL(2, \mathbb{R})/U(1)$ . The same sigma model was found by considering strings rotating with large angular momentum in  $AdS_5 \times S^5$ . The spinning strings were identified with semiclassical coherent states built out of  $SL(2, \mathbb{R})$  spin chain states.

We considered the Super Yang–Mills/spin system map to construct the  $SU(2)$  spin bit model at the level of two loops in Yang–Mills perturbation theory. The model describes a spin system with chaining interaction. In the large  $N$  limit the model is shown to be reduced to the two loop planar integrable spin chain.

In a subsequent paper, we derived the coherent state representation of the integrable spin chain Hamiltonian with non-compact supersymmetry group  $G=SU(1,1-1)$ . By passing to the continuous limit, we found a spin chain sigma model describing a string moving on the supercoset  $G/H$ ,  $H$  being the stabilizer group. The action is written in a manifestly  $G$ -invariant form in terms

of the Cartan forms and the string coordinates in the supercoset. The spin chain sigma model is shown to agree with that following from the Green-Schwarz action describing two-charged string spinning on  $AdS_5 \times S^5$ .

An alternative approach to the calculation of anomalous dimensions in  $N=4$  SYM is based on matrix models, which can be also formulated in terms of a non-commutative field theory on a torus, and whose equivalence with spin-chain/spin-bit models in the  $N \rightarrow \infty$  (planar) and  $N \rightarrow 0^+$  limits is still under study. Indeed, so far we considered the matrix model approach to the anomalous dimension matrix in  $N=4$  super Yang-Mills theory. We constructed the path integral representation for the anomalous dimension density matrix and analyzed the resulting action. In particular, we considered the large  $N$  limit, which results in a classical field theory. Since the same limit leads to spin chains, we proposed to consider the former as an alternative description of the latter. We considered also the limit of small  $N$ , which corresponds to the restriction to the diagrams of maximal topological genus.

## 5 Transport proprieties in low-dimensional systems and spin Hall effect

Recently the idea to use the electron spin in mesoscopic devices has generated a lot of interest: the electron spin offers unique possibilities in order to find new mechanisms for information processing and information transmission so that the "spintronic" opens new perspectives to quantum computation. This part of our activity strongly benefits from putting together the complementary expertises within the group, e.g. the emerging studies of superconductivity in carbon nanotubes are benefitting from the expertise of the Tor Vergata group. Moreover, the Frascati and Roma Tre groups have been complementing each other in describing transport in different regimes, i.e. ballistic and diffusive transport. Both the Tor Vergata and the Roma Tre groups are involved since a long time in the study of transport with different and complementary approaches, whose synergy is being explored. In addition, our activity allows for a strong predictive power on the physics of nanostructures which is the object of extensive experimental investigation at the present time. In particular, we are focussing on the carbon nanotube and quantum dot based systems.

Exploratory investigations of toy-model realizations, capable of describing the physically measurable properties of low-dimensional correlated electron systems were highly successful in the past. For instance, the Tomonaga-Luttinger illustrative model within the context of QED, became concretely realized later in carbon nanotubes. In a similar way we have been studying well-defined models from the mathematical-physics viewpoint, in the hope that they correspond to some concrete realizations of the effective hamiltonians describing the systems considered in our research. For instance, a speculative development of our research is quantum mechanics on the non commutative plane, in the presence of a magnetic field  $B$ . The application of the modern field-theoretical methods, particularly, supersymmetric models, in condensed matter, was a subject of extensive study during a long period. The most recent such intersection was the application of noncommutative theories to the Hall effect, as well as in its recently proposed four-dimensional generalization. The interpretation of the semiconductor models with effective non-constant masses as of the quantum systems on the curved spaces is also well-known. We began apply nontrivial quantum mechanical systems (that are quantum mechanics on curved spaces, supersymmetric quantum mechanics and noncommutative quantum mechanics) to the excitonic effects in quantum dots. Applying the above systems to quantum dots, we have to interpret the curvature of their configuration spaces as a non-constant effective mass; the singularity of these systems on the "equator" could be interpreted as a well of the quantum dots. A supersymmetric extension can allow us to take into account the interaction of the spin of system with a magnetic field. Non-commutativity provides us with a model describing the collective effects in the lowest Landau levels.

Recently, we developed a theoretical framework that applies to the intermediate regime be-

tween the Coulomb blockade and the Luttinger liquid behavior in multi-walled carbon nanotubes. Our main goal is to confront the experimental observations of transport properties, under conditions in which the thermal energy is comparable to the spacing between the single-particle levels. For this purpose we have devised a many-body approach to the one-dimensional electron system, incorporating the effects of a discrete spectrum. We showed that, in the crossover regime, the tunneling conductance follows a power-law behavior as a function of the temperature, with an exponent that oscillates with the gate voltage as observed in the experiments. Also in agreement with the experimental observations, a distinctive feature of our approach is the existence of an inflection point in the log-log plots of the conductance vs temperature, at gate voltages corresponding to peaks in the oscillation of the exponent. Moreover, we evaluate the effects of a transverse magnetic field on the transport properties of the multi-walled nanotubes. For fields of the order of 4 T, we found changes in the band structure that may be already significant for the outer shells, leading to an appreciable variation in the power-law behavior of the conductance. We then foresee the appearance of sizeable modulations in the exponent of the conductance for higher magnetic fields, as the different subbands are shifted towards the development of flat Landau levels.

We developed two theoretical approaches for dealing with the low-energy effects of the repulsive interaction in one-dimensional electron systems. Renormalization Group methods allow us to study the low-energy behavior of the unscreened interaction between currents of well-defined chirality in a strictly one-dimensional electron system. A dimensional regularization approach is useful, when dealing with the low-energy effects of the long-range Coulomb interaction. This method allows us to avoid the infrared singularities arising from the long-range Coulomb interaction at  $D = 1$ . We can also compare these approaches with the Luttinger model, in order to analyze the effects of the short range term in the interaction. Thanks to these methods, we are able to discuss the effects of a strong magnetic field  $B$  in quasi one-dimensional electron systems, by focusing our attention on Carbon Nanotubes. Our results imply a variation with  $B$  in the value of the critical exponent  $\alpha$  for the tunneling density of states, which is in fair agreement with that observed in a recent transport experiment involving carbon nanotubes. The dimensional regularization allows us to predict the disappearance of the Luttinger liquid, when the magnetic field increases, with the formation of a chiral liquid with  $\alpha = 0$ .

We also developed a theoretical approach to the low-energy properties of 1D electron systems aimed to encompass the mixed features of Luttinger liquid and Coulomb blockade behavior observed in the crossover between the two regimes. For this aim we extended the Luttinger liquid description by incorporating the effects of a discrete single-particle spectrum. The intermediate regime is characterized by a power-law behavior of the conductance, but with an exponent oscillating with the gate voltage, in agreement with recent experimental observations. Our construction also accounts naturally for the existence of a crossover in the zero-bias conductance, mediating between two temperature ranges where the power-law behavior is preserved but with different exponent. Recent experiments about the low temperature behaviour of a Single Wall Carbon Nanotube showed typical Coulomb Blockade peaks in the zero bias conductance and allowed us to investigate the energy levels of interacting electrons. Other experiments confirmed the theoretical prediction about the crucial role which the long range nature of the Coulomb interaction plays in the correlated electronic transport through a Single Wall Carbon Nanotube with two intramolecular tunneling barriers. In order to investigate the effects on low dimensional electron systems due to the range of electron electron repulsion, we introduce a model for the interaction which interpolates well between short and long range regimes. Our results could be compared with experimental data obtained in Single Wall Carbon Nanotubes and with those obtained for an ideal vertical Quantum Dot. For a better understanding of some experimental results we also discussed how defects and doping can break some symmetries of the bandstructure of a Single Wall Carbon Nanotube.

## 6 List of Conference Talks by LNF Authors in the Year 2005

1. S. Bellucci, "Higher dimensional Quantum Hall effect", Condensed Matter and Field Theory Workshop, ICTP Trieste, Italy 1 March 2005

## References

1. Stefano Bellucci, Armen Nersessian, hep-th/0512165.
2. S. Bellucci, J.Gonzalez, P.Onorato and E.Perfetto, cond-mat/0512546, submitted to Phys. Rev. B (2005).
3. S. Bellucci, S. Krivonos, A. Marrani, E. Orazi, hep-th/0511249, Phys. Rev. D (in press).
4. S. Bellucci, A. Beylin, S. Krivonos, A. Shcherbakov, hep-th/0511054, Phys. Lett. B (in press).
5. S. Bellucci, P.-Y. Casteill, F. Morales, Nucl. Phys. **B729**, 163-178 (2005).
6. S. Bellucci, A. Yeranyan, Phys. Lett. **B609**, 418-423 (2005).
7. S. Bellucci, P.-Y. Casteill, A. Marrani, C. Sochichiu, Phys. Lett. **B607**, 180-187 (2005).
8. S. Bellucci, A. Galajinsky, E. Latini, Phys. Rev. **D71**, 044023 (2005).
9. S. Bellucci, S. Krivonos, A. Sutulin, Phys. Lett. **B605**, 406-412 (2005).
10. S. Bellucci, S. Krivonos, A. Shcherbakov, Phys. Lett. **B612**, 283-292 (2005).
11. S. Bellucci, S. Krivonos, A. Nersessian, Phys. Lett. **B605**, 181-184,2005.
12. S. Bellucci, C. Sochichiu, Nucl. Phys. **B726**, 233-251 (2005).
13. S. Bellucci, P.-Y. Casteill, F. Morales, C. Sochichiu, Nucl. Phys. **B707**, 303-320 (2005).
14. S. Bellucci, A. Beylin, S. Krivonos, A. Nersessian, E. Orazi, Phys. Lett. **B616**, 228-232 (2005).
15. S. Bellucci, E. Ivanov, A. Sutulin, Nucl. Phys. **B722**, 297-327 (2005).
16. Stefano Bellucci, Armen Yeranyan, Phys. Rev. **D72**, 085010 (2005).
17. S. Bellucci, V.M. Biryukov, A. Cordelli, Phys. Lett. **B608**, 53-58 (2005).
18. S. Bellucci, V.A. Maishev, Phys. Rev. **B71**, 174105 (2005).
19. S. Bellucci, Mod. Phys. Lett. **B19**, 85-98 (2005).
20. S. Bellucci and P. Onorato, Phys. Rev. **B71**, 075418 (2005).
21. S. Bellucci and P. Onorato, European Physical Journal **B45**, 87 (2005).
22. S. Bellucci and P. Onorato, Phys. Rev. **B72**, 045345 (2005) .
23. S. Bellucci, J. Gonzalez, P. Onorato, Phys. Rev. Lett. **95**, 186403 (2005) .
24. S. Bellucci and P. Onorato, Eur. Phys. J. **B47**, 385390 (2005).
25. S. Bellucci and P. Onorato, accepted for publication in Annals of Physics (2005), cond-mat/0510590

26. S. Bellucci and P. Onorato, accepted for publication in Phys. Rev. **B**, cond-mat/0512543.
27. Gianguido Dall'Agata, Riccardo D'Auria, Sergio Ferrara, Phys. Lett. **B619**, 149-154 (2005).
28. Gianguido Dall'Agata, Sergio Ferrara, Nucl. Phys. **B717**, 223-245 (2005).
29. R. D'Auria, S. Ferrara, M. Trigiante, S. Vaulà, JHEP **0503**, 052 (2005).
30. R. D'Auria, S. Ferrara, M. Trigiante, JHEP **0509**, 035 (2005).
31. L. Andrianopoli, S. Ferrara, M.A. Lledó, O. Macia, J. Math. Phys. **46**, 072307 (2005).
32. S. Ferrara, E. Ivanov, O. Lechtenfeld, E. Sokatchev, B. Zupnik, Nucl. Phys. **B704**, 154 (2005).
33. R. D'Auria, S. Ferrara, M. Trigiante, S. Vaulà, Phys. Lett. **B610**, 270-276 (2005).
34. R. D'Auria, S. Ferrara, M. Trigiante, S. Vaulà, Phys. Lett. **B610**, 147-151 (2005).
35. R. D'Auria, S. Ferrara, M. Trigiante, Comptes Rendus Physique **6**, 199-208 (2005).
36. R. D'Auria, S. Ferrara, Phys. Lett. **B606**, 211-217 (2005).
37. R. Raimondi and P. Schwab Phys. Rev. **B71**, 033311 (2005).
38. R. D'Agosta, G. Vignale, and R. Raimondi Phys. Rev. Lett. **94**, 086801 (2005),
39. J. Gonzalez and E. Perfetto Phys. Rev. **B72**, 205406 (2005).
40. E. Perfetto and M. Cini Phys. Rev. **B71**, 014504 (2005).

## PI11

F.Palumbo (Resp.)

### **1 Composite boson dominance in relativistic field theories- S. Caracciolo, V. Laliena and F. Palumbo**

We applied the bosonization method described in Iniziativa specifica PI31 to relativistic field theories. We obtained a general expression for the action of the effective bosons valid also for gauge theories regularized on a lattice. We are now investigating its continuum limit.

### **2 Analytic nonperturbative approach to QCD- Yu. A. Simonov and F. Palumbo**

We make the pure gauge action on the lattice quadratic in the gauge fields by using the Hubbard-Stratonovich transformation (which requires the use of a noncompact regularization). Then we integrate out exactly the gauge fields and investigate the saddle point equations of the resulting effective action for gauge invariant functions with glueballs quantum numbers.

## PI31

F. Palumbo (Resp.)

### 1 Composite boson dominance in many-fermion systems

I developed a new method of bosonization <sup>1)</sup> of fermion systems based on the use of coherent states of fermionic composites. It is applicable when the partition function is dominated by composite bosons with smooth structure functions. Restricting the partition function to such states I get an euclidean bosonic action from which I derive the Hamiltonian. Such a procedure respects all the fermion symmetries, in particular fermion number conservation, and provides a boson mapping of all fermion operators.

I generalized the above method and derived results which hold for arbitrary structure functions and interactions <sup>2)</sup> respecting all fermion symmetries. The generalized method reproduces exactly the results of the pairing model of atomic nuclei and of the BCS model of superconductivity in the number conserving form of the quasi-chemical equilibrium theory.

#### References

1. F. Palumbo, Phys. Rev. C **72**, 014303 (2005).
2. F. Palumbo, cond-mat/0512548.

## ARCHIMEDE

G. Cinque (Resp.), G. Cibin (Dott.), A. Grilli (Tecn.), A. Raco (Tecn.),  
E. Burattini (Ass.), A. Marcelli

### 1 Summary

The INFN-Gr.V project **ARCHI**tects of **Mirror Extreme** ultraviolet **DE**VICES deals with the experimental study of high reflectivity systems to be used at quasi-normal incidence for soft X-rays down to the *water-window*. This research is strategical to the development of soft X-ray optics - e.g. to microscopy in biophysics and microprobe spectroscopy in general - not only for Synchrotron Radiation (SR) but also for future 4<sup>th</sup> generation sources such as Free Electron Lasers (FEL). The commitment of INFN takes advantage of the expertises at the Laboratori Nazionali di Legnaro (LNL) for designing and depositing multilayers, and the soft X-ray vacuum reflectometer developed on purpose at the Laboratori Nazionali di Frascati (LNF). The first *Ni/Ti* and *Ni/TiO<sub>2</sub>* devices grown at the LNL, by a lattice spacing around 14 Å and more than 100 bilayers, have been successfully tested by the  $\theta - 2\theta$  reflectometer completed in 2005 at the LNF. In the second half of 2005, SR soft X-rays have been used to characterize these multilayers at Frascati.

### 2 Activity

The project ARCHIMEDE addresses the demand on novel X-ray reflectors for soft energies, i.e. down to the O and C absorption edges (280 – 540eV). The development of multilayer mirrors is particularly appealing for the microscopy of organic samples in the so called *water-window*, where X-rays provide very good contrast between protein and water environment. Advantages of such artificial Bragg's diffractors include high radiation tolerance and throughput. However, at low energies it is difficult to fabricate reliable devices with layer pair thickness around 30 Å and hundreds of bilayers. The rationale of multilayer researches is the wider solid angle available for focusing X-rays at near-normal incidence with respect to grazing angles of standard X-ray mirrors. Ni-Ti based systems are well-suited candidates for multilayer mirrors due to their optical constant matching, giving high reflectivity nearby *Ti* (450eV) and *Ni* (850eV)  $L_{2,3}$  edges. *Ni/Ti* multilayers designed to work at quasi-normal incidence were successfully grown at LNL for the first time by 300 bilayers. After optimization of the sputtering deposition, completely new *Ni/TiO<sub>2</sub>* multilayers were also fabricated by 150 bilayers. These are, to our knowledge, the first results concerning X-ray reflectors made of pure metal layers (*Ni*) deposited onto different metal oxide (*TiO<sub>2</sub>*) and tested under SR. Preliminary characterizations were obtained by Rutherford Backscattering Spectroscopy (RBS), Nuclear Reaction Analysis (NRA) and X-Ray Reflectivity (XRR). Since summer 2005, the

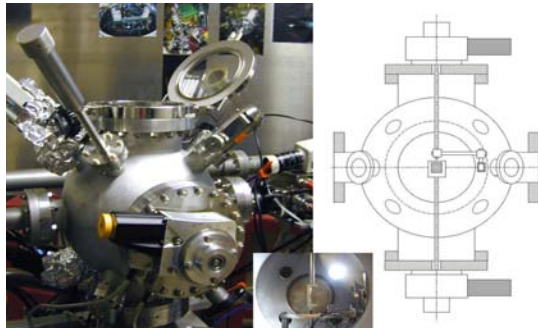


Figure 1: *UHV reflectometer experimental set-up (SR beam coming leftside). At left: external side view. At right: schematic drawing top view. Bottom: inside view from top.*

commissioning and test of the vacuum compatible soft X-ray reflectometer have been completed at LNF, including remote control unit and dedicated software. The whole set-up (Fig. 1) consists in a UHV chamber allocating two high precision/resolution goniometers, coupled to UHV all-magnetic rotary feedthroughs, to perform in-angle scans of the multilayer under X-ray beam and to follow the reflected beam by the detector arm. Extreme precision, accuracy and repeatability of the angular movements (better than  $1/300$  *mrad*) are guaranteed without backlash by the readout of absolute encoders for angle feedback (closed-loop mode). The direct detection of diffracted X ray beams is accomplished by an absolute X-ray photodiode directly connected to a UHV compatible preamplifier. To test the new optics, at LNF the direct characterization of the multilayer reflectivity have been performed using the photons emitted from the wiggler source of DAΦNE. The first experimental measurements were accomplished with the direct measurements by means of X-rays of the first optical-grade multilayers in terms of energy bandwidth (rocking curve) and reflectivity <sup>1)</sup>. Two experimental approaches have been followed, i.e. white-beam  $\omega$ -scans for determining the multilayer rocking curve, and both  $\omega$ - and  $2\theta$ -scan measurements by monochromatic beam at about  $1.2$  *keV*. The measurements performed on a benchmark *Si/Mo* device and the preliminary results obtained on both *Ni/Ti* (see Fig. 2), and *Ni/TiO<sub>2</sub>* devices can be summarized as follows: by comparison of the experiments by SR and conventional X source, the overall reflectivity of the *Ni/Ti* device is estimated to be between 5 to 9%. RBS, NRA and XRR techniques result in *Ni/Ti* and *Ni/TiO<sub>2</sub>* multilayer periods of, respectively,  $13.86 \pm 0.07$  Å and  $12.78 \pm 0.18$  Å.

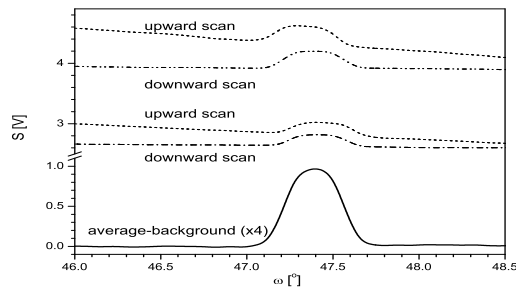


Figure 2: *Ni/Ti* multilayer tests under white-beam at  $45^\circ$ : the lower peak is the average of the four scans plotted above, background subtracted and normalized to a circulating current of 1A.

New experiments are in due course (2006) at LNF for better definition of nickel-titanium devices as a function of photon energy and by  $\theta - 2\theta$  scans. The natural development consists in improving the reflectivity performances to the *about 30%* expected nearby the *Ni L - edges*.

### 3 Acknowledgements

A special thanks is due to M. Pietropaoli and G. Viviani for the technical support at DAΦNE-L Lab, as well as Antonietta Frani for the development of the software interface.

### References

1. G. Cinque *et al*, "Preliminary SR characterization of first multilayer mirrors for the soft X-ray water-window", *Spec. Acta.* **B**, in press (2005).

**CAPIRE**  
**A Program to Develop Large Area Parallel Plate Detectors**

A. Calcaterra, L. Daniello (Tecn.), R. de Sangro, G. Mannocchi (Ass.)  
P. Patteri, M. Piccolo (Resp.), L. Satta (Ass.)

In collaboration with INFN MILANO and INFN TORINO

## 1 Introduction

During 2005 the Collaboration has carried out long term test for a substantial amount of detectors at the Milano Bicocca test facility. About  $10 \text{ m}^2$  of detectors have been kept on and monitored. Results of the test have shown substantial degradation of performances after a period of several months of continuous operation. Electrode analysis has yielded indications of chemical attack of the glass surface by the fluorine contained in the R134A. This has, in turn, led the collaboration to develop a parallel plate detector operating with a freon-less gas mixture.

## 2 Results

Test setup were operational at Milano Bicocca and Frascati to evaluate the long term behavior of relatively large detectors ( $1.1 \text{ m}^2$ ). Nine chambers were kept on gas and voltage for about one year under tightly controlled conditions, temperature and gas moisture were continuously monitored; particular care was taken in order to keep gas moisture well below the 30 ppm value, as such level was deemed to be safe for chamber operation. The data collected showed a definite deterioration of chambers performances: In fig 1 the efficiency maps of the different chambers at the beginning of the run are shown. The spacers are clearly seen as a relatively low efficiency areas.

After few months of continuous operation the efficiency was badly deteriorated Fig 2 shows the efficiency drop as a function of time. The efficiency deterioration was clearly correlated with a sizeable increase of the singles rate in the detectors. Through out the entire running period the moisture level in the chamber gas was below 15 ppm. Temperature, chamber currents and high voltage were monitored as well to ensure smooth operation during the test. After roughly one year of operation the chambers were taken off line; samples of the anode and cathode glass were sent off to be analyzed together with glass samples of chambers built at the same time and never operated. In fig. 3 a measure of the surface roughness is presented for three different samples.

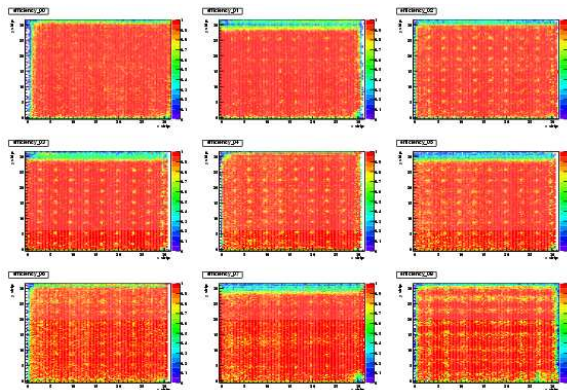


Figure 1: *Efficiency maps of the nine  $1 \text{ m}^2$  chambers at the beginning of the run*

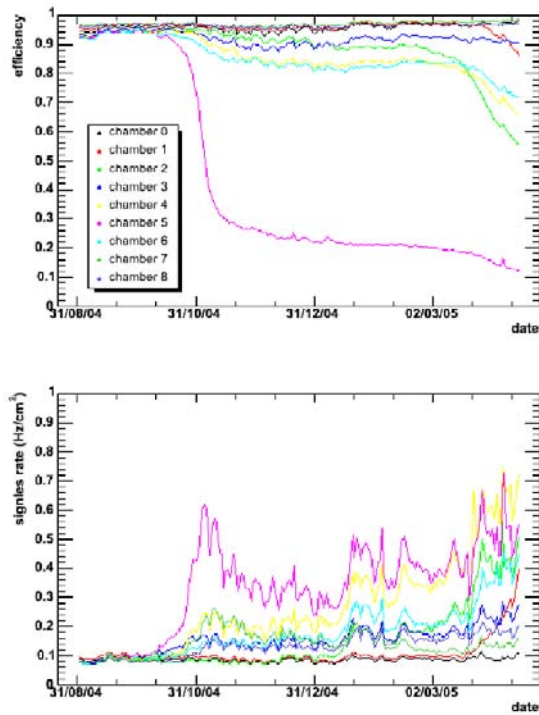


Figure 2: *The time development of the chamber efficiency (upper plot) and the time development of the singles rate for the nine chambers under test .*

It seems clear that Fluorine containing mixtures cannot be safely used in glass RPC, so, we devised a different structure, bound to work by means of a mechanical quenching rather than heavily electronegative gas quenching.

In fig. 4 is shown a new type of RPC that would work with almost pure Argon. The hexacell structure prevents the streamer from spreading and becoming a Geiger discharge. Preliminary test show that efficiency in excess of 80% for minimum ionizing can be obtained with a hexacell 3mm diameter. <sup>1)</sup>

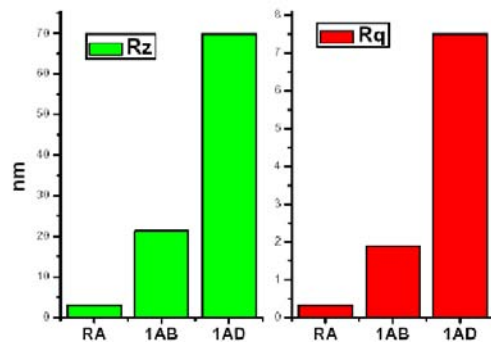


Figure 3: *Two different parameters that measure the electrode surface roughness. The labels RA,1AB and 1AD refers respectively to new glass, good anode after few months of operation and bad anode after few months of operation.*

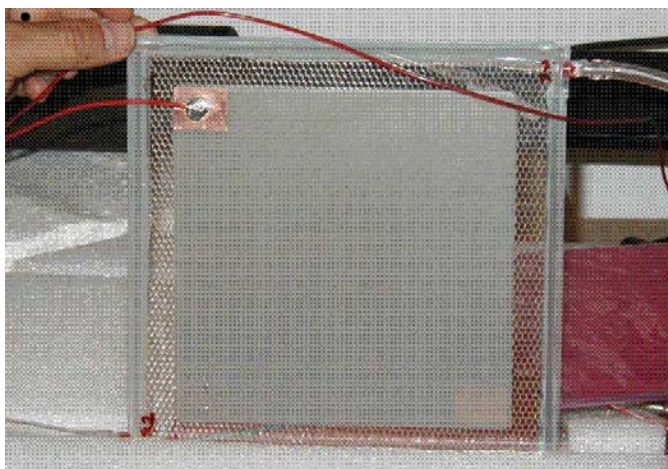


Figure 4: *A photo of the first mechanically quenched RPC.*

### 3 2006 plan

In coming year, the Collaboration, with a new name R2PC, will develop this new breed of parallel plate detector: studies of gas mixtures, performances as a function of the hexacell size, behavior as a function of local rate will be carried out; if these will be successful large area chambers will be built and long term reliability will be checked.

### 4 Conference presentations and Publications

- M.Piccolo, "Contribution to the Muon and special detector session for ALCPG-ILC" Snowmass (USA) August 2005.
- T. Tabarelli de Fatis, "Contribution to IEEE Nuclear science Symposium 2005 " San Juan Puerto Rico, October 2005.

### References

1. A.Calcaterra *et al.*, "A new concept for streamer quenching in parallel plate chamber" **LNF 05/13**, accepted for publication by Nuclear Instruments and Methods.

## E-CLOUD

### Study of the Vacuum Chamber Surface Electronic Properties Influencing Electron Cloud Phenomena

A. Balerna, E. Bernieri, M. Biagini, M. Boscolo, R. Cimino (Resp.), A. Drago,  
S. Guiducci, M. Migliorati, L. Palumbo, C. Vaccarezza, M. Zobov (INFN, LNF)

The e-cloud collaboration has been active, in 2005, on different fronts. We continued studying material surface properties as input for e-cloud simulations <sup>1)</sup>, performing e-cloud related experiments on the actual material in which the LNF Accelerator ring DAΦNE vacuum system is built, and connecting them to simulations <sup>2)</sup>, and presenting the obtained results in different workshops and international conferences <sup>1, 2, 3)</sup>. Experimental studies on the DAΦNE actual Al surface properties were prompted by the notion that despite preliminary simulations predicted e-cloud induced beam instabilities in the positron ring, such calculations were based on literature results on aluminum reflectivity, photon yield, etc., not directly measured from the actual DAΦNE chamber wall material. We show how calculations strongly depend on the assumed reflectivity and photon yield values. These two quantities have been measured using synchrotron radiation on samples prepared and made of the same aluminum alloy (Al 5083) used for the storage ring of DAΦNE . The obtained experimental results are implemented in the calculations. In fact, several codes are

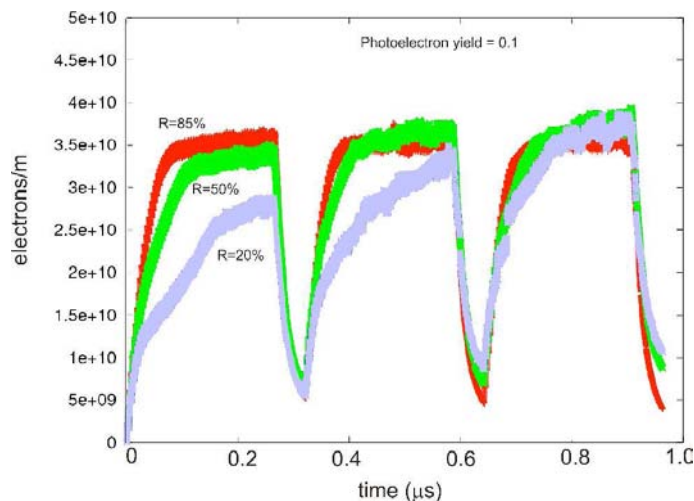


Figure 1: mean e-cloud linear density plotted changing the value of the reflectivity (85%, 50%, and 20%) with a photoelectron yield of 0.1.

available to evaluate e-cloud density around the circulating beam, but most of the parameters are strictly dependent upon the vacuum chamber geometry, the material choice, and its surface finishing. We did concentrate on the relevance of photon reflectivity and photon yield on the simulated e-cloud build up by using the ECLOUD code <sup>1)</sup> to simulate the average e-cloud linear density as a function of reflectivity and photoelectron yield. This is shown in fig 1 where it is clear the importance of using the appropriate parameters by comparing the the electron density obtained by changing the reflectivity. The simulations results confirm the importance of the considered reflectivity value in order to obtain a reliable estimation of the e-cloud effect impact on the collider

performance and its remedy efficiency.

The reflectivity  $R(\omega)$  and the photoelectron yield  $Y(\omega)$  have been measured at the BEAR beamline at Elettra (Trieste, Italy) in the photon energy range from 10 to 1000 eV, using a calibrated photodiode and a picoammeter for the measure of the drain current. The sample is made of the material used for the vacuum vessel (an aluminum alloy Al 5083-H321). We measured the specularly reflected light impinging onto the sample at three different incidence angles ( $85^\circ$ ,  $45^\circ$  and  $5^\circ$ ), and the diffused light setting the photodiode far from the specular direction. The results are presented in Fig 2 as a function of angle of incidence and of the energy of the impinging photons, for specular reflectivity. The diffused light was also measured and was negligible in all cases. The total light intensity reflected by the DAΦNE walls can be than calculated and results to 27% , 0.2% and 0.1% for the incidence angles  $\Theta = 85^\circ$ ,  $45^\circ$ ,  $5^\circ$ . The total PY has been also measured as

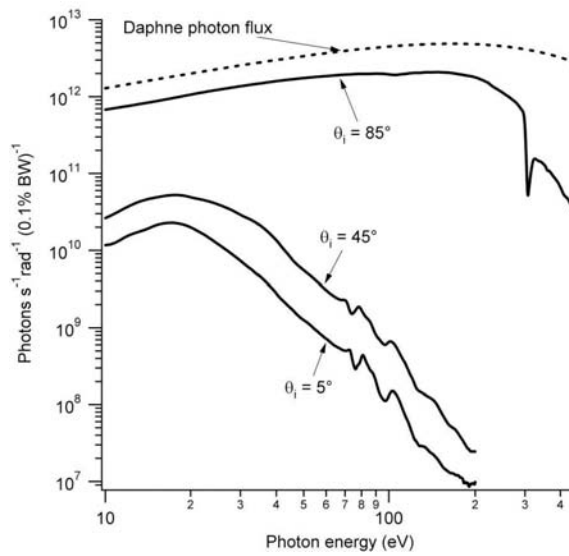


Figure 2: Number of reflected photons obtained by the reflectivity curves at incidence angle  $\Theta = 85^\circ$ ,  $45^\circ$ ,  $5^\circ$ .

a function of photon energy and its integration gives the total number of electrons produced by the material when it is illuminated by photons in the range 10-1000 eV. The total PY is about 0.2 for all the three angles considered even though the shape of the three curves are slightly different. Electron cloud simulations have been performed to study the dependence of the obtained results from the values of reflectivity and photoelectron yield used to perform the simulations. The results suggest the need of using experimentally determined values to extract reliable predictions of the e-cloud build up. Synchrotron radiation studies showed that the parameters used so far in the simulations are different from the experimental data obtained from the Al samples representative of the DAΦNE vacuum chamber. The code has been implemented with the measured values. This suggests the need to extract experimental values for reflectivity and photoelectron yield of the material used in other accelerator machines where electron cloud simulations are required. Together with such studies, an experimental campaign has been launched to measure the effects of the predicted presence of electron cloud detrimental effects on DAΦNE. After the first indications of the e-cloud build-up in the positron ring a signature was looked for in the vacuum behaviour for the two beams. The residual pressure was measured and the gauge readings were recorded every 15 s by the DAΦNE control system and logged in the daily data sheet together with the main operating parameters such as beam current, luminosity, beam lifetime and so on. In both

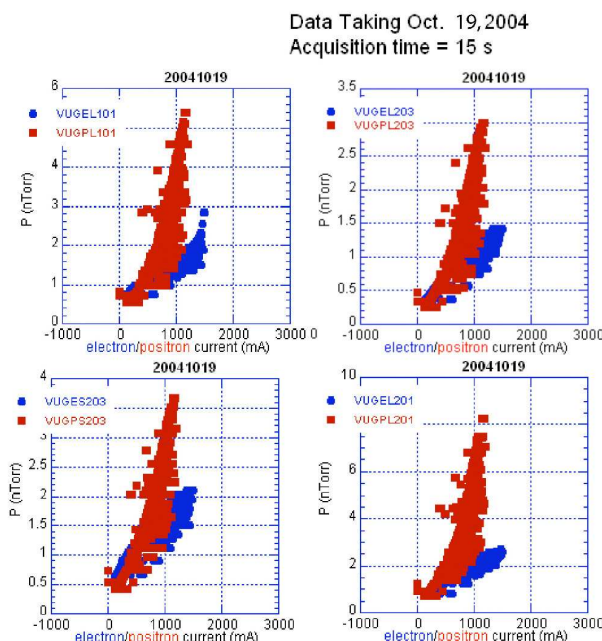


Figure 3: Vacuum pressure read-out vs total current as recorded in four straight section locations for the electron (blue dots) and positron (red dots) rings.

the electron and positron rings 14 Bayard Alpert vacuum gauges are located, one in each of the two interaction regions, one per arc, and one upstream and down stream of each arc respectively. Looking at the gauge readings and comparing the observed behaviour between the electron and positron ring some relevant differences are found as it is shown in Fig 3. In this figure the pressure readings are plotted as recorded from the gauges located in the straight sections in both the electron and positron ring. Looking at the plots over a whole day acquisition the positron beam exhibits a non-linear behaviour of the pressure together with a blow-up for definitely lower current values than those circulating in the electron ring. Also, to refine e-cloud simulations, the measured field-map for the wiggler magnetic field has been included in the code, together with some real DAΦNE surface parameters as come out from the measurements. The simulation results suggest that a significant value of the electron linear density has to be expected for a beam current of  $I_b \approx 1A$ . The study is underway in order to understand whether the obtained electron-cloud density can be related to the observed fast horizontal instability and the large positive tune shift. This study is even more urgent and interesting in view of the proposed upgrade of DAΦNE-2, where significant e-cloud detrimental effects may be expected. The group is also closely connected to the european collaboration EUROTEV, to study, both experimentally and with simulations, the potential presence of e-cloud phenomena in the very performing ILC damping rings.

## 1 List of Conference Talks by LNF Authors in Year 2005

1. N. Mahne, A. Giglia, S. Nannarone, R. Cimino, C. Vaccarezza, “Experimental determination of e-cloud simulation input parameters for DAΦNE”; presented at PAC05 Particle Accelerator Conference, Knoxville, Tennessee, USA, May 16-20, 2005.
2. C. Vaccarezza, R. Cimino, A. Drago, M. Zobov, G. Bellodi, D. Schulte, F. Zimmermann,

G. Rumolo, K. Ohmi, M. Pivi; "Electron cloud build-up study for DAΦNE"; presented at PAC05 Particle Accelerator Conference, Knoxville, Tennessee, USA, May 16-20, 2005.

3. "Surface related properties as an essential ingredient to e-cloud simulations"; R. Cimino, presented in: COULOMB'05 - High Intensity Beam Dynamics September 12 - 16, 2005 - Senigallia (AN), Italy.
4. "SEY measurements and e-cloud studies at DAΦNE", R. Cimino, presented in: EUROTeV meeting, 22-23 June, London 2005.

## References

1. "Experimental determination of e-cloud simulation input parameters for DAΦNE"; N. Mahne, A. Giglia, S. Nannarone, R. Cimino, C. Vaccarezza; proceedings of PAC05 Particle Accelerator Conference, 2005.
2. "Electron cloud build-up study for DAΦNE"; C. Vaccarezza, R. Cimino, A. Drago, M. Zobov, G. Bellodi, D. Schulte, F. Zimmermann, G. Rumolo, K. Ohmi, M. Pivi; proceedings of PAC05 Particle Accelerator Conference, 2005.
3. "Surface related properties as an essential ingredient to e-cloud simulations"; R. Cimino, Nuclear Instruments and Methods in Physics Research A, in print (2006).

## FLUKA2

M. Carboni, M. Pelliccioni (Resp.), S. Villari (Ass.)

### 1 Report year 2005

The investigation on the effect of the aircraft structures on the cosmic ray doses onboard has been concluded. The calculated results have been published (refs. 1 and 3).

The effect of possible changes of the radiation and tissue weighting factors recommended by the ICRP on the doses is currently under evaluation, using a number of data recently calculated by Fluka simulations.

A comparison between the calculated high energy photon vertical flux and experimental data at various locations and altitudes is also in progress.

Finally, the data analysis of the angular dependence of the neutron fluences on altitude, latitude and solar activity, has been initiated.

### 2 List of Publications 2005

1. G. Battistoni, A. Ferrari, M. Pelliccioni and R. Villari, "Evaluation of the doses to aircrew members taking into consideration the aircraft structures", *Advances in Space Research*, 36, 1645-1652, 2005.
2. A. Ferrari, P. Beck, M. Pelliccioni, S. Rollet and R. Villari, "Fluka simulation of TEPC response to cosmic radiation", *Radiat. Prot. Dosim.* 116, 327-330, 2005.
3. A. Ferrari, M. Pelliccioni and R. Villari, "A mathematical model of aircraft for evaluating the effects of shielding structure on aircrew exposure", *Radiat. Prot. Dosim.* 116, 331-335, 2005.
4. F. Ballarini, G. Battistoni, F. Cerutti, A. Ferrari, E. Gadioli, M.V. Garzelli, A. Ottolenghi, V. Parini, M. Pelliccioni, L. Pinsky, P. Sala, D. Scannicchio, "Modeling the action of protons and heavier ions in biological targets: nuclear interactions in hadrontherapy and space radiation protection", *AIP Conference Proceedings* May 24, 2005, Volume 769, Issue 1, pp. 1606-1611, 2005.
5. H. Aiginger, V. Andersen, F. Ballarini, G. Battistoni, M. Campanella, M. Carboni, F. Cerutti, A. Empl, W. Enghardt, A. Fasso', A. Ferrari, E. Gadioli, M.V. Garzelli, K. Lee, A. Ottolenghi, K. Parodi, M. Pelliccioni, L. Pinsky, J. Ranft, S. Roesler, P.R. Sala, D. Scannicchio, G. Smirnov, F. Sommerer, T. Wilson, N. Zapp, "The FLUKA code: new developments and application to 1 GeV/n iron beams", *Advances in Space Research*, 35, 214-222, 2005.

## FREETHAI

V. Andreassi, C. Catena (Ass.), F. Celani (Resp. Naz.), G. D' Agostaro (Osp.),  
A. Marcelli, E. Righi (Ass.), A. Spallone (Ass.), G. Trenta (Ass.), P. Quercia (Osp.)

Collaboration with Companies/University:

EURESYS (Rome); Pirelli Labs (Milan); Centro Sviluppo Materiali (Castel Romano); CESI (Milan); ORIM (Macerata); STMicroelectronics (Cornaredo, Milan); Mitsubishi Heavy Industries (Yokohama-Japan); Univ. Osaka (Japan). Univ. and INFN Lecce; Univ. and INFN Perugia.

### 1 Foreword

Starting from 2004, the experiment FREETHAI included, formally, also the activity of previous INTRABIO experiment (see the Activity Report AR of years 2003 and 2004): biological use of Heavy Water. It was renamed DEUTER in 2004. In such group are involved also Researcher of Perugia, INFN section that have a close collaboration with LNF because some of their scientific activity is performed at LNF using the Infrared Synchrotron Light coming out from DAΦNE  $e^+e^-$  collider.

- At first, we will report the nuclear results, key activity of FREETHAI-LNF and, at the end (shortly), the experimental activities performed at INFN-Univ. Lecce (use of a laser to stimulate the production of “new” elements in Hydrogenated or Deuterated Palladium films).
- Later one we will report about FREETHAI-DEUTER which aim is to explore the possible use of Heavy Water, heavily (17kGy) irradiated with gamma radiation (energies of 1173keV and 1332keV) coming out from a high intensity  $^{60}\text{Co}$  source (“Calliope” facilities at ENEA-Casaccia), as a possible anti-cancer agent.
- The common aspect of all experimental activities, both nuclear and biological, is the use, in most of the cases, of Deuterated compounds as “active” agents and Hydrogenated as “control” one.

### 2 Introduction

The experimental task of FREETHAI (Fusion Research by Electrolytic Experiments: Tritium and Heat Anomalous Increase), 3<sup>rd</sup> year of activity, is to develop innovative and reproducible techniques to maximize the values of Hydrogen (H) and Deuterium (D) concentrations in Palladium (Pd), i.e. the so-called “overloading”, ( $\text{H,D/Pd} \gg 0.95$ ) through light (H) or heavy (D) electrolytic solutions (water and/or hydro-alcoholic). The aim is to get short waiting times for the overloading (50 hours) and long time stability ( $> 4$  hours). It is a further developing of the FREEDOM experiment ended in December 2002: see the AR of such experiment for further details.

Our experimental pathway consists in the development of very innovative methods for overloading Pd (surface and/or bulk) using light H and, later on, in the transfer and adaptation of the successful methods to the use of heavy (water, alcohol) solutions. Such two steps procedure was demonstrated to be overall quite efficient because the experiments using light H didnt need particularly sophisticated cares (for example the solutions are insensible to ambient humidity). The employment of heavy H solutions (i.e. the Deuterium, D) is, on the contrary, very time consuming and experimentally complex. All the deuterated compounds are strongly hydro-scopic:

the H contamination of D solutions (with H arising from ambient humidity), was an uncontrollable parameter in our D-based experiments: it could work as a “poison” with respect to the D electrolyte. The resulting main drawback of such, sequential two-steps, procedure is that it is necessary to build at least a twin experimental set-up, electronics, data acquisition system together with full-time dedicated people.

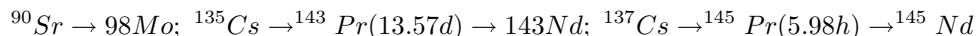
In the case of the D based experiments, we were looking for “the anomalous production” of excess heat, tritium and “transmutations also, i.e. the quite “strange” and unusual thermal and/or nuclear ashes related to the so-called, and still now controversial, “Cold Fusion” (CF) phenomenology. Anyway, recently, the “transmutations” phenomena received a significant acceptance in the scientific community, mainly because of the reproducible experiments carried out at Mitsubishi Heavy Industries Laboratories (Yokohama, Japan). We note that, some of the Mitsubishi Group (headed by Yasuhiro Iwamura) results, were independently confirmed also by our experimental group in Italy at INFN Frascati National Laboratories. We used a complementary methodology: wet electrolytic environment instead of dry gaseous ones. At the present, we have some collaborations with Iwamura group in specific tasks (see following).

In order to understand, fully, the quite complex and unconventional pathway of our scientific activity, it is necessary to read our previous Activity Report of years 2003 and 2004. In this report, we will discuss only the activity performed during year 2005.

The activities were of two types (a & b, c):

- a) Almost “conventional” work about Hydrogen and/or Deuterium overloading, although performed from a completely new point of view: effects of nano-structures and/or fractals on Hydrogen and Deuterium absorption at the surface and into Palladium lattice. The total papers presented, at National and International Conferences, were 5 (Ref. 1; 4; 5; 6; 7). Among them, 3 were Invited Papers, (Ref.1; 4; 7) and 2 Contributed Papers: all presented by Francesco Celani.
- b) Off line analysis of some previous experiments using light electrolytes, about Resistive Thermal Coefficients of H iper-loaded Pd wires ( $H/Pd > 0.95$ ). The measurement approach, in order to cross-check different methodologies, was based on taking advantage of specific cell used, not thermally stabilized: “natural” day-night cycles temperature variation of the environment, paper (Ref. 9) presented, as contributed at ICCF12, by Antonio Spallone.
- c) Efforts, in order to promote the “use” of some of most interesting results of Cold Fusion studies up to now obtained, i.e. the “transmutations” of natural (not radioactive) Strontium (Sr, main isotope  $^{88}\text{Sr}$ ) and  $^{133}\text{Cesium}$  (Cs) into others non radioactive elements (respectively,  $^{96}\text{Molybdenum}$  and  $^{143}\text{Praseodymium}$ ). We proposed to make specific experiments using radioactive ones (i.e.  $^{90}\text{Sr}$  and  $^{135}\text{Cs}$ ,  $^{137}\text{Cs}$ ): nuclear waste remediation.

The expected new elements, according to the experimental results of natural one, would be:



We recall that the radioactive isotopes of Sr and Cs are the most abundant (in total 62.2kg per year of operation of a PWR power plant, operated at 3410MWt, i.e. about 1GWe) and dangerous (because enter in the food chain) fission products coming out from nuclear power plants. Several meetings have been performed with Italian Government and Industry decision makers. Two Invited Papers were presented at International Conferences (Ref. 2; 8): the first was presented by Francesco Celani, the second by Akito Takahashi.

Moreover, during the “Pontignano International Workshop” (Ref. 3), a round table was organized on such specific topic. The opinions expressed were, obviously, quite different each

other and discussion take over 2 hours and 30 minutes. Some critics, expressed from strong opponents to such project, like the impossibility to recover radioactive Sr and Cs from the core of the reactor, were fully solved. I showed documents where are described innovative technical methods: developed, mainly, in Japan and recently, in USA. There exist one video-recording of the round table. Such very innovative experiment, if and when will be approved, will be performed in a joint collaboration between Japanese Companies-Universities and several Italian Companies, including INFN as Research Institution. The Italy-Japan project was named “Scorie Zero”; the dedicated laboratory will be build in Italy, not too far from Frascati.

## 2.1 The nano-structure approach

In the framework of Condensed Matter Nuclear Science, it has been recently shown, by Yoshiaki Arata, at Osaka University, that nano-structures of metallic Palladium, stabilized in a matrix of Zirconium oxide, can rapidly absorb surprisingly large amount of H<sub>2</sub> or D<sub>2</sub>.

According to Arata results and to the Akito Takahashi (Osaka University) theoretical model, atomic ratios (H, D)/Pd  $\gg$  1 can be easily accomplished at a pressure of only a few bars into Pd nano-particles, stabilized in a ZrO<sub>2</sub> matrix. In the Arata experiments, together with the abnormally high D/Pd ratios, a remarkable excess heat and production of 4He were detected. On the basis of such results (and new deeper interpretation of some of our previous experimental results that, although quite interesting from the point of view of experimental effects, didnt get at that time a satisfactory explanation), we are now convinced that most of the high loading ratios (H-D/Pd) and/or anomalous effects, both thermal and nuclear (by using D), obtained (generally in a not reproducible way) by the people involved in cold fusion experiments, can be reasonably attributed to the spontaneous and uncontrolled growing-up of fractal nano-structures on the Pd surface. In our opinion, even the Sr and Cs (both natural) transmutations obtained in the experiments carried out by the Yasuhiro Iwamura team at Mitsubishi Heavy Industries, Yokohama, Japan, which occur on the surface of the Pd/Pd-CaO/Pd multilayer, could be due to the formation of fractal-like structures produced during the multilayer fabrication process. In short, our experimental activity aimed at the production of nano-structures on Pd wires both by anodic oxidation (in situ) and air oxidation (in situ and ex situ). In situ means inside the electrolytic cell, without removing the Pd wire. In the gas experiments, the Pd wire is inside a tick SS chamber, pressurized up to 10bar with H or D gas, usually at room temperature. The “good” key point of new approach is that the substrate, where are located the active nano-particles, is the Pd wire itself, not other external (and not active) materials. The drawback is that the “active zone” is very limited: less then 1 over 1000 of the volume of the wire.

## 3 Experimental activity

### 3.1 Cells and electrolytes

The cell geometry and the experimental set-up, continuously up-graded, were reported in detail in our previous A.R., since 2000. Along the year 2005, about usual electrolytic experiments, we make 2 specific one in order to compare, and cross check, the results about new elements detected by Inductively Coupled Plasma-Mass Spectrometry (ICP-MS), using light and heavy electrolytes. The cell and experimental set-up were almost the same, as described in the reference given in previous AR. We just changed the composition of cell itself (from chemical glass to quartz) in the last experiment with D (b type), as detailed:

- a) Hydrogen loading: main solution 750cc (C<sub>2</sub>H<sub>5</sub>OH 95%, H<sub>2</sub>O 5%); Th(NO<sub>3</sub>)<sub>4</sub>=5cc (with 1cc=1mg of Th in D<sub>2</sub>O); Hg<sub>2</sub>SO<sub>4</sub> = 7cc (concentration 10<sup>-3</sup>M, in D<sub>2</sub>O) – Chemical glass (Schott Duran like, brand Fortuna) cell.

Table 1: Main new elements detected, in light alcohol-water (Scott Duran type) and heavy alcohol-water (quartz) cell. All the reagents  $\text{Th}(\text{NO}_3)_4$  (at 1mg/ml concentration) and  $\text{Hg}_2\text{SO}_4$  ( $10^{-3}\text{M}$ ) are in  $\text{D}_2\text{O}$ . BKG and reagents subtracted. 1 Count = about  $5E10$  Atoms. In bold characters are reported values of new elements, about Deuterium experiments, larger than a factor 10 in respect to Hydrogen one.

Element	H loading Exp. Counts	D loading Exp. Counts	Comments
P	0	6.4E6	BKG=4E3
$^{39}\text{K}$	0	1.8E7	BKG=1E6
Cu	2.3E6 63/65=2.20	2.7E6 63/65=2.11	Nat. 63/65 =2.25
Zn	6.2E6	4.9E7	
Rb	3.1E4	8.2E4	
$^{108}\text{Pd}$ (26.5%)	Normal	Depleted of 5%	
Ag	6.5E4	2.6E5	
$^{140}\text{Ce}$ (88.5%)	1.86E4	1.31E5	
W	1.16E4	4.42E4	
Tl	80	900	
Pb	4.5E5	1.38E7	
U	1.1E3	1.0E4	
$^{195}\text{Pt}$ (33.8%)	4.3E7	10.8E7	Marker Anode dissolution

- b) Deuterium loading: main solution:  $\text{C}_2\text{H}_5\text{OD}$ =1005cc,  $\text{D}_2\text{O}$ =89cc;  $\text{Th}(\text{NO}_3)_4$ =6cc (with 1cc=1mg of Th in  $\text{D}_2\text{O}$ );  $\text{Hg}_2\text{SO}_4$ =8cc (concentration  $10^{-3}\text{M}$ , in  $\text{H}_2\text{O}$ );  $\text{NH}_4\text{OD}$  (0.16M, in  $\text{D}_2\text{O}$ )=6cc. - Ultra pure quartz cell.

### 3.1.1 ICP-MS results

In consideration of the fact that all our previous electrolytic loading experiments in both a) and b) electrolytes, included anodic de-loading cycles and anodic oxidation, we routinely examined electrolytes, wire and sediments in order to check whether some transmutations had occurred.

The results about main new elements, detected by a high resolution ICP-MS, are reported in Tab. 1 and were presented/discussed at JCF6 Meeting (Tokyo, April 2005), Pontignano Workshop (May 2005), SIF Conference (September 2005) and ICCF12 Conferences (November 2005, Yokohama, Japan).

### 3.2 Procedure for the anodic oxidations in situ

The Pd wires were H, D loaded up the maximum of R/Ro (H,D /Pd  $\simeq$  0.75) by a current density of 5-10 mA/cm<sup>2</sup>. The wires were then anodically de-loaded with a current density of 1-2 mA/cm<sup>2</sup> and when the de-loading reaches the point R/Ro 1.1 or less, the current is raised to 5-20 mA/cm<sup>2</sup> and kept for a few minutes until full deloading.

### 3.2.1 Electrolytic H loading after the anodic oxidation in alcohol solution

An example of very good result, using the combined effects of previous Pd anodic oxidation, proper electrolyte composition and effect of cathodic current is shown in Fig. 1: the loading rate is extremely high and after 300s the maximum of  $R/R_0$  is reached and surpassed. After that, the loading proceeds still at a surprisingly high rates up to values of  $R/R_0$  down to 1.2 (right hand side of the Baranowski curve), within  $\simeq 700$ s, and down to 1.15 within 1500s. It should be noticed that without the anodic oxidation the time for loading up to  $R/R_0 \simeq 1.6$ —1.5 (right hand side of the Baranowski curve) is measured by the tens hours.

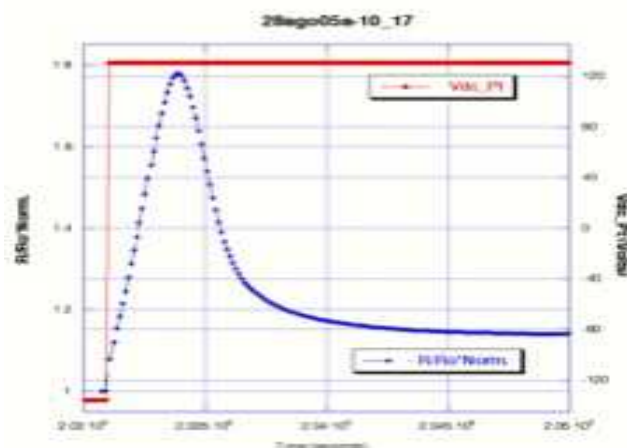


Figure 1:  $R/R_0$  ratio, versus time, using optimized anodic oxidation and electrolyte composition. The solution is quite insulating (main liquid is  $C_2H_5OH$ , few salt are dissolved): the cell Voltage is 135V even at only 30mA of electrolysis current.

These results indicate that a proper anodic oxidation produces a very active surface. On the basis of Arata experiments, such activity could be explained as due to the formation, just at the surface of the wire, of something similar to Arata's nano-particles.

- The, really impressive, experimental result shown in Fig.1 was reproducible.
- The reproducibility problem was one of the most weak- point in Cold Fusion experiments.
- One of reproducibility test was performed even under the eyes of INFN-LNF Director, Prof. Mario Calvetti, at the beginning of September 2005.

### 3.2.2 Electrolytic Deuterium loading after the anodic oxidation

Generally, the loading experiments carried out with electrolyte b-type showed lower loading rates and lower maximum (final) loading with respect to the ones with electrolyte a-type. Typically the maximum loading didn't exceed the one correspondent to  $R/R_0 \simeq 1.6$  (right hand side of the Baranowski curve). Anyway, deuterium based electrolyte some times showed anomalous effect like excess heat and "new" elements as detected by ICP-MS (routinely) and SEM micro-analysis. We think that such anomalies are the "experimental proof" of "cold fusion" related effects.

### 3.3 Air oxidation of Pd and coating

As we have shown, in our electrolytic loading experiments, we observed the phenomenon of spontaneous deuterium loading, i.e. without the application of any electrolytic current (self-loading). After several years of observations and specific tests we realized that large self-loading occurred only at the end of certain anodic cycles, in specific electrolytes. In particular, we found that the self-loading effect obtained with water electrolytes was almost negligible ( $R/R_o \approx 1.1$ ), while with hydro-alcoholic electrolytes, both a) and b) types, the effect was higher. By optimizing the anodic cycle it was possible to reach self-loadings up to  $R/R_o = 1.75$  (left hand side of the Baranowski curve) with  $H_2$  and  $R/R_o = 1.95$  (left hand side of the Baranowski curve) with  $D_2$ . SEM microphotography of the Pd wires, which presented strong self-loading effects, show the presence of thin porous structures on the surface of the wire. It was also observed that during the anodic cycles in hydro-alcoholic electrolytes a significant diffused pitting corrosion occurs both of Pd and Pt electrodes. ICPMS revealed a consistent presence of Pt in the electrolyte, in the sediments and on the Pd surface. These facts suggested that in such electrolytes the anodic cycles produced strong oxidations of the Pd (useful) and Pt (deleterious, see discussion about overvoltage in our previous A.R.) wires. These considerations led us to try a high temperature air oxidation of Pd wires as an alternative and more practical mean for obtaining active palladium surfaces. Since the first trials we found out that this simple procedure is scarcely effective. As a matter of fact it produced slight and unstable self-loadings and only for once. We considered that during the anodic cycles, in addition to anions, negatively charged particles are electrophoretically deposited on the Pd electrode and that this effect is enhanced in an alcoholic environment, so we thought that for a significant self-loading to occur, the presence of an impurity layer, intimately adherent to the oxidized surface, might be a necessary condition. So we resorted to artificially apply such impurities to the oxidized Pd wire in the form of colloidal silica.

#### 3.3.1 Procedure for the preparation of the samples, *ex situ*

A thin ( $50\mu\text{m}$  diameter) and long (60cm) Pd wire was Joule heated in air ( $\cong 600\text{mA}$  for 60 seconds) at about  $700^\circ\text{C}$  in order to get a thin layer of PdO. After such a heat-treatment the wire was immersed into a diluted solution of colloidal silica, and then heated  $\rightarrow$  cooled  $\rightarrow$  heated  $\rightarrow$  cooled again several times. We recall that a virgin Pd wires (no treatment) exposed to  $D_2$  gas at 1atm pressure and ambient temperature, usually reach a maximum loading, corresponding to an electric resistance ratio  $R/R_o \approx 1.8$ , in over 2 days. The wires, treated according to the reported procedure, exposed to Hydrogen or Deuterium in the same condition, instead, showed extremely high loading rates. In fig. 2 is shown the case of a wire exhibiting an astonishingly high loading rate: the electric resistance ratio ( $R/R_o$ ) of the wire exposed to a 1atm  $D_2$  gas, at  $24^\circ\text{C}$ , reached the value of 1.90 in about 100 seconds.

## 4 Conclusions

According to us, almost all of positive experimental results (excess heat, transmutation, particle emissions) in Cold Fusion experiments (Fleischmann, Takahashi, Arata, Iwamura, Mizuno, Celani, Mc. Kubre, Swartz, Storms, Preparata-De Ninno-Del Giudice, Miley, Violante.) can be RATIONALISED as the effect of nano-structures at Pd surface. It is very difficult to produce such nano-structures (almost all, except Arata, Iwamura, Celani) obtained just by change. Moreover, such nano-structures are not stable over time. We begin to develop a SIMPLE procedure to obtain nano-structures, both by electrolysis (routinely produced also during the usual cathodic regime: specific electronic circuitry and procedure developed from our Group since 2004, patenting) and by addition of colloidal silica on oxidised Pd surface (since March 2005, gas loading). In some aspects,

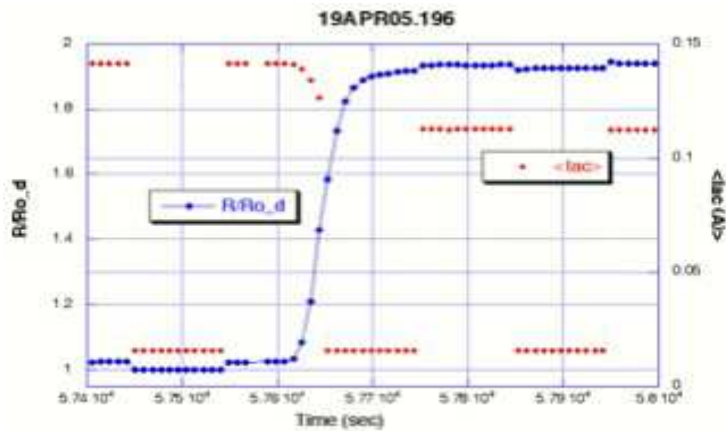


Figure 2: Loading ratio, versus time, of a Pd wire treated by oxidation and silica. D gas loading (1bar).

the latter method is similar to Yoshiaki Arata procedure that was the Pioneer about nano-particles production for Cold Fusion studies. The kind of colloidal silica (5-10nm dimension, low Na content), that up to now give the best results, was specially developed (after 5 years of efforts), by an Italian chemical company, according to our request. We think that the nano-structure interpretation of anomalous effect in deuterated metals will bring soon to some technological device: boiler using liquid electrolyte, even some turbine engine using pressurised high temperature gas loading method. More systematic work is necessary in order to elucidated all the possibilities that come because nano-size materials. BTW, as shortly shown also during ICCF12, we get indications that some anomalous heat seems coming out from a new pressurised cell (SS) using even the Hydrogen gas.

## 5 References

1. Francesco Celani, A. Spallone, P. Marini, V. Di Stefano, M. Nakamura, E. Todarello, A. Mancini, P.G. Sona, E. Righi, G. Trenta, C. Catena, G. D' Agostaro, P. Quercia, V. Andreassi, F. Fontana, L. Gamberale, D. Garbelli, F. Falcioni, M. Marchesini, E. Novaro, U. Mastromatteo, "Further studies, about new elements production, by electrolysis of cathodic Pd thin-long wires, in alcohol-water solutions (H, D) and Th-Hg salts. New procedures to produce Pd nano-structures", invited paper at: The 6th Meeting of Japan CF Research Society, April 27-28, 2005. Tokyo Institute of Technology, Japan. Hiroshi Yamada Ed., Vol.6, pgg. 1-10, 2005. [http:// wwwcf.elc.iwate-u.ac.jp/jcf/](http://wwwcf.elc.iwate-u.ac.jp/jcf/)
2. Francesco Celani. "Italy-Japan Project on Sr and Cs nuclear waste recovery", invited paper at "6th International Workshop on Anomalies in Hydrogen/Deuterium loaded Metals", Certosa di Pontignano, May 13-16, 2005, Italy. <http://www.iscmns.org/meetings>
3. F. Celani and 15 speakers. "Prospects of Radio-Active waste remediation", Round Table at: "6th International Workshop on Anomalies in Hydrogen/Deuterium loaded Metals", Certosa di Pontignano, May 13-16, 2005, Italy. Video-recorded. <http://www.iscmns.org/meetings>
4. F. Celani and same authors of Ref. 1, "Nano-structures at Pd surface: a key condition for anomalous effects in deuterated metals? Results, at INFN-LNF, on electrolytic and

- gas experiments”, invited paper at : 6th International Workshop on Anomalies in Hydrogen/Deuterium loaded Metals”, Certosa di Pontignano, May 13-16, 2005, Italy.  
<http://www.iscmns.org/meetings>
5. F.Celani and same authors of Ref. 1, except C. Catena, “Risultati comparativi di evidenziazione di nuovi elementi, tramite ICP-MS, in celle elettrolitiche idrogenate o deuterate con catodi di palladio filiforme”, Contributed Paper at: XCI Congresso Nazionale Società Italiana di Fisica - Catania, 26 Settembre-1 Ottobre 2005, Italy. <http://www.sif.it>
  6. F.Celani and same authors of Ref. 5, with the addition of O. Giacinti, “Possibile effetto delle nanostrutture superficiali sulla ipercarica di idrogeno o deuterio nel palladio e fenomeni anomali correlati”, Contributed Paper at: XCI Congresso Nazionale Società Italiana di Fisica - Catania, 26 Settembre-1 Ottobre 2005, Italy. <http://www.sif.it>
  7. F. Celani and same authors of Ref. 6, with the addition of E. Purchi, “New procedures to make active, fractal like, surfaces on thin Pd wires”, invited paper at ICCF12, November 27- December 2, 2005, Yokohama (Japan). Publ. by World Scientific.  
<http://www.iscmns.org/ICCF12/>
  8. Akito Takahashi, Francesco Celani, Yasuhiro Iwamura. “The Italy-Japan Project: fundamental research on cold transmutation process for treatment of nuclear wastes”, invited paper at ICCF12, November 27- December 2, 2005, Yokohama (Japan). Publ. by World Scientific.  
<http://www.iscmns.org/ICCF12/>
  9. Antonio Spallone, F. Celani, V. Andreassi, P. Marini, V. di Stefano. “Measurements of resistance temperature coefficient at H/Pd overloadings”, contributed paper at ICCF12, November 27- December 2, 2005, Yokohama (Japan). Publ. by World Scientific.  
<http://www.iscmns.org/ICCF12/>
  10. F. Celani and same authors of Ref. 1. “Thermal and isotopic anomalies when Pd cathodes are electrolyzed in electrolytes containing Th-Hg salts dissolved at micromolar concentration in C2H5OD/D2O mixtures”, paper of ICCF10, (Cambridge-MIT, USA), (2005), pp. 379-398. Peter Hagelstein and Scott Chubb eds. World Scientific. ISBN 981-256-564-7 C.

## FREETHAI-DEUTER

F. Celani, A. Marcelli, G. Onori, E. Righi (Resp. Naz.), G. Trenta (Ass.)

### 1 Experiment purpose and troubles

DEUTER project concerns are physical, chemical and biophysical researches on the irradiated heavy water to understand its effects on living matter aiming at a possible application in cancer therapy. In the last period of the various operational research phases of our group (DOSIME, INTRABIO, DEUTER), we need to face a noteworthy organization troubles mainly due to lack of personnel because of a breaking off of a work contract (INFN contract, Drs. Debora Pomponi) and a fully unexpected retirement (Dr. Carlo Catena, ENEA-Casaccia). So, some efforts were addressed to the reconstitution of the FREETHAI-DEUTER group.

### 2 2005 Results

Our up-to-date results met with the agreement and the interest of qualified ambits (see “Fisica in Medicina” scientific official review of the “Italian Medical Physic Association” AIFM).

**I** – Professor R. D’Amelio, full professor of Clinic Allergology and Immunology at the 2nd Medical and Surgery Faculty of the “La Sapienza” University stated agreement on his participation to the FREETHAI-DEUTER project. To confirm his interest, Professor D’Amelio presented the report: “Sistema Immunitario - Risposta alle basse dosi” attending at the 19th “Corso Avanzato di Radioprotezione Medica” organized by the Padua University and sponsored by INFN and AIRM in Bressanone (Aug. 29-Sept. 2, 2005). The Prof. D’Amelio and Prof. Giuseppe Luzi (chair associated) agreed on the following research topic:

*“Study of the immune parameters in the presence of ROS at low concentration of irradiated D<sub>2</sub>O: comparison with the effects due to the low dose irradiation”.*

**II** – Scientific collaboration agreements are settled with the following Institutions that operate at the research project named: MARINER (Marcatori di Rischio negli Esposti a Radiazioni ionizzanti: verifica di eventuali differenze nella risposta alle radiazioni ionizzanti in base a profili citogenetici e di espressione genica):

- i) “Istituto Nazionale per la Ricerca sul Cancro”, Genoa, Environmental Carcinogenesis,  
Responsible: Dr. Claudia Bolognesi.
- ii) ARPA Emilia-Romagna, Excellence Environmental Carcinogenesis,  
Responsible: Dr. Annamaria Colacci.

The following two topics were proposed to be inserted in the agreement:

- a) to realize a reference national Laboratory of cytogenetic Dosimetry at the National Research on Cancer Institute of Genoa (Dr. C. Bolognesi); this can be done utilizing the experience ripened at LNF in the context of the agreement INFN-ENEA research Protocol on “Nuove metodologie di Dosimetria biologica applicabile alla Protezione della salute dell’uomo” signed on Nov. 4th 1994 by the Presidents of the two Institutions (for the INFN: Prof. L. Maiani). It could be useful to mention that the biodosimetric competence was an important point for

INFN (Frascati Centre) to be acknowledged as Istituto autorizzato for the ionizing radiation protection medical surveillance at national level (D.M. 27.4, 1995 - Gazzetta Ufficiale del 27.7.1995 -Serie Generale n. 174).

b) Citotoxic effect of irradiated D<sub>2</sub>O on oncological cells.

**III** – It was also got the formal consent of the Dr. Gianfranco Giubileo Responsible of the Photoacoustic Laser Spectroscopy Laboratory (ENEA - Frascati) for the research on deuterated ROS (Study on the irradiated D<sub>2</sub>O and its effects on normal and tumor cells).

**IV** – Meanwhile, the collaboration with the research group led by the Prof. Giuseppe Onori of Perugia University is carried on to set-up a spectrophotometric system able to detect the expected concentration of oxidative compounds at about 10-20 $\mu$ M level as it could be found in a  $\gamma$ -irradiated sample. To this aim it was selected horse heart cytochrome c (cyt c), a metalloprotein involved in electron transfer in the mitochondrial respiratory chain. The electron transfer properties of cyt c have been extensively studied using a large number of different low molecular mass substances, such as ascorbic acid, dithionite, hydrogen peroxide and hydroquinones. Some of these compounds give rise to the formation of high reactive free radicals, which can change the oxidation state of the iron of cyt c. The reduced cyt c is characterized by an absorption peak at 550nm which decreases when the oxidation of the iron of the protein takes place. In a first series of experiments we have studied the effect of the oxidizing agent H<sub>2</sub>O<sub>2</sub> and of the reducing one dithionite on cyt c, following the changes in the cyt c absorption band between 400 and 600 nm. These preliminary results clearly show that the depicted system is suitable for our purpose. Namely the system on the one hand allows to estimate oxidizing or reducing agents concentration in water up to an extent of 1 $\mu$ M and to the other show a biological effect on a bio-molecule. We now are studying, with the same approach, the effect of irradiated water on cyt c and, in particular, the redox process between this protein and the free radical produced in irradiated D<sub>2</sub>O and H<sub>2</sub>O. We hope that the quantitative evaluation of the oxidizing or reducing agents in irradiated H<sub>2</sub>O and D<sub>2</sub>O joined to the correlation of the observed biological effects, will be able to allow the better understanding of the responsible mechanism causing the cytotoxic effects of the irradiated water and to clear the differences between the effects due to H<sub>2</sub>O and D<sub>2</sub>O.

### 3 Publications and Conferences

1. Righi E. – “Radiopatologia. Danni stocastici” – Master di 2° livello in “Difesa da Armi Nucleari, Radiologiche, Chimiche e Biologiche” –II Facoltà di Medicina e Chirurgia, Università degli Studi di Roma ‘La Sapienza’, Osp. S. Andrea – febbraio e giugno 2005.
2. Righi E. – “Radiopatologia stocastica. Il Sistema emopoietico” – 1° Corso di formazione e aggiornamento in Radioprotezione medica, AIRM, Roma - marzo 2005.
3. Righi E. – “Interventi nella irradiazione esterna” – Corso di formazione per medici della Polizia di Stato, Istituto Superiore di Polizia, Roma 19 aprile 2005.
4. Righi E. – “La previsione di radiopatologia stocastica a seguito di evento accidentale” – Giornata di studio su nuove emergenze radiologiche, ENEA Frascati, 22 aprile 2005.
5. Righi E. – “Stima degli effetti tardivi a seguito di eventi incidentali” – Corso di formazione e perfezionamento in Radioprotezione Università degli Studi di Napoli “Federico II”, 9 maggio 2005.
6. Righi E. – “Significato e limiti dell’ipotesi lineare senza soglia” – 19° Congresso nazionale AIRM, Mattinata (FG), 7-10 giugno 2005.

7. Righi E. – “Lo sminamento umanitario: Opera di Pace, Sfida tecnologica” – Corso di Formazione “Mine Action: Aspetti multidisciplinari dello Sminamento Umanitario”, CABLIT Operatori di Pace Nazioni Unite, Roma – Palazzo Barberini, 17-18 giugno 2005.
8. Righi E. – “Radiopatologia stocastica: le evidenze contraddittorie del modello LNT” – 19° Corso Avanzato di Radioprotezione Medica, Università degli Studi di Padova con Patrocinio INFN e AIRM, 29 agosto – 2 settembre 2005.
9. Righi E. – “Effetti sull’ uomo e rischi per la salute” – Corso di formazione per gli Addetti alla Vigilanza sulla Radioprotezione, Azienda USL Roma H Albano Laziale (RM), 29-30 settembre e 16-17 novembre 2005.
10. Catena C., Pomponi D., Trenta G., Celani F., Marini P., De Rossi G., Righi E. – “Acqua pesante D<sub>2</sub>O irradiata: dal reattore nucleare alla cellula” – Fisica in Medicina, Vol. 4 (2005), pp. 365-379.
11. Trenta G. – Serie di lezioni su: “Contaminazione ambientale”, “Le armi atomiche”, “Scenari incidentali”, “Contaminazione umana”, “Fisiopatologia dellirradiato”, “Scenari nucleari”, “L’incidente di Chernobyl” Master di 2° livello in “Difesa da Armi Nucleari, Radiologiche, Chimiche e Biologiche” II Facoltà di Medicina e Chirurgia, Università degli Studi di Roma “La Sapienza” Osp. S. Andrea febbraio e giugno 2005.
12. Trenta G. – Serie di lezioni su: – “Principi generali di Radioprotezione”, “Valutazione della Probabilità causale”, “Incidenti nucleari ed altre emergenze”, “Gestione degli interventi sanitari in caso di evenienze accidentali”, “Diagnosi e denuncia di malattie professionali”, “Sorveglianza medica: il polmone” – 1° Corso di formazione e aggiornamento in Radioprotezione medica, AIRM, Roma - marzo 2005.
13. Trenta G. – “La contaminazione ambientale ed umana” – Corso di formazione per medici della Polizia di Stato, Istituto Superiore di Polizia, Roma 19 aprile 2005.
14. Trenta G. – “Scenari possibili” – Giornata di studio su: “Nuove emergenze radiologiche”, ENEA Frascati. 22 aprile 2005.
15. Trenta G. – “IR e NIR: grandezze ed unità di misura” – Corso di formazione e perfezionamento in Radioprotezione Università degli Studi di Napoli “Federico II”, 9 maggio 2005.
16. Trenta G. – “L’ accertamento del nesso causale nelle malattie professionali da raggi” – 19° Congresso nazionale AIRM, Mattinata (FG), 7-10 giugno 2005.
17. Trenta G. – “Medical surveillance” – Scuola Europea di Studi Avanzati in “Tecnologie nucleari e delle Radiazioni Ionizzanti”, Università degli Studi di Pavia, 30 giugno 2005.
18. Trenta G. – “Aspetti medici” in Corso di formazione su Radioattività naturale: Radon, Rischi per la popolazione e per i lavoratori, Servizio Sanitario Regionale Emilia-Romagna - AUSL-Modena, 2 marzo e 29 novembre 2005.
19. Trenta G. – “La Sorveglianza sanitaria nelle esposizioni occupazionali ai CEM alla luce della nuova Direttiva” – Giornata di studio: – “La nuova Direttiva Europea 2004/40/CE sulla protezione dei lavoratori dalle esposizioni ai campi elettromagnetici” – ISS, ISPESL, AIRP, 1 aprile 2005.
20. Trenta G. – “Energia nucleare e salute” – I costi delle scelte disinformate: il paradosso dell’energia nucleare in Italia - 2° Convegno nazionale dell’Associazione Galileo 2001 per la libertà e la dignità della scienza, CNR Roma 9 marzo 2005.
21. Trenta G. – Serie di relazioni su: “ICRP 2005 Draft”, “Linee guida AIRM per la sorveglianza medica dei lavoratori esposti alle radiazioni ionizzanti”, “Improvised nuclear device (IND)

- e terrorismo” – 19° Corso Avanzato di Radioprotezione Medica, Università degli Studi di Padova con Patrocinio INFN e AIRM, 29 agosto – 2 settembre 2005.
22. Trenta G. – “Radiazioni ionizzanti e non ionizzanti: definizione, misurazione, grandezze ed unità di misura” – Corso di formazione per gli Addetti alla Vigilanza sulla Radioprotezione, Azienda USL Roma H Albano Laziale (RM), 29-30 settembre e 16-17 novembre 2005.
  23. Sgrilli E., Trenta G. – “Proposta ICRP 2005 di nuove Raccomandazioni di Radioprotezione” – Fisica in Medicina, Vol. 4 (2005), pp. 305-313.

## MARIMBO

G. Celentano (Ass.), A. Della Corte (Ass.), U. Gambardella (Resp.)

### 1 Purposes of the project

The *MARIMBO* experiment has been generated by the *Ma-Bo* three years program ended last year. *Ma-Bo* was devoted to study potential applications of magnesium diboride  $\text{MgB}_2$  which becomes superconducting at temperatures below 39 K. Thus its potentiality either in wire applications (magnets) or in thin films applications (RF applications or electronics) were considered. As the tape technology has been developed relatively fast, making available 400 m long pieces of  $\text{MgB}_2$  tapes with good transport properties, we proposed to build a demonstrating application of  $\text{MgB}_2$  tapes. The *MARIMBO* experiment in fact concerns the fabrication of a small racetrack coil designed and tested by INFN and realized by Ansaldo Superconduttori SpA. Three INFN sections are involved: Genova (group leader), Milano, and LNF, in collaboration with Ansaldo Superconduttori SpA, Genova.

### 2 The Frascati group activity

The Frascati group, made of LNF and ENEA Frascati researchers, takes care of  $\text{MgB}_2$  tape characterization, analyzing the  $\text{MgB}_2$  superconducting properties by means of current transport as a function of the temperature and the applied magnetic field. The experiments were performed in a gas flow cryostat to study a wide temperature range. Two different kind of wires have been considered for the final model: a multifilamentary copper stabilized tape produced by Columbus Superconductor (Genova) and a multifilamentary copper stabilized round wire produced by Hyper Tech Inc. (Columbus, OH).

#### 2.1 Results of Hyper Tech wires

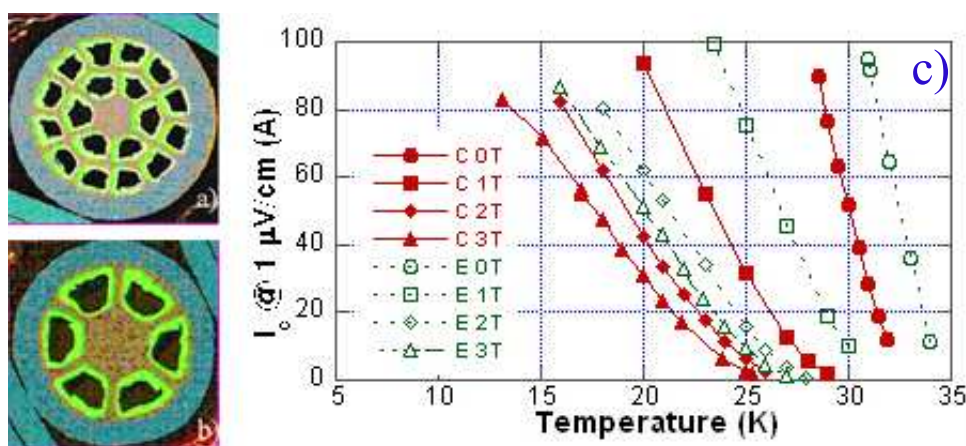


Figure 1: Cross section of the Hypertech wires: # 632 (a), # 684 (b). Critical current measured in two differently reacted # 632 wires (c)

Two kind of wires have been analyzed, # 632 and # 684, shown in figs.1a) and b) respectively. They differ in the number of filaments and their sizes, whilst they keep the same technology: copper stabilized and Nb barrier around the MgB<sub>2</sub> filaments in a monel jacket, with a diameter of 0.84 mm. These wires follow the wind & react technology, thus an heat treatment (700 °C for 15÷20 min) must be performed to grow the superconducting phase, and after that the wire became rigid. Further to test samples reacted by the manufacturer, we also performed reactions and tests on unreacted wires (limited to # 632 only). In 1c) the critical current measurements (corresponding to an electric field of 1 μV/cm) as a function of the temperature, under different applied magnetic field values are shown, concerning two differently reacted wires. The different annealing processes produced different wire performances. However the critical current at 20 K and 1 T may overcome 140 A, useful for low field applications of this wire.

## 2.2 Results of Columbus tapes

The shape of this conductor is a tape, 3.6 mm wide and 0.65 mm thick, manufactured with the PIT (Powder In Tube) method. Also in this case there is copper inside, included in an iron barrier, and finally the MgB<sub>2</sub> filaments are compressed in a Ni matrix. In fig.2 a) it is shown the cross section view of the tape <sup>1)</sup>, where the superconducting fraction is less than 10% of the whole section.

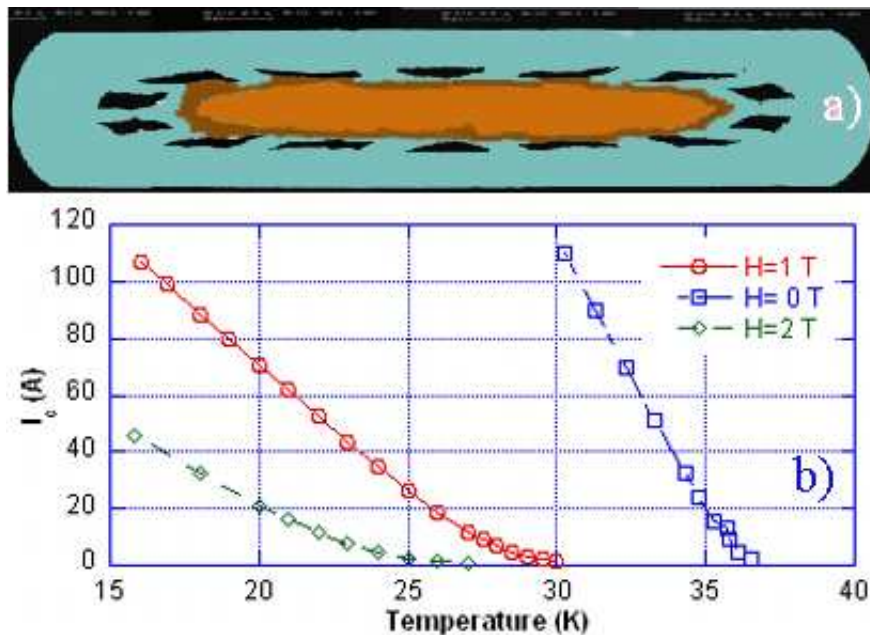


Figure 2: Cross section of the Columbus tape a); critical current behavior of a bended tape as a function of temperature under three values of applied magnetic field b)

In fig.2 b) it is shown the behavior of the critical current as a function of the temperature under different applied magnetic field values. These measures are referred to a bended tape, 25 mm bending radius, performed to ascertain the tape features when used for small windings. The critical current at 1 T and 20 K is 70 A, to be compared to 170 A we have measured for a straight tape in the same conditions, and to 180 A indicated by the tape manufacturer for this kind of straight tape. We deduced that there is no possibility to design any winding having a bending

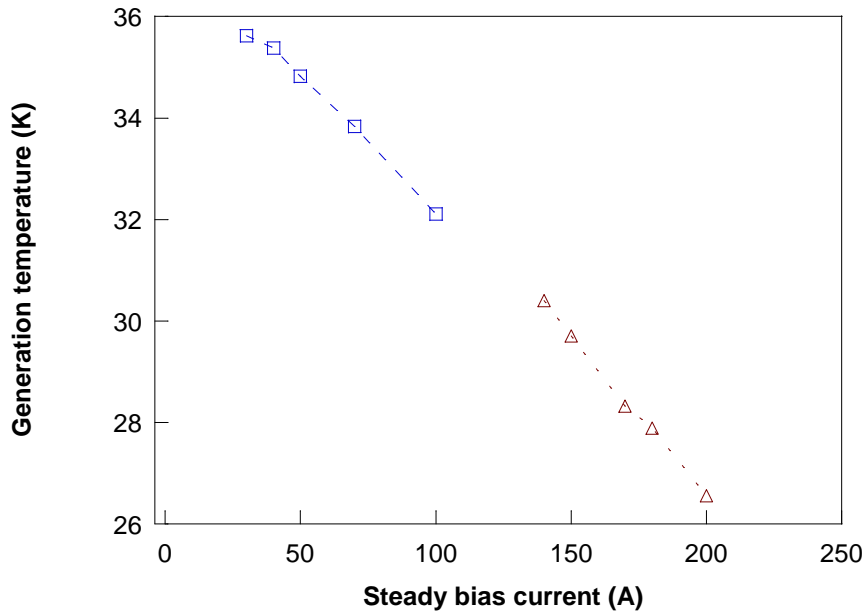


Figure 3: *Measurement of the critical temperature for different bias values of the straight tape*

radius smaller than 60 mm to keep the reasonable operating current. However measurements on short straight tapes, cut from long length production, confirmed the quality assured by the manufacturer, i.e. a critical current at 30 K in self field  $\geq 210$  A. As this kind of conductor is being used for the racetrack winding, basic experiments concerning the stability have also been carried out. Namely we measured the critical temperature when the sample is biased at high current in self field. This corresponds to the maximum operating temperatures which keep the dissipative state below the critical levels generating a quench. In fig.3 these temperatures are reported in our cooling conditions. Further measures will also be carried out as a function of the bias current under different magnetic field values.

## References

1. Thanks to A. Rufoloni, ENEA Frascati, for SEM and microanalysis.

## MINCE

Balasubramanian C. (Bors. PD), S. Bellucci (Resp. Naz.), P. Borin (Perfez.),  
M. Bottini (Ass. Ric.), G. Giannini (Ass. Ric.), A. Marcelli,  
F. Micciulla (Laur.), A. Raco (Tech.), M. Regi (Ass. Ric.).

### 1 External collaborating Institutions:

Univ. Roma La Sapienza (School of aerospace engineering), Univ. Modena, Univ. Roma Tor Vergata-Policlinico Tor Vergata, IHEP-Protvino (Russia), VARIAN (Torino), CSM (Pomezia), HITESYS (Aprilia), Univ. Pune (India), Burnham Institute (La Jolla, CA, USA), Lviv Univ (Ukraine), ILL (Grenoble, France), Univ. Riga (Latvia).

### 2 Introduction

The formation of carbon nanotubes could be traced back to the discovery of the fullerene structure  $C_{60}$  (buckyball) in 1985 by means of Richard Smalley and Harold Kroto. The structure of the buckyball comprises 60 carbon atoms arranged by 20 hexagonal and 12 pentagonal faces to form a sphere. When the buckyball is elongated to form a long and narrow tube with a diameter of approximately 1 nm (10Å), then there are the basic form of a carbon nanotube. The carbon nanotubes casually have been discovered in 1991 from Sumio Iijima. The basic element is the graphite, which is constituted by a series of plane one about the other, and these plans are tied up among them through the Van der Walls strengths. Each plane have a bidimensional covalent structure. Through a series of processes, folding up these planes of graphite, it is possible to create a tubular seamless structure that does not exist in nature. This structure takes the name of carbon nanotube.

Essentially two families of carbon nanotubes exist:

- SWNT or *single wall nanotubes*, that are constituted by only one rectilinear tubular unity;
- MWNT or *multi wall nanotubes*, that are constituted by a series of SWNT among them coaxial and distant about 0.34 nm (same distance among the various planes of the graphite).

Carbon nanotubes can be inert and can have a high aspect ratio, high tensile strength, low mass density, high heat conductivity, large surface area, and versatile electronic behaviour including high electron conductivity. While these are the main characteristics of the properties for individual nanotubes, a large number of them can form secondary structures such as ropes, fibers, papers, thin films with aligned tubes, etc., with their own specific properties. The combination of these properties makes them ideal candidates for a large number of applications provided their cost is sufficiently low. The cost of carbon nanotubes depends strongly on both the quality and the production process. Naturally, another key factor for applications, is the toxicity of carbon nanotubes, as well as nanotube-based composite materials, which are being carefully investigated by our collaboration. Owing to their exceptional morphological characteristics, electric, thermal and mechanics, carbon nanotubes yield a material particularly promising as reinforcement in the composite materials with metallic matrixes, ceramics and polymeric. The key question includes the good dispersion of the nanotubes, the control of the bond between nanotubes and matrix, the density of the mass of the composite and the thin films and the possibility of alignment of the nanotubes. Besides, the type of nanotubes (SWNT, c-MWNT, h-MWNT, etc) and their origin (arc discharge, laser, CCVD, etc) are important variables since they determine the perfection of the structure and the reactivity of the surface.

### 3 Carbon Nanotubes

Carbon nanotubes were synthesized by us in a DC arc plasma system in helium atmosphere at a pressure of 600 torr. The arc was struck between one high purity graphite rod and a block of graphite serving as electrodes. The discharge is typically carried out at a voltage of 20 V and a current in the range of 80/100 A. Some amount of the evaporated carbon condenses on the tip of the cathode, forming a slag-like hard deposit. The deposit consists essentially in a fused tip which has inside bundles of carbon nanotubes mixed with amorphous.

After this, we made characterization analysis by means of SEM, TEM and AFM. We carried out a comparison with the characterizations of earlier samples we produced in the period 2002-2004.

### 4 Nanotubes Composites

Carbon nanotubes are being widely studied for various applications ranging from medical to electronics and also optical devices. We did recent studies of biosensor composites based on functionalized nanotubes and nanoparticles. They are also being studied for the suitability and applications in aerospace and aeronautical field. A useful application in aerospace that we are studying is the improvement of electrical properties of composites made from carbon nanotubes and epoxy resin.

The epoxy resin that we use is a Shell commercial product named Epon828. It is a classical epoxy resin liquid at room temperature. For the application we wanted study we use two mixtures of resin-curing agent. Two mixtures of resin-curing agent have been prepared

- the first sample contains 50 g of resin and 13 g of *A1* curing agent;
- the second sample contains 22 g of resin and 6 g *PAP8* curing agent.

In both samples we put the 20 wt% of graphite. We mix with a glass stick by hands. In this process we take care that air is not present in the mixture.

These two mixtures have been spread, like thin films, on a circuit samples and we have made electrical resistance tests.

Analyzing the test data it is possible to observe that, for the first sample, when we work in different pressure conditions, the resistance changes very little. Instead in the second sample, the resistance undergoes remarkable variations when we work in different pressure and humidity conditions. We can deduce that the *PAP8* curing agent is very sensitive to the humidity variations over a long time period and cannot optimize the performance of the circuits. Instead the *A1* curing agent is not very sensitive to these variations and makes the behavior of the circuit stable.

Preliminary results of these studies present interesting features which are useful in choosing the ideal composition and ratio of the composite material for use in shielding of electrical circuits of space vehicles from radiations of the outer space. A future development of this work will be the use of the same samples of resin and curing agent inserting carbon nanotubes powders instead of graphite and the study of the behaviour of the circuits in the same conditions.

### 5 Field emission

Field emission is a quantum tunneling effect based on the passage of electrons through a barrier with a high electric field. The advantage, in comparison with thermionic emission, yielded by field emission is that no heat is required, in order to extract the electrons. There is a strong influence both of the properties of the material and the shape of the cold cathode on the field emission itself. Since cathodes having a high aspect ratio yield high field emission currents, carbon nanotubes are ideal candidates to replace thermionic emitters, providing several potential advantages, including a higher efficiency, emitted electrons having less scatter, smaller values of the turn-on time.

Moreover, carbon nanotubes allow to improve the robustness and compactness of the emitting devices.

## 6 Main experimental activities

We continued the study of the stability of the emitted current, which is a very important constraint for the proposed applications. We also repeated the measurements of the emitted current for samples obtained using different synthesis conditions. We started sample purification procedures using thermal oxidation, in order to eliminate unwanted forms of carbon. Fourier Transform Infra Red (FTIR) characterization of the nano-AlN samples produced in collaboration with the Univ. of Pune were performed for both mid-IR (600 - 4000  $\text{cm}^{-1}$ ) as well as far-IR (200 - 600  $\text{cm}^{-1}$ ), in collaboration with the LNF Dafne Luce laboratory. In collaboration with the Aerospace Engineering School at the Univ. Rome La Sapienza and the industrial Center for the development of materials (CSM), we carried out structural characterizations of composite materials containing carbon nanotubes, for aerospace applications. In collaboration with the Univ. of Roma Tor Vergata, the Policlinico of Tor Vergata and the Burnham Institute, we characterized carbon nanotube-silica nanobead composite structures for biomedical applications. We also studied the toxicity of nanotubes, in collaboration with the INFN Servizio Medicina del Lavoro.

## 7 List of Conference Talks by LNF Authors in Year 2004

1. S. Bellucci, "Nanoparticles, nanotubes and semiconducting nanostructures: current views and future perspectives", Meeting on Nanostructures vs. Nanotechnology, Univ. Napoli (Italy), 10 March 2005.  
  
S. Bellucci, "Composite materials based on carbon nanotubes for aerospace applications", EUPOC05 european conference, Gargnano (BS, Italy), 2 June 2005.  
  
S. Bellucci, "Neutron characterization of aluminum nitride nanotubes", 1st Int. Conference on neutron Brillouin scattering, Perugia (Italy), 14 June 2005.  
  
S. Bellucci, "Bending of 480 MeV positron beam by deformed crystal", International workshop on Relativistic Channeling and Coherent Phenomena in Strong Fields, Frascati I(Italy), 25 July 2005.  
  
S. Bellucci, "Biomedical Applications of Nanoparticles and Nanotubes", Bressanone (TN, Italy), 1 September 2005.  
  
S. Bellucci, "Carbon Nanotubes-Silica Nanoparticles Composites for Biomedical Applications", Bioforum and Nanoforum, Politecnico Milano (Italy), 29 September 2005.  
  
S. Bellucci, "Applications of Nanoparticles and Nanotubes", Physics Department General Colloquium, Univ. Perugia (Italy), 12 October 2005.  
  
S. Bellucci, "Biomedical Applications of Carbon Nanotubes and the Related Cellular Toxicity", NanoRoadMap Workshop, Univ. Padova (Italy), 10 November 2005.  
  
M. Bottini, "Carbon nanotubes cytotoxicity", School and Workshop on Nanoscience and Nanotechnology, Monteporzio Catone (RM, Italy), 16 November 2005.

S. Bellucci, "Composite nanomaterials as platforms for medical and biotechnological applications", School and Workshop on Nanoscience and Nanotechnology, Monteporzio Catone (RM, Italy), 16 November 2005.

S. Bellucci, "Nanotechnology for Aerospace, Electronics and Bio-medical Applications", MATIMOP Conference, Tel Aviv (Israel), 29 November 2005.

P. Borin, "Synthesis and characterization of carbon nanotubes based composite materials for aerospace applications", Meeting su Compositi e Nanotecnologie per l'Aerospazio, Frosinone (Italy), 7 December 2005.

## References

1. M. Bottini, *et al.*, Toxicology Letters (in press).
2. S. Bellucci, Nucl. Instr. Meth. **B234**, 57 (2005).
3. M. Bottini, *et al.*, Chem. Commun. **6**, 758 (2005).
4. M. Bottini, *et al.*, J. Phys. Chem. **B** (in press).
5. M. Bottini, *et al.*, Journal of Nanoscience and Nanotechnology (in press).
6. S. Bellucci, Phys. Stat. Sol. (c)**2**, 34 (2005).
7. S. Bellucci *et al.*, 3rd International Conference on Experimental Mechanics, Proc. of SPIE **Vol. 5852** (2005), p. 121.
8. S. Bellucci, 3rd International Conference on Experimental Mechanics, Proc. of SPIE **Vol. 5852** (2005), p. 276.
9. S. Bellucci, 9th Topical Seminar on Innovative Particle and Radiation Detectors, Nucl. Phys. **B** (Proc. Suppl., in press).
10. V.T. Baranov *et al.*, Pisma Zh. Eksp. Teor. Fiz. **82**, 638-641 (2005).
11. S. Bellucci, V.A. Maisheev, Nucl. Instrum. Meth. **B234**, 87-98 (2005).
12. A.G. Afonin, *et al.*, Nucl. Instrum. Meth. **B234**, 122-127 (2005).
13. V.M. Biryukov, S. Bellucci, Nucl. Instrum. Meth. **B230**, 619-623 (2005).
14. V.M. Biryukov, S. Bellucci, Nucl. Instrum. Meth. **B234**, 99-105 (2005).
15. V.M. Biryukov, S. Bellucci, V. Guidi, Nucl. Instrum. Meth. **B231**, 70-75 (2005).
16. S. Bellucci, Atti XVII Congresso AIV, Ed. Compositori (2005), p. 61.

## POLYX

G. Cappuccio (Res. Ass.), G. Cibin (Ass.), S. B. Dabagov (Art. 23), A. Esposito,  
V. Guglielmotti (Osp.), D. Hampai (Osp.), A. Marcelli, V. Sessa (Osp.),  
C. Veroli (Osp.), Y. Dudchik, M. A. Kumakhov.

### Participant Institutions:

Italy: INFN - LNF, INFN - Milano Bicocca.  
CNR - ISMN, Istituto Studio Materiali Nanostrutturati, Roma.  
CNR - IPCF, Istituto Processi Chimico Fisici, Pisa.  
UNIV. "Tor Vergata", Dip. Scienze e Tecnologie Chimiche, Roma.

Belorussia: Institute of Applied Physics Problems, Minsk.

Russia: P. N. Lebedev Physical Institute, Moscow.  
IRO - Institute for Roentgen Optics, Moscow.

Switzerland: Unisant S.A., Geneva.

## 1 Introduction

The POLYX project for research and development of polycapillary optics in X-ray applications is supported by the MIUR project: "Impianti innovativi multiscopo per la produzione di radiazione X ed ultravioletta" (Legge 449/97) and is in progress with the participation of the CNR-ISMN and INFN-LNF.

## 2 Activities in 2005

In the year 2005 the X-ray cabinet with all its accessories (X-ray source, HV power supply, detector, etc.) was authorized to work by the LNF Radiation Protection Group after some minor improvements to increase safety.

A set of polycapillary lenses supplied by IRO (Moscow) were tested on the optical bench using a first group of lens holders fixed at the center of a "gimbal" mount along the source-detector axis direction. As it is not possible to use any glue, a couple of "O-rings", pressed by setscrews, were used to fix each lens inside the holder. The alignment test performed with such configuration put into evidence a lacking reliability in the lens clamping. For such reason a new kind of lens holder was designed and made in collaboration with the Group Service SSCR of LNF (Fig. 1). The prototype was realized for a big semi-lens to be utilized in connection with an X-ray laser plasma source at the ILIL laboratory (CNR - IPCF, Pisa). The alignment test was successfully performed using the same procedure of the last year with remotely controlled linear actuators using an "ad hoc" software program. During the second part of the year, according to a proposal by T. Levato of Pisa Group, an experiment was done to evaluate the possibility of using a laser instead of an X-ray beam for polycapillary alignment, even if the visible radiation is not transmitted in the best way by a polycapillary lens which is not made by a set of optical fibers but by a bundle of hollow capillaries. The measurements proved that a preliminary alignment can be done using a diode laser while, the iterative procedure developed by our group, using an X-ray source and a scintillation detector, allows to improve the alignment providing also an evaluation of the optical gain, i.e. the radiation density value at the point where the X radiation is focalized (Fig. 2).

In September 2005 our group participate in the organization of the International Conference ICXOM XVIII held at Frascati; an oral contribution titled "X-ray propagation through polycap-

illary optics: a feature study by PolyCAD” was given and will be published as a special issue of *Spectrochimica Acta B* <sup>4</sup>).

By means of the “CNR - Short Term Mobility Program” Yury Dudchik, one of the main expert in X-ray diffractive optics, was our guest in October 2005, coming from the Institute of Applied Physics Problems (Minsk - Belorussia). X-ray diffractive lenses allow to increase the radiation density on sub-micron surfaces and may be utilized in analytical measurements like micro-diffraction, micro-fluorescence and X-ray microscopy. For such a reason a set of preliminary experiments were carried out using a gold mesh with 5  $\mu\text{m}$  wires as a test object for imaging. A set of images of the X-ray source and mesh were collected and visualized by a CMOS camera.

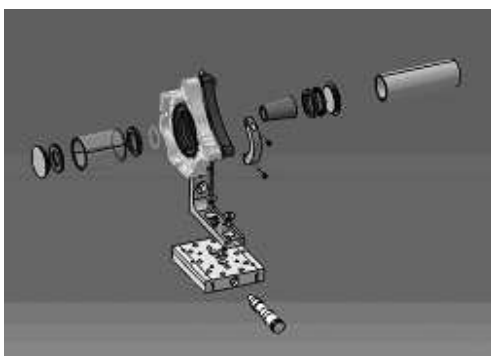


Figure 1: New polycapillary lens holder designed and made by the LNF Group SSCR. The holder, which will operate in vacuum, is equipped with input and output lead-steel slit, a PVC front support for centering the lens and a rear support for fixing with a thrust “O-ring”. Courtesy by A. Tiburzi.

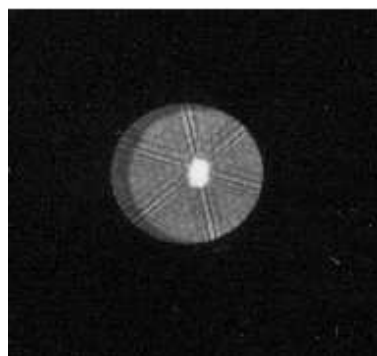


Figure 2: Polycapillary lens alignment using a led laser beam. The light passage through the polycapillary lens generates the radial effect with an hexagonal symmetry.

### 3 Activity in 2006

According to the CNR-MIUR Project, in collaboration with the Institute for the Chemical Physics Processes (IPCF Pisa) and with the Physics Department of the University “Milano Bicocca”, polycapillary lenses will be utilized in 2006 for X-ray microscopy experiments and for micro-diffraction measurements, while diffractive lenses will be tested for X-ray microscopy applications.

### References

1. D. Hampai, S.B. Dabagov, G. Cappuccio, G. Cibin, *Proceedings of SPIE*, Vol. **5943**, 7–14 (2005).
2. D. Hampai, S.B. Dabagov, G. Cappuccio, G. Cibin, *Proceedings of SPIE*, Vol. **5974**, 433–441 (2005).
3. D. Hampai, S.B. Dabagov, G. Cappuccio, G. Cibin, to be published on *Nucl. Instrum. and Methods, B* (2005).
4. D. Hampai, S.B. Dabagov, G. Cappuccio, G. Cibin, to be published on *Spectrochim. Acta B* (2005).

## PRESS-MAG-O

M. Cestelli Guidi, G. Della Ventura, D. Di Castro, D. Di Gioacchino (Resp.),  
A. Marcelli, A. Mottana, M. Piccinini, P. Postorino, P. Tripodi

### 1 Purposes

The *PRESS-MAG-O* experiment, one of the 2005 highlights of the INFN Vth Committee, is devoted to investigate new materials and new phenomena in condensed matter under extreme conditions. The proposal is based on the R&D of an apparatus that will allow performing ac magnetic measurements and magneto-optic experiments on samples under high pressure and high DC magnetic field in a wide temperature range. The device has been designed to perform experiments using SINBAD, the brilliant IR beam line operational at Frascati. In this proposal a large collaboration is involved based on the 'LNF-INFN magneto-dynamic' group, the SINBAD team, the 'High-pressure Raman Spectroscopy group' of the Department of Physics of "La Sapienza" University and the Department of Geological Science of the Roma Tre University.

### 2 *PRESS-MAG-O* Activity

During the first year the main tasks carried out by the *PRESS-MAG-O* collaboration are summarized below: a) the order of the superconducting magnet device; b) the design of a cryostat for the superconducting magnet with optical windows; c) the development of a compact high pressure diamagnetic Diamond Anvil Cell (DAC) for low temperature experiments, d) the R&D of a gradiometer to be inserted in the DAC cell.

#### 2.1 Cryostat and superconducting magnet

We prepared the international tender for the superconducting split magnet. The document with the required parameters has been submitted to four companies. After a carefully analysis of the technical and economical proposal we selected the offer of the AMI Inc. for an 8 T split magnet, whose layout is shown in figure 1. The magnet has been delivered and we plan tests at the LNF in the first months of 2006.

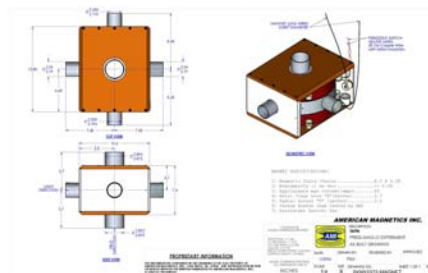


Figure 1: *Schematic layout of the superconducting split magnet.*

After the selection of the magnet device we prepared the tender for the cryostat. This device characterized by four accesses, two of which are dedicated to optical windows, allows the insertion

from the top, of a DAC cell equipped with a magnetometer. The DG-Tecnology Service is the company that has been selected to realize the cryostat. The delivery of the device is expected in the spring of 2006. Using a cryogenic device already available at the SINBAD laboratory and, thanks to the support of the 'Solid State Laser Laboratory' team led by Rosa Maria Montenerali of the ENEA Frascati who provided the laser system, we performed a series of tests to check the technical feasibility via laser heating to control and monitor the temperature on a sample placed inside our DAC cell. Typical results of the tests performed at liquid nitrogen temperature using the cold finger are both shown in Figure 2. The results confirm the feasibility to operate *in situ* with a commercial laser of 3W. From Figure 2 is clear that the temperature at the sample position [thermometer 1] changes while the temperature gradiometer remains almost constant to the value of the cold finger thanks to a thermal shield made by teflon and by a thermal short by a copper sock with the cold finger [thermometer 2].

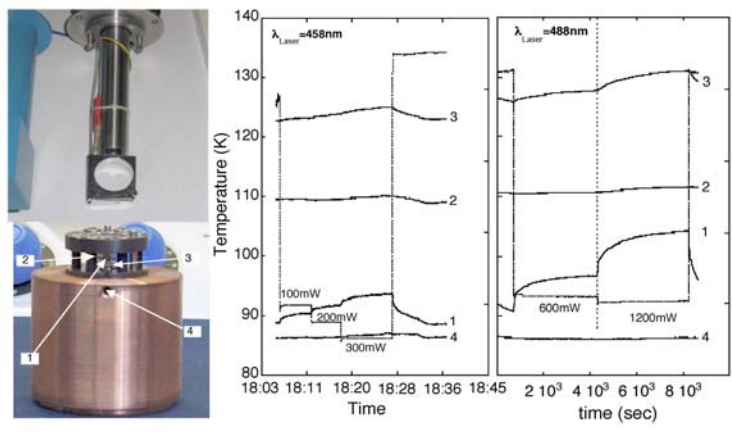


Figure 2: *Left panels: photos of the cold finger and of the temperature control. Right panels: Experimental temperature behavior vs. time. The thermometers inside the DAC cell were located on: the diamond near the sample (1), the DAC gasket (at the gradiometer position) (2), the table of the diamond (3) and the cold finger (4).*

## 2.2 Gradiometer

The development of the miniaturized gradiometer system to place inside the DAC cell is in progress. During the first year, an accurate analysis of the special DAC cell we developed, characterized by a large lateral access (see figure 3) has been performed. A first prototype of the gradiometer (see figure 4) has been designed and assembled to start the characterization on view of the future device that will be optimized for the actual geometry and constraints of the DAC cell. Moreover, a sample of about  $10\mu\text{m}^3$  has been compressed between two diamond anvils and the magnetic noise with a very low fill factor ( $10^{-6}$ ) has been measured. To enhance the magnetic signal and the contrast we are evaluating the possibility to realize a second order differential gradiometer. In figure 4 we shown a symmetric second order gradiometer (right panel) rolled on a PVC support in a split configuration. We manufactured it to simulate the DAC geometry between the pick-up

coils. The system employs 2 identical pick-up coils placed on both sides of the cell. A test using a small YBCO bulk sample has been also performed measuring the ac susceptibility signal. For this sample the superconducting transition around 85K is shown in the left panel of figure 4. An improved gradiometer configuration based on an a-symmetric magnetometer is under construction. In the final configuration, the signal from the pick-up bridge coils will be amplified by a SQUID system whose design will start in 2006.



Figure 3: Photos of the diamond anvil cell (DAC). Top (left) and side (right) views.

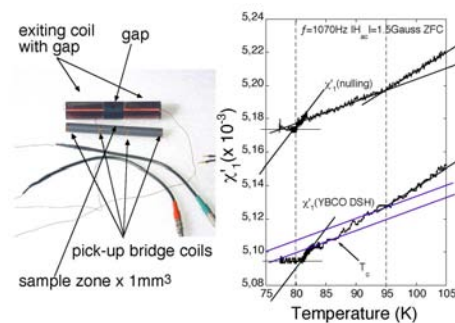


Figure 4: Left panel: photos of the first prototype of the second order gradiometer characterized by a split configuration. Right panel: Data of ac susceptibility of the first harmonic real part vs. temperature with (bottom curve) and without (top curve) a small YBCO sample.

## References

1. D. Di Gioacchino, P. Tripodi, A. Marcelli, M. Cestelli Guidi, M. Piccinini, P. Postorino, D. Di Castro, "PRESS-MAG-O: a new facility to probe superconducting phenomena under extreme conditions", contribution subm. to the Appl. Superconductivity Conference. (Seattle, 2006).

## SAFTA2

D. Alesini (Art. 23), V. Fusco (Ass.), M. Migliorati (R.U.), A. Mostacci (Ass.),  
L. Palumbo (P.O.), B. Spataro (D.T.)(Resp.), M. Zobov (art. 2222)

### 1 Aim of the experiment

The aim of SAFTA2 group is mainly related to the study of the electromagnetic interaction between a particle beam and the accelerator beam pipe wall, the generation of the parasitic fields, the related energy loss and the instability effects. The main investigated subjects are the coupling impedances of the LHC and SPS machines. The activity, done in collaboration with AB/ABP group at Cern, consists of estimating the longitudinal and transverse coupling impedance budget of the LHC and SPS rings in order to evaluate the instability thresholds. Results obtained from simulations have been cross-checked with analytical estimations and, whenever possible, with experimental results.

The energy losses, the parasitic resonances, and the longitudinal and transverse impedances of several beam components and the standing wave accelerating structures have been studied with the MAFFIA3D, HFSS, ABCI, OSCAR2D and SUPERFISH code, and in each case the analysis of the results has suggested an optimization of the design in order to obtain acceptable values of the coupling impedance and energy loss.

### 2 2005 Main results

#### 2.1 Impedance calculations for the LHC synchrotron light monitor (SLM) vacuum chamber

We have performed impedance calculations for the synchrotron light monitor (SLM) vacuum chamber in order to evaluate its contribution to the overall LHC impedance budget and to reveal potentially dangerous higher order modes (HOM). Since the SLM structure is long, we started simulations with the central SLM body containing three attached tubes by assuming the symmetry plane at  $x = 0$  (radial). Already for this structure we have found two distinct trapped modes at about 2.2 GHz and 2.4 GHz. The respective longitudinal wake decays fast but still lasts for a time long enough to catch successive bunches in the LHC train. These modes are near the cut-off frequencies of the central body beam pipe, having azimuthal field variation. The modes propagate at large distances from the SLM central body and can be enhanced if there are additional discontinuities within the region occupied by the mode fields. We have seen this behavior in simulations by adding small tapers attached to the beam pipe. In our opinion this is due to the asymmetric positions of the attached tubes on the central beam pipe. Possible candidates for the incriminated modes are TM<sub>21</sub> and TM<sub>02</sub>, respectively.

As a next step, we added a central conductor in the vertical plane simulating the mirror periscope, as it is shown in Fig. 1. The conductor inserted inside the flange creates a piece of a coaxial pipe with respect to the flange walls. In this case new coaxial type HOM can be excited. Since a coaxial does not have a cut-off frequency some of the modes can have relatively low frequencies. In fact one distinguishes the new HOM modes at frequencies  $f = 0.45, 1.40$  and  $2.4$  GHz.

The SLM structure is not azimuthally symmetric and for this reason the coaxial HOM has a strong vertical component on the beam axis. The relative longitudinal and transverse wake fields have been estimated.

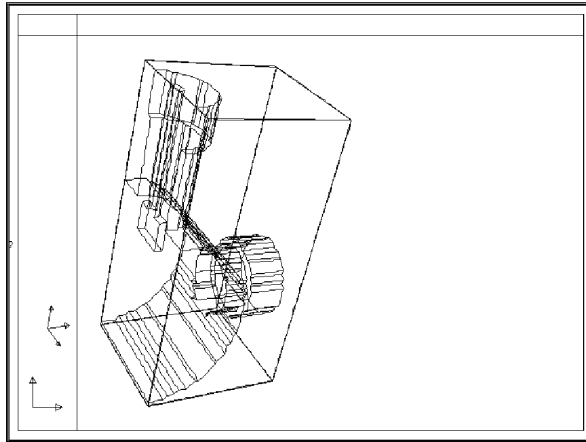


Figure 1: *whole shape of the SLM used for MAFIA simulations (half structure).*

In order to characterize HOM parameters we have performed both the time domain and frequency domain simulations. As a final result, we suggested to install a dedicated antenna for damping the parasitic resonances and to obtain the optimization of the device.

## 2.2 SPS vacuum chamber WAMPAC3 and WAMPAC4 (calorimeter)

The main investigated subject on this vacuum chamber was to estimate and check the power losses, longitudinal and transverse impedances. Calculations have been carried out and the numerical results are in agreement with the experimental ones.

## References

1. B. Spataro, *et al.*, "Impedances of the cold bore experiment, COLDEX, installed in the SPS machine", LNF-05/06 (P), 11 April 2005, accepted for publication on NIM A.
2. L. Palumbo, *et al.*, "Observation of anomalously large spectral bandwidth in a high-gain self-amplified spontaneous emission free-electron laser", Physical Review Letters, v 95, n 5, 29 July 2005, p 054801/1-4.
3. M. Migliorati, *et al.*, "SPARC working point optimization for a bunch with gaussian temporal profile", 2005 Particle Accelerator Conference, pp. 1248-1250, Knoxville - Tennessee, May 2005.
4. D. Alesini, *et al.*, "The project PLASMONX for plasma acceleration experiments and a thomson X-ray source at SPARC", 2005 Particle Accelerator Conference, pp. 820-822, Knoxville - Tennessee, May 2005.
5. M. Migliorati, L. Palumbo, *et al.*, "Start to end simulation for the SPARX project", 2005 Particle Accelerator Conference, pp. 1455-1457, Knoxville - Tennessee, May 2005.
6. M. Migliorati, *et al.*, "Beam dynamics studies for the SPARXINO Linac", 27th International Free Electron Laser Conference, pp. 67-70, Stanford, California, USA, August 2005.
7. L. Palumbo, *et al.*, "Simulations, diagnostics and recent results of the VISA experiment", 27th International Free Electron Laser Conference, Stanford, California, USA, August 2005.

## SALAF

D. Alesini (Art. 2222), R. Boni (D.T.), A. Gallo (P.T.),  
F. Marcellini (T.), M. Migliorati (R.U.), A. Mostacci (Ass.), B. Spataro (D.T.) (Resp.)

### 1 Aim of the experiment

The aim of SALAF group is related to the design, realization and measurements of a compact standing wave accelerating structure operating at 11 GHz to be used for linearizing the longitudinal space phase in the Frascati coherent light source (SPARC). Two different structures have been analyzed, the first one is a 9-cell cavity operating on a  $\pi$  standing wave mode, and the second one is bi-periodic accelerating section operating on the  $\pi/2$  standing wave mode.

The standing wave sections have been designed with the HFSS, ABCI, OSCAR2D, SUPERFISH and ANSYS codes. Prototype for both the structures have been built and the  $\pi$ -mode structure has been successfully characterized.

### 2 2005 Main results

#### 2.1 X-band standing wave accelerating structure working on $\pi$ mode

Concerning the linear accelerating structure operating on  $\pi$  mode at a frequency  $f=11.424$  GHz, a prototype in copper was realized. The section constituted by 9 cells has been designed to obtain a 5 MeV accelerating voltage. To feed the structure there are two lateral antennas, each one at the end cavity, and a waveguide coupling (coaxial-transition) or coupler in the central cell. Then, in each cell is inserted a tuner in order to properly tune the frequency and the field shape of the operating mode.

Calculations for the 2D profile design have been carried out using the e.m. codes SUPERFISH, OSCAR2D while the coupler has been designed using HFSS code. The antennas allow to excite and characterize all the electromagnetic modes of the structure; the dispersion diagram can be measured and compared to the theoretical expectations. The coupler allows to feed the section with high RF power and to get a better separation of the  $\pi$  mode from the closest one as it will be shown later.

At room temperature, bead-pull measurements of the field inside the structure are in good agreement with the numerical results <sup>1)</sup>. Two graduation theses on this activity have been successfully carried out by the students A. Falone and F. Palpini of the Rome University - La Sapienza <sup>2, 3)</sup>. The result was an excellent agreement between the theoretical predictions and the experimental measurements.

In addition to this activity, intensive simulations have been performed to study the feasibility of an innovative hybrid RF gun <sup>4, 5, 6)</sup> and a X band SLED system <sup>7)</sup>. Moreover the experimental and theoretical study of the RF SPARC deflector is still going on <sup>8)</sup>.

As an example, in Fig. 1 we show the measurement setup at the laboratory in University of Rome "La Sapienza" (Energetics department).

The measured frequency spectrum of Fig. 2 is obtained by feeding the section with the lateral antennas (left picture), or by exciting the section by the coupler (right picture). The whole dispersion diagram is reported in Fig. 3 where it is compared to the simulation results (HFSS and SUPERFISH).

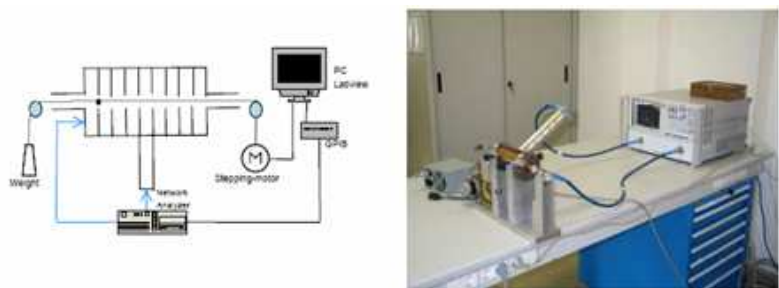


Figure 1: *RF measurement set-up: scheme and picture.*

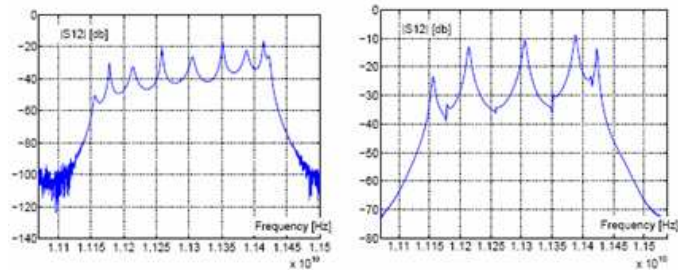


Figure 2: *S<sub>21</sub> frequency spectrum obtained by feeding the antennas or the coupler.*

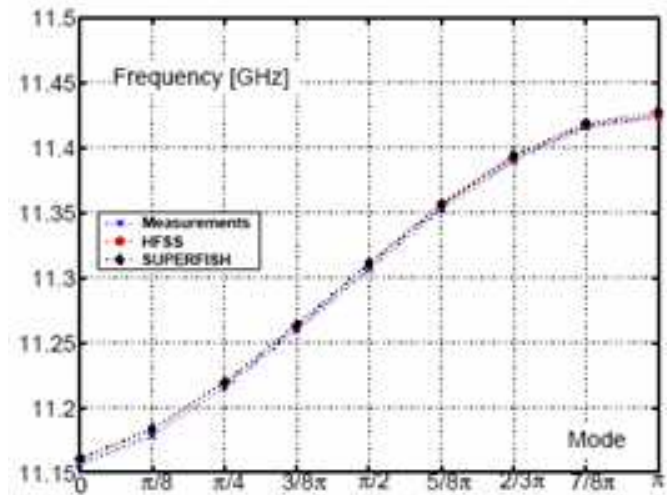


Figure 3: *Measured dispersion diagram compared to simulation results by HFSS and SUPERFISH.*

It is worth noticing that exciting the structure by the coupler we observe only 5 over 9 possible modes of the diagram dispersion because, in doing that, we impose a non-zero field in the coupling cell. On the contrary, by feeding the structure from the antennas, we excite all the 9 structure

modes of the dispersion curve.

Additional measurements like the electric field flatness, the loaded quality factor  $Q_l$ , the structure form factor  $R/Q$  where  $R$  is the longitudinal shunt impedance, have been done and they are shown in fig. 4.

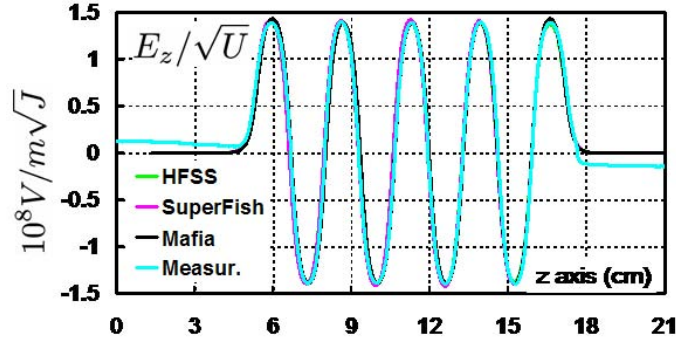


Figure 4: *Measured field inside the cavity.*

Moreover an activity on the design and construction of high frequency, multicell accelerating structures is in progress at Frascati Laboratory using vacuum brazing technique<sup>9)</sup>. An alternative to the standard to standard machining and brazing procedure is the galvanoplastic technique of electroforming. A study on the possibility of obtaining the same final result following this completely different technique is in progress<sup>10)</sup>.

## 2.2 X-band standing wave accelerating structure working on $\pi/2$ mode

The numerical electromagnetic design on the bi-periodic structure has been completed. The study includes: open and closed dispersion curves, design of the coupling cells, field profile optimization, shunt impedance and quality factor calculations. The analysis of the generator-cavity coupling has been carried out using HFSS code and thermal analysis with the ANSYS software<sup>11)</sup>. Then, a prototype in copper has been realized and measurements at room temperature are in progress at the Rome University - La Sapienza.

## 3 Activity 2006

The continuation on the design and realization of the linear accelerating structures is foreseen in order to determine the final choice of the section to be installed on the SPARC LINAC. In particular the behaviour of the thermal stress will be investigated in detail with simulations and by comparing the results with dedicated measurements. In order to get a satisfactory know-how on the design and realization of the linac sections at high frequency, more investigations will be made on the brazing and electroforming procedures. Prototype for the  $\pi/2$  mode structure is ready and its electromagnetic peculiarities will be carefully investigated in details during the next months.

## References

1. B. Spataro, *et al.*, "Design and Rf measurements of an X-band accelerating structure for linearizing the longitudinal emittance at SPARC", NIM A 554 (2005) 1-12.

2. F. Palpini, "Ottimizzazione della misura di campi elettromagnetici nei campi acceleratrici ad 11 GHz", tesi di Laurea di Primo Livello, Università La Sapienza, 2005.
3. A. Falone, "Accoppiatore simmetrico a guida d'onda per strutture acceleranti in banda X", tesi di Laurea Specialistica, Università La Sapienza, 2005.
4. P. De Santis, "Sviluppo e test di una cavità accelerante multi cella ad 11.4 GHz", tesi di Laurea di Primo Livello, Università La Sapienza, 2005.
5. G. Caretti, "Progetto di un cannone ibrido a radio frequenza in banda X", tesi di Laurea di Primo Livello, Università La Sapienza, 2005.
6. D. Santarelli, "Progetto di un foto iniettore ibrido per elettroni in banda S", tesi di Laurea di Primo Livello, Università La Sapienza, 2005.
7. R. Da Re, "Progetto di uno SLED in banda X", tesi di Laurea di Primo Livello, Università La Sapienza, 2005.
8. L. Ficcadenti, "Progetto di uno SLED in banda X", tesi di Laurea Specialistica, Università La Sapienza, 2005.
9. B. Spataro, *et al.*, "First results on vacuum brazing of RF 11GHz linear accelerating structures at Frascati laboratory", LNF-05/22(IR), 14 Novembre 2005.
10. B. Spataro, *et al.*, "An investigation on electroforming procedures for RF 11 Ghz linear accelerating structures at Frascati laboratoty", LNF-05/23(IR), 14 Novembre 2005.
11. B. Spataro, *et al.*, "Studies on bi-periodic X-band structure for Sparc", LNF-03/013(R), 25 Agosto 2003.

## SI-RAD

L. Bongiorno (Ass. Ric.), M.A. Franceschi, G. Mazzenga (Tecn.), M. Ricci (Resp.), B.Spataro

Participant Institutions:

ITALY: INFN LNF, Firenze, Roma Tor Vergata, Trieste; University of Genova

GERMANY: SIS (Darmstadt)

RUSSIA: MePhi, IBMP, RKK "Energia" (Moscow)

SWEDEN: KTH (Stockholm)

ESA European Astronaut Center

### 1 Introduction

The SI-RAD experiment is a continuation of the activity that the Collaboration has carried out for the experiments SIEYE1 and SIEYE2 on board the Russian Space Station MIR and SIEYE3/ALTEINO on board the International Space Station (ISS) in the years 1995-2002. <sup>1, 2, 3, 4, 5, 6, 7, 8)</sup>

The experimental task of the SI-RAD experiment is to develop a detector to be placed on the external part of the ISS. The detector will be used to monitor cosmic rays and radiation environment in Low Earth Orbit. Long (Solar modulation) and short (coronal mass ejections, orbit dependence) of the particle flux and the dose absorbed by the astronauts will be monitored. In addition, data will be compared with measurements taken inside the ISS with Altea and Alteino detectors to validate radiation transport and dose estimation codes. At the same time, the investigation, with a more sophisticated instrument, of the "Light Flashes" phenomenon <sup>9)</sup>, will be conducted to improve and refine the results obtained with the previous SIEYE experiments.

To meet these goals, a precursor mission in space with a high performance cosmic ray detector, LAZIO/SIRAD <sup>10)</sup>, has been accomplished to measure and identify all particles traversing the detector separating nuclei from electrons/positrons, in the energy range 10 to 100 MeV. It is able to record their time of arrival, their line of arrival (pitch angle) and their direction of arrival. A very important feature of LAZIO/SIRAD equipment, which weighs 30 kg, is its very large aperture ( $\sim 60 \text{ cm}^2 \text{ sr}$ ) which allows to perform accurate, real time measurements of the pitch angle distribution within short time intervals (from few seconds to few minutes depending on the position on the orbit). LAZIO/SIRAD has been launched in April 2005 on a Soyuz rocket and placed aboard the ISS by the Italian astronaut Roberto Vittori. Data collection and analysis is currently in progress. Before launch, the apparatus has been exposed to a low energy electron beam at the Beam test facility (BTF) of the INFN Frascati Laboratories <sup>11)</sup>. The accuracy of LAZIO/SIRAD and its sensitivity to all kind of low energy radiation allows a precision monitoring of the radiation collected by the astronauts during their mission. Moreover, LAZIO/SIRAD is equipped with a high precision low frequency magnetometer, which is used to measure the intensity and the variations of the magnetic field within the ISS, in correlating these measures with the measurements of the particle fluxes. LAZIO/SIRAD is also operated in conjunction with the SIEYE3/ALTEINO detector.

The preparation of the next SI-RAD extended mission is progressing with the realization of the full flight instrument consisting of a 16-plane tower of double-sided silicon detectors ( $8 \times 8 \text{ cm}^2$  area) equipped with trigger and anticoincidence counters. The total weight is about 15 kg and the

total power consumption should not exceed 30 W. The hardware set-up is accomplished through three steps by the construction of a laboratory prototype model, an engineering model and the final flight, space qualified model. The activity in 2005 has been focused on the parallel development of the following systems of the engineering model:

- Trigger system.
- Development of Silicon Photomultiplier (SI-PM) technology for space applications and test of different SI-PM configurations at the LNF-BTF beam.
- Design and realization of a highly integrated silicon board (16 cm x 16 cm).
- Realization and test of a low-power, low-mass Digital Processing Unit (DPU).

In 2006, the planned activity includes the completion of the engineering unit and the set-up of the flight configuration equipped with autotrigger capabilities for heavy nuclei and a trigger for crossing protons and nuclei. The interface with the ISS Space Station will be realized with an intermediate CPU to manage the telecommands from ground and the download of the data. Beam tests at the LNF-BTF, GSI/Darmstadt and TSL/Uppsala are also planned together with the continuation of the study and development of the SI-PM technology.

## 2 Activity of the LNF group

The LNF group has taken the responsibility of the design, construction and test of the mechanical structures and interfaces of the three models of the detector also contributing to the integration of the mechanical support for the DAQ. This activity is carried out with the support and the participation of the LNF Service of Development and Costruction of Detectors (SSCR). The activity in 2005 has been mainly devoted to the mechanical support of the engineering model and to the interfaces of the front-end and DAQ with the detector. These issues will be developed for the final flight configuration in the year 2006. The LNF group participates as well in the beam test activities at the above mentioned facilities having the responsibility of the beam trigger counters.

## 3 Publications in 2005

1. F.Altamura *et al.*, "Preliminary results from the LAZIO-Sirad experiment on board the International Space Station", Proc. XXIX ICRC, Pune (2005), SH35 p.101.
2. R.Bencardino *et al.*, "Response of the LAZIO-SiRad detector to low energy electrons", Proc. XXIX ICRC, Pune (2005), SH36 p.101.

## References

1. S.Avdeev *et al.*, "The SilEye nuclei cosmic ray and eye light flash experiment onboard the Mir Space Station", Proc. Proc. XXVII ICRC, Hamburg (2001) p. 1745.
2. M.Casolino *et al.*, "Cosmic ray measurements on board space station MIR with SILEYE-2 experiment", Proc. Proc. XXVII ICRC, Hamburg (2001) p. 4011.
3. V.Bidoli *et al.*, "In-flight performances of SilEye-2 Experiment and cosmic ray abundances inside space station MIR"; Journal of Physics G: Nuclear and Particle Physics **27**, 2051(2001).

4. S.Avdeev *et al.*, “Eye light flashes on the Mir Space Station”; *Acta Astronautica*, **50**, 511 (2002).
5. L.Narici *et al.*, “The ALTEA facility on the International Space Station”; *Physica Medica Suppl. 1* **17**, 255 (2001).
6. M.Casolino *et al.*, “The Sileye/3-Alteino experiment on board the International Space Station”; *Nucl.Phys.* **113B**, 88 (2002) .
7. V.Bidoli *et al.*, “Dual origin of light flashes in space”, *Nature* **422**, 680 (2003).
8. P.Maponi *et al.*, “A syncitium model for the interpretation of the phenomenon of anomalous light flashes occurring in the human eye during space missions”, *Nuovo Cim.*, **116B**, 1173 (2001).
9. G. Horneck, “Radiobiological experiments in space: a review”, *Nucl. Tracks Radiat. Meas.*, **20**, 185 (1992) .
10. F.Altamura *et al.*, “Preliminary results from the LAZIO-Sirad experiment on board the International Space Station”, *Proc. XXIX ICRC, Pune (2005)*, SH35 p.101.
11. R.Bencardino *et al.*, “Response of the LAZIO-SiRad detector to low energy electrons”, *Proc. XXIX ICRC, Pune (2005)*, SH36 p.101.

## SUE

E. Burattini (Resp.), A. Grilli (Tecn.), A. Raco (Tecn), D. Bettega (Ass.), P. Calzolari (Ass.),  
F. Malvezzi Campeggi (Ass.), F. Monti (Ass.), L. Tallone (Ass.), F. Farina, L. Doneda

Skin cancer is the most common human malignancy and is strongly associated with exposure to ultraviolet radiation. The depletion of the ozone layer contributes to increased penetration of the UVB radiation particularly at the shortest wavelengths. As it is known, the UVB biological effectiveness is strongly dependent on the radiation wavelength and increases at the shortest wavelengths. Aim of the SUE experiment is to study the wavelength dependence of UVB effectiveness for neoplastic transformation, cell killing, delayed reproductive death and micronuclei induction in human cells *in vitro*. Irradiation was performed with monochromatic beams at the Ultraviolet (UV) beamline of the DAΦNE-Light Synchrotron Radiation Facility. Details on the irradiation technique as well as on the beamline and on the experimental hutch can be found elsewhere <sup>1)</sup>. In five irradiation sessions up to 2004, cultures of human hybrid cells CGL1 <sup>2)</sup>, <sup>3)</sup> were exposed to monochromatic beams of four different wavelengths (285, 292, 295 and 300 nm) in the dose range between 5 and 100 J/m<sup>2</sup>. Figure 1 shows the survival data and the fitted curves for all the beams studied. The curves are the best fit of the linear-quadratic equation to the surviving fractions determined at five or six doses. Figure 2 shows the cloning efficiency of the progeny of irradiated cells versus the dose given to their progenitors. Delayed reproductive death is induced by all the beams: the effect is large and dose dependent. For all the end-points the UVB biological effectiveness increases with decreasing wavelength from 300 to 285 nm: increase factors up to 4; 7; 14 are found for survival, delayed reproductive death and transformation induction respectively. The biological effectiveness of the monochromatic UVB beams studied relative to that found at 300 nm, ( $a_l / a_{300}$ , where  $a$  is the coefficient of the linear term of the fitted curves) has been compared with the spectral weighting factors ( $S(l) / S(300\text{nm})$ ) used by the International Committee on Non-Ionizing Radiation Protection (ICNIRP) <sup>4)</sup>. For these delayed effects the effectiveness increase at the shortest wavelengths is greater than that of the ICNIRP spectral weighting factors in the same wavelength interval <sup>5)</sup>. The results of this experiment show that with decreasing wavelength from 300 to 285 nm the UVB biological effectiveness increases. The increase is constant with dose, is end-point dependent and is greater in the case of the two delayed effects, i. e. delayed reproductive death and oncogenic transformation, where factors of 7 and 14 were found respectively. In two irradiation session during 2005 cultures of AG1522 were exposed to monochromatic beams of the same four different wavelengths in the dose range between 3 and 100 J/m<sup>2</sup> to determine cell survival and micronuclei formation in the directly irradiated cells and in their progeny at 15 and 30 days after irradiation. Data analysis has still to be completed. In Figure 3 and Figure 4 we report preliminary results on survival of the irradiated cells and of their progeny (15 days after irradiation). These data on AG1522 cells exposed to monochromatics UVB-beams confirms previous results on CGL1 cells, i.e.: the biological effectiveness increases with decreasing wavelength from 300 to 285 nm for cell killing and micronuclei induction in the directly irradiated cells as well as the induction of delayed effects in the their progeny.

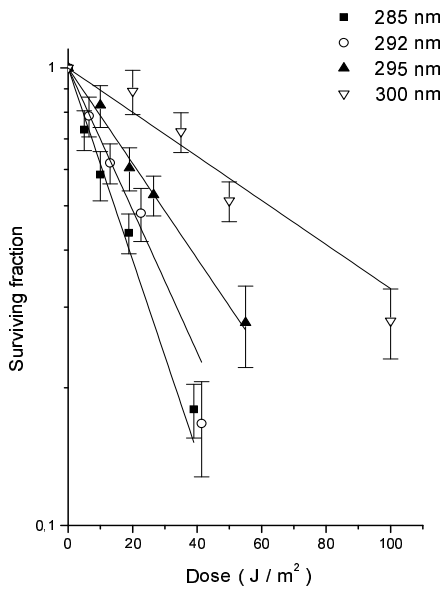


Figure 1: *Survival of the irradiated CGL1 cells vs the dose.*

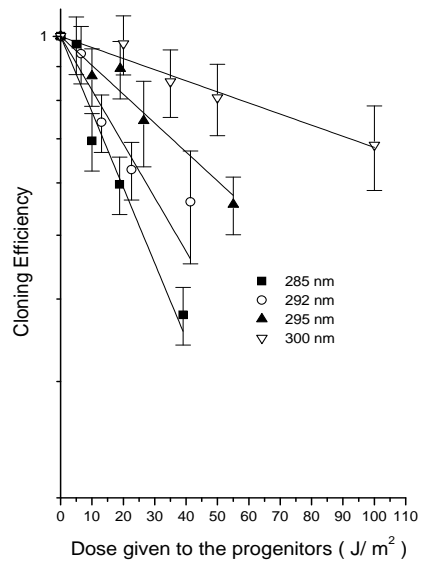


Figure 2: *Cloning Efficiency of the CGL1 progeny vs the dose given to the progenitors.*

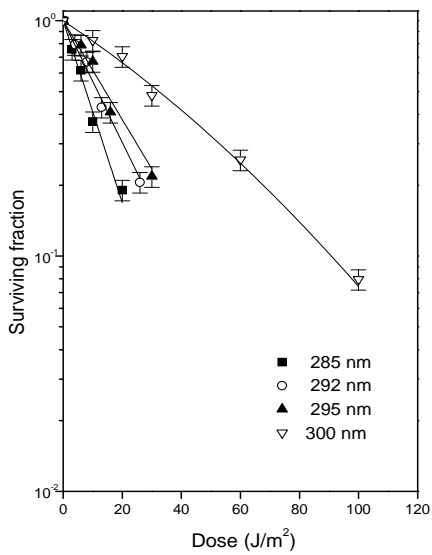


Figure 3: *Survival of the irradiated AG1522 cells vs the dose.*

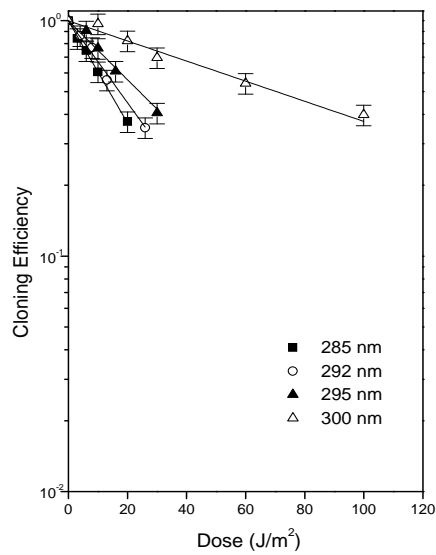


Figure 4: *Cloning Efficiency of the AG1522 progeny vs the dose given to the progenitors.*

## References

1. E. Burattini *et al.*, “LNF 2004 Annual Report”, E. Nardi ed., LNF-05/5.
2. E.J.Stanbridge *et al.*, *Science* **215**, 252 (1982).
3. J.L. Redpath *et al.*, *Rad. Res.* **110**, 468 (1987).
4. *Health Physics* **87**, 171 (2004).
5. D. Bettega *et al.*, *Int.J. Radiat. Biol.*, submitted.

## CSAXS - SMALL ANGLE X-RAY CAMERA

A. La Monaca (Resp.), R. Sinibaldi(Ass.), P. Mariani, B. Salvato

In the frame of a partnership between National Laboratory of Frascati of the INFN, the SASC Department of Polytechnic University of Marche and Department of Biology of Padova University we are renewing a Small Angle X-ray Scattering Camera (CSAXS), an experimental apparatus to measure the X-ray elastic cross section. The instrument, built and developed by INFN, worked for many years with the hard X-rays of synchrotron radiation facility, it was dismissed when the storage ring ADONE was closed. CSAXS was equipped with an original two-dimensional gas detector, synchronized with electron bunches of the storage ring <sup>1)</sup>, an optical and mechanical system suitable for both SAXS and diffraction experiment. The bidimensionality is a very powerful tool and allow performing SAXS experiment on organized but anisotropic system such as amyloid aggregates or quadruplexes complex formed by guanosine basis. Nevertheless the most famous subject of amyloid aggregation in diseases (Parkinson, Alzheimer) the second system is similar to the in vivo ends of DNA strains, where the rich composition of Guanosine basis is essential for the folding of DNA into chromosomes <sup>2)</sup>.

### 1 The instrument

In figure 1 we can see the different parts that compose the CSAXS apparatus. The X-rays pass in the vacuum from the pinhole, throughout sample holder and telescope up to the detector. Different step-motors allow moving the detector up and down in respect to the incident beam for about 40 cm and then turning it around the beam with a goniometer motor. The goniometer can turn for about 90 degree in both direction and in this way the instrument can explore a wide portion of the Ewald sphere. It is very easy to change the sample detector distance manually, moving the sample holder camera on two binary and reducing the telescope's length.

Fast electronic front end and two-dimensional acquisition system compose the CSAXS electronics. The front end is constituted by emitter follower system, low level amplifier comparators connected to the sense wire and to the delay line ends. The acquisition system made by a couple of LeCroy 4204 CAMAC TDCs (time to digital converters), with conversion time of about 1  $\mu$ s and time resolution up to 150 psec. The output from the TDCs is stored into two histogram memories via a separate bus independently of the CAMAC.

### 2 Activity

Our group began this activity in 2005 with the aim to renew this apparatus and to perform future experiment using a traditional hard X-rays source already available in University of Marche. CSAXS is temporary housed in the vacuum laboratory of Accelerator Division of LNF. The instrument was first unmounted and metal components were putted in an anodizing bath or cleaned or changed.

Detector and beam stopper movements were connected to the computer using our custom electronics linked to the computer with a PCI card from National Instrument and Labview package. It was necessary to change the sample holder's micrometers and then to optimize the collimation micro-mechanics.

The acquisition system was completed choosing a CAMAC crate controller model CAEN JNT01 that is possible to use via serial or ethernet ports and allows block transfer from histogram

memories. We verified and partially tested the functionality of the acquisition system with pulse generator using a simple software written in C++. The activity will continue in the first half of 2006: we are going to verify the functionality of the drift chamber detector and to optimize the composition of the gas mixture (Ar, Xe, CO<sub>2</sub>, CH<sub>4</sub>). We will write a program in C++ to view the two-dimensional graphic display of the experimental data in real time and finally the instrument will be moved in the University of Marche where the instrument will be used for some years to investigate biological matter.



Figure 1: *The Small Angle X-ray Camera.*

### 3 Acknowledgements

We wish to thank Prof. M. Calvetti, director of LNF-INFN, for his constant attention to this project.

### References

1. A. La Monaca, M. Barteri, E. Borghi, A. Congiu-Castellano *et al.*, Instruments and Methods in Physics Research A **310**, 403 (1991).
2. F. Federiconi, P. Ausili, P. Mariani *et al.*, J. Phys. Chem. B **109**, 11037 (2005).

## DAΦNE

The DAΦNE Team: D. Alesini, G. Benedetti, M.E. Biagini, C. Biscari, R. Boni, M. Boscolo, B. Buonomo, A. Clozza, G. Delle Monache, E. Di Pasquale, G. Di Pirro, A. Drago, L. Falbo, A. Gallo, A. Ghigo, S. Guiducci, M. Incurvati, P. Iorio, C. Ligi, F. Marcellini, C. Marchetti, G. Mazzitelli, C. Milardi, L. Pellegrino, M. Preger, L. Quintieri, P. Raimondi (Resp.), R. Ricci, U. Rotundo, C. Sanelli, M. Serio, F. Sgamma, B. Spataro, A. Stecchi, A. Stella, S. Tommasini, C. Vaccarezza, M. Vescovi, M. Zobov

The DAΦNE Technical Staff: G. Baldini, P. Baldini, A. Battisti, A. Beatrici, M. Belli, B. Bolli, A. Camiletti, G. Ceccarelli, R. Ceccarelli, A. Cecchinelli, S. Ceravolo, R. Clementi, O. Coiro, S. De Biase, M. De Giorgi, N. De Sanctis, R. Di Raddo, M. Di Virgilio, G. Ermini, G. Fontana, U. Frasacco, C. Fusco, F. Galletti, M. Giabbai, O. Giacinti, E. Grossi, F. Iungo, R. Lanzi, V. Lollo, V. Luppino, M. Marchetti, C. Marini, M. Martinelli, A. Mazzenga, C. Mencarelli, M. Monteduro, A. Palleschi, M. Paris, E. Passarelli, V. Pavan, S. Pella, D. Pellegrini, R. Pieri, G. Piermarini, G. Possanza, S. Quaglia, F. Ronci, M. Rondinelli, F. Rubeo, M. Sardone, M. Scampati, G. Sensolini, R. Sorchetti, A. Sorigi, M. Sperati, A. Sprecacenero, P. Tiseo, R. Tonus, T. Tranquilli, M. Troiani, V. Valtriani, R. Zarlenga, A. Zolla

### 1 Introduction

DAΦNE is an "electron-positron factory" operating at Frascati since 1997. Factories are storage rings for electrons and positrons delivering a high rate of mesons to high resolution experiments which require an extremely large number of events. To reach such high rates, the factories are designed to work at the energies of the meson resonances, where the production cross section peaks. To obtain the required production rate it is also necessary that the collider luminosity (the number of events per unit time of the reaction under investigation divided by its cross section weighted by the acceptance of the detector) is very high, between one and two orders of magnitude larger than that obtained in the conventional colliders with a single ring, where electrons and positrons run on the same orbit in opposite directions. When sharing the same ring the two N-bunch trains cross in 2N points and the maximum obtained luminosity is limited by the electromagnetic beam-beam interaction. The unwanted effects of this interaction can be reduced with a very strong focussing (called "low- $\beta$ ") at each of the crossing points, obtained by means of quadrupole doublets or triplets. At the same time these magnetic structures take up much room and excite chromatic aberrations which must be corrected elsewhere in the ring. A large number of bunches can be stored only with twice the number of low- $\beta$  points and due to the compactness of the DAΦNE machine only two of these regions can be realized, and therefore only a single electron bunch and a single positron one could be stored in a single ring.

This limitation does not hold for the double ring option, consisting in two separate rings crossing at two low- $\beta$  points. The number of bunches that can be stored in such a collider is limited only by the geometry of the IR's.

DAΦNE is a system consisting of a double-ring collider, a linear accelerator (LINAC) an intermediate damping ring to make injection easier and faster and 180 m of transfer lines connecting these machines. The beam accelerated by the Linac can also be switched into a laboratory called "BEAM Test Facility BTF)", for dedicated experiments and calibration of detectors. The accelerator complex has been designed to fit into the existing ADONE buildings (ADONE was the 3 GeV center of mass electron-positron collider in operation at LNF from 1969 to 1993); the complex is shown schematically in Fig. 1.

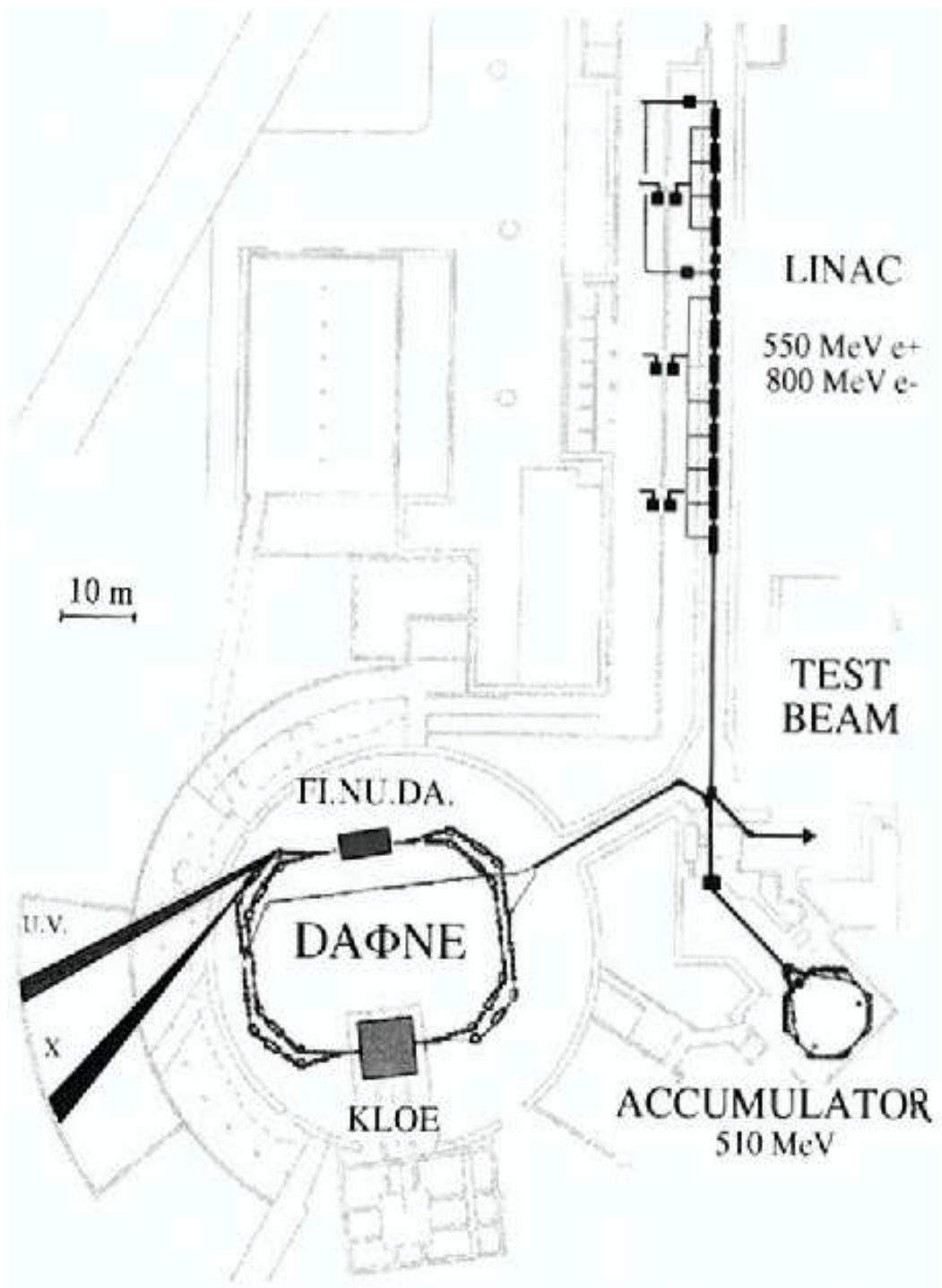


Figure 1: *The layout of the DAΦNE accelerator complex inside its buildings.*

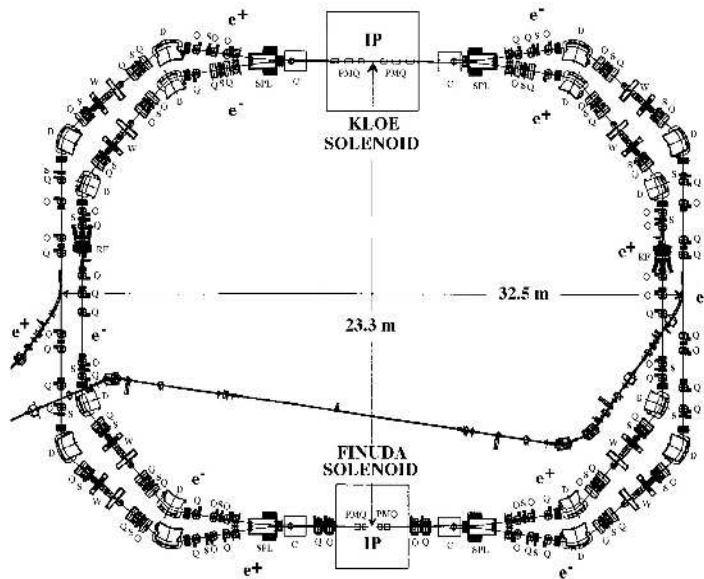


Figure 2: *The DAΦNE Main Rings.*

In the DAΦNE collider the two beam trajectories cross at the interaction point (IP) at an angle of  $\approx 1.5$  degrees in the horizontal plane. A positron bunch leaving the IP after crossing an electron one will reach the following electron bunch at a distance of half the longitudinal separation between bunches from the IP. Due to the horizontal angle between the trajectories of the two beams, the distance in the horizontal direction between the two bunches is equal to the horizontal angle times half the longitudinal distance between the bunches in the beam. The beam-beam interaction can be harmful to the beam stability even if the distance in the horizontal direction between bunches of opposite charge is of the order of few bunch widths at points where the  $\beta$  function is high and this sets a lower limit on the bunch longitudinal separation and therefore on the number of bunches which can be stored in the collider. For DAΦNE the minimum separation is 80 cm, and the maximum number of bunches to be stored in each ring is 120. This number determines the frequency of the radiofrequency cavity which replaces at each turn the energy lost in synchrotron radiation, which must be 120 times the revolution frequency. The luminosity of the collider can therefore be up to 120 times larger than that obtainable in a single ring with the same size and optical functions.

Crossing at an angle could in principle be a limitation to the maximum single bunch luminosity. In order to make the beam-beam interaction less sensitive to this parameter and similar to the case of single ring colliders where the bunches cross head-on, the shape of the bunches at the IP is made very flat (typical r.m.s. sizes are 30 mm in the longitudinal direction, 2 mm in the horizontal and 0.01 mm in the vertical one).

The double ring scheme with many bunches has also some relevant drawbacks: the total current in the ring reaches extremely high values (5 A in the DAΦNE design) and the high power emitted as synchrotron radiation ( $\approx 50$  KW) needs to be absorbed by a complicated structure of vacuum chambers and pumping systems in order to reach the very low residual gas pressure levels necessary to avoid beam loss. In addition, the number of possible oscillation modes of the beam increases with the number of bunches, calling for sophisticated bunch-to-bunch feedback systems.

The double annular structure of the DAΦNE collider is shown schematically in Fig. 2. Both

rings lay in the same horizontal plane and each one consists of a long external arc and a short internal one. Starting from the IP the two beams travel together inside a common vacuum chamber and their distance increases until it becomes  $\approx 12$  cm at the level of the magnetic separators called "splitters" (SPL). These are special magnets with two regions of opposite field which deflect the two beams in opposite directions, allowing them to reach the separate vacuum chambers of the long and short arcs. Each arc consists of two "almost achromatic" bends (deflecting the beam by 81 degrees in the short arc and 99 degrees in the long one) similar to those frequently used in synchrotron radiation sources, with a long straight section in between. Each bend consists of two dipoles, three quadrupoles, two sextupoles and a wiggler. This structure is used for the first time in an electron-positron collider and it has been designed for the particular requirements of DAΦNE: the amount of synchrotron radiation power emitted in the wigglers is the same as in the bending magnets and the wigglers can be used to change the transverse size of the beams. The increase of emitted power doubles the damping rates for betatron and synchrotron oscillations, thus making the beam dynamics more stable, while the possibility of changing the beam sizes makes the beam-beam interaction parameters more flexible.

The straight section in the long arc houses the pulsed magnets used to store into the rings the bunches coming from the injection system, while in the short straight arc there are the radiofrequency cavity and the equipment for the feedback systems which are used to damp longitudinal and transverse instabilities.

The most delicate part of the whole structure are the IR's. The collider can host two experiments, even if up to now only one at a time can get useful luminosity. Three detectors have been realized, KLOE, DEAR and FINUDA. KLOE is permanently installed in the first IP, while DEAR and FINUDA are alternatively running on the second one. The detectors of KLOE and FINUDA are surrounded by large superconducting solenoid magnets for the momentum analysis of the decay particles and their magnetic fields represent a strong perturbation on the beam dynamics. This perturbation tends to induce an effect called "beam coupling", consisting in the transfer of the betatron oscillations from the horizontal plane to the vertical one. If the coupling is not properly corrected, it would give a significant increase of the vertical beam size and a corresponding reduction of luminosity. For this reason a superconducting solenoid magnet with half the field integral of the detector one and of opposite direction is placed near each splitter in such a way that the overall field integral in the IR's vanishes. However, this is not sufficient to obtain full compensation of the beam coupling induced by the main solenoids. In the case of KLOE the low- $\beta$  at the IP was originally designed with two quadrupole triplets. Due to the flat shape of the beam at the IP, the low- $\beta$  is realized only in the vertical plane. The quadrupole cannot be of the conventional electromagnetic type for two reasons: the first is that the iron of the joke would degrade the flatness of the magnetic field in the detector and the second is that the overall transverse size of a conventional quadrupole is at least twice its useful aperture. Therefore quadrupoles realized with permanent magnets have been built, which exhibit an excellent field quality, very small transverse size and are fully transparent to external fields. The region of space around the IP occupied by machine elements, which is unavailable for the detection of decay particles by the experiment consists in two cones with the vertex at the IP and a half aperture of only 9 degrees. In order to obtain a good compensation of the above mentioned coupling effects induced by the solenoids, these quadrupoles are rotated around their longitudinal axis by angles between 10 and 20 degrees and are provided with actuators to finely adjust their position and rotation.

The structure of the FINUDA IR is quite similar. Since its superconducting solenoid magnet has half the length (but twice the field) of the KLOE one, the low- $\beta$  focusing at the IP is obtained by means of two permanent magnet quadrupole doublets inside the detector and completed with two other conventional doublets outside. Both IR's have been further modified during the 2003 shutdown.

The DEAR experiment, which was installed on the IR opposite to KLOE, took data during the years 2002-2003. It does not need magnetic field and therefore only conventional quadrupoles were used for the low- $\beta$ . FINUDA rolled-in at DEAR's place in the second half of 2003 and took data until spring 2004. It was then removed from IP2 in order to run the KLOE experiment with only one low- $\beta$  section at IP1.

Two synchrotron radiation lines, one from a bending dipole and the other from the wiggler are routinely operated by the DAΦNE-LIGHT group in a parasitic mode, providing to users radiation from the infrared to soft x-rays.

The vacuum chambers of the arcs have been designed to stand the high level of radiation power emitted by the beams (up to 50 KW per ring): they consist of 10 m long aluminum structures built in a single piece: its cross section exhibits a central region around the beam and two external ones, called the antechambers, connected to the central one by means of a narrow slot. In this way the synchrotron radiation hits the vacuum chamber walls far from the beam and the desorbed gas particles can be easily pumped away. The chambers contain water cooled copper absorbers placed where the radiation flux is maximum: each absorber has a sputter ion pump below and a titanium sublimation pump above.

The single cell copper radiofrequency cavities, one in each ring, are capable of running at 368 MHz and 250 KV and are designed with particular care to avoid high order modes which could induce longitudinal instabilities in the particular multibunch structure of the beams. This is obtained by means of external waveguides terminated on  $50\Omega$  loads. A sophisticated longitudinal feedback has, however, been built to maintain a reasonable safety margin on the threshold of multibunch instabilities. The system is based on the digital signal processing technique and acts on each single bunch individually. Additional feedback systems on the betatron motion have been also realized following the observation of coherent instabilities during collider operation.

The correct superposition of the beams at the IP is of course critical for the luminosity of the ring. For this reason, 46 beam position monitors are available in each ring and 31 small dipoles can be used to steer the beam and correct orbit distortions caused by alignment errors or wrong currents in the magnetic elements by means of sophisticated software procedures implemented in the Control System of the collider. Additional beam diagnostics are two synchrotron radiation outputs, from which the transverse and longitudinal size of the beam can be measured, total beam current monitors and strip-line pickups delivering the charge of each bunch.

In a low energy electron-positron collider, such as DAΦNE, the lifetime of the stored current is mainly limited by the Touschek effect, namely the particle loss due to the scattering of the particles inside the bunches. In the present operating conditions it is of the order of half an hour. It is therefore necessary to have a powerful injection system, capable of refilling the beam without dumping the already stored one. In addition, flexibility of operation requires that any bunch pattern can be stored among the 120 available buckets. The injection system of DAΦNE is therefore designed to deliver a large rate of particles in a single bunch at the working energy of the collider. It consists of a linear accelerator (LINAC, see Fig. 1) with a total accelerating voltage of 800 MV. In the first section electrons are accelerated to  $\approx 250$  MeV before hitting a tungsten target (called positron converter) where positrons are generated by bremsstrahlung and pair production with an efficiency of  $\approx 1\%$ . The positrons exit from the target with an energy of few MeV and are then accelerated by the second section of the LINAC to their final energy of  $\approx 0.51$  GeV. The positrons are then driven along a transfer line and injected into a small storage ring, called Accumulator, at a frequency of 25 Hz. Up to 19 positron pulses are stacked into a single bucket of the Accumulator, then injection stops and the bunch damps down to its equilibrium beam size and energy spread, which are much smaller than the LINAC ones. Damping takes  $\approx 0.1$  seconds and then the beam is extracted from the Accumulator and injected into the positron main ring at an overall repetition rate of 2 Hz. A powerful and flexible timing system allows the storage

of any desired bunch pattern in the collider. In the electron mode, the converter is extracted from the LINAC and electrons are directly accelerated to 0.51 GeV and injected into the Accumulator in the opposite direction with respect to positron operation. They are then extracted like in the positron case and injected into the electron main ring through the second transfer line.

The Accumulator has been introduced for the following reasons. The first is that the LINAC can deliver 10 ns pulses with a charge of  $\approx 1$  nC. Since the design charge of the main ring at the maximum luminosity is  $1.5 \mu\text{C}$  and the longitudinal acceptance of the main rings is only 2 ns, the number of pulses necessary to fill the ring is of the order of  $10^4$ . In order to avoid saturation it is therefore necessary that at each injection pulse a fraction smaller than  $10^{-4}$  of the already stored beam is lost, and this is not easy to achieve. The Accumulator instead can work with a lower frequency RF cavity and therefore with a larger longitudinal acceptance. In this way the full charge coming from the LINAC can be stored. The number of pulses into the Accumulator is only 19, and after damping the whole charge stacked into an Accumulator bunch can be stored into the main ring. In this way a single main ring bucket can be filled with only one pulse from the Accumulator, reducing to 120 the number of injection pulses into each main ring. As an additional benefit, the transverse beam size and energy spread of the beam coming from the Accumulator are at least one order of magnitude smaller than those of the LINAC beam, and this strongly reduces the aperture requirements of the main ring and, as a consequence, the overall cost of the collider.

## 2 DAΦNE main changes during 2003

During the six months shutdown occurred in 2003 the main machine modifications can be summarized as follows:

- KLOE IR extraction and reassembling according to a modified optics design and vacuum chamber upgrade: the IR lattice was changed from a triplet to a doublet structure in order to have the same low- $\beta^*$  characteristics while lowering the chromaticity with an overall improvement of the beam lifetime and beam-beam performance. At the same time the increased tunability of the low- $\beta^*$  lattice allows to double the number of colliding bunches (from 50 to 100) avoiding the parasitic crossings drawback on the luminosity.
- FINUDA detector installation, together with the insertion of a new Be vacuum chamber and four Permanent Magnet (PM) quadrupoles; as for the KLOE IR, the mechanics has been modified in order to allow for full rotation of the PM quadrupoles.
- wiggler magnets modification to increase the width of the good quality field region and get rid of the high order terms of the magnetic field. The main effect on the beam dynamics is a strong octupole term contribution affecting the dynamic aperture of the ring. A reduction of the octupole term by a factor  $\approx 2.5$  turned out from the measurements.

Further details of the overall machine modifications performed in 2003 can be found in the previous LNF Activity Report. In the following section the activities carried on during 2005 are described in detail.

## 3 Year 2005 activity

In March 2004 the FINUDA experiment completed its data taking and the first phase of its scientific program with the observation of the hypernuclear carbon.

In the following shutdown, started in April 2004, the FINUDA detector has been removed from the collider and parked in the pit. At the same time its Interaction Region has been replaced with a straight section equipped with electromagnetic quadrupoles. It was originally based on four

permanent magnet devices placed inside the FINUDA 1.1 T solenoid and on four conventional quadrupoles outside. With this new section the collider has only one low beta point at the KLOE IR with smooth optical functions in the other IP, allowing for a more efficient separation of the two beams.

DAΦNE operation for KLOE restarted in May 2004 with the goal of delivering  $2fb^{-1}$  integrated luminosity before the end of 2005.

KLOE commissioning started with the compensation of the betatron coupling by rotating the permanent quadrupoles inside the KLOE solenoid, reaching an optimal value of 0.3%. Then, with a continuous optimization involving mainly the main ring optics and the feedback systems, the peak luminosity has been increased above the maximum obtained in the 2002 KLOE run reaching the value of  $1 \times 10^{32}cm^{-2}s^{-1}$  during the next four months and  $1.25 \times 10^{32}cm^{-2}s^{-1}$  by the end of 2004, see Fig. 3.

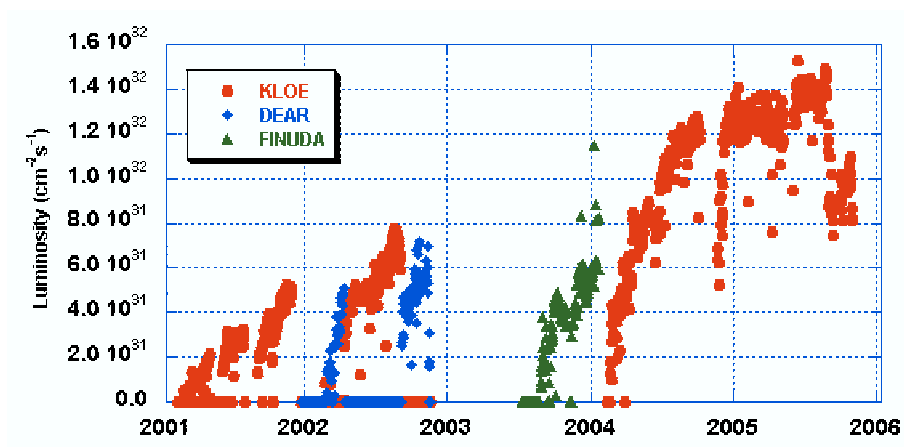


Figure 3: evolution of the DAΦNE peak luminosity since 2001: KLOE (dots), DEAR (squares) and FINUDA runs (triangles).

In November 2004 the field of the wiggler magnets has been increased by 2% to add more damping for the betatron and synchrotron oscillations in order to improve the beam stability and the beam beam interaction. As a result an increase of the geometric luminosity (i.e. the luminosity normalized by the product of the colliding beam currents) and of the integrated luminosity has been observed.

The activity of DAΦNE in 2005 has been mainly dedicated to the KLOE experiment with short periods devoted to machine studies to investigate the limiting factors in the maximum achievable luminosity.

In November 2005 KLOE completed its data taking at the  $\Phi$  resonance. The best collider performances can be summarized as follows:

- number of bunches per beam 105 + 105;
- total current in the colliding beams e-/e+ 1.8/1.3 A;
- peak luminosity  $1.53 \times 10^{32}cm^{-2}s^{-1}$ ;
- maximum integrated luminosity per day  $10pb^{-1}$ ;
- total logged luminosity (May 2004 - Nov 2005)  $2fb^{-1}$ .

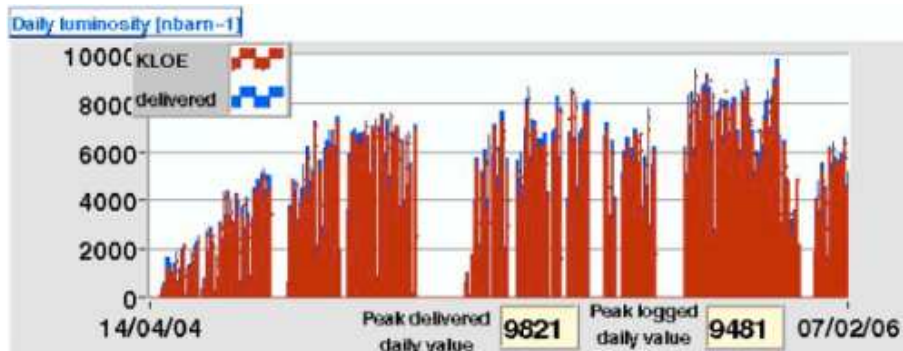


Figure 4: *daily integrated luminosity during the KLOE run. It exhibits a steady improvement and its maximum value of  $\approx 10pb^{-1}$  per day has been obtained in November 2005. The last bins with lower integrated luminosity correspond to the off energy operations.*

The last part of the KLOE program started in November 2005 with the scan of the  $\Phi$  resonance. Collision have been delivered changing the center of mass energy by + 3 MeV, -2 MeV and  $\pm 10$  MeV with respect to the nominal one. Moreover the experimental program required  $200pb^{-1}$  20 MeV below threshold. At each point a new configuration of the injection system has been computed scaling all magnetic elements according to the calibrations. The energy of the main rings has been moved by scaling all the quadrupoles and dipoles while keeping the current in the wiggler magnets constant, since they were working already at their maximum excitation. Moreover the ring optics has been optimized to maintain the proper value of the Twiss functions at the Interaction Point, since the KLOE low- $\beta$  section relies on permanent quadrupoles providing different focusing at different energies. Using this approach it has been possible to minimize the efforts to optimize the collider configuration at an energy different from the nominal and to recovery good performances in a very short time.

An integrated luminosity of  $10pb^{-1}$  has been delivered at each energy during the scan of the  $\Phi$  resonance, with a peak luminosity around  $10^{32}cm^{-2}s^{-1}$ . Eventually the collider has been configured for the off-energy run.

### 3.1 Machine Studies

The bunch length in the electron ring is longer than in the positron one because to the higher impedance due to the ion-clearing electrodes. Moreover the bunch length and bunch vertical size increase with the stored current, as shown in Fig. 5 and Fig. 6, affecting the maximum achievable luminosity. To understand and cope with these effects the dependence of the beam blow upon current, RF voltage and momentum compaction has been studied.

The momentum compaction  $\alpha_c$  is the ratio of the relative trajectory length deviation and the relative energy deviation; the optics used during the KLOE runs has  $\alpha_c = 0.02$ . Measurements have shown that with a higher  $\alpha_c$  it is possible to reduce the transverse blow up and the bunch lengthening, see Fig. 7 and Fig. 8, and that the transverse effects are correlated with the longitudinal microwave instability.

Theoretical simulations predict that, for the same absolute value of the momentum compaction, the bunch length is shorter when  $\alpha_c$  is negative than when it is positive. Moreover in such a lattice there is no head-tail instability with negative chromaticity and beam beam effects as well as synchrotron resonances are less harmful. For this reason several machine runs have been dedicated to study beam dynamics with a negative  $\alpha_c$ . The lattice flexibility and accuracy of

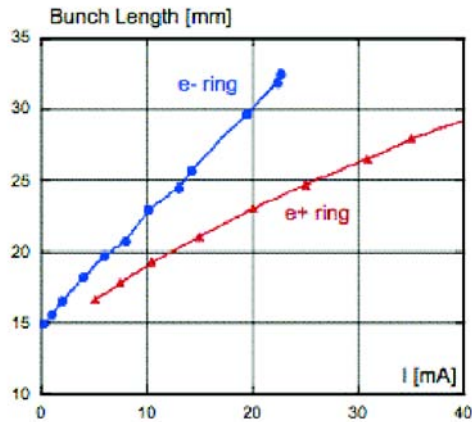


Figure 5: measured bunch length as a function of the stored current in the bunch for the electron (dots) and positron (triangle) ring.

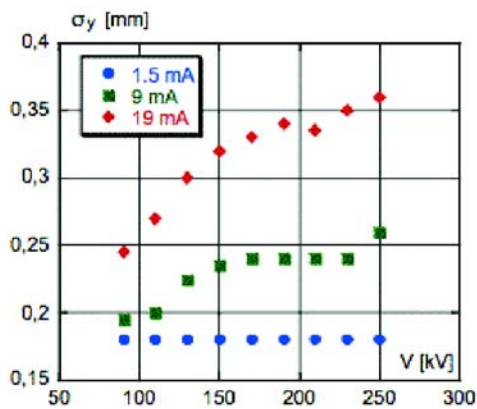


Figure 6: vertical bunch size as a function of the voltage of the radio frequency cavity for several values of the current  $I$  stored in one single bunch:  $I = 1.5$  mA (dots),  $I = 9$  mA (squares) and  $I = 19$  mA (rhombs).

the model have allowed to implement successfully an optics with  $\alpha_c = -0.02$ . Measurements have confirmed the theoretical expectations, observing a 35% reduction in the bunch length, see Fig. 9, and high current bunches have been stored with large negative chromaticity.

1 A current has been stored in both the electron and the positron beams after proper tuning of the radio frequency and the feedback systems. A first trial to perform collisions at low current, 200 mA per beam, has given a luminosity of  $2.5 \times 10^{31} \text{cm}^{-2} \text{s}^{-1}$ , quite similar to the results obtained with the nominal optics with  $\alpha_c > 0$  at the same currents.

Since the restart of DAΦNE operation for KLOE a threshold has been observed in the maximum storable positron current. This phenomenon has been analyzed in detail and it has been found that the threshold is compatible with a fast horizontal instability driven by the secondary electrons extracted from wall of the vacuum chamber by the synchrotron radiation, a very well known effect observed in other colliders, called electron cloud instability. The effect has been cured by improving the transverse horizontal feedback obtaining a maximum positron current of 0.7 A

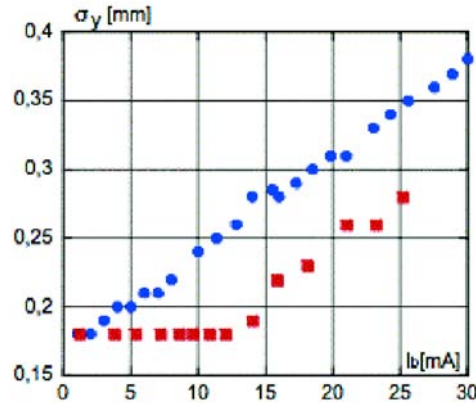


Figure 7: measured bunch length as a function of the current stored in the bunch for different values of the momentum compaction:  $\alpha_c = 0.020$  (dots),  $\alpha_c = 0.034$  (squares).

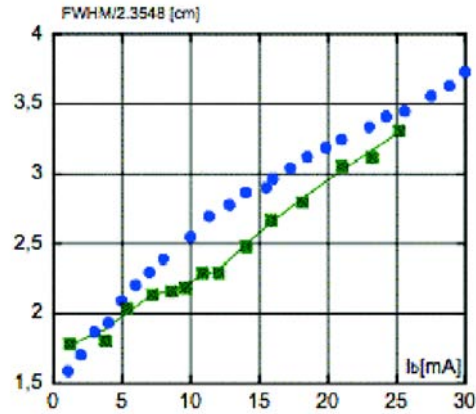


Figure 8: vertical bunch size as a function of the current stored in the bunch for different values of the momentum compaction:  $\alpha_c = 0.020$  (dots),  $\alpha_c = 0.034$  (squares).

in single beam and 1.3 A in collision.

### 3.2 R&D Activity

New kickers have been designed to improve the injection efficiency of DAΦNE, this activity being synergic with the R&D effort for the International Linear Collider (ILC) damping rings. The kicker is a strip line structure and the design has been based on the idea to taper the strips in order to simultaneously reduce the impedance of the device and to improve the deflecting field quality. The design has been done using 2D and 3D electromagnetic simulation codes.

Compared to the present injection kickers the project of the new ones exhibits:

- much shorter pulse ( $\approx 5$ ns instead of  $\approx 150$ ns);
- better transverse uniformity of the deflecting field;
- reduced broadband impedance;
- possibility of 50 Hz repetition rate.

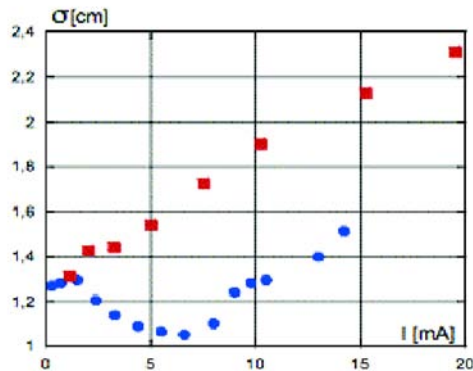


Figure 9: *measured bunch length as a function of stored current stored for negative and positive values of the momentum compaction:  $\alpha_c = -0.02$  (dots),  $\alpha_c = 0.02$  (squares).*

The much shorter pulse perturbs only the stored bunch corresponding to the injected one instead of about 50 bunches as in the present scheme, see Fig. 10. This can strongly reduce the background to the experiment during injection and increase the positron current threshold, as observed when the kicker pulse length was halved from 300 to 150 ns.

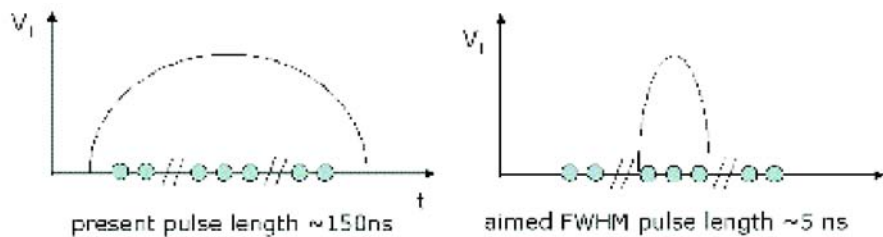


Figure 10: *pulse length of the injection kickers left: present device; right: new project.*

Concerning the reduced broadband impedance, first calculations give a reduction of  $\approx 50\%$  with respect to the present kickers. Moreover, since the new kickers have been designed with the same beam pipe cross section of the dipole region, no tapers are needed between the dipoles and the kicker and this also contributes to the reduction of the overall machine impedance. Finally, the possibility of 50 Hz injection might be useful for future upgrades of the collider.

The mechanical drawing of the device has been prepared and is shown in Fig. 11. The structure is fed with high voltage (50 kV) short (5ns) pulses. Tests on high voltage feedthroughs are under way.

#### 4 Future Plans

The present physics program of DAΦNE is expected to be completed by 2009. KLOE will stop its data collection by the end of March 2006 and the whole detector will be removed from the collider. In the next four years two runs for FINUDA and one for SIDDHARTA have been planned with the following tentative time schedule:



Figure 11: *mechanical drawing of the injection kicker.*

- KLOE removal and FINUDA installation ( $2^{nd}$  run): Apr - Jul 2006;
- FINUDA removal and SIDDHARTA installation: half 2007;
- SIDDHARTA removal and FINUDA installation ( $3^{rd}$  run): spring 2008.

During the shut downs, necessary to switch among different experiments, several smooth upgrades should be implemented to improve the peak and the integrated luminosity relying on the experience gathered during the machine studies. The modifications of DAΦNE will be mainly aimed at reducing the impedance in the electron ring, at increasing the current stored in the positron beam, at reducing the impact of the long range beam beam interaction and at improving the lifetime of the colliding beams.

On the long term the DAΦNE staff is working at the project of a new machine, DAΦNE-2. It is a double ring collider designed to run at the energy of the  $\Phi$  resonance (1020 MeV c.m.) with a luminosity of  $10^{32}\text{cm}^{-2}\text{s}^{-1}$  and at the energy of 2400 MeV c.m with a lower luminosity of  $10^{33}\text{cm}^{-2}\text{s}^{-1}$ . This collider will allow experiments both in the field of high energy and nuclear physics. A conceptual design report will be presented by the end of September 2006.

## 5 Publications

1. Karl L.F. Bane, SLAC; Katsunobu Oide, KEK; Mikhail Zobov, INFN-LNF: “Impedance Calculation and Verification in Storage Rings”, SLAC-PUB-11007, January 2005.
2. D. Alesini, G. Benedetti, M. Biagini, C. Biscari, R. Boni, M. Boscolo, A. Clozza, G. Delle Monache, G. Di Pirro, A. Drago, A. Gallo, A. Ghigo, S. Guiducci, M. Incurvati, C. Ligi, F. Marcellini, G. Mazzitelli, C. Milardi, L. Pellegrino, M. Preger, P. Raimondi, R. Ricci, C. Sanelli, M. Serio, F. Sgamma, B. Spataro, A. Stecchi, A. Stella, C. Vaccarezza, M. Vescovi, M. Zobov, INFN-LNF; C. Pagani, INFN-MI-LASA; E. Levichev, P. Piminov, D. Shatilov, BINP; J. Byrd, F. Sannibale, LBLNL; J. Fox, D. Teytelmann, SLAC: “Proposal of a Bunch Length Modulation Experiment in DAΦNE”, LNF-05/4(IR), 22/02/2005.

3. Gabriele Benedetti: “DAFNE Lattice With Two low- $\beta$  Interaction Regions”, LNF05/ 10 (Thesis), June 1, 2005.
4. M. Zobov, D. Alesini, G. Benedetti, M.E. Biagini, C. Biscari, R. Boni, M. Boscolo, A. Clozza, G. Delle Monache, G. Di Pirro, A. Drago, A. Gallo, A. Ghigo, S. Guiducci, M. Incurvati, C. Ligi, F. Marcellini, G. Mazzitelli, C. Milardi, L. Pellegrino, M. A. Preger, P. Raimondi, R. Ricci, C. Sanelli, M. Serio, F. Sgamma, B. Spataro, A. Stecchi, A. Stella, C. Vaccarezza, M. Vescovi, LNF-INFN; E. Levichev, P. Piminov, D. Shatilov, BINP; J. Fox, D. Teytelman, SLAC: “DAΦNE Operation and Plans for DAFNE2”, Presented at the 2005 Particle Accelerator Conference (PAC2005), Knoxville, Tennessee, USA - May 16-20, 2005; LNF-05/26 (P), 20/12/2005.
5. C. Biscari, D. Alesini, G. Benedetti, M.E. Biagini, R. Boni, M. Boscolo, A. Clozza, G. Delle Monache, G. Di Pirro, A. Drago, A. Gallo, A. Ghigo, S. Guiducci, M. Incurvati, C. Ligi, F. Marcellini, G. Mazzitelli, C. Milardi, L. Pellegrino, M.A. Preger, P. Raimondi, R. Ricci, C. Sanelli, M. Serio, F. Sgamma, B. Spataro, A. Stecchi, A. Stella, C. Vaccarezza, M. Vescovi, M. Zobov, LNF-INFN; C. Pagani, INFN-Milano LASA; E. Levichev, P. Piminov, D. Shatilov, BINP; J. Byrd, F. Sannibale, LBL; J. Fox, D. Teytelman, SLAC: “Proposal of an Experiment on Bunch Length Modulation in DAΦNE”, Presented at the 2005 Particle Accelerator Conference (PAC2005), Knoxville, Tennessee, USA - May 16-20, 2005; LNF-05/26 (P), 20/12/2005.
6. A. Drago, M. Zobov, INFN-LNF; Dmitry Teytelman, SLAC: “Recent Observations on a Horizontal Instability in the DAΦNE Positron Ring”, Presented at the 2005 Particle Accelerator Conference (PAC2005), Knoxville, Tennessee, USA - May 16-20, 2005; LNF-05/26 (P), 20/12/2005.
7. D. Alesini, C. Biscari, R. Boni, A. Gallo, F. Marcellini, M. Zobov, INFN-LNF; Carlo Pagani, INFN-LASA and DESY: “Design of a Multi-Cell, Hom Damped Superconducting Cavity for the Strong RF Focusing Experiment at DAΦNE”, Presented at the 2005 Particle Accelerator Conference (PAC2005), Knoxville, Tennessee, USA - May 16-20, 2005; LNF-05/26 (P), 20/12/2005.
8. A. Drago, M.E. Biagini, S. Guiducci, C. Milardi, M. Preger, C. Vaccarezza, Mikhail Zobov, INFN- LNF: “Phase-Space Dynamic Tracking by a two Pickups Data Acquisition System”, Presented at the 2005 Particle Accelerator Conference (PAC2005), Knoxville, Tennessee, USA - May 16-20, 2005; LNF-05/26 (P), 20/12/2005.
9. R. Cimino, A. Drago, C. Vaccarezza, M. Zobov, INFN-LNF; G. Bellodi, CCLRC/RAL/ASTeC, Didcot; D. Schulte, F. Zimmermann, CERN; G. Rumolo, GSI; K. Ohmi, KEK; M. Pivi, SLAC: “Electron Cloud Build-up Study for DAΦNE”, Presented at the 2005 Particle Accelerator Conference (PAC2005), Knoxville, Tennessee, USA - May 16-20, 2005; LNF-05/26 (P), 20/12/2005.
10. Mahne, TASC-INFN Trieste; A. Giglia, S. Nannarone, TASC-INFN Trieste and Univ. Modena e RE Modena; R. Cimino, C. Vaccarezza, LNF-INFN: “Experimental Determination of E-Cloud Simulation Input Parameters for DAΦNE”, Presented at the 2005 Particle Accelerator Conference (PAC2005), Knoxville, Tennessee, USA - May 16-20, 2005; LNF-05/26 (P), 20/12/2005.
11. C. Biscari: “Bunch Length Modulation in Highly Dispersive Storage Rings”, Phys. Rev. ST Accel. Beams 8, 091001 (2005) [11 pages] [Issue 9 1 September 2005].

## The DAΦNE Beam Test Facility (BTF)

The BTF Staff:

B. Buonomo (Art. 22), G. Mazzitelli (Resp.), L. Quintieri (Art. 23), P. Valente (Art. 23)

The DAΦNE Operation Staff:

G. Baldini, P. Baldini, M. Belli, B. Bolli, B. Beatrici, G. Ceccarelli,  
R. Ceccarelli, A. Cecchinelli, S. Ceravolo, R. Clementi, O. Coiro, S. De Biase, M. De Giorgi,  
N. De Sanctis, M. Di Virgilio, G. Ermini, C. Fusco, O. Giacinti, E. Grossi, F. Iungo, R. Lanzi,  
C. Marini, M. Martinelli, M. Masciarelli, E. Passarelli, V. Pavan, D. Pellegrini, R. Pieri,  
G. Piermarini, S. Quaglia, M. Sardone, M. Scampati, G. Sensolini, A. Sorgi, M. Sperati,  
A. Spreccacenero, R. Tonus, T. Tranquilli, M. Troiani, R. Zarlenga

### 1 Description of the DAΦNE BTF 2005 Activities

During 2004 and 2005 the DAΦNE Beam Test Facility (BTF) <sup>1)</sup> was effectively operating for a about 580 days (more than the foreseen and scheduled availability), delivering beam to 24 research groups (55% of which TARI funded) corresponding to 140 users from all over the world. The complete list of the hosted experiments is reported just below, while the relevant results derived from the measurements performed in BTF are described only for few of these in the next sections.

Regarding the upgrade and new implementations, since September 2005 a photon tagging source is also available in BTF, while a study of feasibility of neutron source has been started and it is still in progress.

The Beam Test Facility staff also continued the optimization of the beam characteristics, the improvement of diagnostic tools <sup>2)</sup>, as well as of the DAQ system, user devices, controls and management software.

### 2 2005 User Experiences

Many test-beam and experiments have used the DAΦNE BTF during 2005, requiring very different beam characteristics and operating conditions. The user experiences are essentially classified on the base of the required beam intensity :

#### **High multiplicity in a wide range of energies:**

AIRFLY <sup>3)</sup>, APACHE <sup>4)</sup>, FISA<sup>1</sup>, FLAG <sup>5)</sup>, RAP <sup>6)</sup>.

#### **Low multiplicity or single electron mode at different energies:**

AGILE-payload <sup>7)</sup>, BENICE <sup>8)</sup>, BTeV <sup>9)</sup>, GRAAL <sup>10)</sup>, LAZIO <sup>11)</sup>, LHCb-LNF <sup>12)</sup>, LHCb-RICH <sup>13)</sup>, CaPiRe <sup>14)</sup>, OPERA <sup>15)</sup>, P326 <sup>16)</sup>, PASSRA <sup>17)</sup>, SIDDHARTA <sup>18)</sup>.

About a month over the year has been also dedicated in parasitic way to experiments and operation tests with educational purpose. Students from Roma II and Roma I universities, as well as students and teachers from high schools, took part in simple experiments or in the operation of the facility.

---

<sup>1)</sup>The LNF radiation protection Group (U.F. Fisica Sanitaria) tested its Bonner Spheres for neutron spectrometry, using neutrons produced by attenuating the BTF electron beam in optimized lead targets. The publication of these results is in progress.

## 2.1 The Photon Tagging Source in BTF: Installation and Performance

The purpose of the Italian space mission AGILE is to detect the gamma rays coming both from inside and outside our galaxy. The AGILE instrumentation consists of a gamma-ray detector and a tracking system for the measurement of the energy and direction of the gamma rays (figure 1 shows the detector core integrated with the upper part of the spacecraft).



Figure 1: The AGILE detector integrated on the upper part of spacecraft



Figure 2: The AGILE instrument and upper part of the satellite on the gamma ray photon beam at the BTF, November 3, 2005

For the calibration of the detector, an exposition of the whole experimental apparatus to a photon beam with energy ranging from 20 to 800 MeV was required. In this frame, at the beginning of 2005, the AGILE team and the DAΦNE-BTF staff started a collaboration to design and realize a Photon Tagging Source in the BTF experimental hall, using the electrons from the DAΦNE-Linac. Photons in BTF are, in fact, produced by bremsstrahlung of electrons (with maximum momentum of 750 MeV/c) on silicon chambers placed at the inlet of the bending magnet downstream in the BTF transfer line. The photons are tagged in energy using the same bending dipole magnet, whose internal walls have been covered by silicon microstrip detectors (the layout of the photon tagging system is shown in figure 3). Depending on the energy loss in the photon production, the electrons knock against different strips, once the dipole magnetic field has been set to a given value. The correlation between the direction of the electron, measured by x-y silicon chambers, and the position where the electron impinges on the silicon module inside the magnet allows the tagging of the produced photons, with an energy resolution  $\leq 7\%$ .

During 2005, the photon tagging system has been successfully implemented and integrated in the BTF equipment and it is now available for scientific use by the community. For the future it is planned to assemble the electronics of the silicon chambers in a more compact structure in such a way to realize smaller modules that can be easily fitted inside the pipeline. The silicon chambers will be also equipped with a motorized system to insert and extract the chambers from

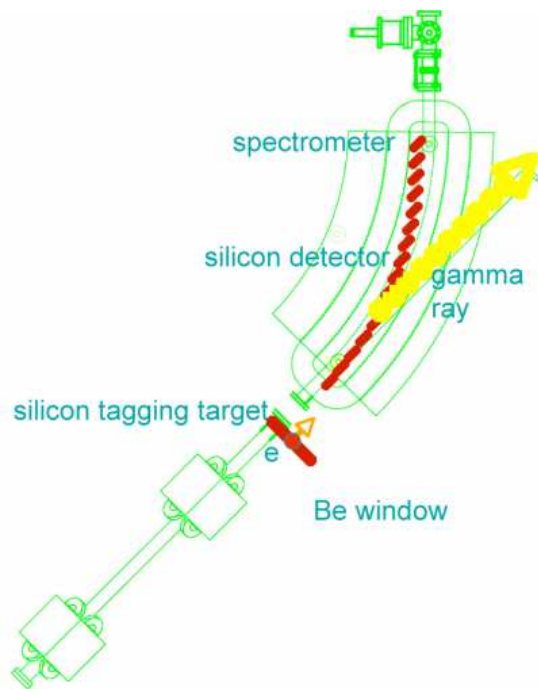


Figure 3: Layout of the photon tagging system: the red lines refer to the silicon detectors respectively placed at the inlet of the bending magnet and on the inner wall of the dipole

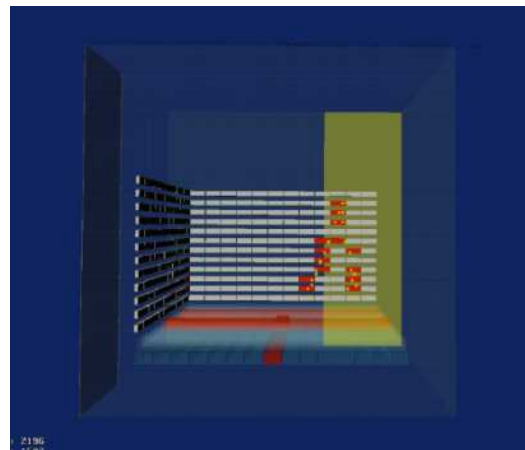


Figure 4: First gamma ray photon detected by AGILE at BTF-LNF

the pipeline according to the user needs.

In what follows it is described the series of tests under beam performed on the main components of the photon source for calibration purposes, in collaboration with the Trieste University section of the AGILE team.

### 2.1.1 Photon Source Calibration

At the beginning of 2005 a module of the photon tag facility (consisting of one silicon detector) has been successfully tested in collaboration with the Trieste section of the AGILE team. The module was put inside the final bending magnet of the BTF transfer line and, adjusting the magnet current in such a way to have the particle beam impinging on the silicon detector, it was possible to calibrate the detector response at different energies. Afterwards the x-y silicon chambers have been inserted upstream the same bending dipole (just before the last quadrupole) in such a way to intercept the electron beam, in order to study the photon production. For this reason the transfer line has been opened and it is still in air for about 7 cm length.

Moreover, the NaI calorimeter positioned at the end of the photon line allowed to measure the energy of the photons so to check the calibration of the silicon spectrometer.

For this part of calibration about 5 shifts were assigned for about 32 days partially shared with other experiments.

## 2.2 Final Calibration of the AGILE Paylod in BTF

The AGILE satellite, that will be launched in 2006 for studying the galactic and extra-galactic gamma rays in the range of 30 MeV-50 GeV, has been completely calibrated at the end of November 2005 at the BTF using photons of known energy produced by the photon tagging system.

The installation of the AGILE instrumentation in BTF started at the beginning of November 2005 and took some days for the positioning and tuning-up of the payload (having a mass of about 200 kg) on the Mechanical Ground Support Equipment (MGSE) in front of the beam (see figure 2). The MGSE is a sophisticated and completely automatized system by which the payload could be translated and rotated with respect the beam line. Moreover the MGSE allowed to control the significant environment parameters (i.e cleanliness, humidity and temperature) of the spacecraft in which the payload has to be hosted.

After 48 hours from the arrival in BTF the first gamma-photon was detected by AGILE (on November 4, 2005) and this event has been reconstructed as shown in figure 4. The first measurements have been taken with photons at 650 MeV, followed by a week of calibration at 463 MeV and, after having reduced the background by suitable lead shielding, the data taking was concluded with measurements again at 650 MeV (from 18 to 20 November).

In order to calibrate in the high energy range, for the first time after the 2004 upgrade the BTF line has been operated at 700 MeV. The AGILE gamma-ray calibration campaign was successfully concluded in November 21st, thanks to a synergic collaboration between the DAΦNE/BTF staff and AGILE team, that allowed the simultaneous optimal operation of both KLOE and AGILE. The LINAC beam was delivered to the BTF with 20 minutes average runs, obtaining about 60% of the DAΦNE collider time and causing a decrease of KLOE accumulated luminosity less than 30%.

Taking into account that the expected rate for the gamma rays in the field of view above 100 MeV is around 500-2000 per day, the gamma-ray events produced in BTF have provided, during the tests, a very satisfactory and useful statistics: the rate of tagged photons had an average value of 1000/h (see figure 5) for an overall production (referring to the entire data taking period) of about 200.000 tagged photons between 20-450 MeV with a 0.5 Hz production rate. In figure 6, the measured spectra of the tagged photons has been also reported.

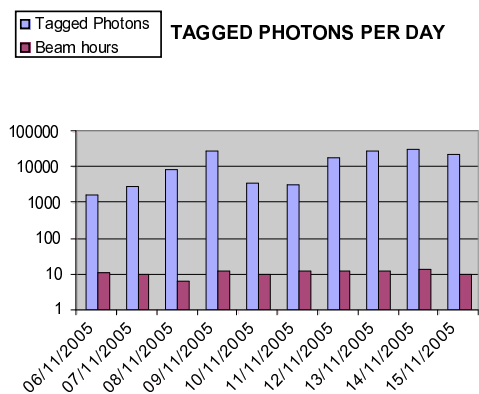


Figure 5: Tagged photons per days and hours of beam delivered in BTF

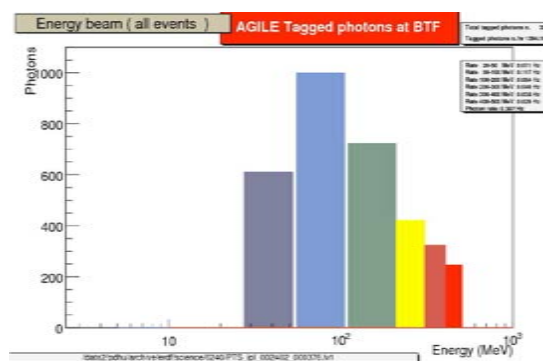


Figure 6: Tagged photons spectra in BTF

The final calibration of the overall AGILE instrumentation required about 20 days, partially shared with other experiments.

### 2.3 LHC-b-RICH Measurements in BTF

In december 2005 a setup has been installed in BTF to test the Pixel Hybrid Photo-Detectors (PHPD) of the Ring Imaging Cherenkov counters for the LHCb experiment.

Each photon detector consists of a vacuum tube closed on one side by a quartz window supporting a photocathode evaporated on its inner surface and on the other side by a pixelised silicon sensor bump-bonded to the encapsulated readout frontend chip (this one running at the LHC 40 MHz clock). Three electrodes provide a cross focussing field between the grounded sensor and the photocathode at -20 kV. This device has been designed to provide the LHCb-RICH detector a high spatial resolution and a good single photon detection efficiency.

For the first time in December 2005, a column equipped with 12 Pixel Hybrid Photo-Detectors and the final electronics chain have been linked together and tested with a charged particle beam at the DAΦNE-BTF. During the tests, the photon detection and data collection efficiency of the LHCb RICH readout system have been measured.

Over one million single electron events were collected on tapes, for a total of 6.5 GB of data.

In figure 7 it is shown the Cherenkov ring obtained with 500 MeV electrons (each pixel corresponds to  $2.5 \times 2.5 mm^2$  on the photocathode) with an integrated run of more than 130000 events collected on a single photo detector. An indirect estimate of the divergence of the BTF beam can be derived using this photo detector imaging: a value of about 2.5 mrad has been obtained, confirming the high quality and strong stability of the beam transported in BTF.

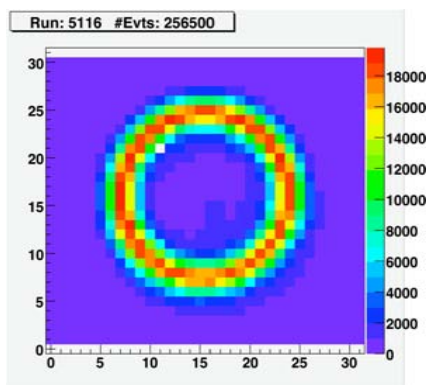


Figure 7: Cherenkov ring on a single PHPD, irradiated with 500 MeV electron beam

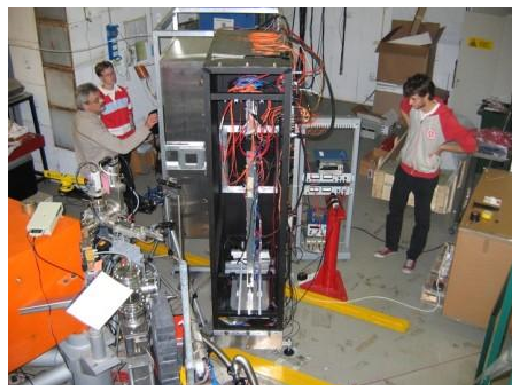


Figure 8: LHCb installation in BTF experimental hall

This experiment had about 10 days assigned in December 2005, partially shared with other experiments, corresponding to a BTF run time of about 50%, that means an availability above the user expectations according the initial agreements.

### 2.4 APACHE (Aerogel Photographic Analysis of Cerenkov Emission)

The experiment aim was to test the light diffusion within the aerogel that negatively affects the performance of the material used as Cerenkov radiator for LHCb-RICH. The measurements in BTF on the uniformity of aerogel tiles for LHCb finished in November 2004. The data analysis was completed soon after and successfully published on journal <sup>19)</sup>, as well as on some master thesis (Ecole Polytechnique Federale de Lausanne, 2005 and in Università di Milano Bicocca).

In November 2005 the same technique was adopted to qualify aerogel samples for the AMS experiment and measurements were successfully carried out in the BTF.

About 5 days (from November 30 to December 4) were assigned to this experiment, partially shared with others BTF users.

## 2.5 Acoustic Detection of Particle in BTF: the RAP Measurements

The RAP (Rivelazione Acustica di Particelle) experiment has the aim to study the mechanical vibrations of small metallic resonant bar to short pulses of high energy electrons, investigating how the conversion efficiency of the particle energy into acoustic vibrations could change between normal and super-conducting state.

The experiment needs of beam spots of large integrated number of particles, in order to release almost 100 TeV in the bar. A low noise beam monitor, placed at the end of the BTF transfer line, has been used to measure the beam intensity.

During May 2005 a niobium bar has been cooled down to 4 K inside a cryostat placed in front of the final bending magnet in the BTF experimental hall (see figure 10), in such a way that the beam could arrive in the middle section of the cylinder, perpendicularly to the cylinder axis. The amplitudes of the first longitudinal mode of the cylindric bar were measured after the collision with a 510 MeV electron beam generated by the DAΦNE-LINAC and compared with the ones expected by the theoretical prediction (Thermo Acoustic Model) <sup>20</sup>.

This is the first time that the Thermo-Acoustical Model has been checked on a superconducting bulk. Moreover, the measurements taken in BTF have allowed to reconstruct the transition curve for the Niobium by a technique (thermo-acoustic conversion) different from the consolidated methodologies normally used in superconducting solid-state physics. The transition curve is shown in figure 9 where the maximum amplitude of the 1st longitudinal mode of the niobium bar normalized to the deposited energy has been reported versus the temperature. In this figure the blue squares refer to the measured values while the green dots are the theoretical predictions using the normal thermodynamic properties of the Niobium and the red ones the theoretical ones estimated using the superconducting properties.

The RAP experiment is partially funded by TARI (Transnational Access to major Research Infrastructures) and during 2005 had assigned 26 days, few of which partially shared with other experiments, while the majority had dedicated runs. Future plans for the RAP experiment foresee to put under beam, in the DAΦNE-BTF, an Al5056 bar, cooled down to 1 K by a dilution refrigerator, by the end of 2006.

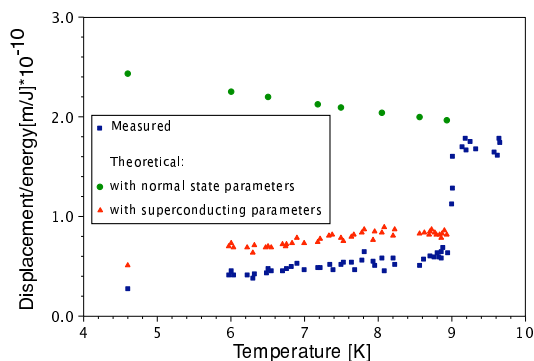


Figure 9: Niobium. Maximum amplitude of the 1st longitudinal mode normalized to the deposited energy vs. temperature.



Figure 10: RAP installation in BTF experimental hall

### 3 Study of Feasibility of a Neutron Source at the DAΦNE BTF facility

The usefulness of neutron sources in the domain of condensed matter research is well recognized and in some case the slow neutrons represents an important complementary investigation tool respect to the synchrotron radiation <sup>21</sup>).

High energy electrons impinging on a target produce a continuous spectrum of bremsstrahlung photons. These gamma rays can generate neutrons via photo-nuclear reactions (the electron directly release few neutrons with respect to the other nuclear mechanisms). As the nucleons are bounded in the nucleus, the ( $\gamma,n$ ) reaction will occur only if the gamma-ray energy is at least equal to the binding energy of the neutron in the target nucleus (the photo-neutron production is a threshold reaction, i.e. can occur only for  $E \geq E_{th}$ ).

#### 3.1 Preliminary Estimation of Neutron Rate achievable in BTF

In order to produce neutrons in BTF, the DAΦNE electron beam has to impinge on a suitable target so that to generate a shower of bremsstrahlung photons, that, consequently, will have an energy spectrum end point equal to the electron beam energy. The maximum energy that the electrons can reach in the DAΦNE-LINAC is about 800 MeV, however, for the calculations developed in the following, the nominal value of 510 MeV has been considered to give some preliminary estimations of the neutron rates.

The rate of neutron produced by photo-absorption depends essentially on the following factors:

- Beam power released in the target
- Atomic number,  $Z$ , of the target nuclei
- Energy of the electron in the beam

For safety reasons, the maximum rate of electrons that, at present time, can be transported in BTF has been set to  $10^3 e^-/s$  (that means a mean of 20 electron per pulse at a repetition rate of 50 Hz), anyway, a requirement to enhance the permitted electron flux (up to the whole Linac flux) has been already presented to the *National Regulatory Authority*.

A first estimation of the maximum beam power that can be released on a target assumes that the DAΦNE beam could be entirely transported in the BTF (disregarding the present safety limit)<sup>2</sup>:

$$P_{beam} = N \cdot f \cdot E = 0.04 \text{ kW} \quad (1)$$

where  $N \simeq 10^{10}$  particles/bunch,  $f=50$  Hz is the repetition injection rate (equivalent to  $4.9 \cdot 10^{11}$  electrons per second) and  $E=510$  MeV is the beam energy.

Using the Swanson formula and the related curves reported in <sup>22</sup>), a preliminary estimation of the maximum neutron rate reachable in BTF has been derived for different materials and the results are listed in the table 3.1

It is important to remark that these values can be applied for target enough thick that all the energy of the ensuing electromagnetic cascade is absorbed in the target (that is for thickness greater than  $5X_0$ , where  $X_0$  is the radiation length).

Montecarlo simulations (by FLUKA code) are in progress in order to give a more accurate estimation of the neutron rate as well as to study the neutron energy spectra and spatial distribution as function of the thickness of a fixed material.

---

<sup>2</sup>Only few tenth of microwatt could be delivered on target with the present limit for the electron rate in BTF

$P_{beam} = 0.04kW @ 510 \text{ MeV}$		
Target Material	Neutron Rate [n/s]	Conversion Rate
Al	$2 \cdot 10^{10}$	$4 \cdot 10^{-2}$
Cu	$4 \cdot 10^{10}$	$8 \cdot 10^{-2}$
Pb	$4 \cdot 10^{10}$	$16 \cdot 10^{-2}$

Table 1: Neutrons produced per second for a given beam of  $4.9 \cdot 10^{10} e^-/s$  at 510 MeV

In fact, the energy spectrum of the neutron depends, once fixed the material, on the thickness of the target, so that an optimum value for which the neutron flux is maximum at a defined energy can be found.

#### 4 Diagnostic Tools Improvement

The DAΦNE-BTF facility has to provide electron and positron beams in a wide range of intensity, from single particle up to  $10^{10}$  particles per pulse, and energy from a few tens MeV up to 800 MeV. This wide range of operation has required the implementation of different beam profile and multiplicity monitors.

For low multiplicity, a Beam Profile Monitor (BPM) made of two strip detectors has been developed. Each detector covers a surface of  $8.9 \times 8.9 cm^2$  with 400  $\mu m$  thick silicon strips<sup>24</sup>). The chambers are able to measure the beam profile with a spatial resolution of about 40  $\mu m$ .

The Silicon Beam Chambers were calibrated by comparing their beam multiplicity readout with the number of electrons derived from the measurement of the total energy deposited in the NaI calorimeter. The beam profile measurements performed for different beam intensity allowed to conclude that the beam spot dimension increases linearly with respect to the number of particles impinging on the detector, as shown in figure 11.

In order to cover efficiently the range of high multiplicity, a beam profile monitor has been also studied and realized in collaboration with the Trieste Section of the AGILE team. In figure 12 the results of the tests on the profile monitor show that the response of the monitor increases linearly with respect to the increasing multiplicity for different energies, also in the range of high beam intensity.

All the devices for diagnostic developed during 2005 have been already integrated in the DAQ system and are going to be available for BTF users.

#### 5 Future Plans and Conclusions

A pulsed power supply for the dipole at the inlet of the BTF transfer line will be mounted during the shutdown maintenance of DAΦNE scheduled for June 2006, in order to make the BTF able to operate in a quasi-continuous regime, that means the possibility to feed the BTF transfer line even during the  $e^-/e^+$  injection in the main rings of the collider.

In fact this power supply object will be used to extract from the beam, accelerated by the LINAC, the particle pulses for the BTF. This will be done essentially in two different operational modes: 1 Hz operation and 2 Hz operation. Thanks to this pulsed power supply for the dipole, the BTF duty-cycle is expected to be better than 90%. The other plans for the year 2005 are, in addition to running the facility for all the available time, to continue the improvements of the diagnostics tools and of the infrastructure.

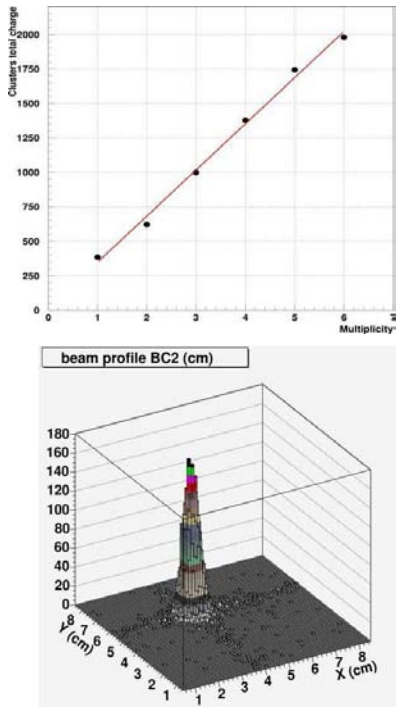


Figure 11: *Top*: Beam multiplicity computed with the number of clusters compared to the number of electrons estimated by the NaI calorimeter. *Bottom*: Beam profile for 433 MeV electrons

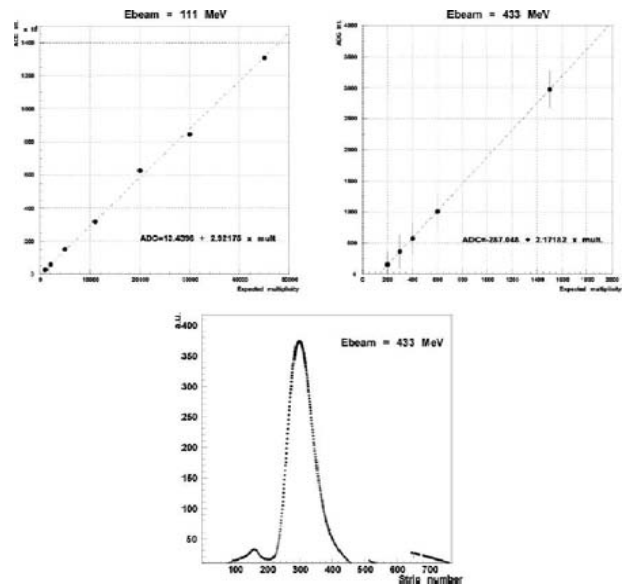


Figure 12: *Top*: Linearity at two different energies of the detector response with respect to increasing multiplicity. *Bottom*: Beam profile in a high multiplicity configuration

## Publication and Conference Talks by LNF Authors in Year 2005

1. AIRFLY Team: Measurement of the Fluorescence Yield in Atmospheric Gases, 29th International Cosmic Ray Conference Pune (2005).
2. B.Buonomo, Profile Monitors for Wide Multiplicity Range Electron Beams, 7th European Workshop on Beam Diagnostic and Instrumentations for Particle Accelerators, Lion (6-8 June 2005).
3. L.Quintieri, The DAΦNE-Beam Test Facility, XCI Congresso Nazionale , Società Italiana di Fisica Catania (26-September).

## References

1. B. Buonomo *et al.*, “Diagnostic and Upgrade of the DAFNE Beam Test Facility (BTF)”, Nucl. Phys. **B150**, 362 (2006) (Proceeding of 9th Topical Seminar on Innovative Particle and Radiation Detectors).
2. M. Anelli *et al.*, “A Scintillating-Fiber Beam Profile Monitor for the DAFNE BTF”, LNF-04/24(IR).
3. F. Arciprete *et al.*, “Air Fluorescence Induced by Electrons in a Wide Energy Range”, in proceeding of 28<sup>th</sup> ICRC (2003).
4. C. Matteuzzi *et al.*, in proceedings of RICH2004 Mexico 2004.

5. D. Filippetto, “Studio Sperimentale della Radiazione emessa da Schermi Fluorescenti attraversati da Fasci di Elettroni Relativistici”, Tesi di Laurea in Ingegneria Elettronica (2003), Università degli Studi di Roma “La Sapienza”.
6. S. Bertolucci *et al.*, “RAP: Acoustic Detection of Particles at the DAΦNE BTF”, Nucl. Instrum. Meth. **A** 518, 261 (2004).
7. M. Prest *et al.*, “The AGILE Silicon Tracker: an Innovative  $\gamma$ -ray Instrument for Space”, Nucl. Instrum. Meth. **A** 501, 280 (2003).
8. S. Bellucci *et al.*, “Making Microbeams and Nanobeams by Channelling in Microstructures and Macrostructures”, Phys.Rev. ST Accel. Beams **6**, 0335032 (2003), TARI proposal n.34.
9. E. Basile *et al.*, “A Novel Configuration for a Strawtube-Microstrip detector”, LNF-04-25(P).
10. Graal Collaboration, “GRAAL: a polarized gamma-ray beam at ESRF”, Nucl. Phys. **A622**, (1997) 110c.
11. D. Babusci *et al.*, “Experimental Trends in Astro-Particle Physics in Space”, LNF-04/26(IR).
12. M. Alfonsi *et al.*, “Triple GEM Detector Operation for High Rate Particle Triggering”, Nucl. Instrum. Meth. **A** 518, 106 (2004).
13. E. Albrecht *et al.*, “Performance of a Prototype RICH Detector using Hybrid Photo-Diodes”, Nucl. Instrum. and Meth. in Phys. Res. Section A - Accelerators Spectrometers Detectors and Associated Equipment 456, 190(2001), ISSN: 0168-9002.
14. S. Calcaterra *et al.*, “Test of Large Area Glass RPCs at the DAΦNE Test Beam Facility (BTF)”, Nucl. Instrum. Meth. **A** 533, 154 (2004).
15. M. Guler *et al.*, “OPERA proposal”, CERN/SPSC 2000-028, SPSC/P318, LNGS P25/2000.
16. G. Anelli *et al.*, “Proposal to Measure the Rare Decay “ $K^+ \rightarrow \pi + \nu\bar{\nu}$ ” at the CERN SPS”, CERN-SPSC-2005-013.
17. S. Bellucci *et al.*, “Crystal Undulator as a Novel Radiation Source”, Phys. Rev. ST Accel. Beams **7**, 02351 (2004), (TARi proposal 35).
18. C. Curceano (Petrascu) *et al.*, “Future Precision Measurements on Kaonic Hydrogen and Kaonic Deuterium with SIDDHARTA”, in proceeding of Workshop on Hadronic Atoms, Trento, Italy (2003).
19. A. Moroni *et al.*, “The Ring Counter (RCo): A high resolution IC-Si-CsI(Tl) Device for Heavy Ion Reaction Studies at 10-30 MeV/A”, Nucl. Instr. and Meth. 556, 140 (2006).
20. B. Buonomo *et al.*, “Particle Acoustic Detection in Gravitational Wave Aluminum Resonant Antennas”, Astropar. Phys. 24, 65 (2005).
21. S. Bartalucci, “High Intensity, Pulsed, Slow Positron and Neutron Sources at INFN-Frascati”, LNF-02/011(IR).
22. W. Swanson, “Calculation of Neutron Yields released by Electrons incident on selected Materials”, SLAC-PUB-2042 (November 1977).
23. P. Swanson *et al.*, “Neutron from Medical Electron Accelerators”, SLAC-PUB-2346 (June 1979).
24. B. Buonomo *et al.*, “Performances and Upgrade of the DAΦNE-Beam Test Facility (BTF)”, Published in IEEE Trans.Nucl.Sci.52, 824 (2005).

## DAΦNE-L Lab

A. Balerna (Resp.), A. Bocci (Dott.), P. Calvani (Ass.), G. Cappuccio (Ass.),  
G. Cibir (Dott.), G. Cinque, S. Dabagov (Art. 23), M. Cestelli Guidi (Art. 23),  
A. Grilli (Tecn.), A. Marcelli (Resp.), F. Monti (Ass.), A. Mottana (Ass.),  
A. Nucara (Ass.), E. Pace, M. Piccinini (Ass. Ric.), M. Pietropaoli (Art. 15), A. Raco (Tecn.),  
V. Sciarra (Tecn.), V. Tullio (Tecn.), G. Viviani (Art. 15).

### 1 Summary

During 2005, DAΦNE-L laboratory continued the synchrotron radiation experimental activity and realized the planned improvements on the existing beamlines. Experiments were performed in parasitic mode during KLOE runs but some dedicated days were given for specific experiments. Italian and European users performed SR experiments on the DAΦNE-L laboratory beamlines. In particular, several EU teams got access within the Integrated Infrastructure Initiative (I3 program for Transnational Access to Research Infrastructure). Following the suggestions of the International Panel Committee who reviewed the Synchrotron Infrared (IR) Beamline (SINBAD), the new IR microscope was installed in the laboratory before the end of the year (figure 1).

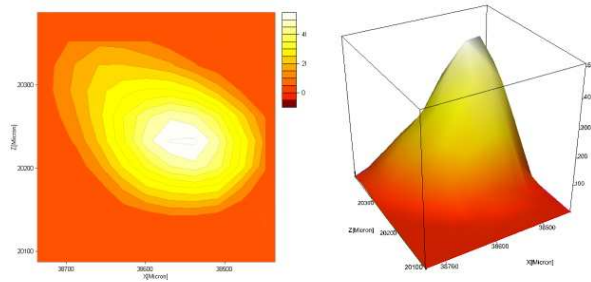


Figure 1: Mapping of the IR synchrotron light source performed with the new BRUKER Hyperion 3000 microscope in the range 2000-8000  $\text{cm}^{-1}$  with a pinhole of 100 micron.

On the soft X-Ray beamline, a good alignment of the optical system with the incoming x-ray beam, thanks to a collaboration with the machine group, gave the possibility to evaluate the optimal e-beam position monitor values that were then fixed and are now reproducible after each injection. With this new situation the negative effects on the measurements, due to the operation during the topping up of the  $e^+$ , have been drastically reduced. Some small changes have also been performed on the software in order to have the chance to use new monochromating crystals and also perform x-ray absorption measurements using different energy ranges. At the end of December, concerning the soft X-ray beamline, all approved projects within new TARI program were successfully completed. At the UltraViolet (UV) branch line, the last dedicated experimental runs to complete the program of the SUE(Solar Ultraviolet Experiment funded by the INFN Vth Committee) were performed. In September the LNF hosted the XVIII International Conference on X-ray Optics and Microanalysis (ICXOM) chaired by S. Dabagov and A. Marcelli. The ICXOM series are conferences devoted to X-ray researches on new developments in X-ray micro-focusing optics and their applications in Physics, Chemistry, Material Science, Earth and Environmental Sciences. The Frascati meeting has been an important forum for the discussion of the challenging

tasks associated to the new X-ray sources, the scientific goals and the new perspectives associated to X-ray optics. Sessions have been dedicated to new techniques in microanalysis and new X-ray instrumentations. Contributions of about 150 participants will be published on a special issue of *Spectrochimica Acta B*. At the end of the year it was available also the final Area Report for the Physics Panel of the CIVR (Committee for Evaluation of Research) devoted to the Italian research for the period 2001-2003. The DAΦNE-Light laboratory was the only activity carried on at Frascati, mentioned in the report: "among the main applications [...] we recall the synchrotron light sources developed at Frascati and universally used in material-science studies - and in the field of radiation detectors."

## 2 Activity

### 2.1 SINBAD

SINBAD is a research facility funded by INFN in the framework of the DAΦNE -Light laboratory. It consists of an infrared beamline composed by three sections: the front-end, the section that transfers radiation from the bending magnet to a focus where the image of the source is demagnified by one ellipsoidal mirror and, finally by a third section that transmits the radiation as a parallel wave to the wedged diamond window located at the entrance slit of the interferometer. At the exit of the BRUKER Equinox 55, an interferometer suitably modified to work under vacuum, at the end of 2005 has been installed the new microscope HYPERION 3000. This is an IR microscope fully automatic, working both in transmission and reflection mode operating in the near- mid- and far-IR range down to about  $200\text{ cm}^{-1}$ . The scientific activity at SINBAD was associated to experiments performed with Italian teams that submitted scientific proposals approved by the LNF Scientific Committee of Synchrotron radiation and by European scientists that get access within the EU framework of TARI access I3 program. Actually, in 2006 we hosted more than 30 experimental teams. The EU funded experimental runs at SINBAD account for a total of 30 users and 331 experimental days. Several Italian scientists, including graduates and PhD had access to the IR beamline performing experiments in cooperation with the SINBAD staff. Almost all of these teams re-applied to continue their researches or their new application is in due course to the next calls. In 2005 not more than 250 hours were dedicated to synchrotron radiation operations mostly spent to perform experiments on sample at high pressure using a DAC cell, for imaging with microscope and alignment of the optical systems. Although working in parasitic regime relevant results were achieved in these months. The extensive list of publications represents only a fraction of the work performed at SINBAD in the 2005 and that is impossible to summarize in a few words. The highlights of the year are represented by the following researches. The pressure-driven insulator-to-metal transition (IMT) is one of the most intriguing phenomena exhibited by condensed matter. The volume compression has usually the effect of both symmetrizing the crystal structure and increasing the overlap among the electronic clouds of the elemental units (ions and/or molecules) leading to a delocalization of the outer electrons. Despite the simplified picture, the actual path followed by an insulating system towards metallization is peculiar and usually complex since volume compression can also modify the balance among microscopic interactions. High pressure is an ideal tool to investigate complex systems where different interactions are simultaneously at work. The SINBAD team, following a research program started in the past years in cooperation with the group of the University *La Sapienza* led by P. Postorino collected the first far-infrared absorption spectra of manganite samples at pressures P up to 10 GPa on  $La_{1-x}Ca_xMnO_{3-x}$  by use of infrared synchrotron radiation. For  $x=0.25$  and  $0.20$  ( $y=0$ ), we may show that the pressure promotes partial metallization at room temperature through a strong reduction of the insulating gap. An Urbach-like model of disordered Jahn-Teller wells has been proposed to fit the far-infrared band edge and allows one to obtain a reliable pressure dependence of the energy

gap. A manuscript summarizing these results has been recently accepted for publication on *Phys. Rev. Lett.*. A second important result obtained within the year was the successful application of the time-resolved IR spectroscopy. Rapid scan time resolved IR spectroscopy has been used to investigate in situ the kinetics of the chemical processes involved in the formation of self-assembled mesostructures. These experiments have been performed in transmission on films casted on a diamond disk using the microscope observing both the time dependence of solvent evaporation and condensation of the chemical species. Moreover, different stages in the films formation have been identified, which well support the general theory of self-assembly. This method set up with the team of the University of Sassari led by P. Innocenzi is a very effective tool for in situ analysis of films formation from a liquid phase (Figure 2)

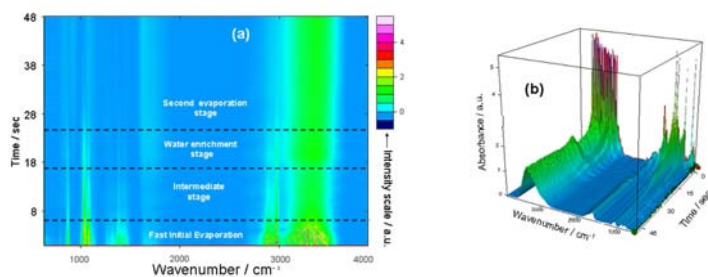


Figure 2: 3D FTIR spectra (bottom view) vs. time obtained during the deposition by casting of a self-assembling titania film. The spectra are recorded by Rapid Scan Time Resolved method. The upper plot is a top view, in false colors, showing the different phases of the process.

The technique we present can be also extended to the study of deposition of films from liquid phases, such as sol-gel films, and can visualize in a simple and direct way (see Fig. 2) the different processes and their relative kinetics. Indeed, using this technique four different stages during film casting of self-assembling films have been clearly distinguished. (work in press on *J. Phys. Chem. B*). The synchrotron light emission is a non-thermal radiation source covering a large energy domain from IR to X-ray energies, with a time structure determined by the length and shape of the stored bunches. With suitable infrared detectors, the pulsed emission can be used to perform spectroscopic experiments at high time and spatial resolution. However, fast infrared detectors can be also applied to investigate the physical structure of the stored particles. Starting from these simple considerations using detectors we are developing for IR imaging, we performed the first characterization of the synchrotron light emission at DAΦNE using detectors optimized in the mid-IR domain with a sub-ns time resolution. Experiments have been performed using the SINBAD beamline, characterizing the emission of the 105 bunches stored in the electron ring of this  $e^+e^-$  collider. With both uncooled photoconductive and photovoltaic infrared detectors we resolved the infrared temporal emission of the electron bunches structure at DAΦNE characterized by bunches separated of 2.7 ns with a rise time of 176 ps and a fall time of 660 ps. (work submit. for publication) (Figure 3).

During these experiments that represent the first direct measurement of the midIR light emission of electron bunches using uncooled fast IR detectors, the best results in resolution time have been obtained with photoconductive detectors optimized to work at 10.6 micron of wavelength and with a response time of about 300 ps. Actually, much faster photovoltaic detectors can be manufactured and a response time as short as 50 ps is achievable with a high frequency optimized devices opening the way towards new diagnostic methods in storage rings that should be also used to monitor source instabilities and bunch dynamics. This research is a part of a larger proposal

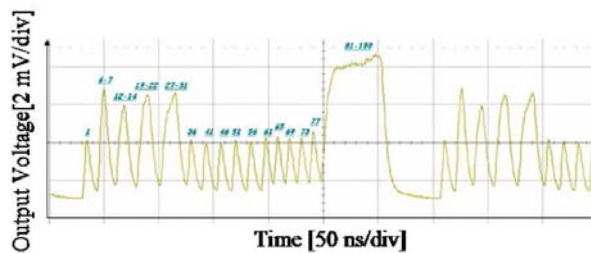


Figure 3: IR signal of a special DAΦNE bunch filling structure. The x and y scales are 50 ns/div and 2 mV/div respectively.

of R&D on IR detector in collaboration with the Florence University (DASS Department), the IMONT (Istituto Nazionale per la Montagna), BRUKER Optics s.r.l. and VIGO systems s.r.l.. Among the many initiatives of 2005, at SINBAD, we may also mention the organization in May of a School of FTIR spectroscopy, organized in cooperation with BRUKER Optics and attended by about 15 people. The school, the first of this type organized by the LNF, was mainly oriented to training and, in addition to introductory lectures it included an experimental session using the SINBAD instrumentations.

## 2.2 Soft X-ray Beamline

The synchrotron radiation (SR) soft X-ray source is a 6-pole equivalent planar wiggler. This wiggler, that gives a critical energy of about 300 eV, forces the electrons to emit a wide fan of electromagnetic radiation that, in the X-ray region is fully polarized in the orbital plane. With a circulating electron current higher than 1 Ampere a very intense flux of soft X-rays is provided. The beamline was designed to accept all the vertical SR divergence, and more than 12 mrad of the photon fan in the orbit plane. A vertical Au-coated silicon mirror is used to deflect, in the horizontal plane half of the SR fan into the UV branch line. Very thin and interchangeable windows separate the vacuum of the beamline from the one of the storage ring. The beamline is equipped with a Toyama double-crystal monochromator in boomerang geometry which ensures a fixed beam exit within the Bragg's angle range  $15^\circ - 75^\circ$ . By a set of crystals including InSb (111), Ge(111) and KTP(011), the x-ray energy spectrum from 1.2 keV upward is covered. The multipurpose experimental UHV chamber can allocate several samples to be measured at RT both in transmission mode and by secondary particles/radiation emission. The implemented detector equipment includes ion chambers and x-ray photodiodes. During 2005, the soft X-ray line has successfully delivered beamtime to Italian, EU and external EU users, in the framework of the INFN-Group V experiments and TARI program. All the experiments related to x-ray absorption measurements were run in dedicated mode with runs of about 25 minutes, very useful to acquire XANES (X-ray Absorption Near Edge Spectroscopy) spectra with good signal to noise ratios. During the parasitic mode, new sample and beamline tests and experiments not requiring long acquisition times, like tests of diamond detectors, soft x-ray multilayers and imaging of lead impurities in leaves were performed. Selected examples of experiments carried out in the dedicated beamtime mode are the following:

1. The extended x-ray absorption fine structure spectrum (EXAFS) of Al was measured in an extended energy range and its Fourier transform is reported in figure 4. Aluminum near-edge region was also measured in magnetic materials (TARI project of J. Chaboy, Zaragoza University) mostly Fe- and Co-compounds. XANES spectra were used to clarify the structural changes due to the lowering of the aluminum amount.

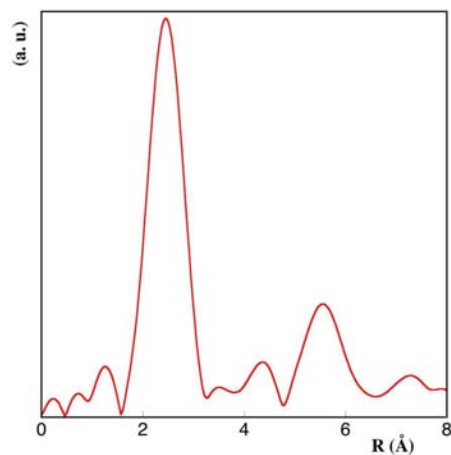


Figure 4: Fourier transform of the extended x-ray absorption fine structure signal of an Al foil.

2. Sulphur XANES spectra were measured for material science on metallic and semiconducting Cr-based spinels and precursors, and on rare earth silicate Intermetallic compounds ((TARI project by A. Kisiel, Jagiellonian University). The measured spectra were related to the differences in local environment due to specific site and symmetry.
3. Sulfur was also measured for biophysics studies on human tissues (hystological sections) (TARI project by Prof. W. Kwiatek and co-workers, Polish Academy of Sciences, proposal Bio-Xanes-IR) and on proteins. The study of sulfur is essential for a wide range of biological functions in cells and tissues. X-ray Absorption Spectroscopy has been used to speciate the redox state of S in biomolecules (proposal by G. Bellisola from Verona University). The XANES data of the model protein systems show significant differences and were interpreted in comparison with the native S and other sulfate standards.

In parasitic mode other SR experiments were done. X-ray imaging tests have been performed on leaves accumulating toxic metals as effective agents for the so-called phytoremediations of polluted environment. Images were taken above and below the lead  $M_V$  absorption edge (A. Reale MIDIX INFN - G. V Committee). XANES spectra at the aluminium K edge have been measured in powders of aluminum nitride nanotubes and nanoparticles. Nanomaterial are nowadays extensively studied since their peculiar mechanical and electronic properties, mostly dominated by the surface state due to their overwhelming surface to bulk ratio (TARI project of E. Kotomin, Riga University). Angle-resolved XANES spectra have been collected for the first time on several natural mica crystals in transmission mode at the potassium K-edge using the polarized SR emission from DAΦNE (proposal by A. Mottana and G. Cibin, Roma III University). Using the multiple scattering theory, the edge of this low-Z atoms was analyzed in terms of the X-ray dichroic behavior of solid layered compounds (2-D structures). Preliminary tests on the performances as x-ray detectors of diamond based detectors were performed (proposal by E. Pace and A. Desio from Firenze University). The sensitivity characterization of these single-crystal devices was performed in the energy range above 1.2 keV. Finally beamtime was given to the ARCHIMEDE (ARCHitects of Mirrors for Euv DEvices) experiment of the INFN - V Committee (see this activity report) for a final set of measurements on new multilayer devices in the soft X-ray energy domain (V. Rigato of LNL and G. Cinque of LNF).

### 2.3 UV branch Line

In 2005 a few shifts of dedicated beamtime was given to the SUE experiment. For a scientific report of the experiment see the SUE pages inside this report. Moreover, during the year, in cooperation with DASS (Department of Astronomy and Space Science) of the Florence University using the existing set up, we continued the tests on detectors based on crystalline diamonds. The results of these researches have been presented at several Conferences and manuscripts have been submitted for publication. From this collaboration, that has been also extended to the team of the Laboratori Nazionali di Legnaro leded by V. Rigato, born the idea for a new project devoted to test of VUV optics for space applications and novel optical devices based on multilayer technology. The proposal submitted by E. Pace of the University of Florence titled SOURCE (Synchrotron Optical & Ultraviolet Radiation for Calibration Experiments) has been approved by the INFN Vth Committee. According to the schedule of the project, in 2006 is planned the upgrade of the UV branch line with a new mirror with a meridional focus, a new UV monochromator and the set up of a larger experimental area.

### 3 List of Conference Talks by SINBAD members in Year 2005

1. A. Bocci, Optimized IR detectors for IRSR micro-spectroscopy and biomedical imaging, 9<sup>th</sup> ICATPP Conference on Astroparticle, Particle, Space Physics, Detectors and Medical Physics Applications - Como, October 2005.
2. A. Bocci, Applications of fast mid-IR detectors as beam monitor in the subnanosecond time domain, ICFA mini-workshop on Frontiers of Short Bunches in Storage Ring - Frascati, Novembre 2005.
3. M. Cestelli Guidi, Performance of the SINBAD beamline for High Pressure Far-Infrared experiments, High Pressure Workshop - Sesto Fiorentino, Marzo 2005.
4. M. Cestelli Guidi, Far-Infrared Synchrotron radiation sources as new facilities for investigations of optical properties of solids in normal and extreme conditions: SINBAD achievements and perspectives, SMEC 2005 (Study of Matter at Extreme Conditions) - Miami, April 2005.
5. M. Cestelli Guidi, Far-infrared pressure driven metal-insulator transition in  $\text{La}_{(1-x)}\text{Ca}_x\text{MnO}_3$  manganites, SPIE 2005 (Strongly Correlated Electron Materials: Physics and Nano-engineering) (San Diego, August 2005).
6. A. Marcelli, Protein structure and function in the time-domain of vibrational spectroscopies. The promising applications of IRSR  $\mu$ -spectroscopy, XL School of Physics - Zakopane, Maggio 2005.
7. A. Marcelli, The DASIM IRSR facilities, 1<sup>st</sup> DASIM Workshop - Daresbury, Luglio 2005.
8. M. Piccinini, FT-IR microspectroscopy on micas: angular dependence in the case of phlogopites, Convegno Micas Italy - Rimini, Febbraio 2005.
9. M. Piccinini, Synchrotron radiation FT-IR micro-spectroscopy on natural mica crystals in the O-H stretching region, International Workshop on Infrared Microscopy and Spectroscopy with Accelerator Based Sources - Rathen, Giugno 2005.
10. M. Piccinini, Synchrotron radiation FT-IR microspectroscopy on micas: angular dependence in the O-H stretching region, The 3<sup>rd</sup> International Conference on Advanced Vibrational Spectroscopy (ICAVS-3) - Delavan, Agosto 2005.
11. M. Piccinini, FT-IR micro-spectroscopy on natural micas: angular dependence in the OH stretching region, 5<sup>o</sup> Forum Italiano di Scienze della Terra 3 - Spoleto, Settembre 2005.

#### 4 List of Conference Talks by LNF Authors in Year 2004

1. G. Cibin, Pleochroism in potassium K-edge XANES on di- and tri-octahedral micas, Convegno Micas Italy - Rimini, Febbraio 2005. G. Cibin, Local structure of the mica two-dimensionally extended interlayer studied by angle-dependent XANES spectroscopy at the potassium K-edge, 18<sup>th</sup> International Conference on X-ray Optics and Microanalysis - Frascati, Settembre 2005.
2. G. Cinque, Preliminary characterization of first multilayer mirrors for the soft X-ray water-window, 18<sup>th</sup> International Conference on X-ray Optics and Microanalysis - Frascati, Settembre 2005.
3. A. Marcelli, Electronic and magnetic properties of iron-containing micas Convegno Micas-Italy - Rimini, Febbraio 2005.
4. A. Marcelli, Il progetto CRYOALP: il ghiaccio nelle Alpi, Convegno Micro-meteoriti e origine della vita - Firenze, Febbraio 2005.
5. A. Marcelli, Polarized XANES spectroscopy: crystal-chemical investigations in natural and synthetic materials 20<sup>th</sup> International Conference on X-Ray and Inner Shell Processes - Melbourne, Luglio 2005.

#### References

1. A. Bocci, M. Piccinini, A. Drago, D. Sali, P. Morini, E. Pace and A. Marcelli, "Detection of the SR infrared emission of the electron bunches at DAΦNE", LNF-05-12 (NT), 15 Settembre 2005.
2. M. Cestelli Guidi, M. Piccinini, A. Marcelli, A. Nucara, P. Calvani and E. Burattini, "Performance of SINBAD, the IR source at DAΦNE", J. Opt. Soc. Amer. A **22**, 2810 (2005).
3. M. Cestelli Guidi, A. Marcelli, P. Calvani, E. Burattini, A. Nucara, M. Piccinini, P. Postorino, A. Sacchetti, E. Arcangeletti, E. Sheregii, J. Polit and A. Kisiel, "Far-infrared synchrotron radiation spectroscopy of solids in normal and extreme conditions", Physica Status Solidi (c) **2**, 236-239 (2005).
4. P. Falcaro, S. Costacurta, G. Mattei, H. Amenitsch, A. Marcelli, M. Cestelli Guidi, M. Piccinini, A. Nucara, L. Malfatti, T. Kidchob and P. Innocenzi, "Highly ordered "defect-free" self-assembled hybrid films with a tetragonal mesostructure", J. Amer. Chem. Soc. **127**, 3838 (2005).
5. P. Innocenzi, L. Malfatti, T. Kidchob, P. Falcaro, M. Cestelli Guidi, M. Piccinini and A. Marcelli, "Kinetics of polycondensation reactions during self-assembly of mesostructured films studied by in situ synchrotron infrared spectroscopy", Chem. Comm. **18**, 2384 (2005).
6. N. Mironova-Ulmane, A. Kuzmin, M. Cestelli Guidi, M. Piccinini and A. Marcelli, "Influence of diamagnetic impurities on mid-IR absorption in antiferromagnetic insulator NiO", Physica Status Solidi (c) **2**, 704-707 (2005).
7. M. Piccinini, M. Cestelli Guidi, A. Marcelli, P. Calvani, E. Burattini, A. Nucara, P. Postorino, A. Sacchetti, E. Arcangeletti, E. Sheregii, J. Polit and A. Kisiel, "Far-IR synchrotron radiation spectroscopy of solids in normal and extreme conditions", Phys. Stat. Sol. (c) **2**, 236-239 (2005).

8. J. Polit, A. Kisiel, A. Mycielsky, A. Marcelli, E. Sheregii, J. Cebulsky, M. Piccinini, M. Cestelli Guidi, B.V. Robouch and A. Nucara, "Vibrational spectra of hydrogenated CdTe", *Phys. Stat. Sol. (c)* **2**, 1147- 1154 (2005).
9. G. Cibin, A. Mottana, A. Marcelli and M.F. Brigatti, "Potassium coordination in trioctahedral micas by K-edge XANES spectroscopy", *Min. Petrol.* **85**, 67 (2005).
10. D. Hampai, S.B. Dabagov, G. Cappuccio and G. Cibin, "PolyCAD: A New X-Ray Tracing Code for Polycapillary Optics", *Proceedings of SPIE Vol. 5943*, 7-14 (2005).
11. D. Hampai, S.B. Dabagov, G. Cappuccio and G. Cibin, "An X-ray tracing code for polycapillary optics", *Proceedings of SPIE Vol. 5974*, 433-441 (2005).
12. D. Hampai, S.B. Dabagov, G. Cappuccio and G. Cibin, "X-ray propagation through hollow channel: PolyCAD - a ray tracing code", *Nucl. Instrum. Meth. B* **244**, 481-488 (2006).
13. S. Tascu, P. Moretti, B. Jacquier, M. Piccinini, R.M. Montereali and F. Somma, "Visualization by SNOM technique of optical modes in LiF channel waveguides", *Physica Status Solidi (c)* **2**, 633-636 (2005).
14. P. Zaidel, A. Kisiel, J. Warczewski, J. Konior, L.I. Koroleva, J. Krok-Kowalski, P. Gusin, E. Burattini, G. Cinque, A. Grilli and R.V. Demin, "The influence of concentration of Sb ions onto the local and electronic structure of  $\text{CuCr}_{2-x}\text{Sb}_x\text{S}_4$  studied by XANES and EXAFS measurements and LAPW numerical calculations", *J. Alloys and Compounds* **401**, 145-149 (2005).
15. G. Cinque, E. Burattini, A. Grilli and S. Dabagov, "The Soft X-ray Beamline at Frascati", *Proceedings of SPIE Vol. 5974*, 448 (2005).
16. W.S. Chu, Z.Y. Wu, S. Agrestini, A. Bianconi, A. Marcelli and W.H. Liu, "Characterization of 3d transition-metal diborides by X-ray Absorption spectra at the metal K edge", *Intern. J. Modern Phys.* **19**, 2386 (2005).
17. E. Burattini, A. De Sio, L. Gambicorti, F. Malvezzi, A. Marcelli, F. Monti and E. Pace, "Second order harmonics suppression with glass filters for synchrotron UV radiation calibration measurements", *LNF Report 05/011(IR)*.
18. M.I. Abbas, Z.Y. Wu, K. Ibrahim, S. Botti, R. Ciardi and A. Marcelli, "XANES study of carbon nanotubes grown without catalyst", *Phys. Scripta* **T115**, 759 (2005).
19. S.J. Li, Z.Y. Wu, T.D. Hu, Y.N. Xie, J. Zhang, T. Liu, C.R. Natoli, E. Paris and A. Marcelli, "A study of the pre-edge X-ray absorption fine structures in Ni monoxide", *Phys. Scripta* **T115**, 223 (2005).
20. Z.Y. Wu, A. Marcelli, G. Cibin, A. Mottana and G. Della Ventura, "Aluminium K-edge XANES study of mica preiswerkite", *Phys. Scripta* **T115**, 172 (2005).
21. G. Iezzi, G.D. Gatta, W. Kockelmann, G. Della Ventura, R. Rinaldi, W. Shafer, M. Piccinini and F. Gaillard, "Low-T neutron powder-diffraction and synchrotron-radiation IR study of synthetic amphibole  $\text{Na}(\text{NaMg})\text{Mg}_5\text{Si}_8\text{O}_{22}(\text{OH})_2$ ", *American Mineralogist* **90**, 695-700 (2005).

## **GILDA**

### **General Purpose Italian Beamline for Diffraction and Absorption - at ESRF**

A. Balerna, S. Mobilio (Resp.), V. Sciarra (Tecn.), V. Tullio (Tecn.)

#### **1 Introduction**

GILDA ( General Purpose Italian BeamLine for Diffraction and Absorption), is the Italian CRG beamline, built to provide the Italian scientific community with an easy access to the European Synchrotron Radiation Facility to perform experiments with a high energy and brilliance X-ray photon beam. GILDA is funded by the three Italian public research Institutes: Consiglio Nazionale delle Ricerche (CNR), Istituto Nazionale per la Fisica della Materia (INFM) and Istituto Nazionale di Fisica Nucleare (INFN). Experimental stations for X-ray Absorption Spectroscopy, Anomalous X-ray Scattering and X-ray Diffraction (XRD) are present at the GILDA beamline. During October 2005, in collaboration with the Italian Society of Synchrotron Radiation (SILS) the VIII Italian School of Synchrotron Radiation was held in the Frascati national laboratory. The school that was chaired by S. Mobilio and G. Vlaic, covered many synchrotron radiation techniques and applications and was attended by 51 students. The next edition will be held in 2007.

#### **2 Activity on the GILDA beamline during 2005**

1) The new second mirror, one meter long having a Si substrate, was installed on the beamline and commissioned. The new performances are very satisfactory because it is now possible to achieve an homogeneous vertical dimension of about  $150\mu$  at the sample position; both absorption grazing incidence technique (REFLEXAFS) and x-ray diffraction will get a large advantage by this improvement. 2) A new system for the measurement of the absorption coefficient using Total Electron Yield (TEY) technique was realized. The system works down to liquid He temperature and is made of a sealed chamber containing gaseous He to amplify the signal. The system can rotate in order to eliminate Bragg peaks when measuring samples grown on crystalline substrates. 3) The detection limit of the fluorescence detection system was improved, by modifying the recording technique. The new system records all the fluorescence spectra of the sample as a function of the incoming photon energy. To extract the desired signal from the background, a fitting is performed on the fluorescence peak of interest; the fluorescence intensity is assumed to be equal to the area of the fitted peak. With this technique, high quality spectra were recorded on impurities of  $5 * 10^{13} \text{at/cm}^2$  of In in Si. 4) The control and data acquisition system of the absorption hutch, previously based on the OS9 operating system, was changed to LINUX. 5) The realization of a magnetron sputtering system to grow nanoclusters was completed. The first tests and depositions are starting.

#### **3 Beamtime use during 2005 and scientific outcomes**

During 2005 ESRF delivered beam for about 5600 hours; 3650 hours were used for user's experiments, about 800 hours for in-house research, 800 hours for beamline improvements, maintenance and alignment; about 350 hours were delivered in single bunch mode and therefore used for tests. Totally 39 experiments were performed, 26 of Italian users and 13 of European users. A result to be mentioned is the following:

The site of Mn in Mn  $\delta$ -doped GaAs studied by X-ray absorption spectroscopy. The interest in these materials comes from their potential use in spintronics devices. In the fabrication

of light emitting diodes, in which the carriers are spin polarized, the spin alignment is made by  $Ga_{1-x}Mn_xAs$  magnetic layers embedded in GaAs. Another promising application of these materials is the development of a Faraday rotator at  $0.98\mu$  to be used with semiconductor laser diodes that pumps Er doped fiber amplifiers, a key component of optical communication systems; ferromagnetic MnAs nanoclusters embedded in GaAs have also shown giant magneto-optical effects. A problem in such materials is the limited solubility of Mn in III-V semiconductors. To overcome this difficulty recently the use of  $\delta$ -doping of GaAs with Mn was suggested. In the resulting material however the Mn concentration is not able to induce ferromagnetism. Only using a modulation doped structure containing Al-GaAs:Be layers, ferromagnetism is achieved. In GaMnAs related materials there is a close interplay between the local Mn structure and the electronic and magnetic properties of the material. Therefore a full understanding of the local structural properties of Mn  $\delta$ -doped GaAs is crucial. For this reason an x-ray absorption spectroscopy experiment at the Mn-K edge in samples grown by molecular beam epitaxy with and without Be co-doping was performed. Mn-Mn atomic correlations have not been found within  $\sim 5$  radius, ruling out the presence of metallic clusters or local Mn enrichment. In samples deposited at  $300^\circ\text{C}$ , Mn substitutionally occupies the Ga site with a local expansion ( $\sim 2\%$ ) of the first-neighbor distance with respect to GaAs; the second neighbors remain at a distance very close to that of the host lattice, indicating that the structural perturbation induced by Mn is very localized. Ab initio simulation of the x-ray absorption near edge structure spectra confirmed that Mn enters the Ga, rather than the As, site. Samples grown at  $450^\circ\text{C}$  exhibit a reduction of the first shell coordination number, suggesting the initial phases of MnAs precipitation. In the case of Be co-doping the downward shift of the Fermi energy leads to the appearance of Mn in tetrahedral interstitial sites, of which a previously unavailable local structural description was provided.

#### 4 2006 - GILDA Forseen Activity

During the 2006, the activity foresees: 1) the completion of the migration of the operating system of the beamline from Microware OS 9 to LINUX; 2) the development of a curved imaging plate detection system in the diffraction hutch, in order to increase the q-range available for the measurements; 3) the installation of a new liquid He cryostat in the absorption hutch in order to increase the thermal stability and to decrease the dead time during measurements; 6) the growth of the first nanocluster samples and their structural and electronic characterization.

#### References

1. C. Monesi, C. Meneghini, F. Bardelli, M. Benfatto, S. Mobilio, U. Manju, DD. Sarma "Local structure in  $\text{LaMnO}_3$  and  $\text{CaMnO}_3$  perovskites: A quantitative structural refinement of Mn K-edge XANES data", Phys. Rev. **B 72**, 174104 (2005).
2. G. Ciatto, H. Renevier, MG. Proietti, A. Polimeni, M. Capizzi, S. Mobilio, F. Boscherini, "Effects of hydrogenation on the local structure of  $\text{In}_x\text{Ga}_{1-x}\text{As}_{1-y}\text{N}_y$  quantum wells and  $\text{GaAs}_{1-y}\text{N}_y$  epilayers", Phys. Rev. **B 72**, 085322 (2005).
3. A. Longo, A. Balerna, F. d'Acapito, F. D'Anca, F. Giannici, LF. Liotta, G. Pantaleo, A. Martorana, "A new cell for the study of in situ chemical reactions using X-ray absorption spectroscopy". J. of Synch. Rad. **12**, 499-505 (2005).

## NTA CANDIA

A. Della Corte (Ass.), G. Celentano (Ass.), U. Gambardella (Resp.)

### 1 Purposes of the project

The *NTA-CANDIA* program comes out from a wider european program NED, (Next European Dipole) carried out in the framework of the CARE activities. It is devoted to study the application of Nb<sub>3</sub>Sn for application in high field dipoles for accelerators. In fact new accelerators will require field as high as 15 Tesla for bending high energy beams. These requirements cannot be fulfilled with the actual wires and new designs must be accomplished. Two developmet steps were originally foreseen: wire development to get 3 kA/mm<sup>2</sup> in 12 T, and the construction of model dipole. Unfortunately, due to the new requirement of developing Fast Ramped Superconducting Dipoles for the FAIR accelerators, this program has been limited to the first one, and the ending activities on the wire realized will merge in the framework of the new NTA-DISCORAP 2006 development program, already approved by NTA committee. Three INFN sections are involved: Genova (group leader), Milano, and LNF, in collaboration with Outukumpu Copper Superconductors Italy, Fornaci di Barga (LU).

### 2 The Frascati group activity

The Frascati group, made of *LNF* and *ENEA* Frascati researchers, takes care of wire characterization, analyzing the Nb<sub>3</sub>Sn superconducting properties by means of magnetization measurements. In fact, because of the high transport current density of the Nb<sub>3</sub>Sn it became advisable to perform magnetization measurements to derive the current density. This technique is much easier and inexpensive to get first informations on the wire ability to carry high currents under applied intense magnetic fields. In fact once the details of the wire are known the critical current density  $J_c$  may be computed with eq.1:

$$J_c(B, T) \approx \frac{3\Delta M}{\mu_0 N_{fil} l d^3 (1 - \eta)^3} \quad (1)$$

where  $N_{fil}$  is the number of filaments,  $d$  and  $l$  are the filament diameter and length respectively, and  $\eta$  is the ratio between Nb<sub>3</sub>Sn and Sn diameters.

As in 2005 the wire designed for CANDIA will not be available our activity has been devoted to support the NED wires developed by different providers and laboratories.

#### 2.1 VSM measurements

The Nb<sub>3</sub>Sn wires are manufactured with either the internal tin, or the PIT (Powder In Tube), or the Modified-Jelly-Roll technology. In this note we just consider the PIT wires with a Nb barrier which are under investigation. The presence of this superconducting barrier, acting as a magnetic shield, introduces further difficulties either in the magnetic measurement or in the features of the wire. To analyse the magnetization  $M$  of Nb<sub>3</sub>Sn wires we used a VSM (Vibrating Sample Magnetometer) which operates in the range [300 ÷ 4] K under a maximum field of 12 Tesla. Small length wires, about 5 mm long, can be easily analyzed. The magnetization measurements were performed with the magnetic applied field either parallel or transverse to the wire axis. In addition to the  $J_c$  value, the measurement of the  $dc$  magnetic moment  $M$  in parallel and transverse field also gives information about the content of Nb<sub>3</sub>Sn and of other superconducting phases. In order

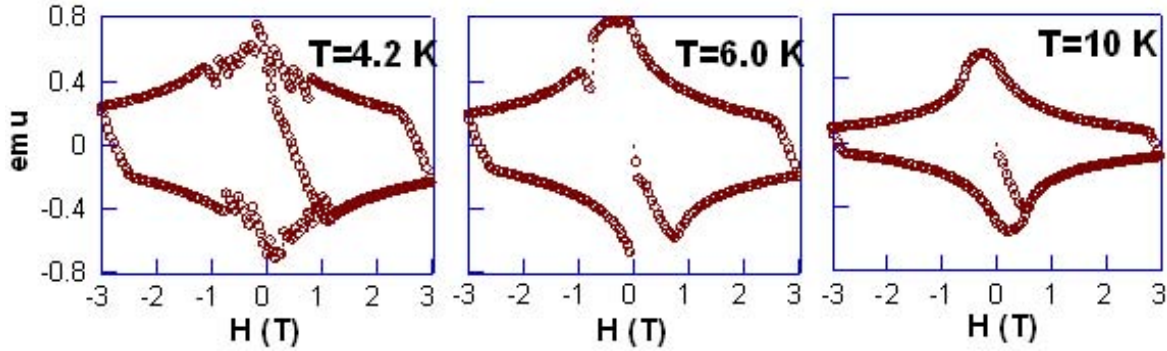


Figure 1: *Magnetization cycle of Nb<sub>3</sub>Sn PIT wire at different temperatures.*

to analyze the Nb<sub>3</sub>Sn phase we performed magnetization cycles above the Nb critical temperature ( $T_c \approx 9.2\text{K}$ ) and at  $4.2\text{K}$ . All the tests were carried out in the ZFC (Zero Field Cooling) situation, to have the opportunity of recording the purely diamagnetic response at low magnetic field, useful for studying the shielding regimes.

The first results concerned the quality and accuracy of the measurements which have been cross compared with different measurements performed in Genova, as well as on known sample geometries <sup>1)</sup>. Incidentally we also first evidenced one of the features limiting the application of high current transport wires: the flux jump phenomena. We observed the occurrence of flux jumps in several samples analyzed as shown in fig.1. It can be summarized as follows: lowering the temperature the critical current achieves very high values, although it is desirable, there is not enough pinning forces to keep fluxoids stationary and the application of even very low magnetic fields induces abrupt changes in the fluxoids positions. This makes the critical current really unstable at low temperature and low fields. In fig.1 it is clearly shown how this mechanism is enhanced while decreasing the temperature. This critical limiting phenomenon may be ascribed to the presence of non completely reacted Nb, which gives rise to impure phases in the wire. Further analysis must be carried out to investigate, and possibly clear, this effect.

## References

1. M. Greco, P. Fabbriatore, C. Ferdeghini, U. Gambardella, “*Magnetization measurements of Nb<sub>3</sub>Sn wires for the Next European Dipole (NED)*”, IEEE Trans. on Magnetics (2006), to be published.

**NTA CLIC  
CLIC Test Facility 3**

D. Alesini, M. Castellano, C. Biscari, R. Boni, B. Buonomo, A. Clozza,  
A. Drago, D. Filippetto, A. Gallo, A. Ghigo (Resp.), F. Marcellini,  
C. Milardi, B. Preger, M.A. Preger, R. Ricci, C. Sanelli, M. Serio,  
F. Sgamma, A. Stecchi, A. Stella, M. Zobov

## **1 Introduction**

The aim of the CLIC Test Facility (CTF3) is to test the two beam acceleration scheme with the final Compact Linear Collider (CLIC) parameters. The acceleration gradient of 150MeV/m is provided by high power 30 GHz radio-frequency generated by a powerful electron drive beam. An international collaboration participates to the construction of the machine and the LNF has realized the first ring, named Delay Loop, of the drive beam recombination system. The Delay Loop has been installed in the existing building at CERN that hosted the LEP preinjector, reusing large part of the existing magnets, power supplies, equipments and ancillary system.

## **2 LNF group contribution in year 2005**

In CTF3 collaboration the INFN Frascati laboratories take full responsibility of the design, realization and commissioning of the first of the two rings of the bunch train compression system, said Delay Loop, and of the Transfer line that connect the Linac to the Delay Loop.

Main components of the vacuum chamber have been realized by Italian firms in the second half of 2004 and early 2005; all the components have been vacuum tested in the Vacuum laboratory in Frascati then shipped to CERN in pure nitrogen overpressure. Magnets and supports of the Delay Loop have been installed during dedicated shifts in winter and spring 2005 sharing the work time with the Linac operation and the high power production experiments. The wiggler magnet and vacuum chamber have been installed in summer and the final test of the vacuum chamber has been completed in autumn; the pressure value achieved before starting the ring commissioning was  $10^{-8}$  Bar without any bake-out procedure after installation. The 1.5 GHz RF deflector has been realized and before the power test the two deflecting cavities have been tuned at the working frequency. Low power measurements of the entire system, composed by klystron, waveguides directional coupler, hybrid junction and twin cavities have been performed. During the operation the full power conditions have been verified after fast conditioning. The Delay Loop commissioning has been started during December. At the Delay Loop exit the  $1.5\mu\text{s}$  continuous train of bunches at 1.5 GHz coming from the linac is recombined in order to create a series of bunch trains and gaps. The bunch frequency and the current in the trains are doubled with respect to the Linac one. The following measurements have been performed:

- energy and energy spread of the electron beam coming from the Linac,
- transverse beam emittance at the chicane exit,
- beam quality in the line end by-passing the delay loop with the RF deflector off,

- efficiency of static injection with correctors instead of RF deflector,
- beam trajectory and its correction,
- optical parameter of the ring with the test optics,
- injection efficiency with RF deflector,
- recombination efficiency of the train of bunches with bunch coding.

Before the winter 2005 shutdown all ring components and systems have been tested and the main characteristics of the Delay Loop have been measured.

### **3 Foreseen activity of the LNF group during year 2006**

The foreseen activities for the year 2006 include the completion of the Delay Loop commissioning and participation to the CLIC Test Facility scientific program. The Memorandum of Understanding of the accelerated CTF3 program foresees the participation of INFN in the realization of the Combiner Ring vacuum chamber.

### **4 References**

1. A. Ghigo, D. Alesini, G. Benedetti, C. Biscari, M. Castellano, A. Drago, D. Filippetto, F. Marcellini, C. Milardi, B. Preger, M. Serio, F. Sgamma, A. Stella, M. Zobov INFN-LNF; R. Corsini, T. Lefevre, F. Tecker, CERN: "Commissioning and first Measurements on the CTF3 Chicane", presented at the 2005 Particle Accelerator Conference (PAC2005), Knoxville, Tennessee, USA - May 16-20, 2005; LNF-05/26 (P), 20/12/2005.

## NTA TTF

L. Cacciotti (Tecn), M. Castellano (Resp), A. Clozza, G. Di Pirro,  
O. Giacinti (Tecn), S. Guiducci, C. Milardi, R. Sorchetti (Tecn), F. Tazzioli, M. Zobov

### 1 Introduction

The TESLA Test Facility (TTF) is an international effort, based at Desy (Hamburg), aiming at the development of the technologies required for a Superconducting  $e^+e^-$  Linear Collider. High gradient superconducting RF cavities, with their high power coupling and tuning device, and low cost cryostats were the main goal of the project, but also the production of a high power, long pulse electron beam from a RF gun was required. This involved the development of new photocathode, an adequate laser source and new beam diagnostics. In addition to prove the possibility of producing and accelerating the kind of beam required for the future superconducting Lineal Collider, TTF has also demonstrated that this beam was of enough good quality to be successfully used for the production of UV coherent radiation with the Self Amplified Spontaneous Emission (SASE) Free Electron Laser process. TTF is now transforming in the TTF VUV/FEL User Facility, becoming a test bench not only for the Linear Collider, but also for the European X-ray FEL Facility. INFN contribution comes from LNF, LNL, Sezione di Milano and Sezione di Roma2.

### 2 Activities in the year 2005

In 2005 the commissioning of TTF VUV/FEL (TTF2) was completed, and a routine delivery of FEL radiation to users started. The linac operation was limited to an energy of roughly 350 Mev, with the last two accelerating modules kept at very low gradient. For this reason, the bunch was compressed only with bunch compressor 2. Nevertheless, in some dedicated shift, the operation of bunch compressor 3 and the bunch length measurement with diffraction radiation and the Martin Puplett interferometer was tested. The results show the sensitivity of the instrument to small variation of the bunch length and, what is more important, its completely non intercepting nature. The bunch length measurement was performed with the beam going through the diffraction radiation slit and the undulator, with the FEL operation totally non affected. In summer we installed in the by pass line a new screen in which two slit were cut, of .5 and 1 mm respectively. The purpose is to verify the possibility of measuring the beam transverse dimension through the analysis of the angular distribution of diffraction radiation in the visible range. Dedicated beam time is scheduled for spring 2006. The whole OTR imaging diagnostic system was strongly operated in the machine commissioning, and its performance were remarkably good, requiring very few maintenance operations.

### 3 Publications

1. K. Honkavaara, F. Loehl, D. Noelle, S. Schreiber, E. Sombrowski, M. Sachwitz, M. Castellano, G. di Pirro, L. Catani, A. Cianchi, "Transverse Electron Beam Diagnostics at the VUV-FEL at DESY", Proc. of the 27<sup>th</sup> International Free Electron Laser Conf. 2005, San Francisco.

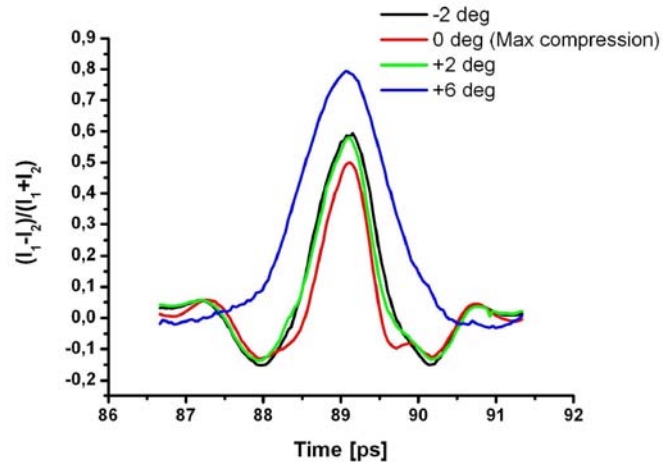


Figure 1: Comparison between bunch length interferograms with different accelerating phases.

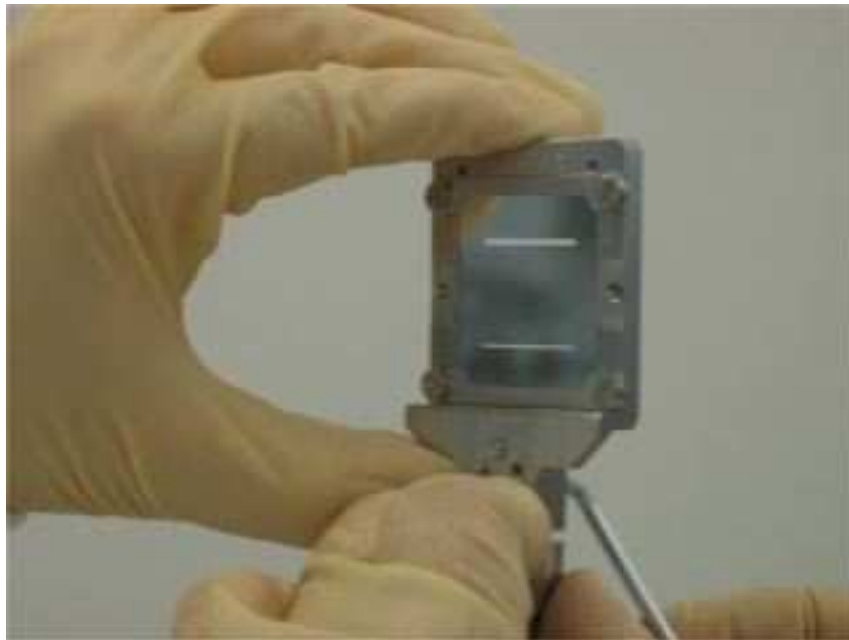


Figure 2: The new Diffraction Radiation screen mounted in the by pass line.

## RADIATION PROTECTINO GROUP

R. Bedogni (Art. 23), M. Chiti (Tecn.), A. Esposito (Resp.),  
A. Gentile (Tecn.), L. Fioretti (Tecn.)

### 1 Institutional duties

The LNF Radiation Protection Group is in charge of the radiation safety and the radiation protection surveillance at the LNF. Environmental and individual radiation monitoring are routinely performed by means of active and passive dosimeters. The environmental dosimetry is based on a lattice of about 100 measurement points distributed over four “rings” around the DAΦNE accelerator complex, up to the boundary of the center. Each point is monitored by means of two dosimeters, provided and processed by the U.F. Fisica Sanitaria itself and the ENEA dosimetry Service, respectively. The same double dosimeter system is used for the individual monitoring of the “Category B” workers. A lattice of active monitoring units, each formed by a rem-counter and an ion chamber, are located around the DAΦNE accelerator complex, and operate as complementary ambient dosimetry system. In case the instantaneous ambient dose rate exceeds a given threshold level, the units provide an “alarm signal” which immediately shuts down the accelerator. Moreover, a confirmation monitoring with active neutron and gamma portable instruments is periodically performed over the center. The radiation induced activity in the components and the instruments inside the accelerator buildings is also periodically assessed. Low background Germanium detectors are used to check the potentially activated component and instruments before clearance or manipulation. The Group is holding a series of Standards for the calibration of the instruments used for the radiation protection surveillance. Whilst radioactivity measuring devices are calibrated with portable alfa, beta and gamma sources, the active and passive dosimeters are calibrated with reference photon and neutron fields.

The Radiation Protection Group is also in charge of the workers classification, the radiation protection and safety training, the dose recording and all licensing and communication activities required by the Italian Radiation Protection Law, D.Lgs. 230/95.

The introduction, detention and use of radioactive sources or X-rays apparatus at the LNF is regulated and controlled by the Group.

The Group is involved in the radiation protection and safety aspects for the commissioning of the following projects: DANAE, SPARC, Plasmon-X, and SPARX.

### 2 Research and Development activities

The LNF Radiation Protection Group is involved in several R&D activities, aimed at verifying and improving the measurement techniques used in the routine radiation surveillance. Moreover, the Group is involved in European and International Working Groups operating in the field of the ionizing radiation dosimetry and metrology. Collaborations with the Universidad Autonoma de Barcelona (Barcelona, Spain) and the “Ospedale S. Maria della Scaletta”, Ravenna, have been set up in the field of the experimental neutron spectrometry.

The following research activities have been performed in 2005:

- *Design and characterization of new thermoluminescence materials (TLDs)*. This study provided passive dosimeters with very high performance in terms of separate neutron and gamma measurements in mixed fields <sup>1, 2, 3</sup>). The calibration tests have been performed at the ENEA Frascati Fast Neutron Generator and the ENEA Bologna Secondary Standard calibration Laboratory. These dosimeter are currently used for neutron dosimetry and spectrometry measurements around the DAΦNE complex.

- *Development of a chemical processing system and an automated reader for CR-39 neutron dosimeters.* A CR-39 based neutron dosimetry system has been set up to augment the environmental surveillance system. A suitable chemical processing unit has been recently installed, and an automated track analysis system has been designed and assembled at the Radiation Protection Laboratory <sup>4)</sup>. This kind of dosimeter provides a valuable contribution to the routine dosimetry, since its response is not influenced by photon radiation. Two external researchers, in the framework of the FAI convention (M. Virgolici) and the collaboration with the Universidad Autonoma de Barcelona (M. J. Garcia) contributed to establish the chemical and reading procedures during 2005.
- *Characterization and clearance of the waste resulting from the decommissioning of ADONE.* The decommissioning of ADONE, in 1993, produced a considerable amount of potentially activated metallic scraps and slightly activated tritiated water. This constitutes a low level radioactive waste repository, that the LNF R.P. Group is managing and routinely monitoring. Moreover, an extensive sampling and measuring procedure is in progress, aimed at an accurate radiometric characterization of the waste for clearance purposes <sup>5)</sup>. An external researcher, in the framework of the FAI convention (J. C. Mora), contributed to this work during 2005. Almost five years are required to complete the work.
- *Characterization and validation of a Bonner Sphere based neutron spectrometer.* A Bonner Sphere spectrometric system, using a 4 mm x 4 mm LiI(Eu) active scintillator, has been studied and its energy response has been validated for use in radiation protection neutron monitoring. The experimental tests have been performed with reference neutron fields at the LNF and the ENEA Bologna Secondary Standard calibration Laboratory. Measurements at the LNF BTF facility have been also performed. A joint neutron spectrometry experimental exercise (May 2005) has been carried out, with the Universidad Autonoma de Barcelona, at the 2.5 and 14.2 MeV monochromatic beams of the ENEA Frascati Fast Neutron Generator. Moreover, an unfolding code for inferring the neutron spectrum from the Bonner Sphere reading has been written in the Group. The spectrometer has been implemented for the environmental surveillance around DAΦNE.

The experimental results obtained with this system have been used as reference data in the computational exercise “Uncertainty assessment in computational dosimetry” organized during 2005 by EU - CONRAD (Coordinate Network for Radiation Dosimetry) <sup>6)</sup>.

The system has been also adapted to be used with Thermoluminescence detectors and gold activations foils, in order to cover experimental needs from very low ( $1 \text{ cm}^{-2} \cdot \text{s}^{-1}$ ) to very high ( $10^8 \text{ cm}^{-2} \cdot \text{s}^{-1}$ ) neutron fluence rate. Whilst the very sensitive TLD version is used for the ambient dosimetry around DAΦNE, the gold foils version has been applied to measure the parasitic neutron spectra arising in medical LINACs. Under request of the “Ospedale S. Maria della Scaletta”, Ravenna, a collaboration in this field has been established <sup>7)</sup>.

- *Secondary Standard calibration Laboratory.* At the R. P. Laboratory, a multi-source irradiation unit is routinely used to calibrate the dosimeters and dose-rate meters with gamma fields ( $^{241}\text{Am}$ ,  $^{137}\text{Cs}$ ,  $^{60}\text{Co}$ ) in the dose rate range from 0.0005 to  $2 \text{ mGy} \cdot \text{h}^{-1}$ . With the aim of obtaining the SIT accreditation as Secondary Standard Laboratory, a standardization and measurement automation <sup>8)</sup> work is in progress.
- *International Commitment in the measurement and standardization of complex workplace radiation fields.* The R. P. Group is involved in the working Group ISO/TC85/SC2/WG2 for the Standardization of the procedures to calibrate radiation protection instruments (WG2, reference radiations). The last meeting, which main task was the establishment of the Standard 12789-2 (Calibration Fundamentals related to the basic quantities characterizing sim-

ulated workplace neutron fields), was hosted by the R. P. Group at the LNF from 17 to 19 October 2005.

In the EU framework, the Group is participating to the working group EU CONRAD WP6/WG8, “Complex mixed radiation fields at workplaces”, aimed at establishing new dosimetric techniques for the characterization of mixed neutron/gamma fields (including high energy and pulsed fields).

### 3 Educational activities

The Group participated to the collaborations between the LNF and the Schools during 2005: “stages invernali”, “stages estivi”, “open Day”, and, for the teachers, “incontri di Fisica”. Participation to the project “Misura della radioattività ambientale” organized for the schools by SIF, INFN, AIF, MIUR and Ministero dell’Ambiente <sup>9)</sup>.

### 4 Archaeometry

Since 2005 the Group is supervising a University thesis in roman archaeology, dealing with the characterization of roman finds by means of X-rays fluorescence technique, using a recently developed experimental apparatus. An external associated scientist (A. Georghinian) contributed to this activity.

### References

1. R. Bedogni, M. Angelone, A. Esposito, M. Chiti “Inter-comparison among different TLD based techniques in a standard multisphere assembly for the characterization of neutron fields”, (in press on *Radiat. Prot. Dosim.*).
2. R. Bedogni, A. Esposito, M. Angelone, M. Chiti, “Determination of the response to photons and thermal neutrons of new LiF based TL materials for radiation protection purposes”, (in press on *IEEE Trans. Nucl. Sci.*).
3. A. Esposito, R. Bedogni, M. Angelone, M. Chiti, M. Pillon, “Characterisation of new LiF based TL materials for use in neutron spectrometry with Bonner Spheres”, *Proc. 2005 IEEE Nuclear Science Symposium / Medical Imaging Conference*, 23-29 October 2005, Puerto Rico.
4. R. Bedogni, “Development of a reader for the routine analysis of CR-39 fast neutron dosimeters: improvement of the dosimetric performance using automatic vision and motion tool”, *Radiat. Meas.* **36**(1-6), 239-243 (2003).
5. J.C. Mora, R. Bedogni, A. Esposito, A. Gentile, “Results of the determination of the possible contamination at the ADONE decommissioned material”, internal Report (2005).
6. CONRAD (European Union - Coordinate Network for Radiation Dosimetry, Work Package 4), “Uncertainty assessment in computational dosimetry - An intercomparison of Approaches”, (2005).
7. A. Esposito, R. Bedogni, L. Lembo, M. Morelli, “Tecniche per la spettrometria neutronica attorno ad acceleratori di particelle: acceleratori medicali”, *Proceedings “Convegno Nazionale di Radioprotezione - La radioprotezione nella ricerca. La ricerca in radioprotezione”*, Catania, 15-17 Settembre 2005. ISBN 88-88648-03-8.
8. R. Bedogni, F. Monteventi, “Development of automatic systems for the ionising radiation metrology at the ENEA-IRP secondary standard laboratory”, *Radiat. Prot. Dosim.* **115**(1-4), 612-615 (2005).
9. R. Bedogni, “Progetto Misura della radioattività ambientale - Radiazioni e radioprotezione, Allegato tecnico”, (2005).

## SPARC

D. Alesini, M. Bellaveglia, S. Bertolucci, M.E. Biagini, R. Boni, M. Boscolo, M. Castellano, A. Clozza, G. Di Pirro, A. Drago, A. Esposito, M. Ferrario, D. Filippetto, V. Fusco, A. Gallo, A. Ghigo, S. Guiducci, M. Incurvati, C. Ligi, F. Marcellini, M. Migliorati, A. Mostacci, L. Palumbo (Resp.), L. Pellegrino, M. Preger, P. Raimondi, R. Ricci, C. Sanelli, M. Serio, F. Sgamma, B. Spataro, A. Stecchi, A. Stella, F. Tazzioli, C. Vaccarezza, M. Vescovi, C. Vicario, M. Zobov (**INFN /LNF**);

F. Alessandria, A. Bacci, I. Boscolo, F. Broggi, S. Cialdi, C. DeMartinis, D. Giove, C. Maroli, V. Petrillo, M. Romè, L. Serafini (**INFN /Milano**);

D. Levi, M. Mattioli, P. Musumeci, G. Medici (**INFN /Roma1**);

L. Catani, E. Chiadroni, A. Cianchi, C. Schaerf, S. Tazzari (**INFN /Roma2**);

### 1 Aim of the experiment

The aim of the SPARC project (Phase 1) is to promote an R&D activity oriented to the development of a high brightness photoinjector to drive SASE-FEL experiments. It has been proposed by a collaboration among ENEA-INFN-CNR-Universita' di Roma Tor Vergata-INFN-ST and funded by the Italian Government and INFN with a 3 year time schedule. The main goals of the SPARC project are: 1) the generation of a high brightness electron beam able to drive a self-amplified spontaneous free-electron laser (SASE FEL) experiment in the green visible light and higher harmonics generation, 2) the development of an ultra-brilliant beam photo-injector needed for the future SASE FEL-based X-ray sources. The machine will be installed at LNF, inside an existing underground bunker. We foresee conducting investigations on the emittance correction and on the rf compression techniques up to kA level.

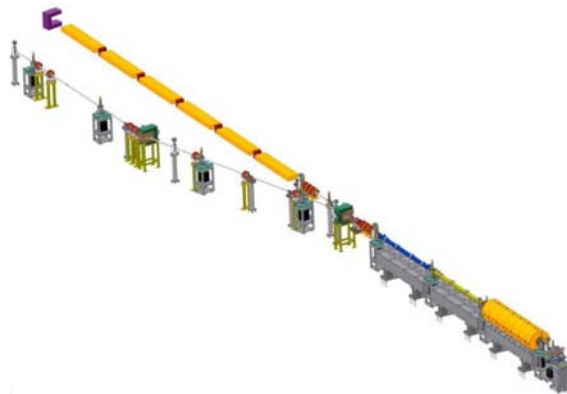


Figure 1: *Layout of SPARC photo-injector, with RF-gun, 3 S-band accelerating sections and FEL undulator (6 modules). Beam line for undulator by-pass is also shown.*

We present in this report the status of the activities concerning the injector that is under the responsibility of the INFN. In the past year the design of the experiment and the main technological

choices have been set up as follows. The proposed system to be built consists of: a 1.6 cell RF gun operated at S-band (2.856 GHz, of the BNL/UCLA/SLAC type) and high peak field on the cathode (120 MV/m) with incorporated metallic photo-cathode (Copper or Mg), generating a 5.6 MeV beam which is properly focused and matched into 3 accelerating sections of the SLAC type (S-band, travelling wave) which accelerate the bunch up to 150-200 MeV.

The choice of the S-band Linac with respect to a L-band is due to compactness of the system, the lower cost, and the existence at LNF of a 800 MeV Linac based on the same technology, with obvious advantages on the side of the expertise and spares components. Moreover, the higher RF frequency leads to a higher peak brightness attainable by an optimized photo-injector. In our case we expect a projected emittance  $< 2$  mm-mrad, a slice emittance  $\sim 1$  mm-mrad with a slice peak current of 100 A.

## 2 Group activity in 2005

### 2.1 Installation of main components

The SPARC project is by now in its advanced installation phase at LNF; tests of related equipments and instrumentation are also under way. The 150 MeV S-band photo-injector and the 12 m undulator for the FEL experiments are located inside an underground bunker, which hosts as well the clean room containing the Ti:Sa laser system driving the photo-cathode. The installation of the RF source and distribution system started during 2005. The klystron pulsed power modulators, supplied by PPT, have been positioned in the SPARC klystron hall, as well as the klystrons (45 MW, 2856 MHz, TH2128C model manufactured by Thales), as shown in Fig. 2. The modulator connections with various controls and ancillary systems are being made. Modulators can switch the klystrons at a maximum rep. rate of 10 Hz, with HV pulses of 310 kV 340 A. The modulator power test have been performed initially with the klystron operating in diode-mode; the installation of waveguide distribution network and RF devices (circulators, shifters, etc.) has been completed in 2005.



Figure 2: *SPARC klystrons with oil tanks installed in the SPARC building (upper facility room or klystron hall).*

The 1.6-cell RF gun and the emittance-compensation solenoid have been delivered at LNF in February from UCLA. The gun supports are being modified to gain full control of the gun axis alignment. The water flow into the gun has been measured up to 5 l/m, a value that should allow control of the gun temperature at the level required for operation up to 10 Hz. The magnetic solenoid yoke has been assembled and it is also going through some minor mechanical modifications.

The solenoid uses 4 different coils that can be independently excited. The magnetic field will be measured to check for axis misalignments and to record longitudinal magnetic field profiles in the different current configurations. Two accelerating sections have been delivered by Mitsubishi, while one of the two sections given by SLAC to SPARC, as part of a collaboration agreement, is under test. As shown in Fig. 1, the first accelerating section will be embedded (see yellow zone) in an array of solenoids, required to produce a magnetic field for additional focusing in order to comply with the Ferrario working point matching conditions for emittance compensation. Thanks to a newly funded European project, EUROFEL, an additional array of solenoids will be built and installed around the second section, in order to further improve the performances of emittance compensation in particular when RF compression is applied. The Ti:Sa laser system, built by Coherent, has passed acceptance tests. The HIDRA-50 amplifier system, made of one regenerative and two multi-pass amplifiers, has already reached the specs in the infra-red, delivering 50 mJ of output pulse energy with 104 fs pulses and good beam quality ( $M^2_x=1.9$  and  $M^2_y=1.6$ ). Preliminary tests in the UV (266 nm), performed after the third harmonic crystal and the UV stretcher, showed the capability to reach 1.8 mJ of pulse energy with quite good pulse-to-pulse stability, i.e. less than 4.5% good beam quality, i.e.  $M^2_x=2.7$  and  $M^2_y=1.9$ . These tests have been completed at LNF. A characterization of the oscillator output spectrum was also performed, showing a quite good behavior (see Fig. 3).

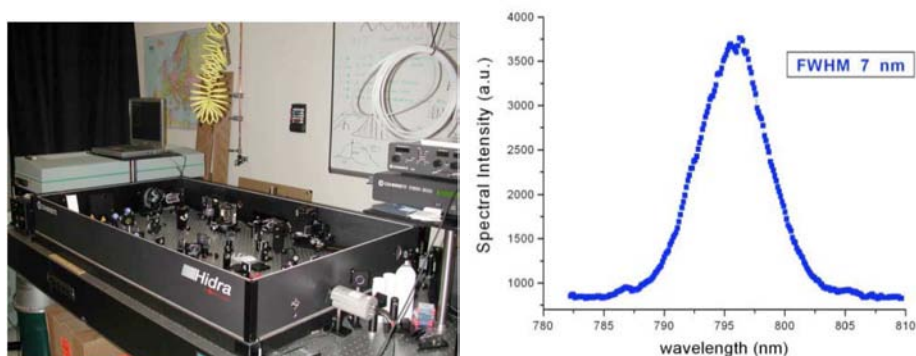


Figure 3: *HIDRA-50 amplifier for the SPARC laser and output spectrum of laser oscillator*

## 2.2 Commissioning of the SPARC movable emittance meter and its first operation at PITZ

The construction of the device was completed in the first part of this year while the beam studies of SPARC Injector with the e-meter are scheduled for the end of 2005. The evidence of a temporal gap between the completion of the e-meter and its first scheduled operations at SPARC suggested the possibility of a temporary installation at DESY Zeuthen for a round of measurements of the PITZ electron beam in the framework of a collaboration aiming on studies and operations with photo injectors. To permit the installation of the SPARC e-meter at PITZ we modified the original design of the system to ensure its mechanical compatibility.

### 2.2.1 Screens and imaging system

The transverse distribution of low-charge beamlets emerging from the slit-mask needs to be measured with high accuracy. It means that radiator screens, used for this purpose, need to have a linear response with beam charge in the range of few tenths of pC and they must guarantee a



Figure 4: *Emittance-meter device with long bellows.*

spatial resolution better than  $20\ \mu\text{m}$ . Same performance are required from the imaging system that should not introduce any degradation to the figure above. Doped-YAG radiators, either crystals or sintered screens, are good candidates because of their high resolution and efficiency. For our application, we focused our attention on Ce:YAG radiators that we tested at the DAFNE Beam Test Facility. We collect forward radiation emitted from Ce:YAG crystal with a mirror at  $45^\circ$  downstream the radiator. As result the radiator is observed at  $90^\circ$  with respect to the rear face thus minimizing the degradation of spatial resolution due to the non-negligible thickness of transparent crystal. The performance of the Ce:YAG radiator has been compared to those of a Cr-oxide radiator used by our group in previous applications. Both radiators have been installed at the same diagnostic station in the DAFNE Beam Test Facility and their performances measured under different beam conditions, within the range of values expected in the SPARC injector. Analysis of results shows that performances of the Ce:YAG screen are superior: efficiency is a factor 2-3 higher than Cr-oxide and resolution is evidently better, as we can observe comparing the two pictures on Fig. 5. At the same time we didnt report any evidence of a deviation from a linear correlation between the light yield from the two radiators varying the charge density of the beam in the range of values expected in the SPARC injector. This confirms a good linearity of the

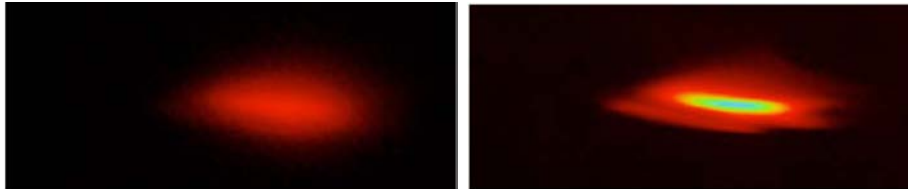


Figure 5: *Electron beam imaging using Cr-oxide (top) and Ce-doped YAG radiators (bottom). Electronic gain of the CCD camera was approximately three times higher in the case of Cr-oxide screen to get comparable pixel values with the Ce:YAG.*

Ce:YAG radiator with charge density in the range of values of interest. Its worth to mention that tests of the imaging system previously made in our laboratory shown that a resolution better than  $11\ \mu\text{m}$  can be achieved.

### 2.2.2 Operation at PITZ

The original design of the SPARC emittance meter has been partially modified during the construction to permit its installation in the Photo Injector Test Facility PITZ at DESY Zeuthen. Mainly the table, being the support for the beamline, was modified by shortening its legs to allow

installation on top of the PITZ girder. Legs extenders have been prepared and they will be used to adjust the height of the modified e-meter to that needed for SPARC. Furthermore we ensured mechanical compatibility between SPARC e-meter and PITZ vacuum beamline. Alignment tools and procedures have been jointly defined. The SPARC e-meter has been installed in the last section of the upgraded PITZ beamline, in the space located after the booster, before the electron beam spectrometer (Fig. 6). The SPARC e-meter has its own control and acquisition system. Two



Figure 6: *SPARC e-meter during installation at the Photo Injector Test Facility PITZ.*

PCs have been installed in the PITZ control room to run control panels and measurements programs. Motors are controlled via CAN bus or RS232 serial interfaces. PCs running control panels communicate with motor controllers via network using a network serialport server. To connect a PC in the control room with digital cameras in the accelerator tunnel, because of limitation of the maximum cable length (4.5 meters), we used a fiber-optic firewire extender. Magnetic steerers are installed at the beginning of the system, clamped around the upstream flange. They can be used to adjust the direction of the electron beam in the x and y plane. Installation of the SPARC e-meter was completed in the beginning of July 2005 and commissioning started. We verified the reproducibility of measurements under different beam conditions and studied the strategies for the optimization of the measurements, e.g. adjusting the distance between the slits mask and the screen (Fig. 7). Although the injector parameters and the transport of the beam are not yet

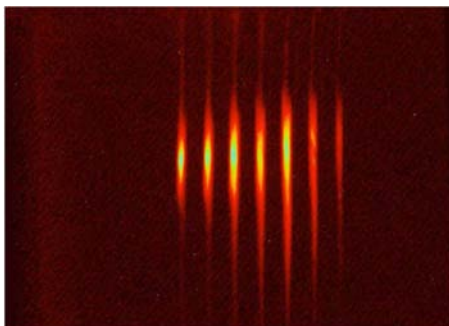


Figure 7: *Picture of the beam at the YAG screen downstream the multi-slit mask.*

optimized since commissioning of the upgraded PITZ facility is still in progress, preliminary measurements confirm the value of transverse emittance, as expected for the current injector settings,

and its variation along the beamline. As an example we report the measurements of the vertical emittance at three different positions along the e-meter (Fig. 8). The measurements show a constant increase of the vertical emittance as function of longitudinal position in the case with booster off while for the higher energy beam accelerated by the booster the value stays almost constant (within the measurement errors). These results are in good agreement with simulations for the current injector settings.

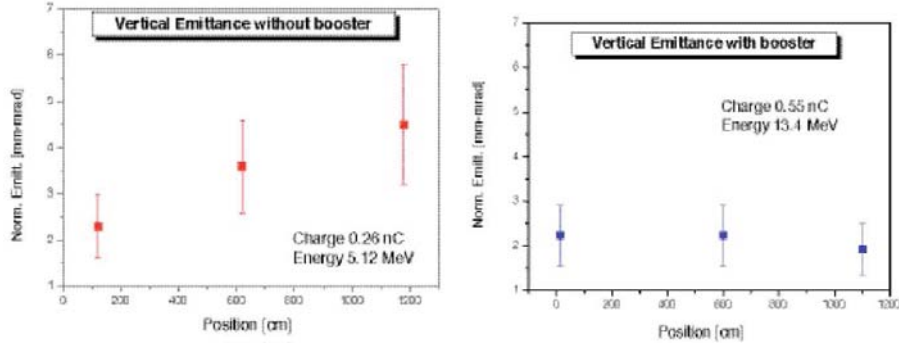


Figure 8: Preliminary result of vertical emittance measurements at PITZ with the SPARC e-meter under different conditions (booster off/on). Note that the three zpositions are not coincident in the two cases; also the beam charge is not identical.

### 2.3 Laser-RF system synchronization

The stability of the synchronization between the laser pulse and the RF reference is crucial task. The laser system will be synchro-locked to a RF/36 signal (79.33MHz) generated in the SPARC timing system. The time jitter of the final UV laser shot respect to the RF synchro-lock has been specified by the laser system manufacturer to be  $\sigma_{t_{laser}} \leq 500 f_{s_{rms}}$ . Pulse-to-pulse phase drifts of the laser-to-RF lock have to be measured and corrected by a dedicated feedback algorithm. In order to measure the stability of the synchronism between the laser shot and the RF reference line, we are proposing the scheme reported in Fig. 9. The laser shot is converted in a long lasting RF

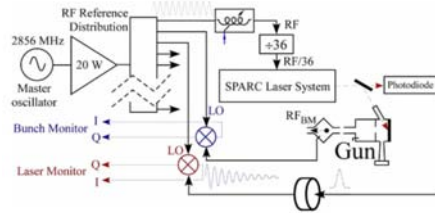


Figure 9: Laser pulse synchronization monitoring.

exponential pulse generated by a RF cavity tuned at 2856MHz excited with a short pulse from a fast photodiode illuminated with a sample of the laser pulse. The RF phase of the exponentially decaying pulse with respect to the RF reference signal is measured again by means of an I&Q mixer. The same phase measurement will be performed on the bunch released by the RF gun. In this case

the exponential pulse will be produced by a 2856MHz bunch monitor cavity placed between the RF gun and the accelerating section S1 excited directly by the bunch. This approach to the phase measurement of pulses whose duration is much shorter than the RF period has been tested on the bench. The measurement layout is sketched in Fig. 10. Short pulses are obtained by exciting a

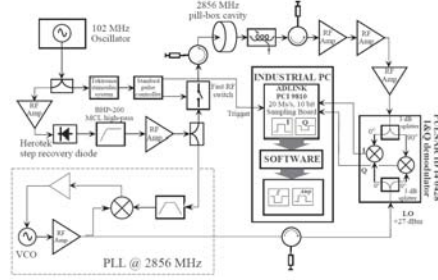


Figure 10: *Short pulse synchronization bench measurement.*

step recovery diode at the 28th sub-harmonics (102MHz) of the linac RF frequency. The repetition rate of the pulses is reduced from 102MHz to 100kHz by gating the pulse train through a fast RF switch. The pulse train emerging from the RF switch is filtered by a 2856MHz cavity that convert it in a series of a RF pulses with exponential profiles and decay time of about 500ns each. The exponential pulses are amplified and demodulated with an I&Q mixer driven with a LO reference signal obtained extracting the 28th harmonics from the original 102MHz pulse train by means of a PLL circuit. The spectral content at 2856MHz of the 100kHz short pulses train is quite low, so it is necessary to put many RF amplification stages along the path to the demodulator input to restore a suitable level of the signal. This should not be necessary in the final layout of Fig. 9 since higher levels of the signals to be monitored are expected. Typical I&Q signals acquired for a single short pulse with this setup and the extrapolated amplitude and phase are reported in Fig. 11. The

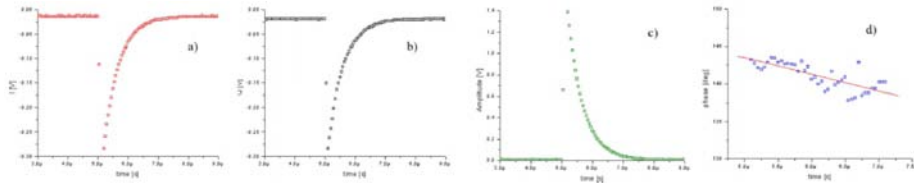


Figure 11: *Typical I&Q signals acquired for a single short pulse (a, b) and extrapolated amplitude (c) and phase (d).*

resolution obtained with this set-up is reasonably good and we believe that it may be improved in the final setup where less RF amplification will be needed and 14-bit, 65Ms/s sampling boards (ADLINK PCI 9820TM) will be used. Other methods for measuring the synchronization stability of short pulses based on triggered oscillators phase measurement are presently under study by the Sincrotrone Trieste group.

## References

1. L. Palumbo, et al., "Recent Results from and Future Plans for the VISA II SASE FEL", Particle Accelerator Conference, Knoxville, Tennessee 2005, pp. 2167-2169.
2. L. Palumbo, et al., "Start To End Simulation for the SPARX Project", Particle Accelerator Conference, Knoxville, Tennessee 2005, pp. 1455-1457.
3. L. Palumbo, et al., "Design and Measurements of an X-Band Accelerating Cavity for SPARC", Particle Accelerator Conference, Knoxville, Tennessee 2005, pp. 1407-1409.
4. M. Ferrario, et al., "Preliminary Results on Beam Dynamics of Laser Pulse Shaping Effects in SPARC", Particle Accelerator Conference, Knoxville, Tennessee 2005, pp. 1315-1317.
5. M. Ferrario, et al., "SPARC Working Point Optimization for a Bunch with Gaussian Temporal Profile", Particle Accelerator Conference, Knoxville, Tennessee 2005, pp. 1248-1250.
6. M. Ferrario, et al., "Optimization of RF Compressor in the SPARX Injector", Particle Accelerator Conference, Knoxville, Tennessee 2005, pp. 1144-1146.
7. M. Ferrario, et al., "Temporal E-Beam Shaping in an S-Band Accelerator", Particle Accelerator Conference, Knoxville, Tennessee 2005, pp. 642-644.
8. M. Ferrario, "Frontiers of RF Photoinjectors", Particle Accelerator Conference, Knoxville, Tennessee 2005, pp. 530-534.
9. D. Alesini, et al., "Status of the SPARX FEL Project", Proceedings of the 27th International Free Electron Laser Conference, 21-26 August 2005, Stanford, California, USA, pp.491-494.
10. D. Alesini, et al., "Simulations, Diagnostics and Recent Results of the VISA II Experiment", Proceedings of the 27th International Free Electron Laser Conference, 21-26 August 2005, Stanford, California, USA, pp.83-86.
11. L. Palumbo, et al., "Beam Dynamics Studies for the SPARXINO Linac", Proceedings of the 27th International Free Electron Laser Conference, 21-26 August 2005, Stanford, California, USA, pp.67-70.
12. M. Ferrario, et al., "Experimental Studies of Temporal Electron Beam Shaping at the DUV-FEL Accelerator", Proceedings of the 27th International Free Electron Laser Conference, 21-26 August 2005, Stanford, California, USA, pp.632-635.
13. M. Ferrario, et al., "Collective Effects in the Thomson Back-Scattering between a Laser Pulse and a Relativistic Electron Beam", Proceedings of the 27th International Free Electron Laser Conference, 21-26 August 2005, Stanford, California, USA, pp.580-583.
14. M. Ferrario, et al., "Status and First Results from the Upgraded PITZ Facility", Proceedings of the 27th International Free Electron Laser Conference, 21-26 August 2005, Stanford, California, USA, pp.564-567.
15. M. Ferrario, et al., "Quantum SASE FEL with a Laser Wiggler", Proceedings of the 27th International Free Electron Laser Conference, 21-26 August 2005, Stanford, California, USA, pp.71-74.
16. M. Ferrario, et al., "Status of the Seeding Experiment at SPARC", Proceedings of the 27th International Free Electron Laser Conference, 21-26 August 2005, Stanford, California, USA, pp.63-66.

**YEAR 2005 FRASCATI PUBLICATIONS**

Available at [www.lnf.infn.it](http://www.lnf.infn.it)

**1 – Frascati Physics Series**

**Volume XXXVII**

*Frontier Science 2004, Physics and Astrophysics in Space*

Eds. A. Morselli, P. Picozza, M. Ricci

Frascati, 14–19 June, 2004

ISBN—88-86409-52-4

**Volume XXXVIII**

*Les Rencontres de Physique de la Vallée d'Aoste – Results and Perspectives in Particle Physics*

Ed. M. Greco

La Thuile, Aosta Valley, February 27 – March 5, 2005

ISBN—88-86409-45-1

**Volume XXXIX**

*II Workshop Italiano sulla Fisica di ATLAS e CMS – Results and Perspectives in Particle Physics*

Ed. G. Carlino

Napoli, October 13 – 15, 2004

ISBN—88-86409-44-3

## 2 – LNF–Frascati Reports

### LNF-05/01(P)

I. Peruzzi

*CP Violation in B Mesons Decays: A Review After Five Years of B-Factories*

Submitted to Rivista del Nuovo Cimento

### LNF-05/02(P)

S. Bellucci

*Nanotubes for Particle Channeling, Radiation and Electron Sources*

To be published in Nucl. Instr. & Meth. B

### LNF-05/03(P)

Il Progetto ScienzaPerTutti: la Fisica in Rete

L. Benussi et al.

Presented at EXPO-Learning 2004, Ferrara

### LNF-05/04(IR)

D. Alesini, G. Benedetti, M. Biagini, C. Biscari, R. Boni, M. Boscolo, A. Clozza, G. Delle Monache, G. Di Pirro, A. Drago, A. Gallo, A. Ghigo, S. Guiducci, M. Incurvati, C. Ligi, F. Marcellini, G. Mazzitelli, C. Milardi, L. Pellegrino, M. Preger, P. Raimondi, R. Ricci, C. Sanelli, M. Serio, F. Sgamma, B. Spataro, A. Stecchi, A. Stella, C. Vaccarezza, M. Vescovi, M. Zobov, C. Pagani, E. Levichev, P. Piminov, D. Shatilov, J. Byrd, F. Sannibale, J. Fox, D. Teytelmann

*Proposal of a Bunch Length Modulation Experiment in DADAΦNENE*

### LNF-05/05(IR)

AA. VV

*Activity Report 2004*

### LNF-05/06(P)

B. Spataro, D. Alesini, M. Migliorati, A. Mostacci, L. Palumbo, V. Baglin, B. Jenninger, F. Ruggiero

*Impedances of the Cold Bore Experiment, Coldex, Installed in the SPS Machine*

Submitted to Nuclear Instruments and Methods in Physics Research, Section A

### LNF-05/07(P)

D. Alesini, A. Bacci, P. Chimenti, V. Chimenti, A. Clozza, A. Falone, V. Lollo, M. Migliorati, A. Mostacci, F. Palpini, L. Palumbo, B. Spataro

*Design and RF Measurements of an X-Band Accelerating Structure for Linearizing the Longitudinal Emittance at Sparc*

To be submitted to Nuclear Instr. & Methods

### LNF-05/08(P)

The Use of a Synchronism Model of the Crystalline Lens of the Human Eye to Study the Light Flashes Seen by Astronauts

Giampietro Nurzia, Renato Scrimaglio, Bruno Spataro, Francesco Zirilli

Submitted to Radiation Research

### LNF-05/09(P)

The KLOE Collaboration: F. Ambrosino, A. Antonelli, M. Antonelli, C. Bacci, P. Beltrame, G. Bencivenni, S. Bertolucci, C. Bini, C. Bloise, V. Bocci, F. Bossi, D. Bowring, P. Branchini, R. Caloi, P. Campana, G. Capon, T. Capussella, F. Ceradini, S. Chi, G. Chiefari, P. Ciambrone, S.

Conetti, E. De Lucia, A. De Santis, P. De Simone, G. De Zorzi, S. Dell’Agnello, A. Denig, A. Di Domenico, C. Di Donato, S. Di Falco, B. Di Micco, A. Doria, M. Dreucci, G. Felici, A. Ferrari, M. L. Ferrer, G. Finocchiaro, C. Forti, P. Franzini, C. Gatti, P. Gauzzi, S. Giovannella, E. Gorini, E. Graziani, M. Incagli, W. Kluge, V. Kulikov, F. Lacava, G. Lanfranchi, J. Lee-Franzini, D. Leone, M. Martini, P. Massarotti, W. Mei, S. Meola, S. Miscetti, M. Moulson, S. M’uller, F. Murtas, M. Napolitano, F. Nguyen, M. Palutan, E. Pasqualucci, A. Passeri, V. Patera, F. Perfetto, L. Pontecorvo, M. Primavera, P. Santangelo, E. Santovetti, G. Saracino, B. Sciascia, A. Sciubba, F. Scuri, I. Sfiligoi, T. Spadaro, M. Testa, L. Tortora, P. Valente, B. Valeriani, G. Venanzoni, S. Veneziano, A. Ventura, R. Versaci, G. Xu

*A Direct Search for the CP-Violating Decay  $K_S \rightarrow 3\pi^0$  with the KLOE Detector at DAΦNE*

Accepted by Physics Letter B, May 26 2005

**LNF-05/10(Thesis)**

Gabriele Benedetti

*DAΦNE Lattice with Two-Low-Beta Interaction Regions*

**LNF-05/11 (IR)**

Second Order Harmonics Suppression With Glass Filters for Synchrotron UV Radiation Calibration Measurement

E. Burattini, A.De Sio, L. Gambicorti, F. Malvezzi, A. Marcelli, F. Monti, E. Pace

**LNF-05/12 (IR)**

Alessio Bocci, Massimo Piccinini, Alessandro Drago, Diego Sali, Pierangelo Morini, Emanuele Pace, Augusto Marcelli

*Detection of the SR Infrared Emission of the Electron Bunches at DAΦNE*

**LNF-05/13 (P)**

A. Calcaterra, R. de Sangro, G. Mannocchi, P. Patteri, P. Picchi, M. Piccolo, N. Redaelli, T. Tabarelli de Fatis, G.C. Trincherò

*A New Concept for Streamer Quenching in Parallel Plate Chambers*

Submitted to Nuclear Instruments and Methods in Nuclear Research

**LNF-05/14 (P)**

Francesco Celani, A. Spallone, P. Marini, V. Di Stefano, M. Nakamura, E. Todarello, A. Mancini, P. G. Sona, E. Righi, G. Trenta, C. Catena, G. D’agostaro, P. Quercia, V. Andreassi, F. Fontana, L. Gamberale, D. Garbelli, E. Celia, F. Falcioni, M. Marchesini, E. Novaro, U. Mastromatteo

*Further Studies, About New Elements Production, by Electrolysis of Cathodic Pd Thin-Long Wires, in Alcohol-Water Solutions (H, D) and Th-Hg Salts. New Procedures to Produce Pd Nano-Structures*

Invited paper at: 6th Meeting of Japan CF Research Society April 27-28, 2005, Tokyo Institute of Technology, Japan Presented by Francesco Celani

**LNF-05/15 (P)**

Francesco Celani, A. Spallone, E. Righi, G. Trenta, C. Catena, G. D’agostaro, P. Quercia, and V. Andreassi, P. Marini, V. Di Stefano, M. Nakamura, A. Mancini, P.G. Sona, F. Fontana, L. Gamberale, and D. Garbelli, E. Celia, F. Falcioni, M. Marchesini, And E. Novaro, U. Mastromatteo  
*Innovative Procedure for the, In Situ, Measurement of the Resistive Thermal Coefficient Of H(D)/Pd During Electrolysis; Cross-Comparison of New Elements Detected in The Th-Hg-Pd-D(H) Electrolytic Cells*

Invited paper at ICCF11, October 30, November 5, (2004) Marseille (France)

**LNF-05/16 (IR)**

A. Balla, M. Beretta, P. Branchini, P. Ciambrone, G. Corradi, E. De Lucia, P. de Simone, G. Felici, M. Gatta, V. Patera

*A 32 Channels Charge Integrating ADC Based on Digital Signal Integration*

**LNF-05/17(P)**

I.I. Bigi, L. Maiani, F. Piccinini, A.D. Polosa, V. Riquer

*Four-Quark Mesons in Non-leptonic B Decays – Could They Resolve Some Old Problems?*

**LNF-05/18(P)**

Antonio Spallone, Francesco Celani, Paolo Marini, Vittorio Di Stefano

*Measurements of the Temperature Coefficient of Electric Resistivity of Hydrogen Overloaded Pd*

Proceedings della Conferenza ICCF12, Yokohama (Japan), November, 2005

**LNF-05/19(P)**

Dariush Hampai, Sultan B. Dabagov, Giorgio Cappuccio and Giannantonio Cibin

*X-ray Propagation Through Hollow Channel: PolyCAD - A Ray Tracing Code*

Nuclear Inst. and Methods in Physics Research, B journal n. 5212

**LNF-05/20(P)**

Tadahiko Mizuno, Tadashi Akimoto, Akito Takahashi, and Francesco Celani

*Neutron Emission from D<sub>2</sub> Gas in Magnetic Fields Under Low Temperature*

**LNF-05/21 (P)**

A. Spallone and F. Celani

*An Overview of Experimental Studies on H/Pd Over-Loading with Thin Pd Wires and Different Electrolytic*

Invited paper at: ICCF11, October 30, November 5, (2004) Marseille (France)

**LNF-05/22(IR)**

P. Chimenti, V. Chimenti, A. Clozza, R. Di Raddo, V. Lollo, M. Migliorati, B. Spataro

*First Results on Vacuum Brazing of Rf 11 Ghz Accelerating Structure at Frascati Laboratories*

**LNF-05/23(IR)**

P. Chimenti, V. Chimenti, A. Clozza, R. Di Raddo, V. Lollo, M. Migliorati, B. Spataro

*An Investigation on Electroforming Procedures for R.F. 11 Ghz Linear Accelerating Structures at Frascati Laboratory*

**LNF-05/24 (IR)**

*A Photon Tag Calibration Beam for the AGILE Satellite*

S. Hasan, M. Prest, L. Foggetta, C. Pontoni, A. Mozzanica, G. Barbiellini, M. Basset, F. Liello, F. Longo, E. Vallazza, B. Buonomo, G. Mazzitelli, L. Quintieri, P. Valente, F. Boffelli, P. Cattaneo, F. Mauri

**LNF-05/25 (IR)**

*High Granularity Silicon Beam Monitors for Wide Range Multiplicity Beams*

A. Mozzanica, F. Risigo, A. Bulgheroni, M. Caccia, C. Cappellini, M. Prest, L. Foggetta, B. Buonomo, G. Mazzitelli, P. Valente, E. Vallazza

**LNF-05/26(P)**

Accelerator Division

*Papers presented at EPAC 2005*

Presented at the 2005 Particle Accelerator Conference (PAC 2005) Knoxville, Tennessee, USA - May 16-20, 2005

**LNF-05/27(IR)**

G. Modestino, G.Pizzella, F.Ronga – for the ROG Collaboration

*Calibration of the Resonant Gravitational Wave Detectors Explorer and Nautilus in 2003 and 2004 Using Cosmic Rays*

**LNF-05/28 (P)**

S. Bianco

*D Meson Spectroscopy*

Invited Review talk delivered at HADRON05, Rio de Janeiro, August 2005

**LNF-05/29 (P)**

Olaf N. Hartmann

*Nuclear and Hadron Physics with Antiprotons: PANDA@FAIR*

Invited talk at the 6th International Conference on Nuclear Physics at Storage Rings, 23-26 May 2005, Julich-Bonn, Germany

**LNF-05/30 (P)**

E.Basile, F.Bellucci, L. Benussi, M. Bertani, S. Bianco, M.A. Caponero, D. Colonna, F. Di Falco, F.L. Fabbri, F. Felli, M.Giardoni, A. La Monaca, F.Massa, G. Mensitieri, B. Ortenzi, M. Pallotta, A. Paolozzi, L. Passamonti, D. Pierluigi, C. Pucci, A. Russo, G. Saviano

*Micrometric Position Monitoring Using Fiber Bragg Gratin Sensors in Silicon Detectors*

Presented by S.Bianco at ICATPP05, Villa Olmo (Como) Italy 2005

**LNF-05/31 (P)**

E.Basile, F.Bellucci, L. Benussi, M. Bertani, S. Bianco, M.A. Caponero, D. Colonna, F. Di Falco, F.L. Fabbri, F. Felli, M. Giardoni, A. La Monaca, F.Massa, G. Mensitieri, B. Ortenzi, M. Pallotta, A. Paolozzi, L. Passamonti, D.Pierluigi, C. Pucci, A. Russo, G. Saviano

*Two-And Three-Dimensional Reconstruction and Analysis of the Straw Tubes Tomography in the BTeV Experiment*

Presented by F. Massa at ICATPP05, Villa Olmo (Como) Italy 2005

**LNF-05/32 (P)**

E.Basile, F.Bellucci, L.Benussi, M. Bertani, S. Bianco, M.A. Caponero, D. Colonna, F. Di Falco, F.L. Fabbri, F. Felli, M.Giardoni, A. La Monaca, G. Mensitieri, B. Ortenzi, M. Pallotta, A. Paolozzi, L.Passamonti, D.Pierluigi, C. Pucci, A. Russo, G. Saviano, F. Massa, F.Casali, M.Bettuzzi, D.Biancon, F. Baruffaldi, E. Petrilli

*A Novel Approach for an Integrated Straw Tube-Microstrip Detector*

Submitted to Transactions on Nuclear Science

**LNF-05/33 (I)**

Eds: Alessandra Fantoni e Caterina Bloise

*A Futuro dei Laboratori*

in press

### 3 – INFN Reports

#### INFN-AE-05-01

G. Cabras, S. D' Auria, D. Cauz, D. Cobai, M. Cobal, B. De Lotto, C. Del Papa, S. Gorokhov, H. Grassmann, L. Santi

*The Silicon Laboratory in Udine: Quality Assurance Tests on the Wafer Sensors for the Atlas Pixel Detector*

#### INFN-AE-05-02

Paola La Rocca and Francesco Riggi

*Analysis of Neutron and Muon Counting During a Forbush Decrease*

#### INFN-AE-05-03

Fabio Cossutti

*Electroweak Corrections Uncertainty on the W Mass Measurement at Lep*

#### INFN-AE-05-04

Katsuya Amako, Susanna Guatelli, Vladimir N. Ivanchenko, Michel Maire, Barbara Mascialino, Koichi Murakami, Petteri Nieminen, Luciano Pandola, Sandra Parlati, Maria Grazia Pia, Michela Piergentili, Takashi Sasaki, Laszlo Urban

*Comparison of Geant4 Electromagnetic Physics Models Against the Nist Reference Data*

#### INFN-AE-05-05

Design and Development of a New Type of Solid in Geant4

Susanna Guatelli, Giorgio Guerrieri, Maria Grazia Pia

#### INFN-AE-05-06

R. Valle, F. Gatti, S. Dussoni, G. Cecchet, M. Rossella and D. Zanello

*Status of the MEG Experiment: Timing Counter Experimental Results*

#### INFN-AE-05-07

Filippo Fichera, Paola La Rocca, Francesco Librizzi, and Francesco Riggi

*An Inexpensive Coincidence Circuit for the Pasco Geiger Sensors*

#### INFN-AE-05-08

J. Albert, G. P. Dubois-Felsmann, D. G. Hitlin, F. C. Porter, G. Bonneaud, S. Playfer, M. Biagini, P. Raimondi, A. Stocchi, France, S. Bettarini, G. Calderini, F. Forti, M. A. Giorgi, A. Lusiani, N. Neri, Superiore and INFN, I-56127 Pisa, Italy, L. Silvestrini, INFN, I-00185 Roma, Italy, M. Ciuchini, Y. Cai, S. Ecklund, D. W. G. S. Leith, A. Novokhatski, B. N. Ratcliff, A. Roodman, J. Seeman, M. Sullivan, U. Wienands, W. J. Wisniewski, D. B. MacFarlane, F. Martinez-Vidal, T. J. Gershon, M. Pierini

*SuperB: A Linear High-Luminosity B Factory*

#### INFN-BE-05-01

Simone Cialdi, Fabrizio Castelli, Ilario Boscolo

*Rectangular Pulse Formation in a Laser Harmonic Generation*

#### INFN-BE-05-02

Simone Cialdi, Ilario Boscolo, Andrea Paleari

*An Optical System Developed for Target Laser Pulse Generation*

**INFN-TC-05-01**

*Esperimento THALAS: Relazione Tecnica Progettazione Meccanica Prototipo Biosusciettometro*  
S. Cuneo, B. Gianesin, M. Marinelli, R. Puppo, G. Sobrero

**INFN-TC-05-02**

S. Cuneo, F. Gastaldo, B. Gianesin, M. Marinelli, E. Oliveri, G. Sobrero  
*Esperimento THALAS: Analisi Dei Rischi e Pericoli Del Prototipo Biosusciettometro*

**INFN-TC-05-03**

G.A.P. Cirrone, G. Cuttone, S. Guatelli, S. Lo Nigro, B. Mascialino, M.G. Pia, L. Raffaele, G. Russo, M.G. Sabini, G. Sabini  
*A New Monte Carlo - GEANT4 Simulation Tool for the Development of a Proton Therapy Beam Line and Verification of the Related Dose Distributions*

**INFN-TC-05-04**

D. Diacono  
*Realizzazione di un Sistema di Autenticazione ed Autorizzazione Centralizzato Basato su Kerberos 5 e OpenLDAP*

**INFN-TC-05-05**

*Microwave Apparatus for Gravitational Waves Observation*  
R. Ballantini, A. Chincarini, S. Cuneo, G. Gemme, R. Parodi, A. Podest, and R. Vaccarone; Ph. Bernard, S. Calatroni, E. Chiaveri, and R. Losito; R.P. Croce, V. Galdi, V. Pierro, and I.M. Pinto; E. Picasso

**INFN-TC-05-06**

Antonio Anastasio, Vincenzo Masone, Pasquale Parascandolo  
*La Scheda Avi (Atom to Vme Interface) per L'Apparato Exodet*

**INFN-TC-05-07**

Raimondo Chiaramonte, Pasquale Parascandolo  
*Un Preamplificatore di Carica per le Interazioni Laser*

**INFN-TC-05-08**

Pasquale Parascandolo, Antonio Vanzanella  
*Una Sonda Attiva a Basso Costo*

**INFN-TC-05-09**

Giorgio Bar, Alberto D'Ambrosio, Franca De Giovanni  
*Manuale di Installazione di un Servizio di Posta Elettronica Completo di Filtri Anti-Virus e Anti-Spam*

**INFN-TC-05-10**

Leonello Servoli, Mirko Mariotti, Francesco Truncellito  
*Design, Implementation and Configuration of a GRID Site with a Private Network Architetture*

**INFN-TC-05/11**

Alfredo Ferrari, Paola R. Sala, Alberto Fass, Johannes Ranft  
*FLUKA: A Multi-Particle Transport Code*

**INFN-TC-05/12**

Valter Bonvicini, Stefano Ciano

*Characterisation and Test of The Power Supply System of the Pamela Experiment*

**INFN-TC-05/13**

Francesca Del Corso, Riccardo Veraldi

*Request Tracker: un Software Open-Source per il Trouble Ticket Management*

**INFN-TC-05/14**

*Conceptual Design for a Polarized Proton-Antiproton Collider Facility at GSI*

F. Bradamante, I.Koop, A.Otboev, V.Parkhomchuk, V.Reva, P.Shatunov, Yu.Shatunov

**INFN-TC-05/15**

Flavia Donno, Maria Santa Mennea

*Using GNU Autotools for the GDMP Package*

**INFN-TC-05/16**

Flavia Donno, Gigliola Vaglini

*Storage Management In The GRID*

## Glossary

These are the acronyms used in each status report to describe personnel qualifications other than Staff Physicist:

Art 15	Term Contract (Technician)
Art. 23	Term Contract (Scientist)
Ass.	Associated Scientist
Ass. Ric.	Research Associate
Bors.	Fellowship holder
Bors. PD	PostDoc Fellow
Bors. UE	European Community Fellow
Dott.	Graduate Student
Laur.	Undergraduate Student
Osp.	Guest Scientist
Perfez.	PostLaurea Student
Resp.	Local Spokesperson
Resp. Naz.	National Spokesperson
Specializ.	PostLaurea Student
Tecn.	Technician